



# 15<sup>TH</sup> INTERNATIONAL RESEARCH CONFERENCE

*Economic Revival, National Security, and Sustainability through  
Advancement of Science, Technology, and Innovation*

29<sup>TH</sup> - 30<sup>TH</sup> SEPTEMBER 2022

ENGINEERING

**PROCEEDINGS**

GENERAL SIR JOHN KOTELAWALA DEFENCE UNIVERSITY



## **15<sup>TH</sup> INTERNATIONAL RESEARCH CONFERENCE**

ECONOMIC REVIVAL, NATIONAL SECURITY, AND SUSTAINABILITY THROUGH ADVANCEMENT  
OF SCIENCE, TECHNOLOGY, AND INNOVATION

**ENGINEERING**

# **PROCEEDINGS**



General Sir John Kotelawala Defence University  
Ratmalana, Sri Lanka

©General Sir John Kotelawala Defence University  
All rights reserved

This book contains the Conference Proceedings of the Engineering Session of the 15<sup>th</sup> International Research Conference of General Sir John Kotelawala Defence University, Ratmalana, Sri Lanka held on the 29<sup>th</sup> and 30<sup>th</sup> of September 2022. No part of this publication may be reproduced, stored in a retrieval system or transmitted in any form, without prior permission of General Sir John Kotelawala Defence University, Ratmalana, Sri Lanka.

**Published by**

General Sir John Kotelawala Defence University, Ratmalana, Sri Lanka

Tel: +94-771002822

e-Mail: irc2022@kdu.ac.lk

Website: <https://www.kdu.ac.lk/irc2022>

**ISBN 978-624-5574-67-4**

**Other Proceedings of the Conference:**

Defence and Strategic Studies: ISBN 978-624-5574-65-0

Medicine: ISBN 978-624-5574-66-7

Engineering: ISBN 978-624-5574-67-4

Law: ISBN 978-624-5574-68-1

Management, Social Sciences and Humanities: ISBN 978-624-5574-69-8

Allied Health Sciences: ISBN 978-624-5574-71-1

Computing: ISBN 978-624-5574-70-4

Built Environment and Spatial Sciences: ISBN 978-624-5574-72-8

Technology: ISBN 978-624-5574-74-2

Criminal Justice: ISBN 978-624-5574-75-9

Basic and Applied Sciences: ISBN 978-624-5574-73-5

Published on

29<sup>th</sup> September 2022

**e-Book Version**

**Patron, Conference Steering Committee**

Maj Gen MP Peiris RWP RSP USP ndc psc MPhil (Ind) PGDM – Vice Chancellor

**President, Steering Committee**

Brig W Chandrasiri RSP USP psc – President

**Conference Chair**

Dr Kalpa W Samarakoon

**Conference Secretary**

Dr Pandula M Athauda-arachchi

**Conference Co-Secretaries**

Lt Col LR Amarasekara

Dr (Ms) GU Jayaweera

Ms MAST Goonathilaka

**Steering Committee**

Brig RGU Rajapakshe RSP psc

Prof KAS Dhammika

Col RKARP Ratnayake RSP USP psc

Prof CL Goonasekara

Lt Col JDB Jayaweera RWP RSP psc

Snr Prof ALS Mendis

Snr Prof SR De Senevirathne

Dr HR Vidanage

Mr VD Kithsiri

Dr LS Liyanage

## **Editorial Committee**

Mr WAAK Amaratunga – President

Dr FMMT Marikkar – Assistant Editor

Dr SHNP Gunawickrama – Assistant Editor

Col PP Serasinghe RSP USP

Maj JPWK Abeyawickrema

Sqd Ldr IKJP Kumara

Snr Prof Swarna Piyasiri

Mr WASMAI Senewiratha

Ms SUW Jayarathne

Dr Varuna Navaratne

Dr Anuji Gamage

Mr BHJ Pushpakumara

Mr FBYR De Silva

Ms NKK Mudalige

Ms BMAHH Balasuriya

Snr Prof P Hewage

Dr UG Rajapaksha

Snr Prof RN Pathirana

Dr R Vijitha

Dr LP Kalansooriya

Mr GIF de Silva

Dr AR Rupasinghe

Archd RGN Lakmali

Mr AARK Amarathunga

Mr PDDD Wickramasinghe

Dr Himali Jayasingheararchchi

Dr EKDHD Siriwardena

Dr PATM Wijerathne

Ms TC Kathriarachchi

Dr MTN Wijetunga

Ms WMUSK Walisundara

Ms BDK Anandawansa

Ms Lakshani Willarachchi

## Panel of Reviewers

Dr A Abeykoon	Dr RMUKGS Bandara
Dr S Abeyrathna	Prof CMM Bandara
Dr RMTB Abeyratne	Prof RMPS Bandara
Dr AM Abeysekera	Mrs K Bandaranayaka
Dr A Abeysinghe	Dr W Bohingamuwa
Maj W Abeywickrama	Dr HKBS Chamara
Dr K Abhayasinghe	Syr KAM Chathuranga
Dr MPKW Abhayasinghe	Dr P Chulasiri
Dr S Adihetti	Prof I Corea
Maj D Aluthge	Dr A Dalpatadu
Dr S Amarasekara	Dr C Dalugama
Prof AATD Amarasekara	Ms LC Damayanthi
Dr NR Amarasinghe	Eng Capt U Dampage
Mr AARK Amarathunga	Dr HDWTD Dassanayake
Mr K Amarathunge	Dr S Daundasekara
Dr S Ambagaspitiya	Dr N Dayanthi
Dr K Ambepitiya	Dr S Jayawardena
Ms K Anandawansa	Ms D De Mel
Dr G Appuhamillage	Dr D De Silva
Ms D Appuhamy	Dr H De Silva
Dr T Ariyadasa	Dr H De Silva
Dr A Ariyaratne	Dr N De Silva
Dr A Asmone	Dr S De Silva
Dr A Athanayake	Dr T De Silva
Dr S Athukorala	Dr T De Silva
Dr S Athukorala	L Cdr V De Silva
Dr P Balasooriya	Mr GIF De Silva
Col (Prof) A Balasuriya	Mr I De Silva
Dr A Balasuriya	Ms LM De Silva
Dr M Balasuriya	Ms O De Silva
Prof A Balasuriya	Dr D De Silva
Prof KASJ Balawardane	Dr AMS Deepanie
Ch Qs KPSPK Bandara	Prof RM Dharmadasa
Dr M Bandara	Mr HKA Dharmasiri
Dr M Bandara	Dr I Dias
Dr R Bandara	Mr U Dikwatta

Syr KA Dinusha  
Prof N Dissanayake  
Dr S Diwakara  
Dr WM Ediri Arachchi  
Ms AA Edirisinghe  
Prof A Edirisinghe  
Ms W Edirisooriya  
Mr I Ekanayake  
Prof S Ekanayake  
Mr DRGWB Ellepola  
Dr N Eranda  
Dr A Fernando  
Dr N Fernando  
Mr L Fernando  
Ms JJRS Fernando  
Dr L Fernando  
Ms IK Galagama  
Wr K Galappaththi  
Dr S Gallolu  
Dr A Gamage  
Dr L Gamage  
Mr I Gamalath  
Ms G Gayamini  
Archt DWK Gayantha  
Dr T Gobika  
Dr M Gogoi  
Prof CL Goonasekara  
Dr D Govindapala  
Dr N Gunarathana  
Mr I Gunarathna  
Mrs DABN Gunarathna  
Prof LHP Gunarathna  
Prof T Gunaratne  
Dr N Gunasekara  
Dr ADAI Gunasekera  
Ms D Gunasekera  
Syr GP Gunasinghe  
Dr MDEK Gunathilaka

Dr HRWP Gunathilake  
Dr WSS Gunathilake  
Prof M Gunathilake  
Prof S Gunawardana  
Dr R Gunawardhana  
Dr N Gunawickrama  
Prof GND Guruge  
Prof RU Halwatura  
Dr IU Hemachandra  
Prof KS Hemachandra  
Dr HMCJ Herath  
Dr HMP Herath  
Dr S Herath  
Mrs HMBS Herath  
Mrs HMB Herath  
Ms LHMIM Herath  
Prof A Herath  
Prof V Herath  
Dr S Herath  
Prof C Hettiarachchi  
Dr J Hettiarchchi  
Dr B Hettige  
Dr K Hettigoda  
Prof CH Hsu  
Dr IMPS Ilankoon  
Ms WMKS Ilmini  
Dr B Indrarathne  
Dr A Isuru  
Ms JAD Jayakodi  
Ms JLR Jayalath  
Prof C Jayalath  
Ms N Jayarathne  
Mrs S Jayaratne  
Dr JMKB Jayasekara  
Dr K Jayasekara  
Ms BKM Jayasekara  
Dr H Jayashignearachchi  
Dr U Jayasinghe

Dr SD Jayasooriya  
Dr P Jayasooriya  
Mr N Jayasuriya  
Dr MRS Jayathilake  
Prof Y Jayathilake  
Eng RHNS Jayathissa  
Dr DGSKL Jayawardana  
Dr V Jayawardna  
Archt N Jayaweera  
Ms E Jayawickrama  
Dr N Joseph  
Dr P Kalansooriya  
Ms SU Kankanamge  
Dr B Karunarathne  
Mr C Karunarathne  
Dr PPCR Karunasekara  
Dr D Karunathilaka  
Mr RDN Karunathilake  
Mr P Kathriarachchi  
Mr RPS Kathriarachchi  
Dr G Kisokanth  
Ms T Kothalawala  
Dr DU Kottahachchi  
Prof J Kottahachchi  
Prof U Kulathunga  
Archt WAPS Kumara  
Mr PPNV Kumara  
Mr WGC Kumara  
Dr N Kumarasinghe  
Dr U Kumarasinghe  
Dr KDKP Kumari  
Dr AI Kuruppu  
Ms H Kuruppu  
Dr AH Lakmal  
Archt RGN Lakmali  
Ms SMM Lakmali  
Dr D Lamabadusuriya  
Dr LCPT Liyanaarachchie

Dr E Liyanage  
Dr L Liyanage  
Mr D Liyanage  
Prof G Liyanage  
Dr N Liyanage  
Dr S llanganthillake  
Ms D Lokuge  
Prof R Lucas  
Dr T Madanayaka  
Prof S Madawala  
Eng P Maduranga  
Ms MKP Madushanka  
Prof A Manawaduge  
Dr S Manilgama  
Dr PG Mantilaka  
Syr KP Manuranga  
Dr T Matthias  
Dr MKDL Meegoda  
Dr NM Mendis  
Dr S Mendis  
Maj HSD Mendis  
Ms BS Menike  
Prof S Methananda  
Prof C Metthananda  
Dr N Miguntanna  
Dr N Mubarak  
Ms NKK Mudalige  
Dr M Mudassar  
Dr J Munasinghe  
Ms MIRK Munasinghe  
Prof H Munasinghe  
Prof A Nagahawatta  
Dr D Nakkawita  
Prof BGTL Nandasena  
Dr V Navaratne  
Archt NMRAT Nawarathne  
Mr NRM Nelumdeniya



Dr AR Nihmiya  
Prof J Niriella  
Archt RAM Padmaja  
Prof P Paranagama  
Archt KNK Pathirana  
Dr S Pathirana  
Snr Prof RN Pathirana  
Dr ML Pathirathna  
Dr T Pathmathas  
Dr HPN Perera  
Dr BJC Perera  
Dr GSN Perera  
Dr N Perera  
Dr S Perera  
Maj M Perera  
Mr D Perera  
Ms ADP Perera  
Ms GAD Perera  
Ms S Perera  
Prof IC Perera  
Prof K Perera  
Dr I Pieris  
Mr K Pieris  
Dr TA Piyasiri  
Maj RMM Pradeep  
Dr HMI Prasanna  
Mr ALI Prasanna  
Archt MLNH Premarathne  
Dr HL Premarathne  
Dr W Premarathne  
Dr P Premaratne  
Ms KGG Priyangika  
Dr S Pulleperuma  
Dr M Punchimudiyanse  
Dr PGRNI Pussella  
Dr U Rahubadda  
Dr U Rajapaksha  
Dr T Ranadewa

Dr AKRN Ranasinghe  
Dr M Ranasinghe  
Dr RJKU Ranatunga  
Syr CP Ranawaka  
Dr M Ranawake  
Mr KKP Ranaweera  
Mr DM Ranga  
Dr DM Ranga  
Dr LM Rankoth  
Dr D Ranthunga  
Prof P Rathnasiri  
Dr I Rathnayake  
Dr M Rathnayake  
Mr C Rathnayake  
Dr N Rathuwadu  
Ms RBWMH Ratnamalala  
Ms RDUP Ratnamalala  
Dr K Ratnayake  
Ms IMA Ratwatte  
Mr O Rodrigo  
Prof I Rodrigo  
Prof T Rodrigo  
Archt HT Rupasinghe  
Dr AR Rupasinghe  
Dr MHF Sakeena  
Ms BLC Samanmali  
Mr R Samarathunga  
Ms WJ Samaraweera  
Dr T Samarawickrama  
Mr K Sandamal  
Ms ERC Sandamali  
Dr TV Sanjeewani  
Ms NA Sanjeewani  
Ms N Sanjeewani  
Dr S Sarasanandarajah  
Dr N Satanarachchi

Mr S Satheesmohan  
Dr A Senanayake  
Dr C Senanayake  
Dr G Senanayake  
Dr C Senarathna  
Dr T Senarathna  
Dr B Senaratne  
Dr A Senavirathna  
Mr SADCS Senavirathna  
Ms DMND Senevirathna  
Dr SMKS Senevirathne  
Prof R Senevirathne  
Ms A Seneviratne  
Mr HKI Shanaka  
Dr S Sharic  
Dr M Silva  
Dr VP Singh  
Ms SCM Sirisuriya  
Mr G Siriwardana  
Dr H Siriwardena  
Snr Prof R Sivakanesan  
Dr T Solomons  
Prof N Somarathna  
Dr I Somaratne  
Dr LHMYK Somaratne  
Dr PDIS Somaratne  
Dr P Sridarran  
Dr SMTD Sundarapperuma  
Prof TS Suresh  
Dr I Thalagala  
Dr M Thayaparan  
Dr C Udayanga  
Dr D Uduwela  
Ms GAI Uwanthika  
Mrs V Vasudevan  
Ms DU Vidanagama  
Dr H Vidanage

Dr R Vijitha  
Dr S Wadugodapitiya  
Dr A Wageesha  
Dr AS Waidyasekara  
Ms U Walisundara  
Dr D Wanasinghe  
Mr A Wanniarachchi  
Mr WAAM Wanniarachchi  
Ms I Wathuhewa  
Dr N Wedasinghe  
Dr BS Weerakoon  
Ms S Weerakotuwa  
Dr L Weerasinghe  
Dr S Weerasinghe  
Mr Y Weerasinghe  
Prof T Weerasinghe  
Prof M Weerasooriya  
Prof T Weerawardane  
Dr AH Wettasinghe  
Mr W Wickramaarachchi  
Prof R Wickramarathne  
Dr ND Wickramasinghe  
Mr YS Wickramasinghe  
Mr RD Widanagamage  
Mr WMSRB Wijayarathne  
Dr S Wijayasekara  
Dr A Wijegunawardhana  
Dr W Wijenayake  
Dr YP Wijerathne  
Mrs M wijesekara  
Dr KAKD Wijesekera  
Dr JSJ Wijesingha  
Mr K Wijesinghe  
Ms PRD Wijesinghe  
Prof N Wijesinghe  
Ms HSMSK Wijesiri  
Ms MPC Wijesooriya  
Mr C Wijesundara

Ms L Willarachchi  
Dr R Wimalasiri  
Dr T Withanawasam

Prof C Yahathugoda  
Dr PN Yapa  
Prof STWS Yapa

## Session Coordinators

Defence and Strategic Studies	Brig RGU Rajapaksha RSP psc Col RKARP Ratnayake RSP USP psc LCdr RMS Jayawardhana Maj RMEK Rathnayake Lsc Maj RAAK Rathnayaka psc Mr Viran Maddumage
Medicine	Air Cdre (Prof) RANK Wijesinghe Dr AD De Silva Dr KDCU Wijeyasiri
Engineering	Capt (E) SU Dampage (Retd) Mrs PPSS Pussesepitiya Mr MKAJ Maldeniya
Management, Social Sciences and Humanities	Mr WAAK Amaratunga Dr Tamara Jayasundera Mr MMLC Gunathilake Ms JT Weeraratne
Law	Mr WS Wijesinghe Mr WAC Perera Ms AP Rathnayake
Allied Health Sciences	Mr ARN Silva Dr CB Ranaweera Ms HPM Dabare
Built Environment and Spatial Sciences	Dr AH Lakmal Dr FR Arooze Mr KT Withanage
Computing	Dr ADAI Gunasekara Ms MKP Madushanka Ms GAD Ganepola
Basic and Applied Sciences	Prof TL Weerawardane Dr AMCSB Alahakoon Dr AMDS Karunarathne
Technology	Dr KMGP Premadasa Dr PATM Wijethunga Dr S Shrestha
Criminal Justice	Deshabandu Prof MADSJS Niriella Mr KS Dharmasiri Mr KBN De Silva

## **Table of Contents**

<i>Welcome Address.....</i>	1
<i>Chief Guest Speech.....</i>	4
<i>Keynote Speech.....</i>	7
<i>Vote of Thanks.....</i>	9
<i>Climate Change and How We Need to Change The Practice of Engineering.....</i>	13
<i>National Defence against Intentional Electromagnetic Interferences.....</i>	18
<i>Towards Net zero: Decarbonising the Construction Industry.....</i>	22
<i>Achieving Sustainability in Buildings.....</i>	24
<i>Home Automation Application Using Raspberry Pi 3 and Windows 10 IoT.....</i>	27
<i>Intelligent Battery Control Mechanism for Electric Bicycles.....</i>	36
<i>Comparison of Printed Circuit Board Fabricated by using conventional method and Laser Cutting Method .....</i>	48
<i>CREEPER: The First Indigenously Developed Hand-Held Digital Mobile Radio (DMR) in Sri Lanka .....</i>	58
<i>A Numerical Study on Effect of Change in Longitudinal Center of Gravity on Planing Capability of a Coastal Patrol Craft: A Case Study, Sri Lanka Navy.....</i>	69
<i>Novel design of Cost-effective Solar Powered Brackish Water Reverse Osmosis Plant: A possible solution for an affordable supply of safe drinking water for the rural communities in CKDu-affected areas in Sri Lanka.....</i>	78
<i>Design and Development of an Autonomous Underwater Vehicle (AUV): For Rip Current Data Collection and Shallow Water Explorations.....</i>	90
<i>Indigenously Designed Addressable Bilge Alarm System for Naval Vessels.....</i>	100
<i>Thermographic Inspection System for Surface Coating Defects on Aircraft Fuselage.</i>	105
<i>Estimation of Lift Hysteresis of an Airfoil in low speed flow.....</i>	117
<i>An analysis of the impact of technical communication on aviation risk mitigation in the context of aircraft maintenance operations in Sri Lanka.....</i>	124
<i>An empirical analysis of the impact of aircraft maintenance technical training on risk mitigation in the Sri Lankan aviation industry.....</i>	133

<i>Predicting the Freezing of Gait in Parkinson’s patients based on Machine Learning and Wearable Sensors: A review.....</i>	142
<i>Local Binary Pattern based features for Prostate Cancer Detection.....</i>	152
<i>Methods of measuring CSF Pressure: A Review.....</i>	163
<i>Ceramic Tile Waste as Fine Aggregate for Marine Concrete Modules In Sri Lanka...</i>	172
<i>Identifications of Pathways for Phosphorus-based Product Recovery from Sewage Sludge using Multi-Criteria Decision Analysis for Sri Lankan Context..</i>	180
<i>Genetic Algorithm-based Path Planning for an Unmanned Aerial Vehicle Considering Energy Consumption and Payload .....</i>	189
<i>Current Phasor Measuring Device for Three Phase Distribution Lines.....</i>	198
<i>Analysis of the Behaviour of Improved Soil under Shallow Concrete Foundations....</i>	207
<i>Improving Turbidity Removal Efficiency in Slow Sand Filter during the Occurrence of High Turbidity Levels in Surface Water.....</i>	215
<i>Study of Issues in Sludge Disposal and Management in Wastewater Treatment Plants.....</i>	221
<i>Assessment of Groundwater Quality due to Leachate Generated from a Solid Waste Dumpsite.....</i>	231

## Welcome Address

Major General Milinda Peiris RWP RSP VSV USP ndc psc MPhil (Ind) PGDM  
*Vice Chancellor, General Sir John Kotelawala Defence University*

Chief Guest, Secretary - Ministry of Defence, General Kamal Gunaratne (Retd), Keynote Speaker, Hon. Prof. Subramanian Swamy, Your Excellencies in the Diplomatic Corps, Chief of Defence Staff, Gen Shavendra Silva, Commander of the Army, Lt Gen Vikum Liyanage, Commander of the Navy, Vice Admiral Nishantha Ulugetenne, Eminent plenary speakers representing our friendly nations, Vice Chancellors of Other Universities, Former Commandants of KDA, Former Chancellors and Vice Chancellors of KDU, Rectors of KDU Campuses and Deputy Vice Chancellors, Deans of Faculties and Centre Directors, Senior Military Officers and Police officers, Academics, Administrative Staff, Students, All distinguished guests including those who connected with us in the cyberspace, Ladies and gentlemen, Good Morning to you all! I am deeply honoured to make the welcome address at this inauguration of the 15<sup>th</sup> International Research Conference (IRC) of General Sir John Kotelawala Defence University. To begin with, I warmly welcome our chief guest this morning, Gen Kamal Gunaratne (Retd), Secretary to the Ministry of Defence for gracing this important occasion. We owe you a great deal of respect for the whole-hearted support extended for the progression of this university at all times. Also, may I have the distinct honour of welcoming our keynote speaker, the esteemed and renowned

personality, Hon Prof Subramanian Swamy from neighbouring India.

Hon Sir, we are extremely grateful to you for accepting our invitation and honouring us with your gracious presence to deliver the keynote address of this two-day international research conference. I am sure that your eminent presence adds great value to the event, and we are looking forward to listening to your words of wisdom, which will surely set the most appropriate tone for this scholarly event.

I also welcome the Chief of Defence Staff, Gen Shavendra Silva, Commander of the Army, Commander of the Navy and all other members of our Board of Management. Let me also warmly welcome the members of the Diplomatic Corps representing our friendly nations, Vice Chancellors and Senior Academics from other universities, Former Commandants of KDA, Former Chancellors & Vice Chancellors of KDU, Other officials of Ministry of Defence, Academics, Senior Military Officers, Plenary speakers, Scholars presenting papers in this two-day conference, and all other distinguished invitees and students joining this event physically as well as on cyberspace. As the Vice Chancellor of KDU, I admire your valuable presence at this occasion.

Reflecting on KDU IRCs held last year and the year before, we held them under the most trying circumstances of the grave pandemic. They really tested our resilience and

defiance against challenges to the very core. Along with the IRCs, we determinedly continued with all academic and other activities of the university with much vigor, and the results are evident in our achievements.

Ladies and gentlemen, today, we are glad that KDU has firmly established its foot print as a unique higher educational model in the world, which even its critics would not be able to disagree with. The best evidence is its steady growth in its popularity as an Higher Education Institute in Asia, as well as the quality of its output, which are evident in the Times Higher Education Impact Ranking, 2022 table, where KDU is ranked 2<sup>nd</sup> in Sri Lanka for Quality of Education and 4<sup>th</sup> in the overall ranking in the country and in the 801-1000 range globally. A more recent indicator of our growth is evident in the world ranking of Law Schools, where the KDU faculty of law took a leap in the world ranking from the 498<sup>th</sup> place in 2021 to the 83<sup>rd</sup> place in 2022, from the 189<sup>th</sup> place to the 25<sup>th</sup> place in Asia, and from the 5<sup>th</sup> place to the 2<sup>nd</sup> place in Sri Lanka.

Ladies and gentlemen, today, we hold the 15<sup>th</sup> consecutive IRC at a time when we, Sri Lankans are in a grave need to pull up our socks as a nation to face the seemingly unsurmountable economic crisis we are in. And we as a university are determined to give our utmost best for the nation at this crucial juncture. We believe that the role of the universities and the intellectual community of the nation is of paramount importance for the resurrection of our economy, and that of the nation's defence university is even more significant as it deals

with the national security perspective which is inseparably linked with the economic crisis and with a possible recovery from the same.

Serious research in defence and security studies needs to go hand in hand with rigorous research in all other fields. This, we believe, is an essential prerequisite for a quick and sustainable recovery from the crisis. So, we carefully selected the overarching theme, *"Economic Revival, National Security, and Sustainability through Advancement of Science, Technology, and Innovation"* for this year's conference, and its scope encompasses a wide range of significant research possibilities to engage in.

Our aim in selecting this theme entails a holistic vision of the complexities of economic and national security perspectives which demand comprehensive inter- and multidisciplinary approaches to resolve contemporary issues. The expectation is to carry forward the research outcomes to the attention of those in authority to consider implementation to resolve related issues. I do not intend to talk any further on this aspect as I am sure our keynote speaker would elaborate on the conference theme and its significance. Ladies and gentlemen, having commenced in the year 2008 in a humble way, the KDU IRC gained gradual momentum as a trustworthy forum for the country's scholarly community to showcase their multi-disciplinary research outcomes. And what is noteworthy is the ever growing increase in the number of research papers submitted for the conference, and more so is



the increasingly higher quality of the papers presented at the conference.

Therefore, KDU enjoys the humble pride of its leading role in strengthening the research culture in the country that is more and more inclined towards product based or problemsolving outcomes in relevant fields, which I believe is the need of the hour. Also the involvement of internationally collaborative research is on the increase. Anyone who visits the KDU IRC Proceedings would note the evolutionary path of the progression in research in the country spearheaded by KDU – You could see the increasingly high numbers of researchers representing almost all the universities, other Higher Education Institutes and research institutes of the country as well as those from renowned universities, Higher Education Institutes and research institutes in the world. So, we are proud of our role in establishing local and international research and scholarly networks that would further enhance creation of new knowledge in diverse disciplines and dissemination of the same.

Ladies and gentlemen, the organizers of this year's research conference too have been doing their utmost best to maintain and upgrade the quality of the annual research conference despite challenges, especially in the face of financial constraints which compelled them to significantly cut down on peripheral expenses.

The circumstances have compelled them to rely on our own resources as much as possible, which I believe is a blessing in disguise in the crisis situation to convert

challenges into opportunities. I appreciate their effort and the support extended from all quarters to make the KDU International Research Conference a resounding success in terms of achieving its objectives. So, let me conclude by once again welcoming our chief guest, the erudite keynote speaker, and all the other distinguished invitees. I convey my congratulations to all researchers who will be presenting their research during the couple of days.

I also request those whose papers were not selected through the double blind reviewing process not to get disheartened because you had competed with many for a placement in the conference. Finally, let me express my heartfelt thanks to the Chairman of the Conference Organizing Team, Dr. Kalpa Samarakoon, Secretary, Dr. Pandula Athawuda Arachchi and the other members of the team for the tireless hours, days and weeks you spent to see the success of this important event.

May the KDU IRC be a haven for establishing scholarly links at national and international levels, which would pave the way for fruitful research, academic and even industrial collaborations for the betterment of our nation, its security and its social, economic and political stability that would in turn pave the way for the creation of a self-sufficient nation in the not so long future. Let us optimistically believe in ourselves and in our potentials to reach that target sooner than later.

Thank you.

## Chief Guest Speech

General Kamal Gunaratne (Retd) WWV RWP RSP USP ndc psc MPhil

*Secretary - Ministry of Defence, Sri Lanka*

Hon. Prof. Subramanian Swamy, Keynote speaker of the 15<sup>th</sup> International Research Conference 2022 of General Sir John Kotelawala Defence University, Your Excellencies in the Diplomatic Corps, Chief of Defence Staff, Commander of the Army, Commander of the Navy, Chief of the Staff of Sri Lanka Air force, Vice Chancellors of Other Universities, Vice Chancellor of KDU, Eminent speakers from friendly foreign nations, former commandants of KDA, former Chancellors and Vice Chancellors of KDU, Rector of KDU Metropolitan Campus, Rector of KDU Southern Campus and Deputy Vice Chancellors, Deans of Faculties and Directors, Senior Military Officers and Police officers, Distinguished guests, Ladies, and Gentlemen's. Good morning to all of you.

I consider it as a great pleasure and privilege to be present here today as the chief guest of the inauguration ceremony of General Sir John Kotelawala Defence University's International Research Conference, which is taking place for its 15<sup>th</sup> consecutive time.

Without a doubt it provides as opportunity for academics, professionals, researchers and practitioners from all around the world to share their research findings and expertise addressing mutual challenges in their fields. Further it provides an opportunity for a wide interaction and networking with national and international scholars in respective fields which in turn proved beneficial for the

participants to broaden their horizons of knowledge through intellectual discussions most importantly despite the global pandemic situation and the reason economic, social and political setbacks in effect it is truly inspiring to see that the KDU is continuation the conduct of this conference with renewed spirit and commitment

Therefore, ladies and gentlemen at this moment I would like to encompass

My sincere appreciation to the Vice Chancellor and the conference organizers for the invitation extended for me to be the chief guest to the most significant academic events of this University. In this context of promoting an excellent academic culture generation of knowledge and subsequent applications of it led to innovations and novel technologies that are crucial for the advancement of humanity, well-being, and sustainability. The knowledge is generated by scientific research and at this backdrop, it is delightful to see that the theme of this year's conference reads economic revival, National Security, and Sustainability through the advancement of Science, Technology, and Innovations, which is a well-timed theme reflecting directions that we should pursue as a country irrespective of the boundaries of time and era.

Further, at this moment, ladies and gentlemen, I will be failing in my duty if I do not acknowledge the distinction of a brilliant keynote address conducted by the former Minister of Commerce Law and the Justice

Republic of India, Honorable Professor Subramanian Swamy. Sir, we as Sri Lankans truly appreciate the accept acceptance of our invitation extended to attend and maintain throughout the past in continuation of the display of your friendliness towards Sri Lanka. The ideas that would be shared by you in this eminent forum today will indeed bring a sparkling light to the discussions to be conducted during this conference that will become highly fruitful with your intellectual input.

All the foreign and the local participants including the senior officers of tri-forces and police would be immensely benefited by the inputs that would be given by you to broaden the Horizon of their knowledge.

Moving on the the focus of the conference I must emphasized that with the effects of globalization in effect the growing international independencies affecting the Sri Lankan National security as well as reasons concerns raised by economic and political implications. There is a recognized need for assessment of the potential to national security, that may emerge during the thrive towards revival of national economy and sustainability.

As per my belief given the importance of certain sectors to the effective functioning of the Sri Lankan society the said need for a deeper conceptual understanding of the threats that may impact the implied economic revival and sustainability in all aspects focusing on technological scientific and innovative faces would be comprehensively discussed with in the earnest gathering of intellectuals during these two days.

A strategic standpoint keeping the past and also most recent lessons learned

In mind a newfound leadership of the present government, Sri Lanka should call for national determination where all sectors of Sri Lankan society including civil organizations, security institutions, political entities and business associations come together to discuss fundamental issues such as national identity, national reconciliation, transitional justice, governance structure, economic revival and many more.

This is a fundamental step towards building consensus and religious legitimizing state institutions and private organizations in the country towards a common goal. Not only would such an effort-based process serve as the foundation for a national pact addressing the country's issues, pointing out how it would concurrently compel every group in society to work towards state building and the sustainability of a secure country due consideration to scientific and technological innovations.

Furthermore, giving high priority to providing solutions to the country's most freezing matters of concern to improve the world's image of Sri Lankans society the Sri Lankan government must take every step necessary to recover high-priority initiatives in the fields of the economy, institution-building, and political reform.

Whilst giving true meaning to the said initiatives in order to address emerging challenges promoting more research and development becomes a task of topmost priority bestowed upon all of us who are present here today.

Fortunately, as a secretary Defence and the Chairman of the KDU Board of Management, I

feel tremendously proud and content to state that KDU is at the forefront of researching the development and security related problems holistically.

In this context, one of the unique aspects of KDU IRC in comparison to a plethora of symposia that we witness in the country and beyond its borders remains to be its firm commitment to defence and strategic aspects of the contemporary world with emphasis on local and regional trends.

In that this conference continues to pioneer in upholding the notion that security is a prerequisite for the viability of achievements in all other areas in which mankind relies on in order to facilitate such outcomes it maintains a seamless association of defence and security with other core areas such as Sciences, Medicine, Engineering, Build environment and Spatial Sciences, Technology, Management, and Humanities. We are fundamental knowledge images. To be honest, I personally acknowledge this pragmatic philosophy as a remarkable achievement of KDU and thereby of the country as a whole. Resulting in interactions and dialogue across apparently distinct disciplines will certainly usher increasing exchanges and collaborations among experts in diverse areas, therefore, I am well certain that all faculties of Sir John Kotelawala Defence University with their interest and commitment to knowledge in diverse

academic disciplines and outside researchers' inputs would contribute immensely to this year's research conference theme.

The knowledge that you are giving to another and sharing during this conference would be an immense benefit not only to the academic community but to the entire humankind to make their lives better.

In conclusion, ladies and gentlemen, at the current context we are on the average of striving to accomplish serenity and excellence in an economic revival, national security, and sustainability through unexploited frontiers of technological innovations as a nation. Therefore, conferences of this nature are instrumental in clearing our fond of mind for the betterment of establishing solutions, therefore, let me express my sincere appreciation to the Vice Chancellor and organizers of the 15<sup>th</sup> KDU IRC 2022 for inviting to this occasion as the chief guest and giving me an opportunity to speak to you. Let me appreciate all the efforts and congratulate all of you for working your way towards a timely and appropriate theme. Finally, I wish all the participants all the very best in their research endeavors and the KDU research conference for 2022 to be successful in every way.

## Keynote Speech

Hon Prof Subramanian Swamy

*Former Minister of Commerce, Law & justice, India*

Hon. Professor Subramanian Swamy, former Cabinet Minister of India made insightful remarks in the keynote address and initiated his speech by extending his gratitude towards Vice chancellor Major General Milinda Peiris for the invitation bestowed on him and went on to acknowledge the presence of the chief guest, Secretary to Ministry of Defence, General Kamal Gunaratne stating, how the Indians themselves couldn't put an end to a major terrorist problem in the region. Professor Swamy recollected how Sri Lanka has never been defeated throughout history, exempting a few setbacks. Furthermore, Professor Swamy remarked how the 21st century isn't going to distinguish between large nations and small nations, as it's a new era with innovations. Speaking from his experience as a trained economist, Professor Subramanian Swamy recalled how all economic development took place when the share of innovation calculated within the GDP rounded up to at least 55%, indicating the development of the USA, Europe and China as examples. He explicating further, mentioned that the growth rate of GDP would be dependent upon the extent to which one innovates. Professor Swamy also recognized the role that could be assumed by the universities in the development of the concept of innovation.

Professor Swamy, elaborated on the inception of the definition of – National security relating to its historical context. He expressed that for most of the 20th century national security had

been a matter of military power, and explicated with the dawn of the 21st century, non-state actors posed most of the challenges to national security as opposed to conventional military warfare. Moreover, professor Swamy emphasized that long-term unsustainable practices make the state more vulnerable to internal and more resilient to external threats. Professor Swamy pointed out the “economic factor “as the primary reason behind Sri Lanka's recent upheaval. Furthermore, he scrutinized the removal of democratically elected people from office, which in turn would disallow them to complete their full term, which he recognized as a blow to the country's national security.

Professor Swamy detailed important aspects that need to be regarded in policy formulation; clearly defined structure of objectives, the order of priorities, strategy to achieve them, and resource mobilization. He also stated that no country should be too dependent on one country, and pointed out how Sri Lanka owes a single country, a staggering 52% in internal and external debt. He further resonated that the world has moved from the notion of “development” to “sustainable development”, “sustainable economic development and sustainable national security” during the course of the last thirty years of the 20th century. Professor Swamy asserted that the most stable system of governance is democracy. Furthermore, he perceived economic security, political security, energy security, homeland security, and new

technology and innovations to be primary elements that constitute sustainable national security. Honourable professor Subramanian Swamy concluded his speech by stating that the sustainable national security of a country

is the ability to provide comprehensive protection and holistic defence of citizenry and climate change, other issues of globalization, terrorism and many more.

## Vote of Thanks

Dr Kalpa W Samarakoon

*Conference Chair, 15<sup>th</sup> International Research Conference,  
General Sir John Kotelawala Defence University*

The Chief Guest, General Kamal Gunarathne, Secretary to the Ministry of Defence, The keynote speaker, Hon Prof Subramanian Swamy, Chief of the Defence Staff, Commander of the SL Army, Commander of the SL Navy, The Representative of the Commander of the SL Air force, The Vice Chancellor of KDU, The Rector KDU Southern Campus, The Rector KDU Metropolitan Campus, The Deputy Vice-Chancellor (Defence & Administration), The Deputy Vice-Chancellor (Academic), Deans of Faculties, Directors, Senior Professors, Senior Officers of tri-officers, and Police, Distinguished invitees, Colleagues, ladies, and gentlemen. Good morning!

Sri Lankans have been suffering an economic slowdown in the post covid era, in particular, with a social and economic crisis, food insecurity, and inequitable provision of health and education, due to its over-reliance on traditional exports, tourism, and constant geopolitical battles. In this context, KDU has been successful in organizing its 15th consecutive International Research Conference. We, strategically analyzed the role of academia of the country to collectively come together and facilitate the transfer of knowledge, skills, and solutions using science, technology, and innovation.

The IRC theme selection for 2022, aims to provide a multi-professional platform to all the scholars based in Sri Lanka and overseas

to bring in their innovative research ideas to fulfil this national responsibility thrust upon us, to revive the nation's economy, to achieve sustainable economic growth coupled with an environment of justice and enhanced security for all. This year's conference attracted more than six hundred and ninety paper submissions in 11 sessions the highest-ever submissions since the inception of IRC. This indicates the amount of novel knowledge generated in our country. This year is the conference's inaugural technology and criminal justice sessions.

With deep appreciation and gratitude, I would like to express my heartiest thanks to General Kamal Gunaratne, the secretary to the Ministry of Defence who is our Chief Guest today at KDU-IRC 2022. Sir, your gracious presence in this occasion despite other commitments is truly appreciated and encouraging, and it has certainly added glamour and value to this important event on the KDU calendar. The same goes with Hon. Prof. Subramanian Swamy. He is a renowned academic and has been a distinguished politician in India and even beyond. Sir, I greatly appreciate your willingness to be our keynote speaker. It is truly an honour, privilege, and inspiration to witness your presence among the KDU community today.

I would like to take this opportunity to express my heartfelt gratitude and deep appreciation to the Vice Chancellor of General Sir John Kotelawala Defence

University, Maj. General Milinda Peiris, with your leadership, guidance, and timely decisions, prevailed throughout the event organization. The event would not be bound to be a success without your active input, particularly under the current difficult context. Thank you indeed Sir.

I will be failing in my duties if I didn't acknowledge the crucial involvement of KDU Deputy Vice-Chancellor (Defence and Administration), Brigadier W. Chandrasiri. He in fact steered KDU-IRC 2022 organization effort providing correct and pragmatic directions successfully even when the team was at difficult crossroads. I would also like to thank the Deputy Vice-Chancellor academic and all faculty Deans and Directors, who held the responsibilities for organizing and conducting forthcoming academic sessions.

Ladies and Gentlemen, as I said before, It has been a seemingly overwhelming challenge to organize, coordinate and conduct a research conference of this magnitude at this time.

I must appreciate the support of our sponsors. Platinum Sponsors, together with banking giants namely, Bank of Ceylon, People's Bank, and special sponsors, Gamma interpharm and George Stuart Health.

Let me take this opportunity to thank generously, conference secretary, Dr Pandula Athaudarachchi, Senior lecturer and consultant interventional cardiologist, and the tremendous work done by the three co-secretaries, Dr. Gihani Jayaweera, Lt Col Lasitha Amarasekara and Ms. Sandali Goonathilaka, who stood alongside me ever since work has been commenced in mid of 2022 with exceptional commitment. I also

thank all the session coordinators who supported tirelessly around the clock from the moment. I am certainly indebted to them for the success of KDU-IRC 2022.

I deeply appreciate all the presidents of the committees, and committee members, faculty committees, Office of Vice-chancellor, Office of DVC, officers of Bursar, Officers of the registrar, Adjutant, co-admin who held and executed the roles and responsibilities over the IRC. A special thank goes to the media and communication team led by the Director of IT, Publishing, printing and editorial committees.

I take this opportunity to thank all authors who shared their valuable research works at KDU-IRC. I thank both internal and external reviewers who perused and evaluated the submissions. Please be assured that your expertise shown and valuable time spent in critical reviewing is duly appreciated.

An event of this dimension cannot happen overnight. The wheels start rolling months in advance, it requires meticulous planning and execution and an eye for details. I cannot thank everyone enough for the involvement they have shown, So please bear with me if I would not have named all the supporters.

I expect that participants of the two-day conference that commenced just now will have an occasion that broadens their horizons of own know-how and improve networking in a refreshing environment which all of us at KDU has attempted to facilitate.

I wish you the very best at the conference.

Thank you very much!



# **ENGINEERING**

## **PLENARY SESSION**

# Climate Change and How We Need to Change The Practice of Engineering

Professor Jayantha Obeysekera

*Director and Research Professor, Sea Level Solutions Center  
Florida International University, Florida*

It's always a pleasure to share my research experience. I pick this sort of a catchy title to send the message to young engineering professionals, this idea of climate change and how we need to change the practice of engineering.

I will share some background on climate change and the causes of it. This will cover Greenhouse gas effect. The carbon dioxide measurement in Hawaii is basically increasing continuously and this warming is actually a good thing for us. I mean too much of a good thing. Otherwise, we will not be able to live on this planet but more importantly, the question is, what effect it has on the environment? This is the key message I will be delivering.

Climate change is a type multiplier, and we need a new paradigm in practicing of engineering, and I'm going to share some of my ideas and experiences and research outcomes. This message called stationary is dead and you will know what stationary means after my speech. Hopefully, we can continue to practice engineering building up the infrastructure, the same way we have learned in school laws in how we do things in practice.

Basically, the climate change itself undermines the assumptions that we have been using historically, for management of water supply demand service. Now my focus

will be primarily on water resources, also I'll touch on transportation, but it can apply to many areas of civil engineering in general.

The message I like to convey is that you need to come up with a new paradigm to plan projects under future conditions which is what we are not doing now. For the most part, we need to adapt the engineering curriculum to this concept that icon called resilient sustainability, the sustainability we've been talking about for decades but now we have to be resilient in doing that and you will see why because of this concept is non-stationary. The other important message I'm going to convey in this short time is, how do we deal with this deep uncertainty and I'm going to introduce this concept of dynamic adaptation.

The figure depicts the science of climate change, all these arrows going up signifies the increasing data behind every one of climate change factors and the arrows going down also indicate the variation of climate change. So these are all consistent with what is being predicted. In climate change science, the metrics that indicate where we are in terms of carbon dioxide global temperatures sea level and others.

This is the background in my speech and the fact is that we have a global scale in which

we have already some indications about, more than a degree Celsius in warming on the planet. Since the pre industrial era this global warming is evident. Then, there's the sea level rising and it seems to be accelerating currently at the rate of 3.3 to 3.4 millimeters per year, which for low lying areas could be significant.

Climate change, basically alters the hydrological cycle and it is like a human on steroids, because of the increased energy that is on the planet is due to much of the climate change. About 90% of energy from climate change that comes as heat is absorbed by the ocean. So that's a big storage of heat and that could be something that causes changes in climate globally.

Our primary variables of interest in our planning of design is the temperature, precipitation is your procrastination in sea levels. As you all probably agree with me, it will have implications for ecosystems and human health, Water Management Energy, Agriculture economics and many more, including other sectors like transportation.

I have been looking at Sri Lankan data for some time on and off. I've been away from Sri Lanka for probably about 40-50 years but still I've been in touch with Sri Lanka on many occasions. Therefore, this is the work we did with my help on basically looking at trends in the map of Sri Lanka where about 20 stages and all the arrows are red, diamonds indicate the warming trend. These are all statistically significant and you have, in general, a variation of about point 1-5.2 degrees per decade and you probably all see that and the figures show that the sea

had been warming continuously for each decade. You can see that the circle is becoming bigger and bigger, that means in every month, we are becoming warmer and warmer and I'm sure many of you who live in these areas like Colombo are feeling it.

So another aspect is you know what will happen to the sea level; As per 'Lena' we are surrounded by sea level rise. Lena is a wonderful tool from NASA that you can go to and globally look at the sea level rise rate. The point closest to Sri Lanka and you can see by 2100 we will have one meter or more depending on the greenhouse gas scenario emissions as shown in the figure. Warming is not going to stop and the sea level is going to rise continuously. And that's something we have to be cognizant on when we are planning or designing projects all along the coastline and I'll show you some examples of what's happening, or what could happen.

This particular side also tells you different scenarios which you can expect, let's say, half a meter one bit of sea level rise. Obviously, it all depends on the greenhouse gas scenarios but the current trend is not being enough to mitigate the greenhouse gases to slow down the warming. This two degree centigrade limit might be set up as not achievable by 2050 as someone wanted to. When you look at the scene of what happened in any kind of landscape there are what we call compounding effects of track multipliers. They could be sea level rise on the coastline.

These big storms like hurricanes which are known as cyclones in our part of the world also cause rising groundwater levels,

particularly in coastal areas, because the highest levels been flooding due to potential changes in rainfall patterns. We saw all these threat multipliers, one research we are conducting is, what are the compounding effects of joint probabilities of this threat multipliers that we have to deal with many parts of the world. We wanted to see of climate change, where some figure show flooding in Florida, also in places like Miami Beach twice. In the West, there was a neighborhood that flooded for 60 days continuously just from tide which is rising and not having a significant effect on other neighborhoods.

But on the other extreme, you also have a drought, the western US is having an unprecedented drought, very low water levels in rest of the areas was having major implications for water supply for agriculture. Another issue was the hurricanes that come through that you never see very often, a New York subway being flooded due to a storm, for example, right now. The heart of the hurricane that came over from the west coast in Florida, had storm surges of 10 to 15 feet and flooding have implications for infrastructure and others.

This much flooding is a medical concern and the picture shows Houston streets were flooded for days and then more recently in Pakistan another same kind of climate we never used to have. We need to think about that when we planned, you know, engineering projects in the future. On the occurrence of extremes, I just want to point out the category of storms coming on shore in Florida, not too long ago it's still going

through a state of a major storm event and these things are happening more and more frequently. It's expected to be stronger and more frequent in the future, particularly the major storms and the climate change.

When you look at the, the cost of these events, what we call billion dollar disasters. They're increasing significantly and this might be the result of development, without any planning and that is a sign that we are going to have more and more losses in the future. One aspect that we should think about which is not really happening in Sri Lanka, in my opinion, is this whole idea of floodplain management if you dig major river basins in Sri Lanka, every one of the basins will be flooded now more and more frequently. But I think we need to think about floodplain management in the context of climate change and that's something I've been trying to promote in Sri Lanka for some time.

The other aspect we don't talk much about as a civil engineer is this crown water. So what inclusion effect, in particularly along the coastline, we have this situation the saltwater inclusion will basically affect high rise buildings, other buildings. This salty water coming in and affecting the foundations and maybe even piles that you construct. This video I'm showing from YouTube is on a collapse of building in Miami Beach, and you will see that this poor building has collapsed and everybody was wondering what the engineers had done. So, this is what happened after the building collapse everybody was wondering we don't build engineering buildings or design buildings to collapse like that but what is happening on the ground is probably the main culprit.

This whole word inclusion due to sea level rise, basically corroded the foundation, and since something that might be sort of like a thread on the ground that we don't know about and that's something we need to think about. This whole concept of stationary at a non-station or it is something Professor Fernando mentioned that I've been doing research on lately. Traditionally, in engineering practices we assume station ID is not constant but the basic laws and patterns will remain the same, the path climate is an indication so when we designed for the future. We assume this probability of extreme still remain the same through time. The idea is the past is a key to the future and we use the concept of return period that many of you engineers might be very familiar with. Now on the non-stationary, the probability distribution basically will be changing with time and basically lifting up with time, because of this trend we might experience in the future. There are many challenges in analyzing and we have done some research on how to plan for the four projects on the future conditions this.

Basically, in this case the past is not a good indication of the future and we need to think about what could happen in the future, can we extend this trend into the future. Those are some of the challenges. So we have a situation of dynamic return period that I will explain that in two minutes. In other words the return period as a fixed quantity cannot be used for planning anymore in this paradigm.

This is an example of sea level rise again. When designing bridges or old way infrastructure, the dynamically changing extreme probabilities will require you to have a new paradigm for planning and design. The graphic go through all the details of that, the return period will actually decrease if you design well. For example, it will have maybe a 50 year return level auditor area by 2040. In other words, your level of protection is decreasing. It's same with another location, this is for the sea level rise on the west and flooding on the right. In other words the return period concept that we've been using as engineers for generations, will not work anymore in this kind of setting.

We've done research, I'm not going to go to all the math on this but we have redefined the return period as what we call expected waiting time. We have come up with other definitions of how we plan for changing frequency of flooding in the future and have come up with this return period concept where we can determine what we need to design for today, in order to deal with these changing conditions in the future.

Also, another concept that we are looking for is the risk based concept. This is the risk formula for non-stationary day and one of the things that I have is what was developed for the National Climate Assessment in the United States. So, under stationary day with your design life your risk is going to increase that is natural, under stationary. But under non stationary you're going to have a higher risk even for the same design life. So we have come up with ways of, If you specify let's say 50%, what you need to design for, so this risk based design is an approach that could

be expanded to incorporate damage in terms of monetary terms.

One thing we have done is to come up with this concept of adaptation portfolio and what are the things that we could do in the future. I'm now going to go through each one of those so that is something that we have developed for the state of South Florida area, what are the options we can use again, keeping in mind this concept of manifestation. So the concept that I want to promote, dynamic Adaptive Path, is what we have worked with the Dutch on. The whole idea is that we are in an existing situation with highly vulnerable conditions and we have had that for generations. There's no change in that we still have an aging infrastructure, but we have this current situation but the future is not in stationery, and due to climate change.

It is uncertain because prediction of climate change is not easy and we have what we call a situation of deep uncertainty. So how do we plan for that kind of uncertain future. So, the approach is basically looking at different adaptation pathways and looking at tipping points. So, this concept of dynamic adaptation or dynamically adaptive pathways is a wonderful technique that we should think about in dealing with non-stationary climate change in engineering. One example we looked at is Miami, for

example, we looked at various options or portfolio of measures. Basically elevating the roadways and houses so the idea here is like how to face these solutions in and we came up with this pathway concept.

At sea level rise magnitude we need to resort to another measure in this set. Finally, I want to leave with five resilience principles.

So, compared to what we have been doing, working in engineering in the past we need to think, have a systems approach we can't just isolate one area and need to look at the environment and other aspect of a project, which you might already be doing.

We also need to think about beyond design events, because I think we are going to have a higher stronger event in the future and we need to look at those as well.

Number three is we need to think about how we design a project using this concept to remain functioning. Just because you fail once, maybe the project does not need to be abandoned how we make sure. They can be used at all design the project in a way that they can be enhanced or rebuild very easily. Improve the recovery capacity by also looking at social and financial capitals, working with the community. And then basically how do we remain in the future by looking at this concept like stationary.

I will stop here and take questions.

# National Defence against Intentional Electromagnetic Interferences

Professor Chandima Gomes

*Distinguished Professor & Chair EPPEI-HVAC, School of Electrical & Information Engineering,  
University of the Witwatersrand, Johannesburg, South Africa*

Two models were to be discussed namely the Risk and the Business model. However, due to the time constraint the latter was not taken into the discussion. Firstly, taken into discussion was the lightning phenomena. Lightning is a natural unintentionally electromagnetic source. The lightning causes an approximate 50 V to 100 V induced voltage between few hundred meters. This leads to the destruction of electronic equipment and components.

Though lightning provides unintentional natural electromagnetic interferences the voltage dips caused by plugging and operating motors in households will contribute to the electromagnetic interferences in other equipment. The television screen having it's images distorted whilst the blender is operational is a classic example which many households faced during the latter part of the 20<sup>th</sup> century. Most fuel stations prohibit customers to use their mobile phones while getting their vehicle pumped. Electromagnetic radiation emitted from the mobile phone can trigger a micro voltage arc with the ionized particles of the fuel causing severe fire risk. Though a possibility of such hazard prevails there are not much quantitative research on the topic. The

mentioned falls under unintentional artificial electromagnetic interferences. These artificial unintentional electromagnetic interferences can be armed into intentional EMPs. A terrorist mounting an EMP emitter in his/her vehicle and activating it in a fuel station could result in a catastrophic incident. Since modern world practices such as the bank industry and the administrative services are based on electronic modes of communication, they can be collapsed due to intentional electromagnetic interferences. The danger

poses in electromagnetic terrorism is that the infiltrator could come to the target until he/she is successful without rising any alarms. By intentionally electromagnetic interference, a skilled person can generate and direct an intentional electromagnetic signal, not only to a remote-control system but also to a wire control system does interfering with the controlling mechanism of the system. Further, the worst case is that the intruder taking over the control of the system in addition to the Intentional Electromagnetic Interference (IEMI). Therefore, mal operation standstill, or even destruction of equipment through IEMI to disrupt the civil society is a commonly known as electromagnetic terrorism or intentional electromagnetic interference.



The textbook definition of IEMI, is intentional malicious generation of electromagnetic energy introducing noise or signals into electrical and electronic systems, thus disrupting, confusing or damaging these systems for terrorist, criminal and industrial sabotage purposes. It was further explained by stating that electromagnetic emission that may cause an incident field, which exceeds 100 V/m, corresponding to a plane-wave free-space power density of 26.5 W/m<sup>2</sup>, is treated as a high power environment where the exposed electrical equipment may encounter a range of issues from temporary signal losses to permanent hardware damage.

When discussing about the risk involved an electromagnetic emitter can be mounted to a vehicle and can be brought near a power line. By illuminating the emitter, it can totally collapse the power grid leading to a regional brown out due to the induced voltage impulse. Further, it will also cause permanent damage to other ancillary services such as communications lines too.

Terrorists, criminals, careless and stubborn people and maniacs are some who could use electromagnetic weaponry. Terrorists attack enemy target to achieve military and political gains, public services to disrupt the normal civilian life and make chaos among the people is common. Criminals may use electromagnetic weapons for personnel rivalries, gang warfare, mafia type attacks, etc. robberies, attacking locks security and alarm systems communication systems, etc. frauds illegal interfering with computer systems for accessing financial statements

secret documents, passwords, etc. The later is more defined in cyber security aspects.

The careless and stubborn people is a person who simply forgets or refuses to turn off a cellular phone or laptop computer radio, or any signal imaging device at critical places becomes a potential terrorist, even if he does not realize that. Therefore, it is essential to educate the public that even normal citizen can be a terrorist who kills hundreds of people due to the carelessness and stubbornness.

The maniacs are ordinary people who have psychological imbalances and instability momentary. Therefore, persons with high knowledge in electromagnetism can destruct, destroy, or even sabotage systems, without any reason, without any particular reason just because they are mentally unstable.

There are numerous sabotaging devices reported recently. A very simple and cheap device can be designed with the microwave oven if one is skillful. Then an electromagnetic weapon can be created. A small inflatable umbrella antenna would give the device an effective 30 dB gain thus it can generate a field of 500 V to 1000 V per meter at a 10 m distance. This is strong enough to up-set most electronics used in banking, security, military, medical and public service control operations.

Impulse generators like TITAN Spectro Super Realtron can be bought from the shelves Ukraine, or most of the former Soviet Union countries. Many other extremely powerful he was generators like for 400,000 V, Russian RADAN, and there

are several others can be bought in the similar manner.

Nowadays, telecommunication towers too can be used as an amplifier to for electromagnetic impulses.

Firstly, are the weak noises such as blenders and most household electrical equipment. These have taken better electromagnetic compatibility measures at the manufacturing stage, compared to 10 years or 15 years ago. Though there are much equipment in this range they are momentary and does not affect the system that much. Next is the RF jammers which is used by police and military. Thirdly are the ultra-wideband emitters, which can disrupt up to some extent, however, when ascended to narrow band, and high-power electromagnetic emitters the damage level increases as well. Finally, the top of the pyramid, are the high-power electromagnetic pulses which are usually generated by exploding nuclear weapons at high altitudes, so it can illuminate a very large area at ground level.

In the latter part of the last century many incidents have been reported. However, in 2004 and 2005 most developed countries blanketed this information from the public as the risk took a crescendo.

In today's world the normal electromagnetic generators can be mounted in drones and fly over critical installations, destroying the electronics. As far as the military is concerned aviation is at the risk of being attacked by IEMI. A landing aircraft would typically be at the height of 100 m at 2 km from the edge of the runway. Therefore, an

adjacent road having normal traffic can impose this threat. An electromagnetic field can be generated by mounting a radiator of reasonable size in the order of few hundred thousand of volts per meter if the source is HPM and few thousand volts per meter if it is UWB. In case the aircraft is not compatible enough to withstand such radiation level, the internal electronic network may fibrillate resulting the collapse of the aircraft. Further consequences will be severed if such happens to the control tower of the airport.

In the present context, an even graver scenario is the illumination of vulnerable positions at ground level with HPM or UWB by a low flying light enemy aircraft or drone. Such an aircraft or drone may carry a sizable radiator and kill many electronics without arousing much alarm in the neighborhood. An air mission that destroys security and alarm systems together with a synchronized ground mission may result a damaged beyond repair to the nation. The main emphasis which needs to be considered is that the attacker can attack multiple times without the victim knowing.

When Germany introduced antilock braking system there was a problem as it interfered with the radio transmitter nearby. It is conclusive that the speeding vehicles can be stopped via electromagnetic interferences.

The effects of the GHz range RF on living beings are available, up to some extent in documented literature in public domain, but such information is not available on the human effect.

A military academia combined research taskforce should be employed to investigate the vulnerability of vital electronic and electrical system to an electromagnetic attack. Consequently, systems should be strengthened in order to withstand a possible undesired electromagnetic illumination. In addition, detectors can be developed, improved or improvised at national level and installed at vital places, which emit warning signals of possible electromagnetic attacks. A team should be appointed to investigate the probability of electromagnetic intrusion to the control systems of public services and be ready to take measures before intolerable threats surface out. The government should also take precautions to protect computer data and software of legal and political importance, which may be prime targets of state terrorists and criminals.

Finally, it is proposed to the KDU in coordination with the Minister of Defense to assign a task force to formulate a mechanism to develop R&D and industry related to IEMI and EMC in Sri Lanka. Further, a task force is to liaise with countries that are in the forefront of research and industrial advancements in the field. The Sri Lanka standard institution is recommended to become at least an O-member at IEC TC 77 that works on electromagnetic compatibility and participates especially at TC 77C. If such regulations and guidelines are in motion it could pave the way to a sound business model that could attract sizable foreign income.

# Towards Net zero: Decarbonising the Construction Industry

Professor Priyan Mendis

*Professor of Civil Engineering, Department of Infrastructure Engineering  
University of Melbourne, Australia*

COP26 climate summit has accelerated the global market push toward reducing emissions from infrastructure projects and operations. Research and innovation are key drivers of a circular economy. Taking a circular economy approach offers the construction industry a major opportunity to deliver decarbonisation targets and whole-life efficiencies. This presentation explored the use of various types of recycled materials, and how they could help to deliver some of those targets especially in the concrete industry. The presenter is a leader in introducing innovative low carbon construction solutions and discussed innovations and challenges in those projects. The use of recycled materials and recovered resources will be included in specifications and therefore will be mandatory in projects in the future. How these materials can be used effectively in construction projects was discussed in the presentation.

The effect of greenhouse gases on the climate is well known. With the increase in global temperatures, the concentration on net zero emissions have gained more prominence. The depletion of the ozone layer, the increased emission of CO<sub>2</sub> and global temperature rise have given us much to think about. For example, Australia has come up with a target of 43% reduction in emissions by 2030. Recent increases in draughts, floods and landslide in Sri Lanka have brought the effects of climate change

much closer to us. Glasgow summit there has been a lot of discussion on working on de-carbonization. The focus here will be on how the construction and demolition industry could contribute towards achieving sustainability goals.

A comparison was made between linear and circular economy. Three principles of circular economy are driven by design. Elimination of waste generation and pollution gets us to de-carbonization. Circulating materials in use at their highest value is design for reuse. Regenerating natural systems eliminated use of natural resources.

Modular construction done in factories is a great way to reduce demolition cost, and waste material in building sites. Section of buildings are constructed in factories and transported at conveniently to be integrated to building sites. The convenience of prefabricated building construction was illustrated with examples of schools, railway stations, and health care facilities.

Emphasizing of the use of recycle waste materials to elevate circular economy it was highlighted that after water, concrete is the most consumed substance in the world. Waste materials are used as filler in construction materials. Concrete is the most consumed substance in the world, at the same time causing immense pollution. One ton of cement produces one ton of Carbon

Dioxide. 8% of the emissions in the world is produced by the cement production process, where limestone is heated to high temperature to produce lime and carbon dioxide as a byproduct.

We are trying use waste material such as tires and glass in a positive way. We seek methods of reusing waste material by taking advantage of the positive properties. For example, rubber which has an increase tensile strength can be used on roads to get rid of shrinkage cracks and temperature cracks. Further we add value to construction materials. For example, insulation properties can be increased by putting tire crumbs. In the Metro project in Australia, glass waste based concrete is used for temporary concrete elements. Further work is carried out in upcycling plastics and using artificial intelligence for waste identification and creating databases and training.

Graphene oxide based Nano modified high performance concrete is currently being research upon. It consumes 20% less cement and less natural aggregates in concrete. Also it has 25% less embodies carbon in concrete while having enhanced properties such as increased compressive strength, tensile strength and abrasion resistance. Vein graphite, which is the purest form of graphite in the world is produced in Sri Lanka. It has a high carbon purity of 99.5% which significantly reduces the manufacturing cost of graphene products. Graphene enables the use of waste materials in concrete by regaining mechanical strength and durability. For the first time in the world, two columns and

slabs were casted using graphene concrete at Design Office of Civil and Structural Engineering Consultants (Pvt) Ltd, Sri Lanka. Blended concrete contains a range of waste material such as graphene oxide, plastic(PHD), rubber, crushed glass, bottom ask, recycled concrete aggregates, textile and hair.

The carbon footprint calculation is a key for any project, in our quest to work towards net zero. Thus the carbon content in concrete will be another parameter which is to be considered, apart from cost and strength, in the choosing the optimum material for a construction. Further work is being carried out in investigating the possibility of introducing paper and textile waste into concrete. These endeavors enhance the properties of the concrete as make a positive impact on the environment in the world.

A couple of few examples were discussed from circular economy. The first was modular construction, where components are dismantled and relocated elsewhere, thereby reducing demolitions and creating versatile connections that can be removed anytime. The second example in circular economy is the use of waste materials in the construction industry, since we are running out of conventional construction materials like sand. Thus we can take care of the environment by using these newer methods and materials in the construction industry

# Achieving Sustainability in Buildings

Eng. Chandana N. Dalugoda

*Managing Partner and Lead Consultant of Chandana Dalugoda Consultants and  
Director of Green Building Council of Sri Lanka (GBCSL)*

“If something can go wrong, it will definitely go wrong.” - The Murphy’s Law. To provide needs for the present, without detracting from the ability to fulfill the needs of the future. In simpler terms, it is required to stop waste and save for future.

Most of the buildings are the culprits of carbon emissions. Reducing carbon footprint of buildings is a very pragmatic way to achieve sustainability. Carbon emissions are twofold, one is operational carbon and the second is embodied carbon. Operational carbon emissions are those associated with the energy used to run the building equipments where as embodied carbon emissions are those associated with the building materials and products including the production, construction, replacement, demolition, disposal items and transportation.

It is important to reduce operational carbon emissions, as much as possible. To achieve this it is important to reduce heat gains. For an example, the latest innovation is AAC blocks (Autoclaved Aerated concrete) which has high thermal resistance. Using high performance glasses against just 16 millimeter normal glasses is another example for taking measures to reduce heat gain. By thermal insulation and painting white, the roofs can reduce the heating inside building.

The equipment which are used inside the buildings needs to comply with the standard ASHRAE 90.1.

To reduce the building energy usage, HVAC equipments complying with ASHARE 90.1 can be selected with minimum efficiency requirement. Also by using the building management systems incorporating energy saving strategies will directly support to reduce building energy usage.

The concept of green with regard of building systems is based on with the awareness and respectfulness towards the nature. It is a design that minimize the negative human impacts on the natural surroundings, materials, resources and processes. The performance of green building is measured using the consumption, atmospheric emission, discharge of harmful liquid effluents, impact on site ecosystem and quality of indoor environment.

Green building of Sri Lanka has a building certification system. Certified rated, silver, gold and platinum. The certified buildings has lower carbon footprint.

Carbon footprint is CO<sub>2</sub> emission per year for electricity. By using Emission Factor (EF) and the electricity usage, it can be calculated. EF is CO<sub>2</sub> mass per unit volume of fuel. Carbon calculations are carried out by

associated professionals of GBCSL, LEED or BREAM.

With the knowledge of the carbon foot print of the building, the owners/ users can

reduce the foot print by taking suitable measures.

## **TECHNICAL SESSION**



# Home Automation Application Using Raspberry Pi 3 and Windows 10 IoT

T Kugaranan<sup>1#</sup>, SK Jaslin<sup>2</sup> and WGCW Kumara<sup>3</sup>

<sup>1</sup>*Department of Electrical and Telecommunication Engineering, Faculty of Engineering, South Eastern University, Sri Lanka.*

<sup>2</sup>*Department of Electrical and Electronics Engineering, Faculty of Engineering, University of Peradeniya, Sri Lanka.*

<sup>3</sup>*Department of Computer Science Engineering, Faculty of Engineering, South Eastern University, Sri Lanka.*

#tkugaranan@seu.ac.lk

**Abstract:** In the present situation demand for electricity stack, up with population growth is one of the major challenges all over the world. Inadequate amounts of electricity create an awareness to conserve energy in all viable methods. As a result, we made an appliance to minimize the energy wastage by the concern of Smart Home. Home automation refers to controlling home appliances and domestic features by local networking or remote control. The devices' respective apps in smart homes allow users to track energy usage over time. They can also get an estimate of how much they are paying for whatever they have plugged in. By and by this will have an impact on consumer behaviour and will help people to be more energy conscious and, in the long run, responsible. Apart from that, the current commercial home automation systems are general and have not to consist specific designed for the Sri Lankan contest. So, we designed a smart home automation system with the sense of Sri Lankan electricity tariffs and practices. This scheme involves the design and construction of individual control home appliances using Raspberry Pi 3, Arduino, and Windows 10 IoT core. This combination can implement the primary home automation functions by using numerous sensors, with that it will deliver suggestions and illustrate the process of the electricity tariff system to the users. With this

attempt, the consumer can reach optimum power consumption.

**Keywords:** *Raspberry Pi, Arduino, Smart Home Automation, Power Measurement, IoT*

## 1. Introduction

The Ceylon Electricity Board is the largest electricity company in Sri Lanka. With a market share of nearly 100%, it controls all major functions of electricity generation, transmission, distribution, and retailing in Sri Lanka. It is one of the only two on-grid electricity companies in the country; the other being Lanka Electricity Company. One of the major problems in Ceylon Electricity Board (CEB) is producing higher demand electricity with allocated funds. The financial crisis of CEB is not only a problem for the CEB but also a problem for the development of the country. For example, due to the financial crisis, CEB is keeping a non-payment of Rs.35 billion (On the date of Sep 29, 2017) to Ceylon Petroleum Corporation. Lack of knowledge among consumers about their electricity tariff system is the major reason for the problem. The end solution is a simple single device that can act as smart home automation as well as assist and give suggestions to the users to optimize their power consumption to reduce their electricity tariff. On the other hand, it supports a lot to the

CEB to overcome their financial crisis, so better for the development of the country.

Generally, the benefits of the Smart home project are by no means limited to convenience, although this is a compelling feature. Smart homes also have the potential to be greener and cheaper. This program is to optimize energy consumption and reduce our electricity bills. And, this technology offers the prospect of significant improvements in living standards.

Application of the Home automation system is moving at the rate of high, they are used to grand comfort, convenience, high quality of life, and smart security for householders. At present days, many home automation systems are used to provide support to elderly and disabled people and they eliminate the manpower in the production of services and goods [1-2]. The Home automation system can be designed and created by using a single controller which has the strength to curb and monitor different interconnected appliances such as power plugs, lights, temperature and humidity sensors, smoke, gas, and fire detectors as well as emergency and security systems [3].

The best superiority of a home automation system is it can be controlled and managed easily from an array of devices such as smartphones, tablets, desktops, and laptops [4]. The rapid growth of wireless technologies influences us to use smartphones to remotely control and monitor home appliances around the world [5-6]. Many home automation systems use them automatically connect with a wireless handset communication technology, such as Bluetooth [7], GSM [8], ZigBee [9], Wi-Fi [10], and EnOcean [11]. Smartphone sequential network communication application errand users can modify their system settings and personal equipment. Different types of home automation systems provide a wide range of services and services, some typical functions include instrument control, temperature control, Remote lighting, video surveillance, monitoring

of a re-view camera, and a real-time text warning.

All the power consumers can be potential customers due to the home automation and remote controlling feature. But to fully utilize the whole system with the power assistance and suggestion feature, the power consumers who fall under the domestic user section and who consume more than 60 units per month in Sri Lanka.

Home automation is very common nowadays, but it can only perform home automation and remote control. There is no knowledge-building or awareness-raising process for the home automation, so we have developed a system called Smart Home Application which can perform the basic operations of home automation as well as creates awareness of Sri Lanka's electricity system and how can we utilize the electricity system effectively. The project Smart Home Automation Application helps the end-users to identify their power consumption pattern and from that, they can optimize their power usage.

Features of the Smart Home Electricity Assistant are as follows.

- Electrical appliances can be controlled via a dedicated display panel.
- Electrical appliances can be controlled remotely using smartphones and tablets.
- The power consumption of each appliance can be monitored.
- The status of a room such as Temperature, Light intensity, and Presence of humans can be observed.
- The home lighting system can be controlled automatically with room light intensity and the presence of humans.

- Automatic switching between fan and air-conditioner concerning room temperature.
- Sri Lanka's electricity tariff system and ideal power-saving tips in the contest of Sri Lanka can be observed in the information tab, from which the consumer can perform some demand-side management and he can reduce his tariff.

The rest of the paper explained related work, the proposed method, and results and discussion.

## 2. Related Work

### A. Evolution of home automation application

The idea of home automation is not a recent concept anyhow it has been more of a case of technology catching up with the idea. It all started with the wireless remote control, which was first unveiled by Nikola Tesla in 1898 when he controlled a miniature boat by sending it radio waves. The 20th century started with the boom in home appliances such as the engine-powered vacuum cleaner in 1901 and the electric-powered vacuum 6 years later.

The idea of home automation was flirted with in the 1930s but it wasn't until 1966 Jim Sutherland developed the first home automation system "Echo IV" which would make a shopping list, control temperature, turn appliances on and off but this was never commercially sold. 1969 saw the Honeywell Kitchen Computer which was a commuter that would create recipes, although this had no commercial success due to the price. The microprocessor came in 1971 and this meant a rapid price fall in electronics, which meant technologies become more accessible to everyone. The term Smart Home was first coined by the American Association of house builders in 1984. Through the 1990's there was a new focus on combining gerontology which technology to help improve the lives of the elderly and less able. Gradually as technology became more

affordable, these technologies slowly become integrated into our homes. Along this, we take the smart home a step forward with the Internet of Things (IoT) and assistive.

### B. Existing Work

The application has been developed based on the android system [2]. An interface card has been developed to assure communication between the remote user, server, raspberry pi card, and the home Appliances. The application has been installed on an Android Smartphone, a web server, and a raspberry pi card to control the shutter of windows. Android application on a smartphone issue command to raspberry pi card. An interface card has been realized to update signals between the actuator sensors and the raspberry pi card. A smart home based on Raspberry Pi, Arduino, and Windows IoT has been proposed [3]. The Project offers a Windows application for operating several devices from a single device remotely where users can control lights, fans, the temperature of heaters, the speed of the fan, and switches from one place. In the case of lights, the system will turn on the lights if the motion sensor is active and natural light is below the required density. Similarly, fan speed is automatically controlled based on room temperature. Shih-Pang Tseng et al. [4] proposed Smart House Monitor & Manager (SHMM), based on the ZigBee, all sensors and actuators are connected by a ZigBee wireless network. They designed a simple smart socket, which can be remote controlled via ZigBee. PC host is used as a data collector and motion sensing, all sensing data are transferred to the VM in the cloud. The user can use the PC or Android phone to monitor or control through the Internet to power-saving the house.

Arduino microcontroller to receive user commands to execute through an Ethernet shield. This house organize framework utilized together both wireless ZigBee and wired X10 advancements [5]. This system followed smart task scheduling with a heuristic for the

Resource-constrained- scheduling problem (RCPSP). The mobile device can be either wired to the central controller through a USB cable or communicated with it wirelessly, within the scope of the home. Arduino contains the web server application that communicates through the HTTP protocol with a Web-based Android application. The system is highly flexible and scalable and expandable. PIC16F887 microcontroller for home appliances controls with GSM for control of the appliances [6]. It has high availability, coverage, and security but the cost of SMS. AT commands can be sent through the GSM network to control the home devices. The system does not have any state information related to the devices and expects the user to keep track of it.

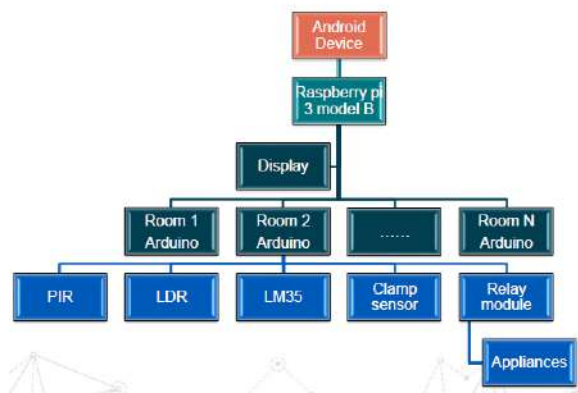


Figure 1. Block diagram of Home

### 3. Proposed Method

As shown in Figure 1, Raspberry Pi 3 Model B was used as the main master device. The Raspberry Pi 3 is running on Windows 10 IoT core. The Raspberry Pi 3 controls and monitors all slave devices that are Arduino UNOs through the I2C bus protocol. Raspberry Pi 3 has Wi-Fi and Bluetooth connectivity compare with other microprocessors. Also, it has a very big performance boost and 1.2 GHz quad core processor.

Each Arduino UNO controls one room. Arduino UNO collects all the sensor data and its device's statuses, then it just sends the data to the master device which controls everything. In the case of wireless device connectivity, an Arduino Pro Mini is used to manage the wireless devices. NRF24L01+ module is used to create the 2.4 GHz wireless channel. Users can interface with the system via the dedicated display at the master device or from their smart mobile devices which have Wi-Fi connectivity. The wireless unit was designed such that users can just plug in and use it. The automation process of lights and fans was assigned to the slave device Arduino UNO to reduce the load on the master device Raspberry Pi. The controlling software and the GUI platforms were designed using C#.

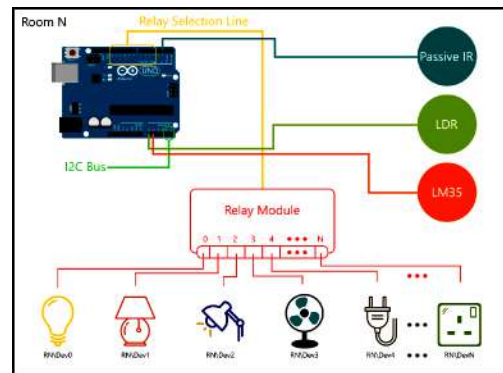


Figure 2. Block diagram of Room

Extensible Application Markup Language (XAML) was used to create the GUI for the application and the application was developed using C# because the Windows 10 IoT core is the best suited with C#. Microsoft Visual Studio 2017 was used as Integrated Development Environment (IDE) for the application. This IDE was selected because the targeted OS platform and the IDE both were from the same developer Microsoft, so it has greater debugging options and compatibilities.

Figure 2 elaborate how sensors and relay module are connected with Arduino. One relay

module can connect several devices. The main reasons for selecting particular types of components are given in Table 1.

Table 1. Used components and properties

Type of component	Properties
Raspberry Pi 3 Model B	Processor Broadcom BCM2387 chipset, Operating system Windows 10 IoT Cortex-A53, Inbuilt wireless connectivity, Memory 1 GB, 1.2GHz Quad-Core ARM
Arduino UNO (Atmega328 microcontroller)	Clock speed 16 MHz, Flash memory 32 kB, SRAM 2 kB, EEPROM 1 kB
DS1820 Temperature sensor	Accuracy $\pm 0.5$ °C from -10 to 85 °C
PIR HC-SR501 Motion sensor	Sensitivity up to 7 m, Beam angle 120°
LDR sensor	Sensitivity 3 ms
Clamp sensor SCT 013-030	Opening size: 13mm*13mm, Non-linearity $\pm 3\%$ (10%—120% of rated input current)
NRF24L01+ module	Maximum data rate 2 Mbps, 125 RF channel operation, True single-chip GFSK transceiver

The current transformer (clamp sensor) and voltage transformer method was used to measure current and voltage because this is a

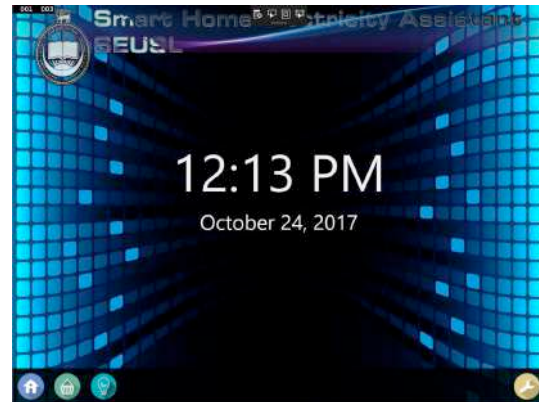
non-invasive method. Here the measuring circuit does not electrically connect with the working circuit, so isolation protection is ensured.

### C. Communications Protocols

Three types of communication protocols were used in this project which are I<sup>2</sup>C, SPI, and 1-wire.

I<sup>2</sup>C – I<sup>2</sup>C (communication is used between Raspberry Pi 3 and Arduino UNO) stands for Inter-Integrated Circuit, which is a synchronous serial interface useful for communicating with other peripheral devices. Multi-master configuration is also possible. SCL and SDA are the basic ports of I<sup>2</sup>C. SCL (Serial Clock Line) is used to transmit clock signals, and SDA (Serial Data Adapter) is used to send data.

SPI – SPI stands for Serial Peripheral Interface, which is a synchronous protocol that allows only



one master device to initiate communication with slave devices. SCK, MOSI, and MISO are the basic ports of SPI. As this is a synchronous protocol a clock signal is needed, this signal is fed through SCK. MOSI (Master Out Slave In) is used to send data by the master. MISO (Master in Slave Out) is used to get the data from the slave.

1-wire – 1-Wire bus uses only one wire for signaling and power. Communication is asynchronous and half-duplex, and it follows a strict master/slave scheme. One or several slave devices can be connected to the bus at the same time. Only one master should be connected to the

bus. The bus is idle high, so there must be a pull-up resistor present.

There is no theoretical limitation in the number of connectable devices with the above protocols. Mainly the physical limitation is the factor that governs the maximum connectable number of devices. The physical limitations are the length of the bus, capacitive loads on the bus, Electrical drive type, and Speed of the data in the bus. So practically the limitation of the number of devices is 1008, 125, and 32 respectively. I<sup>2</sup>C allows asynchronous and needs less wire for communication, so this protocol was used between Raspberry Pi 3 and Arduino UNO. The 8-bit address was used so 255 rooms can be connected to one master device. I<sup>2</sup>C is not well defined for wireless communications at the same time the radio module that we used (NRF24L01+) is designed for SPI protocol, so the SPI protocol was used between Arduino UNO and Arduino Pro mini. A maximum of 125 wireless units can be connected. 1-wire protocol was used to connect the digital temperature sensor with the Arduino UNO.

#### D. Graphical User Interface (GUI) Design

The GUI has consisted of four tabs those are home tab, the Room tab, the Information tab, and the Configuration tab.



(a)



(b)

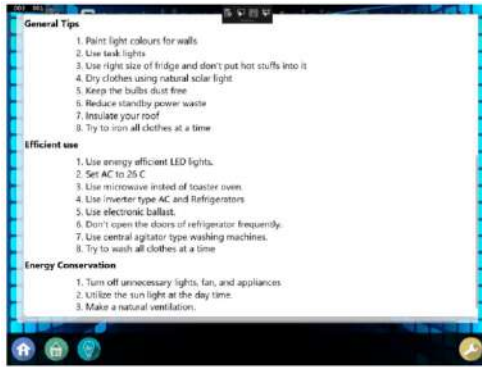


(c)

Units (kWh)	Unit Charge (Rs./kWh)	Fixed Charge (Rs./month)
If consumption is less than 60 units/month		
0-30	2.50	30.00
31-60	4.85	60.00
If consumption is higher than 60 units/month		
0-60	7.85	-----
61-90	10.00	90.00
91-120	27.75	480.00
121-150	32.00	490.00
>150	45.00	540.00
If consumption is based on Time of Use		
Peak (18:30-22:30)	54.00	540.00
Day (6:30-18:30)	25.00	540.00
Off-peak (22:30-05:30)	13.00	540.00

**Power Saving Tips**  
General Tips  
1. Paint light colours for walls.

(d)



(e)



(f)

Figure 3. Smart device application tabs. (a) Home, (b) Room, (c) Inside room window, (d) Information, (e) Tips, (f) Configurations.

As shown in Figure 3, the room tab (c) can show the all rooms (Living Room and Kitchen) which have been set in the configuration tab. The living room was set with one bulb and a fan. The human detection state, light intensity, room temperature, and power consumption can be seen from the left side of the window respectively. Here all the values have been shown as zero because this GUI was not connected with the Raspberry Pi3 when the photo was taken.

The Sri Lankan electricity tariff system for domestic consumers, as well as the Time of Use (ToU) system, have been shown in the upper

portion of the information tab (d). The lower part carries some tips to reduce and save energy (e). Finally, the configuration tab has the choice of connected devices inside the room (f).

#### 4. Results and Discussion

This topic briefly discusses the clamp sensor sensitivity test, Wi-Fi module range measurements, temperature accuracy test Voltage calibration, and limitations of this project.

##### A. Clamp sensor sensitivity test

In this sensitivity test, an Incandescent lamp, CFL lamp, Bouth, Phone charger, and Glue gun were selected and the current through them was measured using a multimeter and using home automation application (proposed system). The readings are shown below in Table 2.

Table 2. Comparison between the digital multimeter and proposed system reading

Device	Multimeter reading (A)	Proposed system reading (A)	Error (%)
Incandescent lamp (100W)	0.440	0.435	1.1
CFL lamp (23 W)	0.100	0.098	2.0
Bouth (30W)	0.090	0.078	6.0
Phone charger	0.050	0.048	4.0
Glue gun	0.250	0.239	4.4

According to the clamp sensor sensitivity test results, we found that the error is too small and it can be negligible in the proposed system.

##### B. Wi-Fi range measurements

The NRF24L01 module works with the help of SPI communications. These modules can either

be used with a 3.3 V microcontroller or a 5 V microcontroller but they should have an SPI port.

NRF Wi-Fi Module was tested in normal condition, with the cover condition, and with cover and walls ranges were measured. The readings are shown in Table 3.

Table 3. NRF Wi-Fi module range results

Normal condition (m)	With cover condition (m)	With cover and walls (m)
40.8	36	5.2

According to the specification in the datasheet, the NRF Wi-Fi module can work maximum range is nearly 60 m. But, using covers and obstacles it can work up to 5.2 m.

#### C. Temperature accuracy test

The temperature was measured using the proposed application and phone sensor. For the comparison, online weather reading was used. The results are shown in Table 4.

Table 4. Temperature accuracy test results

Application (°C)	Phone sensor (°C)	Online weather (°C)
31.19	31.18	31

Here proposed application temperature reading is more accurate than other readings.

#### D. Voltage Calibration

Voltage calibration for the system was done to get accurate readings. Initially, the voltage at a particular point was measured by a TM-87 digital multimeter. The voltage reading of the multimeter is 222 V. Then, again the voltage was measured in our system. Finally, the error between the multimeter and our system was reduced by setting the calibrating resistor. To

obtain 222 V in transformer 47 kΩ variable resistor was used.

#### E. Limitations

The advantages of smart home systems are easy to understand and user-friendly, but at the same time, there is a drawback in the learning curve for most people. For anyone already immersed in technology, converting it will be a breeze, but for anyone not so tech-savvy, it makes for a lot of time spent to understand. The IoT is a diverse and complex network. Any failure or bugs in the software or hardware will have serious consequences. Even power failure can cause a lot of inconveniences.

Delay functions in the Arduino programming were used, because of excess use of delay function the I2C communication between Raspberry Pi 3 and Arduino became utterly slow. The need for the excess delay function came up due to the greater number of sensors and automation processes. Also took too much time for automation processes. As a solution, we implemented jump instruction and we removed delay functions, so the delaying process occurred when only necessary not for all executions. So, the communication became high.

Less reading resolution: The maximum value of the LM35 is 1V, but the internal ADC uses 5V as a reference, so 80% of the ADC was wasted. So, we manually set the reference voltage as 1.1V. So, we can optimize the whole resolution.

## 5. Conclusion

Recently, the home automation market is a very promising field that is growing very fast and needs a vast range of developments that can be carried out in the concept of the smart home. In this project, the main concept of the system is to perform the basic home automation function by using numerous sensors. The system mainly consists of control of the home appliances, reducing energy consumption, and providing awareness. Using the system public can obtain a



piece of knowledge regarding the Sri Lankan tariff system. At the same time, it will motivate them to use an adequate amount of electricity without wastage. Since this system is introduced for the home appliances it can work 100% efficiency when it uses in 230V appliances.

Finally, the system helps to produce the optimum amount of electricity in Sri Lanka. In the future, a new tab window can be added for CEB, where CEB can directly communicate and share information with consumers and CEB can get the power usage of the consumers directly without visiting personally.

### References

"Annual report 2017 | CEB." [Online]. Available: <https://report-2017.coebank.org/en/>. [Accessed: 19-Dec-2019].

Hayet Lamine and Hafedh Abid, "Remote control of domestic equipment from an Android application based on Raspberry pi card", IEEE transaction 15th international conference on Sciences and Techniques of Automatic control & computer engineering -STA'2014, Hammamet, Tunisia, December 21-23, 2014.

B. S. Rao, S. D. V. Prasad, and R. M. Mohan, "A prototype for Home Automation using GSM technology," in Power, Control and Embedded Systems (ICPCES), 2010 International Conference on, 2010, pp. 1-4.

The Journal of the Korea institute of electronic communication sciences, vol. 10, no. 10, pp. 1139- 1144, 2015.

Y. Zhai and X. Cheng, "Design of smart home remote monitoring system based on embedded system," in Computing, Control and Industrial Engineering (CCIE), 2011 IEEE 2nd International Conference on, 2011, vol. 2, pp. 41-44.

S.-P. Tseng, B.-R. Li, J.-L. Pan, and C.-J. Lin, "An application of Internet of things with motion-sensing on smart house," in Orange Technologies (ICOT), 2014 IEEE International Conference on, 2014, pp. 65-68.

C. Severance, "Eben Upton: Raspberry pi," Computer, no. 10, pp. 14-16, 2013.

C. W. Zhao, J. Jegatheesan, and S. C. Loon, "Exploring IoT application using raspberry pi," International Journal of Computer Networks and Applications, vol. 2, no. 1, pp. 27-34, 2015.

C.-Y. Chen, Y.-P. Tsoul, S.-C. Liao, and C.-T. Lin, "Implementing the design of the smart home and achieving energy conservation," in Industrial Informatics, 2009. INDIN 2009. 7th IEEE International Conference on, 2009, pp. 273-276.

B. Li, P. Hathaipontaluk, and S. Luo, "Intelligent oven in the smart home environment," in Research Challenges in Computer Science, 2009. IRCCS 09. International Conference on, 2009, pp. 247-250.

<https://zeusintegrated.com/blog/item/a-brief-history-of-smart-home-automation>. [Accessed: 20-Dec-2019].

K. Baraka, M. Ghobril, S. Malek, R. Kanj, and A. Kayssi, "Low-cost Arduino/android-based energy-efficient home automation system with smart task scheduling," in Computational Intelligence, Communication Systems and Networks (CICSyN), 2013 Fifth International Conference on, 2013, pp. 296-301.

N. Noury, G. Varone, P. Barralon, J. Ye, V. Rialle, and J. Demongeot, "New trends in health smart homes," in enterprise networking and computing in the healthcare industry, 2003. Healthcom 2003. Proceedings. 5th international workshop on, 2003, pp. 118-127.

M. Narender and M. Vijayalakshmi, "Raspberry Pi based advanced scheduled home automation system through E-mail," in Computational Intelligence and Computing Research (ICCIC), 2014 IEEE International Conference on, 2014, pp. 1-4.

S. Jain, A. Vaibhav, and L. Goyal, "Raspberry Pi based interactive home automation system through E-mail," in Optimization, Reliability, and

Information Technology (ICROIT), 2014 International Conference on, 2014, pp. 277–280.

H. H. Hadwin and Y. P. Reddy, “Smart Home Control by using Raspberry PI and Arduino UNO,” International Journal of Advanced Research in Computer and Communication Engineering, vol. 5, no. 4, pp. 2278–1021, 2016.

L. Jiang, D.-Y. Liu, and B. Yang, “Smart home research,” in Machine Learning and Cybernetics, 2004. Proceedings of 2004 International Conference on 2004, vol. 2, pp. 659–663.

M. E. Morris et al., “Smart-home technologies to assist older people to live well at home,” Journal of aging science, vol. 1, no. 1, pp. 1–9, 2013.

S. Khedkar and G. M. Malwatkar, “Using raspberry Pi and GSM survey on home automation,” in Electrical, Electronics, and Optimization Techniques (ICEEOT), International Conference on, 2016, pp. 758–761

# Intelligent Battery Control Mechanism for Electric Bicycles

UVH Sameera<sup>1#</sup>, KLATM Ranasinghe<sup>1</sup>, RMPMD Rajapaksha<sup>1</sup>, GMSM Gaspe<sup>1</sup>, WSM Melvin<sup>2</sup>

<sup>1</sup>*Department of Mechanical Engineering, General Sir John Kotelawala defence University, Sri Lanka*

<sup>2</sup>*Research and Innovation Center, Sri Lanka*

#sameerauvh@gmail.com

**Abstract:** Transportation is a basic requirement of humans. Currently, fossil fuels are the main source used in automobiles and the trend is moving towards electric vehicles which is more environmentally friendly. Battery is one of the main components in an electric vehicle. This paper aims to introduce an intelligent battery control system which integrates a dual battery mechanism and four riding modes. Two lithium-ion battery packs with 48V and 16AH each are used. Full electric, pedal assist, neutral and continuous charging are the four driving modes. The pedal assist mode is implemented with new Control mechanism and continuous charging is a new concept to E-bicycles. An alternator is used as an energy harvesting mechanism. The state of charge of each battery pack are automatically detected and pack with lower state of charge is assigned to store the energy harvested from regenerative mechanism. The battery pack with higher state of charge is allotted to drive the bicycle. System will automatically interchange the role of each pack when the driving pack reaches to its acceptable minimum state of charge. Proposed system will allow both battery packs to charge or discharge within its full nominal range which is not linear. Thus, that allows an increase in per charge travelling distance. The inter connection between subpacks are controls through a relay panel based on voltage readings. Finally, the bicycle was subjected to road trials under three drivers with different weights. Proposed system helps to cover 41.6km under electric mode and covers 49.4km in pedal assist mode. Bicycle needs to

cover 61km in continuous charging mode to fully charge the battery.

**Keywords:** *E-bicycle, Dual-Battery Mechanism, Driving modes.*

## 1. Introduction

Transportation is a basic requirement of people in the present. Almost every family in urban areas has their own vehicle. But, due to lack of space in houses, there's a tendency of increase in usage of smaller size vehicles in the world and as well as in Sri Lanka. Among small size vehicles, two wheelers have become more famous due to several reasons. Affordable price, less parking space, low maintenance, easy to ride are some of those. Nowadays there is a trend in people to move towards E vehicles. But E-bikes or electric bicycles are not a new trend, it has been around for decades. An electric bike is a regular bike with the addition of an electrical drive system. This consists of a battery, a motor, a way to integrate the motor's power into the drivetrain, and a way to control that power. (Krung, 2019) E-bicycles also have limitations like, per charge travelling distance, top speed, battery life span, charging time etc. Among those, this research is focusing on increasing the per charge travelling distance through integrated mechanism of dual battery mechanism with four driving modes. Through the research conducted by Lijun and the team on "Dynamic Lithium-Ion Battery Model for System Simulations" it was observed that the Charging and discharging of Lithium-ion cells are not linear. Figure 1 shows the

experimental (Dark line) and simulated (Lighter line) results of above research. It can be observed that the discharge rate at the beginning is low. In the charging cycle also the initial charge rate is lower, which means charging and discharging curves does not coincide. The proposed system allows the batteries to charge and discharge through its full cycles without overlapping. Usually, lithium-ion cells are not discharged up to 0V level. It is also demonstrated through below Figure 1. (Gao , et al., 2002)

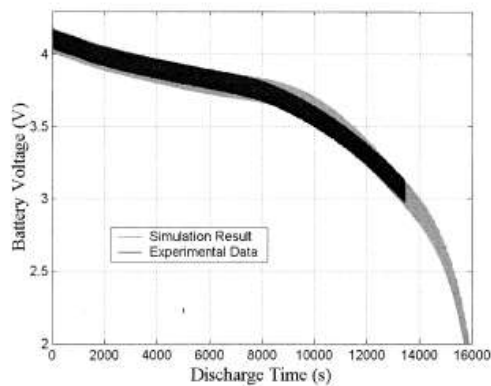


Figure 1. Simulated & Experimented results of 18650 Lithium-ion cell discharge cycle.

Source: (Gao , et al., 2002)

## 2. Methodology

Online research based on research, leading brands and local market research was carried out to collect data on electric bicycles, battery charging mechanisms, energy harvesting mechanisms, rechargeable cell chemistry and geometry, battery management systems, bicycle chassis simulation methods, bicycle motor controllers, and driving modes. Based on the collected data, design consideration was one of existing techniques and methods to make this research distinctive. Based on results of the design consideration, conceptual designs were done. Calculations, 3D modelling, Material selection and design simulations were carried out simultaneously as shown in the Figure 2.

Calculations were carried out to select the motor and the controller. Some modifications were done in calculations and selected 3D model based on the simulations and available components and materials. The finalized design was fabricated in a workshop. Then the prototype was subjected to road trials. A mobile app was used to take track the route, the distance travelled and to measure the top speed. Voltage readings were noted, and results were evaluated.

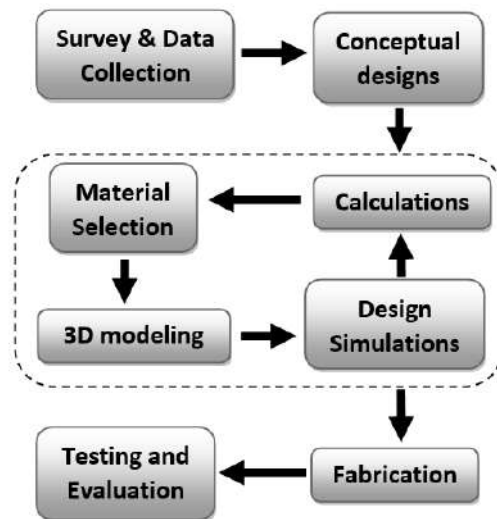


Figure 2. Methodology of the research.

Source: Designed by authors.

## 3. Design, Simulation and Testing

### A. Battery Pack and Control Circuit

One of the most important parts of an electric bicycle is the battery pack. It is because the performance of the bicycle dependent on it. Currently, Variable Regulated Lead Acid Battery (VRLA), Nickel Cadmium (NiCd), Carbon Zinc (C-Zn), Lithium Ion (Li-Ion), Lithium polymer (LiPo) are some of the cell types available in the industry. When selecting a suitable battery type for an electric vehicle, Energy Density (Wh/kg), Specific Energy (Wh/l), Power Density (kW/kg), Charging and Discharging timing, life cycles and eco friendliness like specifications were considered. The Table 1 shows a summary of

properties of each cell type according to the research done by Ashish. (Ashish, et al., 2016)

Based on data in Table 1 it could be observed that Li-ion has higher specific energy that only seconds to Li-Po. Also, Li-

Table 1. Properties of cells used in Electric Vehicles.

PROPERTIES	VRLA	C-Zn	NiMH	NiCd	Li-ion	Li-Po
Specific Energy (Wh/Kg)	33-42	36	60-80	40-60	90-133	150-260
Specific Energy Density(Wh/l)	60-110	92	140-300	50-150	250-676	250-730
Specific Power (W/Kg)	180	10-27	250-1000	150	250-340	300-350
Life Cycles	500-800	N/A	500-2000	2000	400-1200	600-800
Cost Of Development(US\$/kWh)	150	90-110	250-300	300	250	N/A
Charge-Discharge Efficiency (%)	50-95	50-60	66	70-90	80-90	80-95

Source: (Ashish, et al., 2016)

ion has a comparatively higher specific power and charge discharge efficiency. According to the report “Design and Analysis of a Battery for a Formula Electric Car” done by Samuel Reineman, MIT, has mentioned that “getting maximum energy and power from lowest mass possible is a main factor when choosing a proper power source for an EV. The acceleration is depending on the power and travelling distance is depending on the energy is important. To get high energy and high power from low mass, cells with higher specific energy (Wh/kg) and higher specific power (W/kg) are suitable.” (Reineman, 2013). Figure 3 shows the comparison between specific power and specific energy. Lithium-ion cells shows more prominent features among cell types.

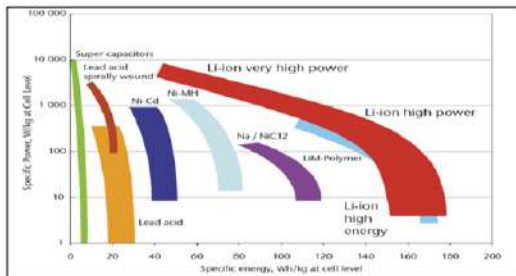


Figure 3. Cell Comparison (Specific Power vs. Specific Energy).

Source: (Reineman, 2013)

Among the lithium iron cells with different geometrical shapes, 18650 cells were chosen because of its flexibility in designing a custom shaped battery pack. Motor selection was done considering the acceleration force, rolling resistance, grade resistance, and air drag. Based on the calculations, required motor was 48V 500W BLCD motor. Thus, the battery pack was designed in 48V and 16 Ah to achieve the maximum per-charge distance. Based on following equations, a model was developed to calculate the number of cells required.

Calculation consideration,

- Expected Nominal Battery pack voltage = 48V
- Battery cell Nominal voltage = 3.7V
- Battery Cell Capacity = 2.2Ah
- Peak C-rate of a cell = 2C
- Continues C-rate of a cell = 1C
- Average Energy Consumption per km = 12whkm<sup>-1</sup>
- Per charge distance = 35km

$$(E_{bc}) = (C_{bc}) \times (U_{bc}) \dots \dots \dots (1)$$

$$(E_{bp}) = (E_{Avg}) \times (D_v) \dots \dots \dots (2)$$

$$(N_{cs}) = ((U_{bp}) / ((U_{bc})) \dots \dots \dots (3)$$

$$(E_{bs}) = [(N)_{cs}] \times [(E)_{bc}] \dots \dots \dots (4)$$

$$(N_{sb}) = ([(E)_{bp}]) / ([(E)_{bs}]) \dots\dots\dots (5)$$

$$(C_{bp}) = [(N)_{sb}] \times (C_{bc}) \dots\dots\dots (6)$$

$$(N_{cb}) = (N_{sb}) \times (N_{cs}) \dots\dots\dots (7)$$

$$(I_{spc}) = [(C)_{rate bcp}] \times (C_{bc}) \dots\dots\dots (8)$$

$$(I_{bpp}) = (I_{spc}) \times (N_{sb}) \dots\dots\dots (9)$$

$$(P_{bpp}) = [(I)_{bpp}] \times (U_{bp}) \dots\dots\dots (10)$$

$$(I_{scc}) = [(C)_{rate bcc}] \times (C_{bc}) \dots\dots\dots (11)$$

$$(I_{bpc}) = (I_{scc}) \times (N_{sb}) \dots\dots\dots (12)$$

$$(P_{bpc}) = (I_{bpc}) \times (U_{bp}) \dots\dots\dots (13)$$

- Battery Cell Energy =  $E_{bc}$
- Battery cell Capacity =  $C_{bc}$
- Battery cell voltage =  $U_{bc}$
- Battery Pack total Energy =  $E_{bp}$
- Average Energy consumption =  $E_{Avg}$
- Vehicle range =  $D_v$
- No of cells connecting in series =  $N_{cs}$
- Nominal battery pack voltage =  $U_{bp}$
- Energy content in of a series string =  $E_{bs}$
- Required no of Strings =  $N_{sb}$
- Battery pack Capacity =  $C_{bp}$
- No of cells of the pack =  $N_{cb}$
- String peak current =  $I_{spc}$
- Peak C - rate of a cell =  $C_{rate bcp}$
- Pack peak current =  $I_{bpp}$
- Pack peak Power =  $P_{bpp}$

- String continuous current =  $I_{scc}$
- Continuous C-rate of a cell =  $C_{rate bcc}$
- Pack continuous current =  $I_{bpc}$
- Pack continuous Power =  $P_{bpc}$

Based on the calculations 192 cells were needed for the battery pack. As the space available in the bicycle is limited, a custom shaped battery pack was modelled using Solidworks. Then the batteries used in the project was subjected to internal resistance test and capacity test. The sub battery packs were spot welded and kept for top balancing before connected to BMS's. Through internal resistance test it is checked whether the batteries discharge themselves. For capacity test, 18650 battery discharger is used where batteries are discharged under a constant current through a resistor. The Final voltage of the battery pack was 48V and capacity was about 16mAh.

Nickel plates are used to spot weld the battery connections in sub-battery packs as shown in Figure 4. For each sub battery pack, a BMS and a voltage sensor is connected. Eight BMS units were connected to the 16-relay panel through higher gauge wires as it switches supply with higher amperages.

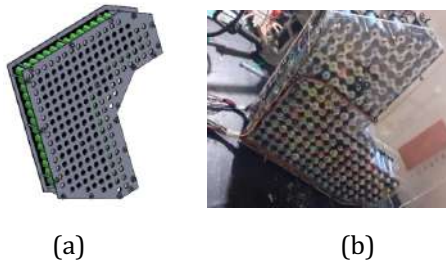


Figure 4. (a) 3D model (b) Fabricated battery pack

Source: Designed by authors.

Battery switching circuit monitor the voltages of each battery pack and battery with higher voltage is assigned to drive bicycle and other pack is used to store the energy harvested from the bicycle. The circuit is automatically switching the role of each battery pack when the driving pack reaches its accepted minimum discharge limit. Proposed circuit is allowing each battery pack to charge or discharge within its full range. As the battery pack is 48V, the supply from alternator (13.5) (Energy Harvesting Mechanism) needs to be converted to 48V using DC-DC converter which would limit the maximum current supplied to the battery pack. Thus, that could result in increase in charging time. As a solution, each battery pack was again divided into four 12V sub-battery packs to charge directly from alternator. To interchange the connectivity between 12V packs to obtain 48V when discharging and 12V when charging, a relay circuit is introduced. Relay circuit was designed and simulated through Proteus software, and it was optimized to 16 relays. Figure 5 shows the block diagram of battery switching circuit.

### B. Driving Modes and Control circuit

There are many different types of electric bikes with different ways of activating the electric assist. According to the way which the electric bike use the electric assist E bike have their modes. For that they use different throttle types (twist grip, thumb, push button), pedal assist

types (torque sensor and cadence sensor) and user can choose different modes by those. In this model, four driving modes as Electric, Pedal assist, Neutral and continuous charging are introduced. Engagement of motor and the alternator is different in each mode.

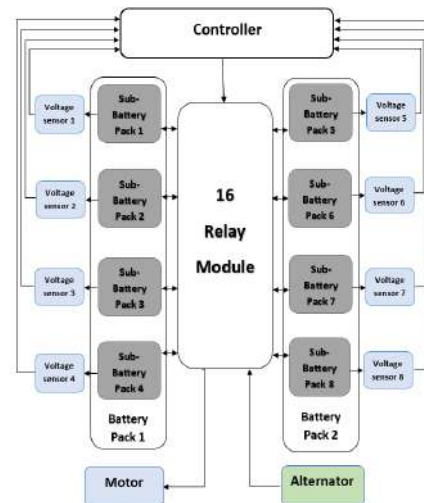


Figure 5. Battery switching circuit.

Source: Designed by authors.

The Electric mode is similar to how a motorcycle or scooter operates. When the throttle is engaged the motor provides power and propels you and the bike forward. A throttle allows you to just kick back and enjoy a “free” ride. According to “Electric Bike Modes: Throttle vs. Pedal Assist” (Zhu, 2018), “A lot of E-Bicycles in the US have bike is not allowed; only pedal assist”. “Twist Throttle”, “Thumb Throttle” and “push button throttle” are currently available in Electric bicycles as throttle options. In this E-Bicycle, the Twist throttle type is used. Thus, there will be no connection between paddling and the motor. Motor will only consider the input from throttle and act accordingly.

Pedal assist is another mode that provides power only when you are peddling. The pedal assist mode will generally give you more range when compared to the throttle mode. With the development in E-bicycle field, different types of sensors like torque sensors, speed sensors and

cadence sensors are being used to take the input for assist mode. In this model, an IR sensor is used with encoder wheel which is with 96mm diameter and 80 pulse per turn for the speed sensor. To detect the peddling effort/speed, following equations were used to calculate the peddling velocity via Encoder IR Sensor Module shown in Figure 6.

$$rpm = ((60 \times 1000)/(pulses \text{ per turn})) \quad (14)$$

$$velocity (kmph) = ((rpm) \times \pi \times (d) \times 60)/1000000 \quad (15)$$

Based on the calculated velocity, scaled pulse is given to the motor controller to drive the motor. A separate relay is used to bypass the throttle signal and connect scaled pulse from controller when pedal assist mode is actuated.

Continuous Charging is the next driving mode which is introduced in this model. This mode is also actuated by rider preference. The energy harvesting mechanism, or the alternator is continuously engaged to the drive strain to charge the batteries. The alternator engaging and disengaging mechanism briefly engaged in under “Engaging and Disengaging Mechanism of motor and alternator”.

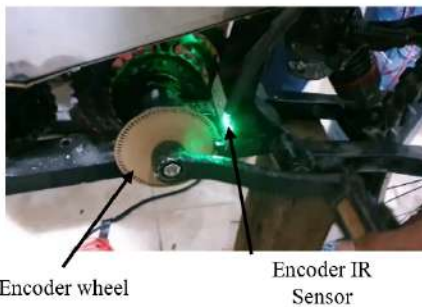


Figure 6. IR Sensor and Encoder wheel.

Source: Designed by authors.

Final driving mode is the neutral mode, which is similar to a conventional bicycle. Both motor and

alternator will be disengaged from the driving strain in this mode.

A slope detection mechanism is added to the bicycle, which is a unique feature to actuate the energy harvesting mechanism while moving on a slope. A Gyroscope sensor was used for this purpose and trials were carried out on a conventional bicycle and on a motor bike to simulate the real conditions and to detect the threshold level to detect a slope. This feature is actuated in any mode and will help to reduce the speed of the bicycle and charge battery. Likewise, the Alternator is also actuated in any mode when brakes are applied. Brake sensors will give the signal to the controller and that will actuate the alternator clutch. Figure 7 shows a block diagram with inputs and outputs connected to controller to actuate driving modes.

### C. Engaging and Disengaging Mechanism

The reason of implementing an engaging and disengaging mechanism for mid driven motor and alternator (Energy Harvesting mechanism) is to avoid unwanted drag on rider. Since both motor and an alternator are used in the model, the drag would be doubled. As a solution, the electro-magnetic clutch mechanism was selected due to its inbuilt mechanism to engage and disengage clutches. Usually, the electromagnetic clutches are used in AC compressors of automobiles, correct alignments when coupling is critical. So, the motor, alternator and the EM-clutches were 3D modelled using SolidWorks software to do the development.



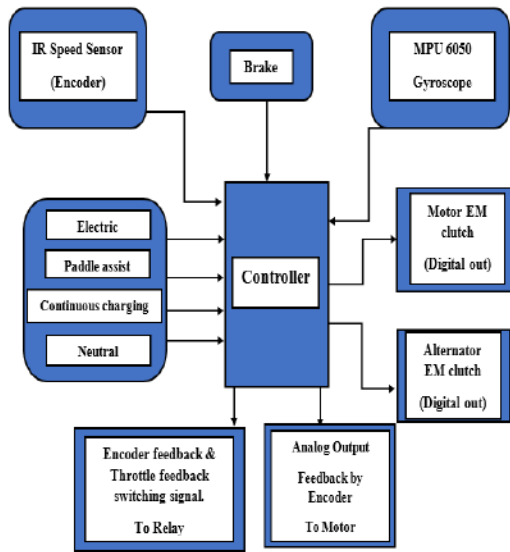


Figure 7. Driving modes control circuit.

Source: Designed by authors

Then the models were modified to a cassette wheel driving mechanism as shown in Figures 8 and 9. Main concerns in this designing were to maintain proper alignments in the motor, alternator, and EM clutch shafts and to maintain concentric positioning between cassette wheel and shafts.

Table 2 shows a summary of Motor and alternator engagement in each driving mode.

Table 2. Motor an alternator engagement in different modes.

Mode	Motor	Energy harvesting Mechanism (Alternator)
Electric (throttle) Mode	Fully engaged, released only in slopes and when brakes applied.	Engaged only in sloped and when brakes applied.

Pedal Assist Mode	Engaging only with encoder signal, released in slopes and when brakes applied.	Engaged only in sloped and when brakes applied.
Continuous charging Mode	No engagement.	Continuously engaged.
Neutral mode	No engagement.	Engaged only in sloped and when brakes applied.

Source: Designed by authors.

#### 4. Results and Discussion

The main aim of this research is to introduce an Intelligent Battery Control system integrated with Dual battery mechanism and driving modes. The project was categorized in to sub sections to reduce the complexity in developing each section. Since each sanction is crucial for the success of the project, it was always concerned to do the fabrications aligned with the design.

The batteries used in the project was subjected to internal resistance test and capacity test. Through internal resistance test, the batteries below 4.0V and batteries bellow 2200mAh after capacity test were not used. Initial battery switching circuit had 22 relays and after simulation it was optimized to 16 relays.

Then the working prototype, as shown in Figure 10, was subjected to road trials in different modes. A mobile app was used to measure the travelled distance, top speed, and the route. The results are as follows.

*D. Electric (Throttle) mode*

To compare the introduced system, few trials were conducted without the system in same bicycle. The per-charge distance without the system was 34.4 km. That means the charging and discharging is undertaken by same battery pack. Thus, the charging and discharging cycles are overlapped. Under the proposed system, eight trials were conducted, and the trial results are given in Table 3.

Table 3. Summary of trial results under Electric mode.

Trial	Initial Voltage (P1)	Final Voltage (P1)	Initial Voltage (P2)	Final Voltage (P2)	Distance Covered
1	49.52	47.12	44.42	44.50	4
2	47.10	44.05	44.50	45.12	5
3	4.05	41.52	45.12	45.71	4.5
4	41.50	38.96	45.71	46.83	4.5
5	38.95	36.55	46.83	46.50	5
6	36.55	37.14	46.50	44.23	4
7	37.14	37.51	44.23	41.92	4
8	37.51	38.12	41.92	39.85	3.5

Source: Developed by authors.

Through above trials, it was observed that per charge distance as 41.6 km and it is about 19% increase in per charge distance.

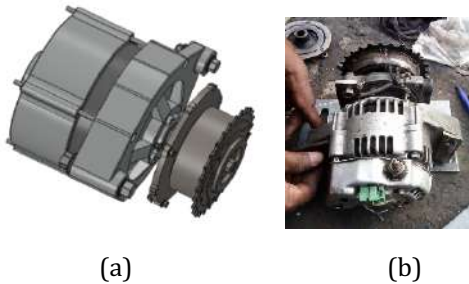


Figure 8. (a) 3D model, & (b) alternator coupled with EM clutch.

Source: Designed by authors.



Figure 9. (a) 3D model & (b) motor coupled with EM clutch.

Source: Designed by authors.

*E. Pedal assist mode*

Five trials were conducted under pedal assist mode covering 11km. The per charge distance was calculated based on the collected data as 49.4 km. Though this is more than the full electric mode, the expected per charge distance under pedal assist mode was 55km. This may be based on the road conditions. Table 4 shows the summary of trial results under pedal assist mode.

Table 4. Summary of trial results under Pedal assist mode.

Trial	Initial Voltage (P1)	Final Voltage (P1)	Initial Voltage (P2)	Final Voltage (P2)	Distance Covered
1	46.23	45.33	39.22	39.23	2
2	45.33	44.20	39.23	39.65	2.5
3	44.20	43.31	39.65	39.89	2

4	43.3 1	42.1 2	39.8 9	40.2 4	2.4
5	42.1 2	40.1 8	40.2 4	40.4 1	2.1

Source: Developed by authors.

#### F. Continuous charging mode

Under continuous charging mode, alternator is always engaged with the drive train. Due to that, paddling was bit



Figure 10. Prototype of the E-bicycle

Source: Designed by authors.

difficult. Thus, the short trials were conducted covering 3.7km. Thus, the rider needs to ride almost 61kms to totally charge under this mode. Table 5 shows a summary of trial results under continuous charging mode.

Table 5. Summary of trial results under Continuous charging mode.

Trial	Initial Voltage (P1)	Final Voltage (P1)	Initial Voltage (P2)	Final Voltage (P2)	Distance Covered
1	42.62	42.62	39.43	39.88	1
2	42.62	42.62	39.88	40.42	1.2
3	42.62	42.62	40.42	41.13	1.5

Source: Developed by authors.

## 5. Conclusion and Recommendations

This research is to implement an intelligent battery control mechanism which is an integration of dual battery mechanism with four driving modes. Here the rider could choose the driving mode they prefer. Based on the trials conducted in electric mode, integrated system has improved the per charge travelling distance from 34.4 to 41.6 km. So, it has improved per charge travelling distance by 19%. By fabricating the bicycle chassis using a much lighter material, the per charge distance could be improved. Though the pedal assist mode is a common mode in electric bikes, a new mechanism to measure riders' input and assist the paddling is introduced here. The per charge travelling distance in pedal assist mode is 49.4km, which could be higher in flat roads like Colombo. Continuous charging mode is a unique feature in this bike, where if any rider needs to burn extra calories, it will be a side benefit. It is observed that if rider needs to fully charge the battery only from continuous charging mode, it takes 61 kms. This could be reduced using a much-developed alternator and using a mechanism to improve the rpm of the alternator. From the statistics produced, it can be concluded that the introduced mechanism has improved the per charge distance of the E-bicycle.

## References

- Abagnale, C; Cardone, M; Idoice, P & Marialto, R (2016): Design and Development of an Innovative E-bicycle, Energy Procedia, 101, pp. 774-781.
- Ashish, U, Bishav, R & Kumar, A (2016): Design and Fabrication of an accumulator container/ Battery pack for a formula student vehicle, International Journal of Research in Engineering and Technology, 05(03).
- Belekar, R; Subramanian, S; Panvalkar, P V; Desai, M and Patole, R (2017): Alternator charging system for Electric Motorcycles.

International Research Journal of Engineering Technology, 04(04), p. 1759-1766.

Chandratre, A; Saini, H; Vemuri, S H & Srinivas, M (2011): 'Battery Management System for E-bike: A Novel Approach to Measure Crucial Battery Parameters for a VRLA Battery,' India International Conference on Power Electronics 2010 (IICPE2010).

Cheng, Y C; Lee, C K; & Tsai, M T (2016): Multi objective optimization of an on-road bicycle frame by uniform design and compromise Programming, *Advances in Mechanical Engineering*, 8(2), pp. 1-15.

Covill, D; Begg, S; Elton, E; Milne, M; Morris, R and Katz Tim (2014): 'Parametric Finite element analysis of bicycle frame geometries,' Conference of the International Sports Engineering Association, 72, pp. 441-446.

Gao , L; Liu, S & Dougal, R A (2002): Dynamic Lithium-ion Battery model for system simulation, *IEEE Transactions on Components and Packaging Technologies*, 25(3).

Hsu, C; Yu, C; Chao, S and Huang, M C J (1989): Electric Bicycle. U.S. Patent 4871042.

Hunt, I A; Zhao, Y; Patel, Y & Offer, G (2016): Surface Cooling Causes Accelerated Degradation Compared to Tab Cooling For Lithium -Ion Pouch Cells, *The Electrochemical Society*, 9, p. 163.

Krung, F, n.d. Electric Bikes vs Regular Bikes: The real Difference by EVELO. [Online] Available at: <https://www.evelo.com/blog/electric-bikes-vs-regular-bikes/> [Accessed 17 February 2020].

Li, Z; Zuo, L; Luhrs, G; Lin, L & Qin, Y (2013): Electromagnetic Energy-Harvesting Shock Absorbers: Design, Modeling and Road Tests, *IEEE transactions on vehicular technology*, 62.

Maughan, R (2017): What is the Best Electric Vehicle Battery Cooling System.

Pellitteri, F; Boscaino, V & di Tommaso, A C (2013): E-bike battery charging: methods and circuits, 2013 International Conference on Clean Electrical Power (ICCEP).

Rashid, M I M & Osman, J R A J (2017): 'Design and Implementation of Battery Management System for Electric Bicycle,' MATEC Web of Conference.

Reineman, S (2013): Design And Analysis of a Battery For a Formula Electric Car, Massachusetts Institute of Technology.

Saw, L H; Ye, Y & Tay, A A (2015): Integration issues of lithium -ion battery in to electric vehicle battery pack, *Journal of cleaner Production*.

Vasic, D; Chen, Y -Y & Costa, F (2013): Self-Powered Piezoelectric Energy Harvester for Bicycle. IECON 2013 - 39th Annual Conference of the IEEE Industrial Electronics Society, pp. 1856-1861.

Yang, Y; Yeo, J & Priya, S (2012): Harvesting energy from the Counterbalancing (Weaving) Movement in Bicycle Riding. *Sensors*, 12, pp. 10248-10258.

## Abbreviations and Symbols

DC – Direct Current

E-bicycle – Electric bicycle

SOC – State of charge

DOD – Depth of Discharge

SOH – State of Health

Li-Ion – Lithium Ion

Ni-Cd -Nickel Cadmium

VRLA – Variable Regulated Lead Acid Battery

NiMH - Nickel Metal Hydride

C-Zn – Carbon Zinc

LiPo – Lithium Polymer

## Acknowledgment

Authors would like to extend their heartfelt gratitude to the Mechanical Engineering Department of General Sir John Kotelawala Defence University, Ratmalana and supervisors for their expertise, guidance, supervision and support for the research.

## Author Biography



U.V.H. Sameera. BSc. (Hons) in Mechatronics Engineering Graduated from Mechanical Department of General Sir John Kotelawala Defence University, Sri Lanka in 2021.

He recently worked at Nikini Automation Systems (Pvt) Ltd as a Control Engineer Trainee and joined KDU as a Temporary Demonstrator to pursue his career in academia.



K.L.A.T.M Ranasinghe. BSc. (Hons) in Mechatronics Engineering Graduated from Mechanical Department of General Sir John Kotelawala Defence University, Sri Lanka in

2021. He is currently working at ITC ONE Colombo 1 project as an ELV Engineer in Building Management Services industry.



R.M.P.M.D. Rajapaksa. BSc. (Hons) in Mechatronics Engineering Graduated from Mechanical Department of General Sir John Kotelawala Defence University, Sri Lanka in

2021. He is currently working at Nikini Automation Systems (Pvt) Ltd as an Electrical & Controls Engineer in Industrial Automation sector



Mrs. G.M.S.M Gaspe is a Lecturer (Probationary) of the Mechanical Engineering Department at General Sir John Kotelawala Defence University, Sri Lanka. She graduated with B. Tech (Hons) in Mechatronics from Uva Wellassa University, Srilanka and completed her M.Sc. in Applied Electronics from University of Colombo, Srilanka. Her research interests include Intelligent System Control, Automation and Robotics.



Mr. W.S.M Melvin is a Research and Innovation Senior Engineer who currently works in Scotland. He completed his M.Sc. from Salford University, Manchester UK, B.Eng. from Wolverhampton University, London, UK, and NDT from University of Moratuwa, Srilanka. Within 9 years of service in research and innovation sector Srilanka, he worked in Peacock Technology Ltd, MAS holdings Pvt Ltd, Jinasena Innovation Centre and Camso Loadstar

# Comparison of Printed Circuit Board Fabricated by using conventional method and Laser Cutting Method

DALP Karunarathne<sup>1#</sup>, WSP Fernando<sup>1</sup>, PSH Pallemulla<sup>1</sup> and MKAJ Maldeniya<sup>2</sup>

<sup>1</sup>Department of Mechanical Engineering, Faculty of Engineering, General Sir John Kotelawala Defence University

<sup>2</sup>Department of Mathematics, Faculty of Engineering, General Sir John Kotelawala Defence University

#lahirukarunarathna@gmail.com

**Abstract:** *There are multiple methods of manufacturing printed circuit boards (PCB). The approach used by electronic enthusiasts is ironing the circuit from the glossy paper onto the copper plate (the homemade method). Industrial PCB manufacturers use laser cutting or computerized numerical control milling to cut the pathways, thus etching the circuit on the board. The former is time-consuming and the latter carries the risk of damaging the board during the manufacturing process, in addition to several other drawbacks. The approach that is presented in this paper avoids these disadvantages. In the proposed method, a polyvinyl chloride sticker is pasted on the copper board and unwanted sections of the sticker are removed by using laser cutting. Subsequently, the copper board with the sticker is immersed in a ferric chloride solution, washed off and the remaining parts of the sticker are removed. The advantages of this approach are the capability of accurately obtaining fine tracks (of 30 mil in width) and being comparatively less time-consuming than other methods used by electronics enthusiasts. In this paper, the procedure for making a PCB with the proposed method is laid out. Then, the function and design of a low-power laser cutter to accomplish the former is discussed.*

**Keywords:** *printed circuit board, laser cutting, polyvinyl chloride sticker*

## 1. Introduction

A printed circuit board (PCB) is used to connect electronic components with one another, forming a compact circuit. These components are fastened to the surface of the PCB, which are then electrically connected via conductive tracks. When developing a circuit on a PCB, components are typically soldered on to the board to hold them in place. High-quality PCBs are fabricated for industrial applications by large-scale manufacturers but many electronic enthusiasts use relatively simple methods to develop PCBs of their own, which they can use for minor projects.

In the typical method that electronic enthusiasts use to make a PCB, the circuit is first printed on photo (glossy) paper and a hot iron is used to apply pressure and heat to transfer the ink on the paper to a copper plate. This method has the disadvantages of being time consuming as the copper plate has to be printed, ironed slowly, washed and dried. Ironing may have to be done multiple times to get an acceptable print of the tracks on the plate. Moreover, it can be difficult to achieve perfect tracks by ironing, thus resulting in improper electrical connections when electronic components are soldered onto the board. In large-scale manufacturing, a variety of processes are used (Mitzner 2007), including laser cutting (Durillo, Falcon & Aranda 2018; Triano & Collins 2013; Sooraj & Vasa 2020), (Plesha & Kycia 2020), milling

(Choudhary et al. 2017; Basniak & Catapan 2012; Madekar et al. 2016) and maskless lithography (Hansotte, Canigan & Meisburger 2011), (Lee 2010). The most prominent of these methods are the use of a laser cutter or a computerized numerical control (CNC) milling machine to etch the circuit onto the conductive plate. Both these processes are subtractive i.e. removing material from the conductive plate in order to obtain the tracks. This results in the possibility of the board being damaged due to the cutting. Another drawback is that fine tracks and gaps between tracks cannot be obtained due to the diameter of the tool in CNC milling (Bogatin 2021), (Shinde & Mutthurajan 2016) and the width of the beam in laser cutting. The drawbacks mentioned above may result in a common problem faced by users of printed circuit boards, which is the intermittent malfunctioning of the circuit. This problem may also be caused by imperfect connections on the copper plate due to loose or damaged connections caused by handling the PCB. The unreliability of the electrical connections of the PCB has resulted in users testing their circuits on a breadboard to check whether the PCB circuit is working as intended. Such redundancy can be avoided if the tracks on the PCB are properly cut out. To avoid such difficulties, the researchers have proposed a novel approach.

In the proposed approach, a polyvinyl chloride (PVC) sticker is pasted on a copper plate instead of using glossy paper and an iron. The parts of the sticker, where the tracks are to be etched, are cut away by a laser cutter. To achieve fineness in the tracks and minimize thermal damage to the PVC sticker, a CNC laser cutter has been designed for this purpose. The design and the functioning of the laser cutter are provided in Section II B of this paper. After this subtractive process, the copper board with the sticker is immersed in a solution of ferric chloride. The board is then

washed with water and the remainder of the sticker is removed.

When the PCB is made with this approach, finer tracks can be obtained compared to other methods. It is also relatively cheap and the fabrication of the board is fast. The results that confirm these facts are presented and discussed in this paper. In order to obtain an objective metric of similarity, an image processing approach is used to compare the results of the homemade method with that of the proposed method.

In this paper, Section II details the steps in the fabrication of the PCB, the function of the laser cutter and calculations related to its input signal. In Section III, the quality of PCBs made using the homemade method and the proposed method are discussed, followed by an assessment of the time taken to cut the PCB tracks using multiple power/cut-rate combinations in the proposed method. A comparison between the time taken to complete the PCB fabrication process in the homemade method and the proposed method is also made in the same section. Lastly, in Section IV, the feasibility of using the proposed method is commented on.

## **2. Methodology**

### *A. PCB fabrication*

The method proposed in this paper uses the following components: a copper board, a PVC sticker (e.g. ORACAL 100G or 100M series), sandpaper, a laser cutter/engraver, Ferric Chloride as the etchant solution and a plastic flat container.

First, the copper board is cut into pieces and the piece to be used as the PCB must be sanded down using the sandpaper. Such a piece is shown in Figure 1. Then, the PVC sticker is pasted on the piece. Subsequently, the piece must be placed in the laser cutter, to which the PCB tracks have been programmed. After the laser cutter has

finished cutting the tracks, the remaining parts of the sticker must be removed and the piece must then be placed in the etchant solution so that it is completely immersed. An immersed copper piece is shown in Figure 2. It is well-known that the etchant solution can be produced by mixing hydrochloric acid and hydrogen peroxide or iron (III) chloride. The copper will gradually dissolve in the solution and when the final trace of copper has been removed, the piece must be dried to stop the chemical reaction. Once dried, any remaining stickers must be removed to obtain the proper PCB tracks. The final product is shown in Figure 3.



Figure 1: A copper piece that has been sanded down

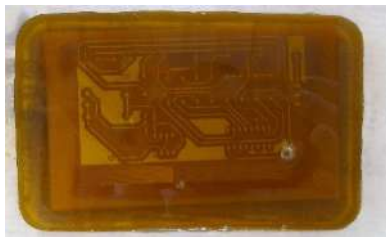


Figure 2: A copper piece with the laser-cut PVC sticker immersed in the Ferric Chloride etchant solution

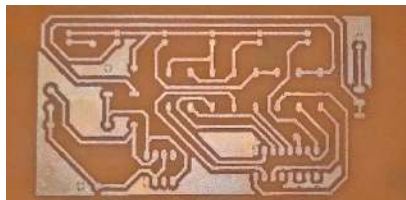


Figure 3: Copper piece after being removed from the etchant solution and dried

### B. Function and Design of the Laser Cutter

The laser cutter is an integral part of the proposed approach as it provides a means of generating a low-power laser beam (up to 3.5 W) that is capable of printing the PCB with no damage to the PVC sticker. A wavelength of 450 nm is used for the laser, generating a blue light. The diameter of the laser spot at this wavelength is  $\leq \Phi 0.08$  with a lens of focal length 20 mm. In contrast to lasers in industrial laser cutters that exhibit fluctuations in power, the proposed design generates a laser of stable power.

Figure 4 shows the block diagram of the CNC laser cutter. In the figure, the computer (A) has the Universal G-code Sender (UGS) platform installed. UGS enables communication between the computer and the laser cutter via universal serial bus (USB) (B). The sketch of the PCB tracks must be drawn by the user and it must be converted to G-code, using appropriate software. Software capable of performing these functions are freely available. The G-codes are then transmitted to the laser cutter by the UGS via the USB.

The G-code stream is sent directly to the microcontroller unit (C), which is pre-programmed to convert the received G-codes to motor-controlling and laser-controlling commands. The G-code handling in the microcontroller is achieved with the GRBL software, which is installed for the express purpose of generating control commands from G-code input.

The laser driver (D) receives control commands from the microcontroller and generates the laser accordingly. Transistor-transistor logic (TTL) modulation is used to enable, disable and modulate the laser diode. TTL modulation has been chosen to maintain the overall cost at a



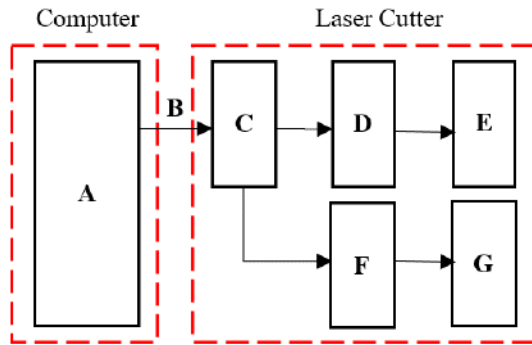


Figure 4: Block diagram of the laser cutter where A – computer, B – USB communication, C – microcontroller, D – laser driver, E – laser module, F – stepper motor driver, G – stepper motor

minimum, in order to facilitate budgeting in minor- and moderate-scale projects. The laser module (E) generates a 450 nm wavelength blue laser in accordance with the commands received from the laser driver.

The stepper motor (F) receives control signals and a pulse-width modulated signal for operation. One pulse of the pulse train, when transmitted to the stepper motor, drives it one microstep. A simple stepper motor model with a STEP input, such as the NEMA 17 can be used here. The NEMA 17 is ideal, since it enables compact design with high torque, when supplied with 12 V.

Figure 5 shows a possible design of the laser cutter that adheres to the block diagram shown in Figure 3.

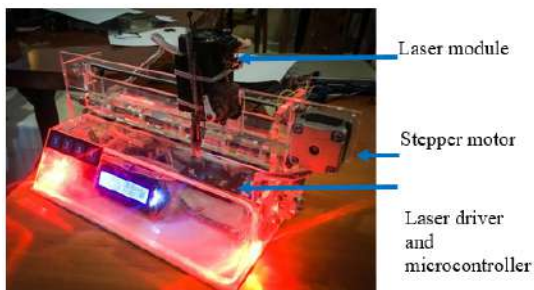


Figure 5: Components of the laser cutter

### C. Pulse Width Modulation

Different brands of PVC stickers require varying cutting power and cutting speeds for obtaining a smooth cut. These specifications can be extracted from the sticker’s datasheet. The power of the laser module designed above varies between 0 W and 10 W. However, due to a portion of the energy dissipating as heat, the optical output of the laser beam is only 3.5 W. A pulse train, as shown in Figure 6, has to be transmitted to the laser module. The calculation required to compute the pulse width of this signal is presented below.

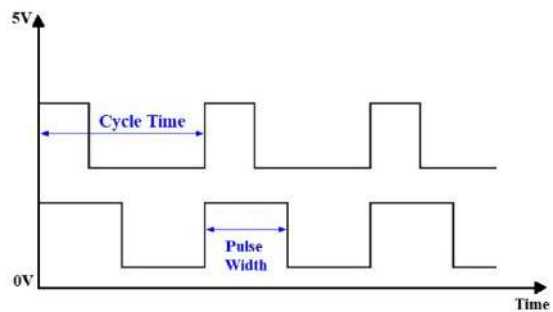


Figure 6: Pulse train to be transmitted to the laser module

The pulse width (PW) of the signal can be calculated from its cycle time (TC) and the duty cycle (DT) as shown in Equation (1).

$$PW = TC * DT \quad (1)$$

TC can be calculated by taking the inverse of the microcontroller output pulse frequency (FC) as in Equation (2).

$$TC = 1 / FC \quad (2)$$

DT can be obtained by dividing the required output power (OP), determined from the datasheet, by the total power (TP) as in Equation (3).

$$DT = OP / TP \quad (3)$$

Equations (1), (2) and (3), can be combined to Equation (4), which shows how PW can be calculated when FC, OP and TP are known.

$$PW = OP / (TP * FC) \quad (4)$$

For example, for a pulse of frequency 490 Hz, if the total power required is 0.5 W and the total power is 3.5 W, the width of the pulse train is.

$$PW = 0.5 / (3.5 * 490) = 0.000291 \text{ s} = 0.291 \text{ ms} \quad (5)$$

Once the pulse width is known, the microcontroller must be programmed to produce the appropriate pulse train.

### 3. Results and Discussion

#### A. Comparison of PCBs made using the Homemade Method and the Proposed Method

In this subsection, the conformance of the output PCB to the PCB template drawn using software are discussed. Additionally, the outputs of the homemade method and the proposed method are compared. In order to do the comparison, binary images of a PCB made using the homemade method and a PCB made using the proposed method were obtained by a simple thresholding process. The original images of the PCBs and the results of their binarization are presented in Figure 7.

In Figure 7, (a) is the template of the PCB designed using software and (d) is the same image with inverted colour. Colours are inverted so that the PCB tracks are displayed in white and the rest of the PCB is displayed in black.

(b) and (c) show the outputs of the homemade method and the proposed method respectively. To obtain the binarized images (e) and (f), (b) and (c) are rotated, resized and then subject to a thresholding process. Otsu's method has been used to automatically calculate the optimal

threshold value for (b) and (c). It should be noted that the two aforementioned images have been captured under uniform illumination so as to minimize any image artifacts and noise after the thresholding.

When comparing the homemade PCB (b) and the template (a), one can clearly note gaps in the tracks in the former. This non-continuity of the tracks can lead to loss of electrical connection between any components that may later be soldered on to the PCB. The imperfect tracks are caused by several reasons, the first of which is the improper transfer of ink from the glossy paper to the PCB after ironing. Figure 8 shows how a considerable amount of ink is still left on the glossy paper, which remains a major drawback in the homemade method. Printing the circuit on the glossy paper at a higher resolution will mitigate, but not completely eliminate, this issue.

The second reason for poor tracks in the output, is the quality of the etchant solution. Etchant solutions, especially ferric chloride, stored for a long time may undergo a chemical reaction with oxygen, which consequently lowers the concentration. Overly dilute solutions lead to incomplete dissolution of the copper plate, resulting in sketchy PCB tracks. This remains a problem in both the homemade method and the proposed method.

When comparing the PCB made using the proposed method (c) and the template (a), one can observe that the output conforms with the template to a greater degree than (b). A majority of the PCB tracks are continuous, with the exception of a few tracks on the right edge, which are caused by imperfections in the etchant solution.

To determine the similarity of a PCB (either (b) or (c)) to the template (a), the images, (b) and (c), are first cropped so that only the circuit area is visible. Then, the images are rotated and scaled so that they match the orientation and size of the template image. Afterwards, the images are

binarized using a threshold computed by Otsu's method, after which the logical AND of the binary images are obtained. This results in matching pixels appearing in white and non-matching pixels appearing in black. Subsequently, the number of white pixels are counted and expressed as a fraction of the white pixels in the template image. Hence, if the two images match perfectly, a score of 1.0 will be obtained. This calculation provides a method to compute a similarity score between a PCB and the template.

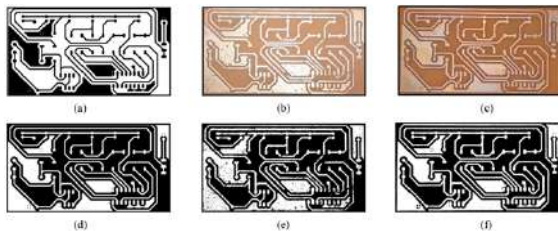


Figure 7: Images of (a) Template, (b) PCB made using the homemade method, (c) PCB made using the proposed method, (d) Template with colours inverted, (e) Binary image obtained from b, (f) Binary image obtained from c.

Comparing the binary image of the homemade PCB (e) to that of the template (a) results in a similarity score of 0.6334. A comparison of the binary image made using the proposed method (f) with that of the template results in a similarity score of 0.9265. The higher similarity score for the latter further reinforces the fact that the proposed method results in PCBs of higher quality that conform with the template, when compared with PCBs manufactured with the homemade method.



Figure 8: Ink remaining on the glossy paper after ironing, when making a PCB with the homemade method

#### A. Variation of Laser Power, Cut Rate and Time

In the proposed method, once the vinyl sticker is pasted on the copper plate, the tracks must be cut using the laser cutter. The time required to cut the tracks at different cut rates and power of the laser cutter were measured and are presented in Table 1. The sticker used is a PVC waterproof sticker of brand Oracal 651.

Table 1. Time taken to cut PCB tracks at different cut rates and power of the laser

Power (W)	Cut rate (mm/s)	Time to Cut (s)
1.65	5	480
1.95	20	448
2.25	35	416
2.4	50	385

Since the laser is low-power (between 1.65 W – 2.4 W), the risk to the operator's safety is minimal. However, laser safety goggles are recommended when working near a laser beam of any power. Apart from the lower risk to the user, the

potential for the PVC sticker to be damaged by excess heat is also low (Owen 2001).

The results of the laser-cut PVC sticker pasted on the copper plate at each of the power/cut-rate

to frictional forces. This is entirely eliminated in the proposed method. When the two processes were timed, the method used by electronic enthusiasts took an average of 44.0 minutes to

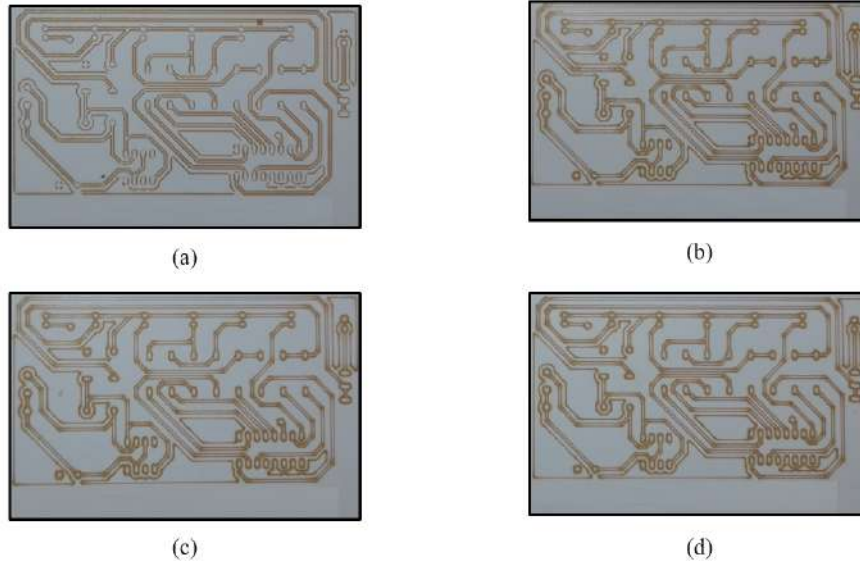


Figure 9: PVC sticker pasted on the copper plate after cutting by laser (a) at 1.65 W and 5 mm/s, (b) at 1.95 W and 20 mm/s, (c) at 2.25 W and 35 mm/s, and (d) at 2.4 W and 50 mm/s

combinations given in Table 1 are shown in Figure 9. It can be observed that cutting at the lowest power and cut rate causes broken lines to be cut on the sticker (a). These are caused by low power in the laser due to heat dissipation, coupled with less time spent on the cutting area. On the other hand, using higher power/cut-rate combinations has caused all lines to be cut continuously, with no gaps in the lines as seen from a), (b) and (c). No significant difference can be seen among these three images.

The proposed approach is less time-consuming when compared to the typical method that electronic enthusiasts use, even when the laser is operated at its lowest power and lowest cut rate i.e., 1.65 W and 5 mm/s. One major reason for this is that the tracks don't have to be printed on the paper and pasted on the copper plate. Printing on glossy paper has another drawback, which is the possibility of the printed lines being erased due

complete, whereas the proposed approach took an average of 16.0 minutes. 5 PCBs each were fabricated by each approach in order to get these results. The maximum speed and power of the laser has been used when timing the proposed approach i.e., 50 mm/s and 2.4 W, respectively. It should be noted that the copper plate has to be immersed in etchant solution in both methods, which took an average of 10.5 minutes for each method.

Assuming the optimum laser power as 2W, obtained similarity scores for different cutting rates.

Table 2. Similarity score of PCB tracks at different cut rates while keeping the power at a constant value

Power (W)	Cut rate (mm/s)	Similarity Score
2	5	0.6884
2	20	0.9265
2	35	0.8638
2	50	0.7965

According to the data obtained, similarity score behaviour shows in Figure 10. It can be observed that low cutting rates causes broken lines to be cut due to heat dissipation and higher cutting rates also causes broken lines to be cut due to inadequate heat supply to the board.

Based on Table 2, a function of similarity score is interpolated as

$$f(x) = 0.00001462716049x^3 - 0.001546074074x^2 + 0.04684592593x + 0.4909938272 \quad (6)$$

where the variable  $x$  is cutting rate. There it uses Lagrange interpolation and graph of  $f(x)$  is given in Figure 10. The function  $f(x)$  has a local maximum and minimum respectively at  $x = 22.04943411$  and  $x = 48.41646733$ , on the range  $0 \leq x \leq 60$ . Equation (6) can be used to obtain the highest similarity score.

Although industrial manufacturing methods such as CNC milling are capable of mass-producing PCBs at a fast rate, there is a risk of damaging the copper plate since it is a subtractive process. Another drawback of CNC milling is that fine tracks cannot be obtained due to the diameter of the milling tool (Bogatin 2021), (Shinde & Mutthurajan 2016). Laser cutting by directly applying heat to the copper plate also has the same drawback due to the width of the beam. One past study (Durillo, Falcón & Aranda 2018) suggests painting the copper plate with black

synthetic spray paint and then drying before applying the laser beam to the plate to minimize any damage. However, this overcomplicates the process and slows it down.

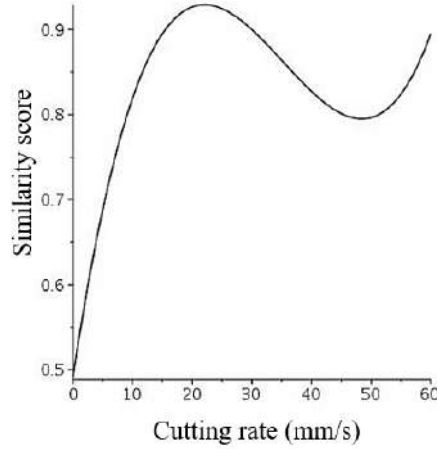


Figure 10: Similarity score and Cutting Rate

One research on convenient PCB fabrication (Alex & Sawn 2013) proposes the use of an ultraviolet (UV) laser on UV-sensitive copper clad boards. The PCB printer developed in the aforementioned study is very similar to the approach proposed in this research, except that the copper board still has to be immersed in, not one, but two solutions (developer solution and etchant solution) in order to get the finished PCB. Another research (Sooraj & Vasa 2020) proposes a cutting method with nanosecond laser ablation, but makes use of Laser Induced Breakdown Spectroscopy. This trades off speed and convenience for extreme accuracy, which is not needed for most small- to moderate- scale PCB-based projects, in general.

The drawbacks of the proposed approach is that it has the possibility of inflicting thermal damage on the sticker pasted on the copper plate, if the laser has unstable power. It is noteworthy that this may also happen in industrial laser cutting methods. Burnt stickers lead to smaller tracks in the PCB. Although finer tracks are preferable in most circuits, those transmitting large or high-

frequency current may be disadvantaged by wider tracks. The disadvantage occurs in the form of energy loss in the form of heat, which may warp the copper plate, if it is considerably thin (Yang et al. 2019), (Chung et al. 2013). High heat may even melt the solder attaching electronic components to the PCB if the temperature rises above a critical value (Anand, Singh & Ladwal 2019). Secondly, since a pulse train is used to signal the microcontroller to generate the laser, step-skipping may occur at high pulse frequencies.

#### 4. Conclusion

Existing methods of fabricating PCBs take up a significant amount of time, especially for short-term projects. Additionally, they carry other drawbacks such as improper electrical connections in the finished PCB or the risk of damaging the copper plate while it is being processed.

The approach proposed in this paper provides a better trade-off between speed of fabrication and accuracy of the finished PCB than existing techniques. This method is expected to contribute to accelerating prototyping in projects of minor or moderate scale. In this research, we succeeded in making a PCB of much higher quality than a PCB made using the homemade method in considerably less time.

#### References

Triano, A & Collins, S (2013): 'Development of a PCB printer using an ultraviolet laser diode', 2013 IEEE Long Island Systems, Applications and Technology Conference (LISAT), p. 1-6.

Anand, V; Singh, V & Ladwal, V K (2019): 'Study on PCB Designing Problems and their Solutions', 2019 International Conference on Power Electronics, Control and Automation (ICPECA), pp. 1-5.

Basniak, R & Catapan, M F (2012): 'Design of a PCB milling machine', ACBM Symposium Series in Mechatronics, pp. 1339-1348.

Bogtin, E (2021): Bogatin's Practical Guide to PCB Design for New Product Development, Artech.

Choudhary, R; Sambhav; Titus, S D; Akshaya, P; Mathew, J A & Balaji, N (2017): 'CNC PCB milling and wood engraving machine', 2017 International Conference On Smart Technologies For Smart Nation (SmartTechCon), pp. 1301-1306.

Chung, S, Heo, G, Kwak, J, Oh, S, Lee, Y & Kang, C (2013): 'Development of PCB design guide and PCB deformation simulation tool for slim PCB quality and reliability', 2013 IEEE 63rd Electronic Components and Technology Conference, pp. 2157-2162.

Durillo, J C M; Falcón, P M & Aranda, A R (2018): 'Low-cost Laser Cutter and PCB exposure', 2018 XIII Technologies Applied to Electronics Teaching Conference (TAE), pp. 484-493.

Hansotte, E J; Canigan, E C & Meisburger, D (2011): 'High speed maskless lithography of printed circuit boards using digital micromirrors', Proceedings of SPIE - The International Society for Optical Engineering.

Lee, D -H (2010): Optical System with 4  $\mu\text{m}$  Resolution for Maskless Lithography Using Digital Micromirror Device, Journal of the Optical Society of Korea, 14(3) pp. 266-276.

Madekar, K J; Nanaware, K R; Phadtare, P R & Mane, V S (2016): Automatic mini CNC machine for PCB drawing and drilling, International Research Journal of Engineering and Technology (IRJET), 03, pp. 1106-1110.

Mitzner, K (2007): Complete PCB Design Using OrCAD® Capture and Layout, Newnes Publications.

Owen, M D (2001): Electronic Packaging: Electrical Interconnects, LIA Handbook of Laser Materials Processing, First Edition, Magnolia Publishing Inc.

Plesha, C E & Kycia, J B (2020): Resonant Frequency Adjusting of an MSA via Laser Ablation of the Input Coil, IEEE Transactions on Applied Superconductivity, 30(8), pp. 1-4.

Shinde, S & Muthurajan, H (2016): 'PCB fabrication unit for electronics circuit prototyping', 2016 IEEE International Conference on Advances in Electronics, Communication and Computer Technology (ICAECCT), pp. 1-5.

Sooraj, S & Vasa, N J (2020): 'Pulsed laser assisted micro-scribing of PCB combined with LIBS based depth monitoring', 2020 Conference on Lasers and Electro-Optics Pacific Rim (CLEO-PR), pp. 1-2.

Yang, D; Cheng, Z; Li, H; Won, S; Zhou, B & Tian, J (2019); PCB Layout Optimization of High-Frequency Inverter for Magnetic Coupled Resonance Wireless Power Transfer System, IEEE Access, 7, pp. 171395-171404.



currently a Senior Lecturer at General Sir John Kotelawala Defence University.

PSH Pallemulla BSc. (Hons) in Mechatronics Engineering graduated from the

Department of Mechanical Engineering of General Sir John Kotelawala Defence University in Sri Lanka in 2016. He is currently a Lecturer (Probationary) at the same university and is reading an MPhil at the University of Moratuwa.



MKAJ Maldeniya BSc. in Mathematics, graduated from the University of Jayawardenepura, Sri Lanka and completed an MS in

Mathematics at the New Mexico State University. He is currently a Senior Lecturer at the Department of Mathematics at General Sir John Kotelawala Defence University, Sri Lanka.



#### **Author Biography**

DALP Karunarathne BSc. (Hons) in Mechatronics Engineering graduated from the Department of Mechanical Engineering of General Sir John Kotelawala Defence University, Sri Lanka. He is currently the Managing Director of his own company, which specializes in industrial automation. He is also an independent researcher.



WSP Fernando BSc. (Hons) graduated from the Department of Computer Science and Engineering of University of Moratuwa, Sri Lanka and specialized in the field of control systems. He has also completed an MPhil from the University of Moratuwa. He is

# CREEPER: The First Indigenously Developed Hand-Held Digital Mobile Radio (DMR) in Sri Lanka

RMGC Navarathne<sup>1#</sup>, SRR Peiris<sup>1</sup> and RAMH Ranasinghe<sup>1</sup>

<sup>1</sup>Centre for Defence Research and Development - Ministry of Defence, Sri Lanka

#geethnavarathne@gmail.com

**Abstract:** Communication plays a crucial role in the context of military operations. The Revolution of Hand-Held radio from Analogue to Digital Technology reached up to many advanced radios with the application of Modern Technology. A famous means of communication which is utilized in modern military warfare is Digital Mobile Radio (DMR). However, due to highly expensive DMRs, it cannot be easily catered to suit various requirements. This paper aims to discuss the first Hand-Held DMR designed and developed for the Sri Lanka Military named the Creeper (The unique bird who can sing vast frequency bands). Creeper aims to reduce the capital cost investment on expensive DMR and provide flexibility for future improvements. The Creeper DMR is checked against existing DMRs such as Racal Cougar, tested on the field, and made many improvements. A Voice Coder (Vocoder) is used to meet the VHF frequency bands designed and then further developed to work on both VHF and UHF bands. The test results were satisfactory in the field and are currently same being used by Tri-services in Sri Lanka. Creeper has successfully provided a cost-effective solution and would stand out as possible future foreign market.

**Keywords:** Creeper, Digital Mobile Radio, Military communication, UHF, VHF, Vocoder

## 1. Introduction

Early communication was mainly based on smoke, hand gestures and signal flags, which then evolved to communication via Morse code

and Telegraph. However, these modes of communication were constrained by different terrain features and distance constraints. With the advent of military warfare, communication tactics had a drastic transformation from communication by means of animals to radios ("War Communication during WWI," n.d.). World War II, which took place from 1914 to 1918, played a major role in developing military communication. The Motorola SCR-300 was the original walkie-talkie radio used by the Army Signal Corps, which allowed real-time communication on the battlefield despite the harsh terrain (The History of Radio, 2022). Also, with the development of digital signal processing techniques, a more robust set of radios replaced the old bulky analogue-based radios with digital technology. These Digital Mobile Radios (DMR) is a system that sends digital signals to small devices called radios (DMR Radio Facts and Figures: A Look at the Current State of DMR Radio. - Newshunt360, 2021). It was standardized under the European Telecommunications Standards Institute (ETSI) Standard TS 102 361 parts 1-4, which is later commercialized for worldwide use (About ETSI, 2013).

Digital Mobile Radios (DMRs) have become a popular candidate in enabling efficient communications, especially in military communication. DMRs, in general, provide both Digital and Analogue mode compatibility. Also, they are embedded with noise cancellation and



secure measures to overcome eavesdropping and spoofing attacks (DMR Radios - Digital Mobile Radios | Hytera, 2022). These features of the DMR are the facilitating advantages for the popularity of DMR. However, the main disadvantage of DMR includes the inability to radio build quality over the whole spectrum.

Sri Lanka Army, Navy, Air Force and Police use various types of radio transceivers in order to achieve their daily operations. The most common type of currently used radio set for this purpose is the infamous Racal CougarNet System (COUGARNET, 2021). However, these radio transceivers are very expensive and no spares available. Also, require a considerable capital cost. In order to overcome these implications, Centre for Defence Research and Development (CDRD) consider addressing this issue as both an opportunity and a challenge. This paper mainly focuses on providing a viable and robust solution, which has already been tested and successfully deployed on the field by initiating the first hand-held Digital Radio Set for Sri Lankan Military named as Creeper. The product was released in three different versions and improved based on previous feedbacks and timely requirements. The first version of the Creeper DMR (V1.1) only was capable of communicating in the VHF frequency band. In the second version (V1.2), UHF frequency band was included along with Global Positioning System (GPS) for navigation. For the latest of third version (V1.3) has IP67 standard were included in order to adhere to Ingress Protection Regulations.



Figure 1. Creeper Logo

The research project aimed to produce the following research objectives:

- i. Locally producing operationally viable and economically advantageous DMR for military services.
- ii. Addressing custom requirements tailored as per the services of operation.

The paper is structured as follows; Literature review section will shortly describe previous similar work that has been undertaken. Following that Methodology section will discuss the design and development procedure as proposed. The results and discussion section will present the results and further improvements. Finally, the conclusion section will conclude the paper.

## 2. Literature Review

Speakeasy is a software-based digital mobile radio initiated to emulate more than five military radios (Upmal, 1995). The designed radio, however, supports a mostly outdated Frequency Division Multiple Access (FDMA) communication scheme, which imposes severe downsides when compared to modern DMR. Modern military communication methods are envisioned (Viswanathan, 1993), where Quadrature Phase Shift Keying (QPSK) digital modulation schemes and trends. As well as Very Large-Scale Integration (VLSI) technologies are expected to boom in military communication via Digital Mobile Radios. Viswanathan mainly has focused on cellular-based radios, which impose conventional implications as in conventional cellular networks. Various solutions, such as utilizing Long Term Evolution (LTE) which offers eNodeB Radio Access Network (RAN) to provide Time Division Multiple Access (TDMA) to provide a communication channel for DMR in congested regions, are evaluated (Qaddus, 2016).

Also, significant research has been conducted on the feasibility of existing Digital Audio Radio Services (DARS) for military applications (Hale & Ballinger, 2002), which are extremely expensive and cannot be deployed in the context of Sri Lanka. A narrowband communication radio was developed, which supports both UHF and VHF frequency bands, with 2.4kHz bandwidth which cannot achieve the required voice quality in the context of military applications (Boucher, Jolly, Lodge, & Dery, 1990). Moreover, this proposed tactical radio didn't have DMR capabilities.

According to the review of literature, it was evident that no progress has been made on developing a hand-held DMR counterfeit for Sri Lankan military applications. Therefore, the initiated Creeper DMR by CDRD is the first hand-held DMR to be developed customized for Sri Lankan military applications.

### 3. Methodology

This section discusses the methodology followed in developing the solution. Since 2015, many research officers have attended to the development of Hand-Held radio, the project initially focused on three aspects of designing. The project's initial stage aimed to produce Voltage Control Oscillator (VCO) with a phase lock loop to produce the required frequency range of interest. Then, the design of the Direct Digital Synthesis (DDS) based transceiver was to be developed to generate an analogue waveform, usually a sine waveform, by generating a time-varying signal in digital form and then performing a digital-to-analogue conversion.

In the first stage, CDRD developed a handset only with a UHF frequency band radio set and tested the prototype. However, further enhancements were proposed due to its bulky nature, the long antenna design, and less efficient battery life.

Secondly, CDRD developed a VHF radio set using the Racal CougarNet System.

In the second design phase, the battery was replaced by a Ni-Cd battery, however, considerable battery life was not obtained. Moreover, the radio communication range was limited to 1km.

However, due to lack of technical feasibility and limitations, the proposed methodology has reformed, and a different approach was implemented. As the final step, a Digital Signal Processing (DSP) based programmable transceiver (RDA1846S) was developed. This can be programmed according to various operational requirements. This methodology was employed in the design phase of the initial circuit design of the proposed DMR. To design the concept as shown in figure 2. The modulation and demodulation standard intercom dedicated chip named as HR\_C5000 family used to interface with trans-receiver to process communication smoothly. This chip is product of Hong Rui independent research and development in China. This is in line with standard digital intercom dedicated chip. Same used 4FSK modulation and demodulation technology, 12.5K channel using 2-slot TDMA communication mechanism to achieve 2 Way digital voice and data communication transmission, support full-duplex, half-duplex communication.

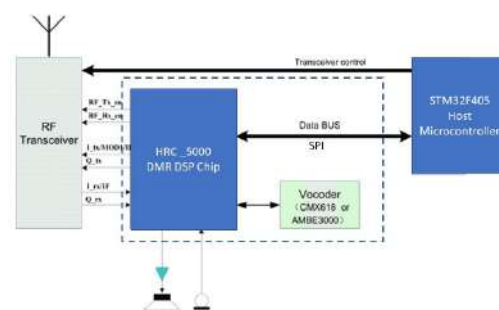


Figure 2. The block diagram of the main concept

HR\_C5000 chip design with the physical layer, data link layer and call controller. Also, application of this chips are digital intercom handsets, private cluster terminals, low-speed data, voice transmission terminal applications support for trunk and end-to-end use. Chip used C-Bus and McBSP interface seamless docking of vocoder chips such as CMX638 (Consumer Microcircuits Limited) or AMBE3000 (Digital Voice Systems, Inc.). The Creeper DMR has used AMBE3000 Vocoder and same type Vocoder used by Motorola. Hence the Creeper is satisfying the Motorola communication standard Tire I and Tier II, Also, it has used standard Serial Peripheral Interface (SPI) for flexible selection of vocoder, support for encrypted voice, data interface, Digital voice recording, playback, Display connections and a tone input providing difference interface with the use of Microcontroller STM32F405. Chip built-in high-performance as shown in figure 3, dual-channel AD / DA unit to support baseband In-phase Quadrature (IQ) inputs which can be configured to IF IQ, this can be configured to IF, two Point modulation and other RF interfaces to provide independent IQ bias voltage adjustable design. In IQ modulation, it can set a standard Analog walkie-talkie processing unit to support 12.5KHz / 25KHz channel communication. The power supply of 3.3VDC to the chip is supporting built-in power management module in order to achieve low-power usage and long battery life.

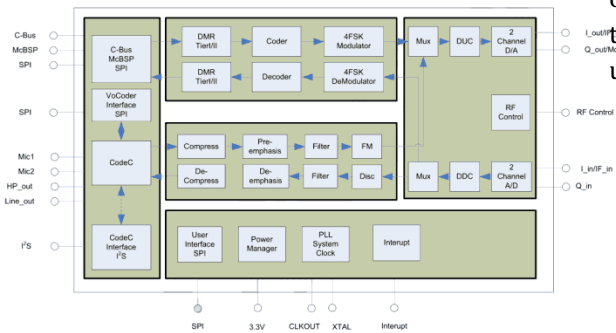


Figure 3. The block diagram of main hardware

With this initial technical knowledge and experience, CDRD Radio and Electronics Wing able to design indigenous Creeper DMR Set for the first time in Sri Lanka. This was developed in three different versions with the customization with difference end users from Tri-servicers. A summary of the version-wise features is listed in Table 1.

Table 1. Version wise features of Creeper DMR

Version	Chip used	VHF Band	UHF Band	GPS facility	IP67 Standard
V1.1	HR_C5000	✓	-	-	-
V1.2	HR_C6000	✓	✓	✓	-
V1.3	HR_C7000	✓	✓	✓	✓

For the Creeper, 2000mAh Li-Ion battery was used. Also, two types of Antennas of whip antennas were designed, as shown in Figure 4. The extended Antenna is capable of operating in long range. Where, the short Antenna is capable of operating in short ranges. During range testing it was found that range difference while using both Antennas are 2 to 3 Km.



Figure 4. Two types of whip Antennas

It has been faced major difficulties in designing in such complex circuit boards and enclosures. To address that various software on enclosure and circuit designing tools such as AutoCAD, MATLAB and Applied Wave Research (AWR) software were used. This software had utilized to designed and finalized the two layers PCB and enclosures. Due to the lack of technical feasibility, resources, requirements and knowledge gap on ability to design of PCBs in Sri Lanka, it found difficult in fabricating PCBs and enclosure in Sri Lanka. Hence a different approach was implemented. As all PCBs and enclosures sent to China for fabrication. The footprint of the circuit board is shown in the figure 5 and figure 6. Printed Circuit Board (PCB) design consisted of Eight layers is shown in figure 7.

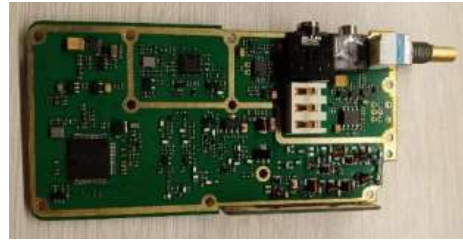


Figure 7. Final PCB Design

Moreover, to the requirement, the initial battery charger pack was custom-made to enable two charging slots to reduce the charging time and enhance the product efficiency, Figure 8.



Figure 8. Two-way battery charger for Creeper DMR

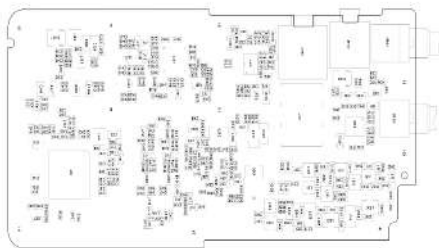


Figure 5. Footprint - Top Layer

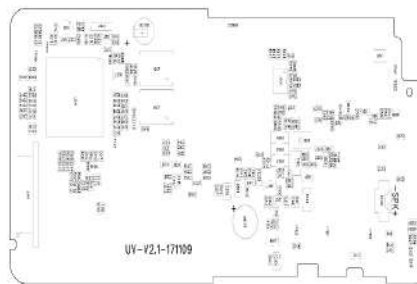


Figure 6. Footprint - Bottom Layer

The Creeper DMR chip HR\_C5000 by default has a programmable user-friendly software. Same has design and modified and customized accordingly requirement mainly focusing on military use. The main window of the software is shown in Figure 9.

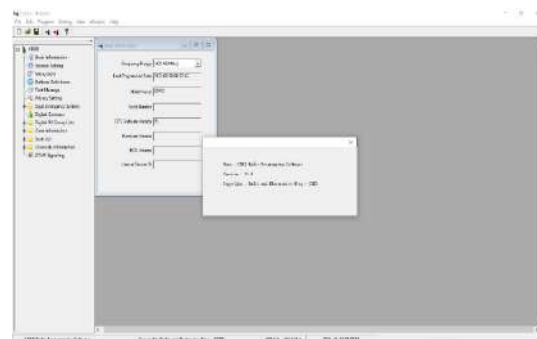


Figure 9. Software Main Window

The same software can be used to read and write necessary information to the radio. Moreover, it is capable of altering general settings of the radio such as Radio Name, Radio ID, Power ON Password, Alert ON and PC Programming Password. As well as Channel Settings which include settings such as Channel Mode (Analogue/Digital), Channel Name, Channel Bandwidth, RX / TX Frequency and Power Output (1W / 5W).

#### 4. Results and Discussion

This section will describe product specifications and briefly discuss its significance. Then, tested results on field testing are provided to validate the operational and functional features of the DMR in the field.

The product is based on main communication chip of HR\_C5000/HR\_C6000 (Miklor, 2017). The Creeper V 1.2 and V 1.3 is operated in both VHF and UHF frequency bands. The VHF band frequency band is 136 - 174 MHz and UHF frequency band is from 400 - 480 MHz. These radios use technology on either Frequency-Division Multiple Access (FDMA) or Time-Division Multiple Access (TDMA) technologies. The final product Three versions of 'CREEPER' as shown in the figure 10.



Figure 10. The CREEPER

The Creeper uses TDMA as the digital function. TDMA is a less power-consuming scheme when compared to FDMA, which consumes power. Moreover, the FDMA scheme is only feasible where the number of channels is small and FDMA cannot afford high transmission speed. In contrast, TDMA in an environment of small multipath delay TDMA can achieve high transmission speed. Also, the spread spectrum technique can increase the number of transmission channels using the TDMA scheme (Jiang, 1987).

For the basic encryption, the DMR is built with software-based encryption. Software-based encryption is vital in ensuring unauthorized eavesdropping. However, the launch of signaling and user identification is unencrypted. Further security is guaranteed using Dual Tone Multi-Frequency (DTMF) function, which allows operating the radio when there is interference in the radio system.

Main features of DMR are listed below:

- i. Frequency Band VHF 136 MHz – 174 MHz
- ii. 1000 Programmable Channels
- iii. 250 Programmable Zones
- iv. Voice Operated Exchange (VOX)
- v. Digital Coded Squelch (CTCSS / DCS)
- vi. High / Low Power Modes
- vii. Wide / Narrow Bandwidth

Technical specification of the developed DMR is listed below:

- i. Frequency Range: VHF channels: 136 - 174 MHz  
UHF channels: 400 - 480 MHz

- ii. Channel Spacing: 12.5 kHz
- iii. Operating Voltage: 7.4 V
- iv. Operating Temperature: +5 °C to +40 °C
- v. Audio Output Power: ≤1000mW @ 16 Ω
- vi. Dimension: 131 x 61 x 36 (mm)
- vii. Weight: 258g
- viii. Output Power: ≤5W (HIGH) / ≤ 1W (LOW)
- ix. Vocoder Type: AMBE+2TM
- x. Spurious Radiation: Antenna: 9 kHz – 1 GHz ≤-57 dBm / 1 GHz – 12.75 GHz ≤ -47 dBm

Further functional and operational details are given in the own created user Manual with the product for reference. The main parts of the Creeper DMR are shown in Figure 11.

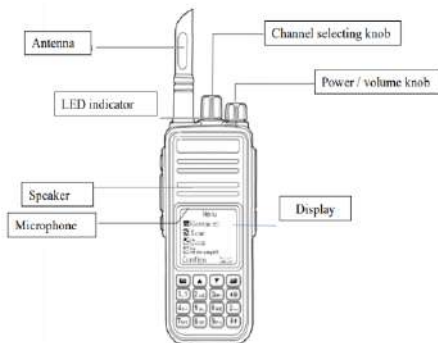


Figure 11. Main Parts of the Creeper DMR

The performance of the DMR is first predicted on the basis of the specification given in details during research phase and same tested by the CDRD with available resources. Range testing has carried out in difference terrain in various weather conditions. Table 2 summarizes the maximum distance achieved in different terrains

Table 2. Maximum distance achieved in different terrains

Terrain	Distance
Flat Ground with no many obstructions (LOS)	10-12 km
Urban/Jungle Area	4-5 km
Inside multi-stories buildings	Upto 20 floors

However, on several fields tests the DMR underperformed the specifications provided as expected. According to the Sri Lanka Navy field test (DGL, SLN HQ letter DGL.560/C/SD/1/2021 dated 12 August 2021), suggestions were made to adhere to Ingress Protection (IP Ratings) and GPS facility to help navigation. These were then considered and included in the latest versions of the DMR. Especially for Sri Lankan Navy, IP67 was included in the latest version to adhere for the Ingress Protection Rating, where it is totally protected from dust and from immersion between 15cm and 1m for 30 minutes (IP Ratings Explained | IP Rating Chart - Rainford Solutions, 2014).

After the modifications of all end user requirements, the CDRD was finally succeeded to deliver 200 numbers of Creeper DMR V 1.3 to Sri Lanka Navy. During the second field test conducted by Sri Lanka Navy, (SLN HQ letter CWL/05/05 dated 21 February 2022), tested each and every parameter of the Creeper DMR and from the given data following test results were observed for analyzation.

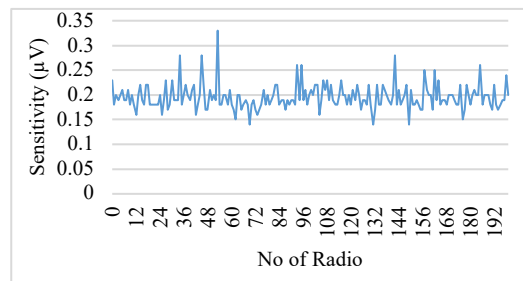


Figure 12. Sensitivity of radios

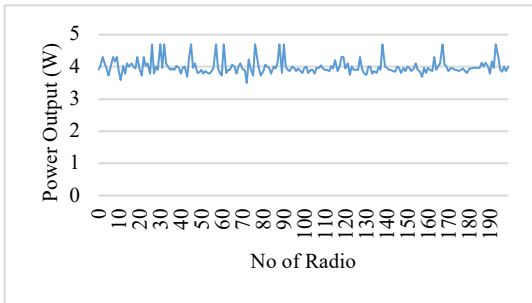


Figure 13. Power Output of radios

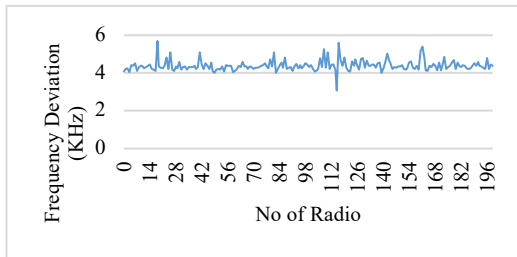


Figure 14. Frequency Deviation of radios

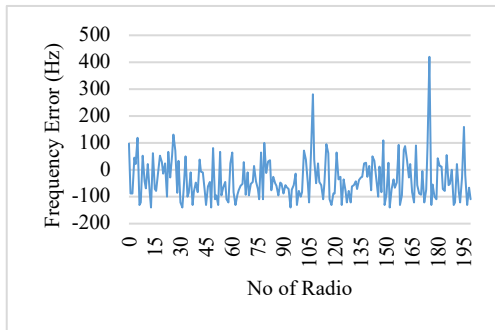


Figure 15. Frequency Error of Radios

According to the data obtain from test results from Sri Lanka Navy field test above graphs are plotted. figure 12 shows the voltage sensitivity of the Creeper. In general, as per naval standard any given hand-held communication set receiver sensitivity to be read as less than  $0.25 \mu\text{v}$ . In the plot in figure 12, 07 No's radios have exceeded aforesaid value. Then only 3.5% radios voltage sensitivity given some high values. This can be neglect when communication process doing in Digital mode.

The output power of the Creeper is plotted in figure 13. As per specification radio power output is 5W. However, result shows that output is varying approximately from 3.8W to 4.8W. This result shows that slightly some deviation in the expected results from the finish product. However, during range test in the difference field found all radios are working satisfactory. Moreover, this kind deficiencies will be taken in the future for upgraded Creeper versions as feasible.

Figure 14 shows the frequency deviation and figure 15 show the frequency error of Creeper. According to the plotted graphs results 09 No's radios shows that  $\pm 1$  KHz deviation in frequency and only 02 No's radios given some frequency error (more than 200 Hz). That indicate 5.5% radios only have some frequency issues and all other radios are working satisfactory. When consider the average of working satisfactory percentage of Creeper radios is 95.5%.

From the test result and feedback obtain from end users following pros and cons are came up. Some pros are as follows and those deficiencies to be addressed properly in future considerations:

- i. **Audio Volume and Quality:** Good response for low frequencies even in the noisiest environments.

- ii. **Rugged Construction:** IP67 compliant and thus waterproof for 30 min. submerged in up to 1m of water.
- iii. **Multi-colored LCD Display:** Having a multi-colored LCD display on the radio allows for easy use and programming while on the move.
- iv. **Front Panel Programming:** This radio is capable of being programmed via the keypad, allowing users to make limited changes without a PC.
- v. **Antenna Connector:** The Antenna connector for this radio uses a SMA connection This allows it to easily to be connected to an external Antenna.

Some cons are as follows:

- i. **Software Polish:** There are a number of oddities/complexities within the firmware of the radio that impacts its overall user experience.
- ii. **Bluetooth Capability:** This radio is not Bluetooth capable, so the use of wireless audio accessories is not possible.

Considering commercially available difference type of Dakota Alert, Icom, Motorola and Wouxun hand held communication sets with creeper hand held sets comparison chart is given in following table 3.

Table 3: The comparison chart of various H/H com sets

Items	Dakota Alert (M538HT)	Icom (VIOMR)	Motorola (RMM2050)	Wouxun (PLC-904EM)	Creeperv1.1	Creeperv1.2	Creeperv1.3
Frequency band (VHF)	✓	✓	✓	✓	✓	✓	✓
Frequency band (UHF)						✓	✓

FM Radio			✓	✓	✓	✓	✓
LCD Display	✓			✓	✓	✓	✓
Adjustable Squelch		✓		✓	✓	✓	✓
Power Save	✓	✓	✓	✓	✓	✓	✓
Selectable Power Level			Hi /Lo	Hi /Lo	Hi /Lo	Hi /Lo	Hi /Lo
PC Programmable			✓	✓	✓	✓	✓
CTCSS / DCS			✓	✓	✓	✓	✓
VOX				✓	✓	✓	✓
Text Messaging				✓	✓	✓	✓
Privet calling					✓	✓	✓
GPS facility						✓	✓
IP standard		IP 67	IP 54/55	IP 55	IP 61	IP 61	IP 67

### 5. Discussion

Military communication plays a crucial role in military operations and in maintaining proper order and governance. With the advent of Digital Mobile Radios, rising popularity was gained by DMR, especially in the context of military communication. However, such commercialized DMR imposed a significant drawback in terms of capital cost, which also accounted for a considerable amount costing of military and security services. Identifying this issue, CDRD Radio and Electronics Wing initiated a robust solution which is also promisingly scalable to address the problem by initiating the first hand-held Digital Radio Set for Sri Lankan Military named as Creeper.



Creeper was initiated with the VHF frequency band, which then integrated UHF frequency band along with all other modern features such as GPS that are readily found in modern DMR. However, all these features were developed without incurring much of the capital cost that would otherwise be invested on importing comparably expensive DMR. It is also provided with a user manual along with the software to easily customize according to the end-user need.

According to field deployed tests and field operations, Creeper successfully achieved the expected outcome set by Radio and Electronics wing of CDRD. With that it can be concluded, all the 200 numbers of DMRs are given excellent performance according to the specification of the Creeper with some minor deficiencies. By obtaining these radios by Tri-servicers, it could save Millions of rupees flowing to other countries and saving foreign reserves in the country.

In future work, considering all minor deficiencies it is ready to produce upgraded Creeper DMR version 1.4, incorporating of the Sri Lankan Army 1:50,000 map feature as expected. Also, incorporating the Creeper in disaster management operations and developed further.

In present scenario, the following numbers of DMR Hand-Held Sets used in Tri-servicers and there are working satisfactorily with good performance. Very recently, due to the good performance of same, some numbers of radios have already despatched to use for peace keeping force in Mali to enhance the communication capabilities.

- i. Sri Lanka Army - 110 Nos
- ii. Sri Lanka Navy - 210 Nos
- iii. Sri Lanka Air Force - 10 Nos
- iv. VIP duties - 20 Nos

## References

About ETSI. (2013). Retrieved July 13, 2022 from <http://portal.etsi.org/portal/server.pt/community/ERM/306?tbId=624>

Boucher, L., Jolly, Y., Lodge, J. H., & Dery, S. (1990). A narrowband tactical radio for the VHF and UHF frequency bands. In Proceedings - IEEE Military Communications Conference (Vol. 3). Retrieved from <https://doi.org/10.1109/milcom.1990.117613>

COUGARNET. (2021). Retrieved July 13, 2022, from <https://radiohistory.uk/cougarnet.htm>

DMR Radio Facts and Figures: A Look at the Current State of DMR Radio. - Newshunt360. (2021). Retrieved July 13, 2022, from <https://newshunt360.com/dmr-radio-facts-and-figures-a-look-at-the-current-state-of-dmr-radio/>

DMR Radios - Digital Mobile Radios | Hytera. (2022). Retrieved July 15, 2022, from <https://www.hytera.com/en-products/digital-radio/dmr-two-way-radios/>

Hale, A., & Ballinger, D. (2002). Military applications for Digital Audio Radio Service (DARS). IEEE Aerospace Conference Proceedings, 3. Retrieved from <https://doi.org/10.1109/AERO.2002.1035232>

IP Ratings Explained | IP Rating Chart - Rainford Solutions. (2014). Retrieved July 14, 2022, from <https://rainfordsolutions.com/products/ingress-protection-ip-rated-enclosures/ip-enclosure-ratings-standards-explained/>

Jiang, T. (1987). COMPARISON BETWEEN THE THREE MOBILE DIGITAL COMMUNICATION SYSTEMS. IEEE Vehicular Technology Conference, 359-362. Retrieved July 14, 2022 from <https://doi.org/10.1109/VTC.1987.1623570>

Qaddus, A. (2016). Real Time Performance Analysis of Digital Mobile Radio (DMR) and APCO Project 25 (P-25) Radio Systems in Land

Mobile Radio (LMR) Systems. International Journal of Computer Engineering and Information Technology, 8(3), 49–55. Retrieved July 15, 2022 from [www.ijceit.org](http://www.ijceit.org)

The History of Radio. (2022). Retrieved July 13, 2022, from <https://armedforcesentertainment.com/news/afe-presents-a-celebration-of-radio-history/>

Miklor. (2017). Retrieved July 14, 2022, from <https://www.miklor.com/MD380/>

Upmal, D. W. (1995). Speakeasy: The Military Software Radio: The Speakeasy Phase II radio will use programmable processing to emulate more than 15 existing military radios. Speakeasy is a challenge, even with recent advancements in DSP technologies. The benefits, however, make the challenge highly worthwhile. IEEE Communications Magazine, 33(5), 56–61. Retrieved July 15, 2022 from <https://doi.org/10.1109/35.392998>

Viswanathan, M. S. (1993). Tactical Military Communication Networks of the Future. Defence Science Journal, 43(1), 71–78. Retrieved July 15, 2022 from War Communication during WWI. (n.d.). Retrieved July 13, 2022.

### Abbreviations and Symbols

CDRD - Centre for Defence Research and Development

DMR - Digital Mobile Radio

DTMF - Dual Tone Multi Frequency

FDMA - Frequency Division Multiple Access

IQ - In-phase Quadrature

LTE - Long Term Evolution

PCB - Printed Circuit Board

QPSK - Quadrature Phase Shift Keying

SPI - Serial Peripheral Interface

TDMA - Time Division Multiple Access

### Acknowledgment

CREEPER: The First Locally Developed Hand-Held Digital Mobile Radio (DMR) Set for the Sri Lanka Military which were initiated and developed by the Centre for Defence Research and Development - Ministry of Defence, Sri Lanka.

### Author Biography



**Captain RMGC Navarathne**, is Professional, experienced Electrical, Electronics, and Telecommunication Chartered Engineer with proven skill levels, with the goal of achieving the highest as an Engineer and higher skill level manager with great capacity on carrying out research & development up to culminating point and capacity to work any field of Electrical, Electronics, and Telecommunication.



**Major SRR Peiris**, a Research Officer to the Radio and Electronics Wing of Centre for Defence Research and Development - Ministry of Defence, Sri Lanka. Rajitha previously completed his undergraduate in Department of English, University of Colombo.



**RA Muditha H Ranasinghe AMIMEchE**, a Research Officer to the Radio and Electronics Wing of Centre for Defence Research and Development - Ministry of Defence, Sri Lanka. Muditha previously completed his undergraduate from the Sri Lanka Institute of Information Technology with a Bachelor of Science of Engineering (Honours) in Mechanical Engineering (Mechatronics Specialization).

# A Numerical Study on Effect of Change in Longitudinal Center of Gravity on Planing Capability of a Coastal Patrol Craft: A Case Study, Sri Lanka Navy

DS Bogahawatte<sup>1#</sup>, PMKC Chandimal<sup>1</sup> and LAKR Athukorala<sup>2</sup>

<sup>1</sup> Department of Mechanical Engineering, Faculty of Engineering, General Sir John Kotelawala Defence University, Sri Lanka

<sup>2</sup> Directorate of Naval Design, Sri Lanka Navy, Sri Lanka

#ds-bogahawatte@kdu.ac.lk

**Abstract:** The pressure acts on the wetted surface area of the vessel always maintains the equilibrium with the weight of the vessel. The acting pressure comprises with two elements as hydrostatic, relates to buoyancy and hydrodynamic, relates to speed of the vessel. The authors involved in planned novel design of this monohull Coastal Patrol Craft with unknown capabilities of the dynamic behaviour with planing at initial stage. The research objectives were to, estimate the total weight, compare resistance for different LCG positions, and the dynamic wetted area comparison for different LCG positions, Effective power demand comparison for different LCG positions, dynamic trim comparison for different LCG positions, and planing capabilities for different LCG positions. Five different LCG positions were considered during the study to realize the craft's behaviour. According to the numerical approach, craft's behaviours explored with the change in LCG positions and anticipated effect on the resistance, effective power demand, dynamic trim, and planing capabilities. Based on the results, a small initial trim angle is required for the CPC to display optimal performance at speeds in the upper range of the planing regime. On the other hand, an initial trim by aft would increase the performance of the CPC at speeds lower than the planing region but would adversely affect the performance at higher speeds as the trim further increases due to

dynamic behaviour. Further, this increase in trim at higher speeds would result in dynamic instability and be detrimental to the performance of the craft.

**Keywords:** Longitudinal Center of Gravity, Planing, Hydrodynamic Forces

## 1. Introduction

The weight of a vessel is always balanced by the pressure acting on the wetted keel length developed by the vessel. This pressure is composed of two components: hydrostatic, related to the buoyancy, and hydrodynamic, related to the speed of the vessel. Many scholars classify the vessels according to the kind of pressure field acts during their steady motion:

- i. Displacement vessels: if hydrostatic pressure is much higher than hydrodynamic pressure (Froude number of less than 0.4).
- ii. Semi-displacement/semi-planing vessels: if hydrostatic and hydrodynamic pressure have the same order of magnitude (Froude number from 0.4-1.2)
- iii. Planing vessels, if hydrostatic pressure is much lower than hydrodynamic pressure (Froude number beyond 1.2).

planing hull is a hull where its displacement is raised in the direction of the water surface mostly by hydrodynamic forces upon enough propulsive power and boat speed is maintained. Thus, hydrodynamic forces are more significant than hydrostatic components. In this scenario, the entire body of the hull performs like a lifting surface and generates the lift force against its weight as the boat speed increases. Upon the boat achieves the planing capability its bare hull resistance declines with the benefit of the reduced draft. Significant research on the hulls which bound to be planed was made by Baker and Millar (1912). Authors further studied the previous works by Sottorf (1932), Shoemaker (1934), Sambraus (1938), Sedov (1947), and Locke (1948) of constant deadrise prismatic planing planes hydrodynamic characteristics which operate with fixed trim, fixed mean wetted length, and constant speed of operation. The seminal studies on the planing hulls were made by Savitsky (1964). In this study, the authors embark on a comprehensive analysis of the hydrodynamic features of the Coastal Patrol Craft (CPC) with a proposed planing hull. The empirical formulae proposed by Savitsky were employed in this conceptual design with a proposed planing hull.

At present, the attractiveness of planing hulls in the applied research area has been developed with the help of developments in Computer Fluid Dynamics (CFD) and computational infrastructure. Authors examined the work of Su et. al.(2012) on hydrodynamic performance of the planing hulls with the employment of CFD software as a numerical approach. One step further, the work of Yu-Min et. al. (2014) hydrodynamic performance of a planing multihulls has been explored with the commercial CFD software.

The basic concept of planing could be depicted in Figure 1 below, which indicates the Pressure and Velocity distribution beneath a planing flat plate in a self-explanatory manner. The hydrodynamic

pressure at stagnation point is very high, since all kinematic energy is converted into pressure.

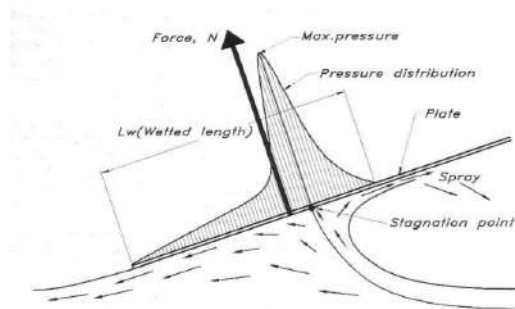


Figure 1. Pressure and velocity distribution beneath a planing flat plate

Source: (Larsson & Eliasson, 2000)

Figure 2 describes the Bow down moments (Pressure force, Appendage resistance, Frictional resistance), and Bow up moments (Thrust force). Accordingly hull automatically attain a trim angle cancelling all moments (i.e. net moment becomes zero). If a net moment to trim by bow occurs the trim will become smaller and the pressure force  $N$  moves forward until balance is achieved. If a bow down trim is applied, when craft at optimum trim angle, new trim becomes smaller, due to that hydrodynamic pressure is reduced. However, wetted surface is increased and the lift may be large enough. If it's not hull will sink down until hydrostatic pressure makes up for the loss.

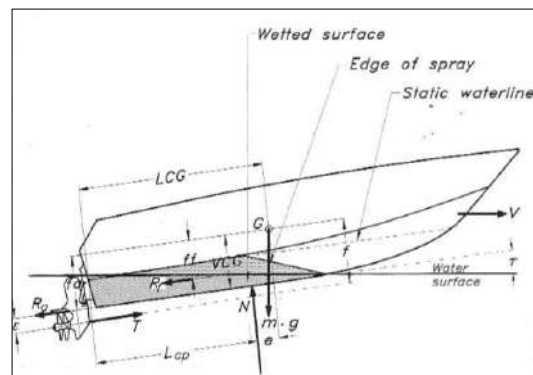


Figure 2. Forces on a planing hull

Source: (Larsson & Eliasson, 2000)

- N: The pressure force (hydrodynamic and hydrostatic)
- $R_f$ : The friction force
- T: Thrust Force
- $R_a$ : Resistance of the propeller drive (a denotes appendage)
- G: Weight centre of gravity
- ff: Lever arm for friction force
- fa: Lever arm for appendage resistance force
- e: Lever arm for pressure force
- f: Lever arm for thrust

The Planing hulls could employ in numerous applications in marine transport including patrol boats, sea taxis, passenger carriers, and pilot boats. A major impact on Planing hulls could be observed in the racing boat industry.

Naval Architecture shall understand the 'Porpoising' phenomenon as a continued, tiresome motion, which leads a boat's bow to jump up and down from water, even at still waters. Negative affect are un-comfortability for fares, and loss of boat control, and even destruction to the construction of boat.

The Naval Architecture shall understand design criteria and promote the ability of boat planing as design input. The principal factors were found to be Displacement and Longitudinal position of Buoyancy and Gravity. The geometrical parameter named Longitudinal Center of Buoyancy (LCB) shall not change during the manufacturing stage if it was manufactured as per the blueprint. Yet the Longitudinal Center of Gravity (LCG) may perhaps be uncertain leading to general arrangement changes, material options, or supplementary burdens from the ship owner.

Due to the machinery selections at later stages and by naval architectural design changes in the boat could lead to an undesired loading state

which might have an adversarial consequence on the boat's hydrodynamic performance. An unexpected initial trim (trim by forward) at the loading condition may prevent the boat from achieving its planing speed. Savitsky (1964) studies leading to LCG behaviours and subsequent development of formulas by him discuss, even if the initial trim could be brought to the desired status with extra ballast weight, this might deteriorate the hydrodynamic performance of the boat, as it leads to an increase in boats wetted surface area, thereby the increment in total hull resistance. Consequently, many authors discuss the phenomenon and came to lime light as many planing hulls remain agonized from the absence of planing capability for this simple reason.

The authors engaged in this novel design and, the dynamic behaviour with planing capabilities of the proposed craft was unknown at initial stages. Thus, it comprehends the research problem. More specifically authors extensively studied the proposed LCG positions for the designed Coastal Patrol Craft for Sri Lanka Navy as a planing hull. The objectives were to (a) estimate the total weight of the craft, (b) comparison resistance for different LCG positions, (c) the dynamic wetted area comparison for different LCG positions, (d) Effective power demand comparison for different LCG positions, (e) The dynamic trim comparison for different LCG positions, and (f) Planing capabilities for different LCG positions. Thereby this study included five different LCG positions (5.4 m, 5.6 m, 5.8 m at fore, 5.98 m at neutral, and 6.15 m at astern) to fully comprehend the study. This paper discusses the results of those tests (numerical approach) with their comparative influence on the change in the LCG position of the CPC.

## 2. Methodology and Experimental Design

The authors obtained the customer requirements from Director General Operation.

Then principal project proposal was submitted to the Ministry of Defence and National Planning Authority. Upon receipt of approval, the detailed design process of CPC (to be manufactured with Fibre Reinforced Plastic) was commenced. As per the SLN requirement, discarded steel hull of 'French Dvora' was used as the plug to develop these CPC moulds (Hull, Deck, and superstructure). Further, mould(s) were improved to cater habitability, transom for demoulding requirements, decks to incorporate hatches, and a custom wheelhouse was designed.

During the study the change to the LCG was considered keeping in mind that a significant change in the LCG would affect the other factors in the Ship Design Spiral such as stability, structural strength, and General Arrangement. Thus, these graphs are to be developed early in the design stage to select the most optimum LCG.

Once the hull mould was completed, the principal dimensions were obtained from the mould, and a lines plan was developed. The body plan of the planing hull used in the study is depicted in Figure 3 below. Then used the Rhino3D software to complete the 3D hull of the CPC, which was a necessity to import CPC dimensions/features for other software for the stability studies, hull drag, powering and structural design.

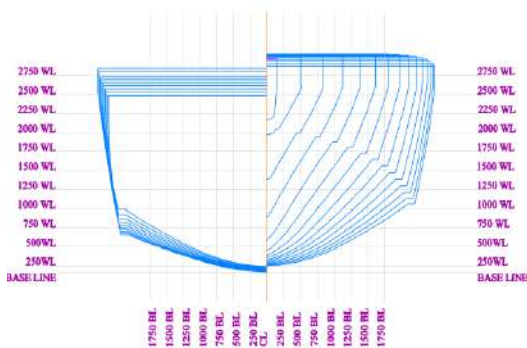


Figure 3. The body plan of the planing hull used in the study

The estimation of CPC weight and determining the principal features were the first step. In this endeavour, the concept of the Ship Work Breakdown Structure approach was employed. The basic equation for weight estimation of individual components using the ratiocination method is depicted as follows. Textbook formulas were considered (Enclosure 1) for different components to find corresponding coefficients. The principal coefficient estimations based on benchmarked parent hull is depicted at Table 1 below.

$$\text{New ship component weight} = \text{Parent hull component weight} * \frac{\text{New ship dimension}}{\text{Parent ship dimension}}$$

Table 1: Ratiocination values comparison

Description	CPC Ratiocination Values	Parent Boat Ratiocination Values
L (m)	15.76	13.50
B (m)	4.38	3.00
D (m)	2.79	1.40
Displacement (T)	27.50	10.40
SHP	2400.00	838.00
V (knots)	35.00	35.00
Cp	0.60	0.55
T (H) (m)	0.80	0.68
KW	21.50	5.7
LD	44.02	18.90

LB	69.03	40.50
$L*(B+2D)$	157.06	78.30
$\frac{L*D*(2D+B)^2}{2}$	4371.89	635.80
$LBD^2*C_p$	323.09	43.66
$LD^2$	122.94	26.46
$L(B+D)$	113.05	59.40
$2*(D-H)*L$	62.82	19.44
LBD/100	1.93	0.57
Crew	12.00	12.00

The weight, LCG, and Vertical Center of Gravity (VCG) derived from above approach and with data obtained from AutoCad and Rhino3D software were used as input data for Savitsky Programme to determine Hull Drag, Trim Angles, Effective Horse Power (EHP), etc. The basic inputs for the Savitsky Programme is depicted at Table 2 as follows.

Table 2: Input data for Savitsky programme

Length of Waterline	$L_{WL}$	15.767	m
Beam	B	4.380	m
VCG	VCG	1.469	m
Displacement	$\Delta$	27,000	kg
Deadrise Transom @	$\theta_T$	12.000	degree
Deadrise Amidships @	$\theta_A$	21.000	degree
Distance to Amidships	$L_A$	7.884	m
	$\theta$	2.724	degree

Angle of Thrust Line	$\alpha$	5.000	degree
	f	0.305	m
Minimum Speed	$V_{min}$	7.000	knots
Maximum Speed	$V_{max}$	45.000	knots
Length Overall	LOA	19.059	m
Maximum Beam	$B_{max}$	5.000	m
Moulded Depth of Hull	$\nabla$	2.850	m
Number of Propellers	N	2	

### 3. Results and Discussions

VCG, Transverse Center of Gravity (TCG), and LCG for each component weights were obtained from the General Arrangement plan and AutoCad drawings. The report was generated for three conditions (full load, arrival load, and lightship condition). The outcome was to finalize the CPC total weight, VCG, LCG, and TCG. The result for full load condition is depicted at Table 3 below. The position of the origin for the longitudinal moments is Transom.

Table 3: Total weight estimation

Weight Group	Weight (T)	VC G (m)	Moment (m-T)	LC G (m)	Moment (m-T)
Hull Weight	8.6	1.7	14.6	7.7	65.9
Engine Room	6.7	0.7	4.5	2.4	16.2
Aux Machinery Room	2.3	0.8	1.8	5.8	13.3
Berthing Areas	0.3	1.1	0.3	10.0	2.8

Wheel House and Galley	0.8	3.2	2.5	8.7	6.7
Flying Bridge	0.3	5.6	1.5	5.9	1.6
Deck	0.7	3.0	2.0	10.0	6.7
Full Load components	6.5	1.1	7.2	6.4	42.0
Sum	26.1		34.4		155.3
Full Load Weight	27.04	VC G (m)	1.47	LC G (m)	5.98

Note: According to SNAME margins for naval vessels or special ships following criteria were used.

- i. Weight Margin - 5% added to the lightship weight
- ii. VCG Margin - 0.5 ft added

Thereafter worked out a few LCG values (+) and (-) around the initial neutral value of LCG to understand the sensitivity of LCG for bare hull total resistance and other parameters. The results are depicted at Figure 4 below. It was evident with increase LCG additional drag in the form of hump is decrease at low boat speed (20 knots), yet adverse effect beyond 40 knots. Since CPC designed operate with 35 knots, minimum resistance below the planing regime was observed with LCG on or beyond neutral LCG.

Authors studied the steady dynamic wetted keel length comparison for different LCG positions and results are depicted at Figure 5. The power demands for the resultant LCG positions were compared as per the method described in ITTC Quality Manual 7.5-02. -05-01 and results are depicted in Figure 6. According to this association, the LCG on or near the initial neutral

position seems to be the optimum case, an CPC hull needs to operate sub planing speeds as well as the beyond the planing speeds with minimum EHP.

Finally, the dynamic trim comparison for different LCG positions is depicted at Figure 7 below. It was evident, at neutral LCG or beyond it CPC display low trim angles and around 20 knots CPC depicts planing features for all LCG values.

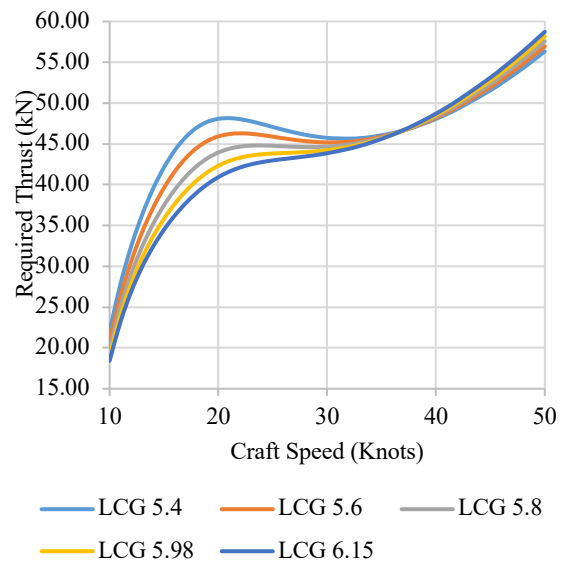


Figure 4. Change in Total Resistance with LCG Positions



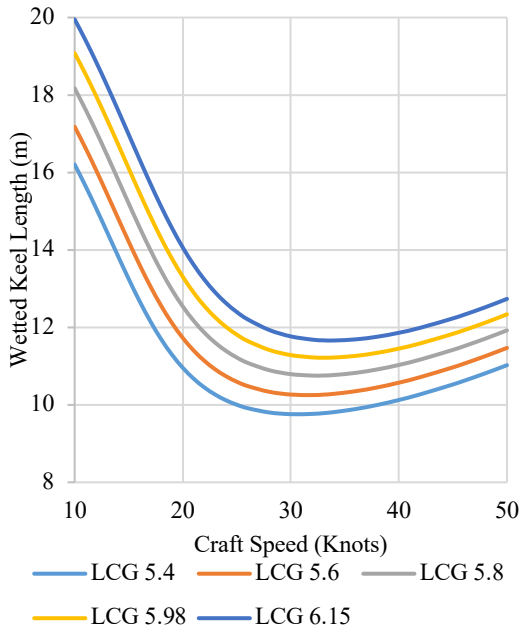


Figure 5. Dynamic wetted keel length comparison for different LCG positions

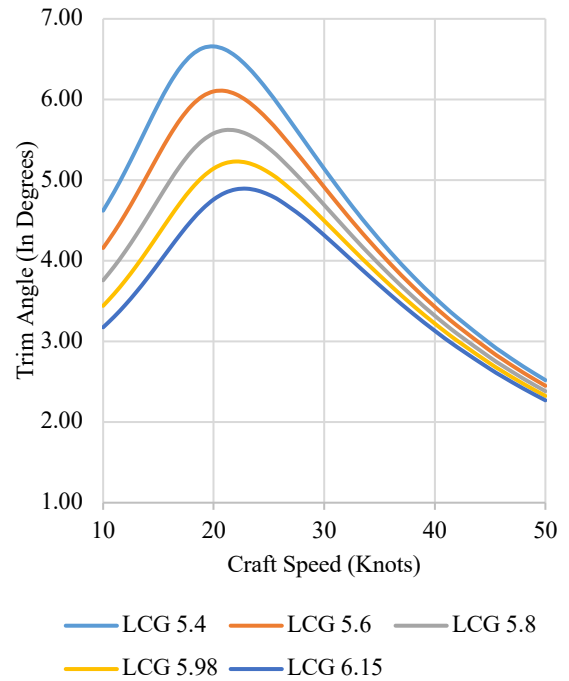


Figure 7. Change in dynamic trim angle with LCG

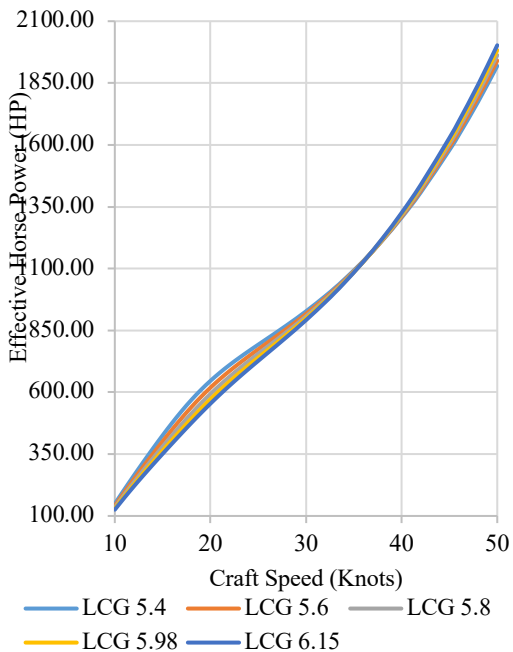


Figure 6: Effective Power Demand Comparison for Different LCG Positions

Authors then studied the Planing capabilities for different LCG positions with the spreadsheet written by Dingo Tweedie, October 2004. The various results are tabulated at Enclosure 2 to this article. It specifies the CPC speed which start Planing the craft. With increase of LCG from transom the speed required to plan the craft increases.

The NavCad commercial software with its database was used to validate the above outputs.

#### 4. Conclusion

Authors explored the behaviour of monohull Coastal Patrol Craft with the change in craft LCG positions and anticipated effect on the resistance, effective power demand, dynamic trim and planing capabilities based on numerical approach. Authors worked out a few LCG values (+) and (-) around the initial neutral value of LCG

to understand the sensitivity of LCG. Based on the results, a small initial trim angle is required for the CPC to display optimal performance at speeds in the upper range of the planing regime. On the other hand, an initial trim by aft would increase the performance of the CPC at speeds lower than the planing region but would adversely affect the performance at higher speeds as the trim further increases due to dynamic behaviour. Further, this increase in trim at higher speeds would result in dynamic instability and be detrimental to the performance of the craft. With the increase of LCG from transom the speed required to planing the craft increases. When LCG increases, to plan the craft, trim angles become large with higher speeds and cause dynamic instability a phenomenon called 'Porpoising'.

## References

- Baker, G. S. & Miller, G. H., 1912. Some experiments in connection with the design of floats for hydro-aeroplanes.. ARC R&M, p. 70.
- Larsson, L. & Eliasson, R., 2000. Principles of Yacht Design.
- Locke , F. J., 1948. Tests of a flat bottom planing surface to determine inception of planing, Navy Department, BuAer, Research division report.
- Sambraus, 1938. Planing-Surface Tests at Large Froude Numbers-Airfoil Comparison (No. NACA-TM-848).
- Savitsky, D., 1964. Hydrodynamic design of planing hulls. Marine Technology and SNAME News, Volume 1(04), pp. 71-95.
- Sedov, L., 1947. Scale effect and optimum relations for sea surface Planing (No. NACA-TM-1097).
- Shoemaker, J., 1934. Tank tests of flat and v-bottom Planing surfaces (No. NACA-TN-509).
- Sottorf, W., 1932. Experiments with planing surfaces (No. NACA-TM-661).

Su, Y., Chen, Q., Shen, H. & Lu, W., 2012. Numerical simulation of a planing vessel at high speed. ,. Journal of Marine Science and Application, Volume 11(2), pp. 178-183.

Su, Y., Wang, S., Shen, H. & Du, X., 2014. Numerical and experimental analyses of hydrodynamic performance of a channel type planing trimaran.. Journal of Hydrodynamics, Volume 26(4), pp. 549-557.

## Acknowledgment

Authors would like to acknowledge the Sri Lanka Navy for providing opportunity and required resources for Naval Architectural discipline.

## Author Biographies



Captain, Dinuk Sakoon Bogahawatte, Chartered Marine Engineer, perform as Head of Department at KDU. Last six year shouldered the responsibility of Manager Naval Boat Building Yard, Sri Lanka Navy. Graduated with BSc Eng (Hons) in Marine Engineering from KDU. Possess MBA from University of Moratuwa and Masters in Manufacturing Management from University of Colombo. Expert for Fast Attack Craft & Fast Missile Vessels fleet repairs.



Lieutenant Commander, PMKC Chandimal has graduated with BSc Eng (Hons) in Marine Engineering from KDU and also the Chartered Marine Engineer, perform as Lecturer (Probationary) at Department of Mechanical Engineering, KDU.



Lieutenant Commander, LAKR Athukorala has graduated from the United States Coast Guard Academy with a BSc. Eng (Honours) in Naval Architecture and Marine Engineering. Currently serves in the capacity of Staff Engineer Officer (Naval Architecture) at the Directorate of Naval Design, Sri Lanka Navy. Further, Visiting Lecturer on Marine Vehicle Design at the KDU since year 2020.

# Novel design of Cost-effective Solar Powered Brackish Water Reverse Osmosis Plant: A possible solution for an affordable supply of safe drinking water for the rural communities in CKDu-affected areas in Sri Lanka

MCP Dissanayake#

Department of Marine Engineering, Faculty of Engineering, General Sir John Kotelawala Defence University, Sri Lanka

#dissanayakemcp@kdu.ac.lk

**Abstract:** The government of Sri Lanka has established a Community-Based Organization (CBO) to supply safe drinking water on a payment basis through the application of electrically driven Brackish Water Reverse Osmosis (BWRO) plants in CKDu-impacted areas. Due to major drawbacks such as cost, issues in regular maintenance, membrane clogging, lack of expertise to rectify the defects encountered in electrically driven BWRO plants, etc. In this design, a multistage centrifugal high-pressure pump was integrated with the BWRO plant and drastically, bring down the manufacturing cost. Then, evaluate the performance of the Brackish Water Reverse Osmosis system powered by solar electric energy under Sri Lankan weather, and environmental circumstances, and enhance the recovery ratio up to 75% through an automated mixture. The novel design of the solar-powered BWRO plant can be manufactured locally at a low cost, and hence it would be the ideal replacement for imported BWRO plants to access high-quality drinking water for the farming community who could not have sufficient wealth to obtain safe drinking water on a payment basis. The solar-powered BWRO plant is considerably reduced the government overheads to subsidize the water purification cost up to 90% of the existing expenses. Further, it leads to protecting the environment by reducing Green House Gas (GHG) emissions with a more than 75% of recovery ratio.

Further, cost comparison of SLN manufactured BWRO vs imported BWRO in a similar capacity revealed that the SLN-manufactured BWRO plant was 7fold cheaper than that of the imported BWRO plant.

**Keywords:** Brackish Water Reverse Osmosis; Chronic Kidney Disease unknown etiology, Safe Drinking Water; Sri Lanka; Net Metering System

## 1. Introduction

A newly published United Nations (UN) world water development report 2019 mentioned that the climate is continuously changing and it impacts societies mostly due to decreasing water bodies (International standards for drinking water, 2019) . Further, this article brings out the facts; that water contamination is one of the major catastrophes that lead to jeopardizing global sustainable development goals and threatening the lives of billions of people . According to the water quality standards defined by World Health Organization (WHO), Total Dissolved Solids (TDS) in safe drinking water should be below 500 mg L-1 [1]. However, in seawater TDS is 35, 000 mg L-1 or more while in brackish water it is around 1000 to 15 000 mg L-1.

Brackish Water Reverse Osmosis (BWRO) is an elementary water purification application; that

is more commonly used to overcome freshwater scarcity in many regions of the world. However, it is contributing to Green House Gas (GHG) emissions. Therefore, many scientists and engineers are investigating integrating renewable energy with BWRO plants as a possible alternative solution to reduce the production cost of product water. Countries such as Australia, Singapore, Spain, and Arabian countries are the usual contenders in reverse osmosis operation in a global context and accessing safe drinking water to billions of people without operational difficulties. However, the operation of the BWRO plant is an energy-intensive process; and the manufacturing cost is also very high. Therefore, this BWRO application is not practically feasible for lower-income communities that are combating to access clean drinking water

Due to the deaths of over 22,000 people from CKDu in Anuradhapura district in the North Central Province (NCP) in Sri Lanka since it was first identified in 1991, WHO had recommended several measures to control the prevailing situation such as regulating fertilizers and agrochemicals use, providing safe drinking water, better health facilities, and also financial support for the victims (Wanasinghe, et al, 2018) Therefore, the government of Sri Lanka has established a Community-Based Organization (CBO) to supply safe drinking water through the application of BWRO plants in CKDu-impacted areas on a payment basis (Dissanayake, et al, 2021). Further, Sri Lanka National Water Supply and Drainage Board (NWSDB) and Non-Governmental Organizations (NGOs) also installed BWRO plants that had been imported from Israel and the USA at a very high cost. However, due to several reasons such as insufficient wealth of the farming community to obtain safe drinking water on a payment basis, walking a longer distance to access purified water, regular membrane clogging, non-availability of skilled personnel for defect rectifications, repairing, high power

consumption and low recovery ratio, the government could not have achieved the expected outcomes (Indika, et.al, 2021).

Sri Lanka Navy (SLN) has been pioneering Reverse Osmosis operations on board naval vessels since 1992 and therefore, SLN is sufficient with expertise, modern workshop facilities, and skilled personnel to handle any situation, in BWRO techniques. Economic feasibility has been recognized as the major concern while developing improved BWRO plants for the continuous supply of clean water to rural communities with low income in CKDu-impacted areas in Sri Lanka. Hence, it is necessary to consider manufacturing costs, enhance the product water supply (recovery ratio), and ease up the existing situation. Sri Lanka lies within the equatorial belt and thus substantial solar energy can be acquired mostly throughout the year for any applications. The main aim of this research was to develop a novel design of a solar-powered efficient BWRO plant with a multistage high-pressure centrifugal pump and efficient membrane arrangement to optimize manufacturing cost, and produce more units to supply safe drinking water for the impacted communities, enhance the recovery ratio, and membrane lifetime.

## **2. Methodology and Experimental Design**

The capacity of the BWRO plant was defined as 10 tons/day to initiate the proposed project and the most vulnerable locations of CKDu prevailing areas in the country such as Vavuniya (Irrattaperilakulam), Sri Lanka Naval Ship Pandukabaya (SLNS) (Poneewa), Madawachchiya Town (Mithreepala Senanayake Central College), Dutuwewa Village and Kadawthrabewa Village in the Madawachchiya area at Anuradapura district were targeted (Ranasinghe, et al., 2019).

### **A. Water Quality Analysis**

Water quality parameters of collected feed water samples from those targeted areas were tested

at the Industrial Technology Institution (ITI), Sri Lanka to determine the nature of the water quality of the collected water aiming at designing suitable BWRO plants for those targeted locations. Physical water quality parameters (pH, Colour, and Turbidity) were tested through APHA 4500 - H+B, APHA 2120 B, and APHA 2130 B respectively. Then, chemical water quality parameters (hardness, alkalinity, metal cations, and anions) were tested by APHA 2340 C, APHA 2320 B, APHA 3125 B, and APHA 4500 CI- respectively. Product water samples were tested at Sri Lanka Water Board.

### B. Designing a Low-Cost BWRO Plant

1) Selection of a Feed Water Pump: The effective pre-treatment process is crucial to improve the quality of the feed water to the level that would result in the reliable operation of the BWRO filtration practice. According to the raw water quality, the pre-treatment application was designed with the following, all or some treatment steps; incorporate chlorination process, apply with lime treatment, fix with media filtration, pH adjustment, water sterilization (Ultraviolet (UV) filter) and fix with micron filters as the final step (Knops, et al., 2007).

The capacity of the feed pump was decided considering the capacity of the BWRO plant, and calculations were done as follows;

Required outlet pressure bar	=	3
Gross Feed Flow rate for filtration m <sup>3</sup> /hr	=	2.5
Capacity 0.7457 kW (1 HP)	=	

2) Designing of Multimedia Filters: Gross Feed Flow rate for filtration is the most concerning factor to design vessel sizes.

$$F_f = F_{fn}/N_f \quad (1)$$

Where,  $F_f$  is feed flow per filter

$N_f$  is the number of filter units

$F_{fn}$  is feed flow to a filtration plant

$$N_f = 2$$

$$F_{fn} = 2.5 \text{ m}^3/\text{hr}$$

$$F_f = 2.5\text{m}^3/2 = 1.25\text{m}^3/\text{hr}$$

Required cross-sectional areas for multimedia filter vessels are as follows;

$$A_f = F_f/F_{sd} \quad (2)$$

Where,  $A_f$  is the cross-sectional filtration area per filter

$F_f$  is feed flow per filter

$F_{sd}$  is service down-flow rate

A downflow of a sand filter is one of the key factors for calculating the cross-sectional filtration area. Further, downflow sand filters are directly impacting to separate from solid to liquid at flow rates up to about 18 m<sup>3</sup>/h m<sup>2</sup> of filter (Ezzeghni, 2018)[11].

$$A_f = 1.25/18 = 0.0694 \text{ m}^2$$

$$A_f = \pi/4 (ID)^2 \quad (3)$$

Where, ID is required internal diameter

$$ID = 0.3 \text{ m}$$

Then, two commercially available filter vessels (12' x 52') were selected for this application and they were filled with sand and active carbon up to 50% of their capacities while keeping 50% freeboard to allow bed expansion during the backwash cycle.

3) Selection of a High-Pressure Pump: A detailed study was carried out on the operating pressures of existing imported BWRO plants that

were functioning at Naval Bases in NPC, and it was revealed that the operating pressures were always maintained below 12 bar, with half load conditions even in the driest season (Table 1). Subsequently, it was realized that there was a high routing maintenance cost and a very high monthly electrical bill during this type of BWRO operation. When the high-pressure pump of the BWRO plant was checked, it was revealed that there was a positive displacement (gear pump) with the overpressure protection. Therefore, a comparison between the Positive Displacement Pump and Centrifugal Pump was carried out to select the suitable high-pressure pump for this BWRO design (Supplementary Table 1).

Table 1. Level of Total Dissolved Solids of feed water and operating pressures of imported BWRO plants at Sri Lanka Navy Bases, North Central Province

Location	Total Dissolved Solids (TDS) mg L <sup>-1</sup>	Maximum Operating Pressure (bar)
SLNS Pandukabaya	707	10
SLNS Tammanna	814	12
SLNS Shiksha	710	10
SLNS Gajaba	796	12
SLNS Buwaneka	823	12

The operating pressures of imported BWRO plants were studied to select a suitable high-pressure pump for this low-cost BWRO application (Table 1).

4) Selection of a Membrane: A spiral wound of 10.16 x 101.6 cm<sup>2</sup> (4 x 40 inch<sup>2</sup>) membranes was matched with this new design according to the

availability of membranes in the local market, productivity, feed water hardness, and TDS. Subsequently, it was decided to fix membranes in serial with each other to the BWRO plant for enabling enhanced productivity (Jayasumana, et al., 2016) (Figure 2). The membrane specifications are as follows;

- i. Capacity - 250 LPH
- ii. Type -10.16 x 101.6 cm<sup>2</sup> (4 x 40 inch<sup>2</sup>) spiral wound
- iii. Make -Vontron
- iv. Effective Area -7.9 m<sup>2</sup> (85 ft<sup>2</sup>)
- v. Material -Polyethylene
- vi. Model - 400
- vii. Operating Pressure -200 psi

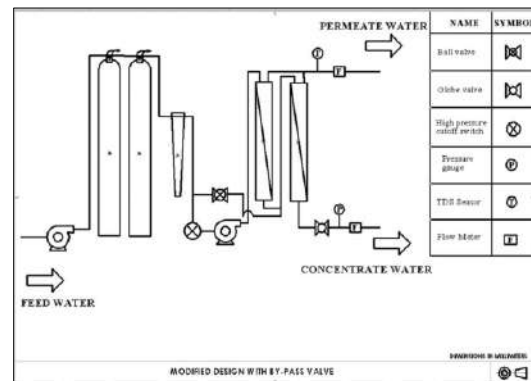


Figure 1. Modified design with by-pass valve (Ahn, et al., 2008)

### C. Setting up of the BWRO Plant

The BWRO plant setup was comprised of a raw water tank, feed pump, multimedia filter, cartridge filter, high-pressure pump, RO modules, and two flow meters (McMordie, et al., 2013). The spiral wound membrane [(brand Vontron) 10.16 X 101.6 cm<sup>2</sup> (4 X 40 inch<sup>2</sup>)] with an effective membrane area of 7.9 m<sup>2</sup> (85 ft<sup>2</sup>) was installed with this BWRO Plant. The experiments were conducted at ambient

temperature with a fully operational mode to get safe drinking water. The BWRO system was encompassed with Polypropylene Random Copolymer (PPR) pipes that sustain 25 bar pressure. The capacity of the feed water tank is 5000 L, and the feed pump was operating under 3 bar pressure for the pre-treatment process by an overhead tank. Then, pre-treated water was pressurized by the 15-bar multistage centrifugal high-pressure pump and the permeate was taken off from one pipe and connected to a 1000 L tank, and allowed rejection flow through another pipe to reject water collected to another 1,000 L tank. In this BWRO process, both the membranes were installed to the system in serial to each other, and then parameters were investigated (Qiu & Davies, 2012)(Figures 2&3).



Figure 2. The Brackish Water Reverse Osmosis Plant with a capacity of 10 tons/ day was developed by Sri Lanka Navy.

Table 2. Cost Comparison of Locally made Brackish Water Reverse Osmosis Plant Vs Imported Brackish Water Reverse Osmosis Plant in Similar Capacity (10 tons/Day)

Description	Qty (Nos)	Rate (US\$)	Cost for Local Plant (US\$)	Cost for Imported Plant (US\$)
Feed water pump (1HP, Single Phase)	1	195	195	2,450

Sand filter (13"X54")	1	170	170	800
Carbon filter (13"X54")	1	240	240	800
15 L Chemical dosing pump	1	130	130	1,250
40 L Chemical tank	1	42	42	400
Low-Pressure sensor (0-3 bar)	1	25	25	500
High-Pressure pump (0-15 bar)	1	650	650	4,500
Control panel (Locally made)	1	265	265	1,400
20" Filter Housing	1	25	25	150
20" Filter element	1	10	10	150
10" Filter Housing	1	10	10	100
10" Filter element	1	2	2	50
Membrane housing & membranes	2	240	480	8,600
PPR Pipes and joints	1	590	590	2,800
BWRO skid	1	210	210	1,100
Panel mount flow meter	2	20	40	200
Line mount flow meter	3	25	75	350
<b>Total</b>			<b>3,159</b>	<b>25,600</b>

#### D. Design of Solar-Powered Control System



In this research, BWRO plants of Vavuniya (Irrattaperilakulam) and Madawachchiya Town (Mithreepala Senanayake Central College) were connected to the Net Metering System concerning product water requirement, the electrical conductivity of feed water, and atmospheric temperature. Further, the focal point of this novel system is to achieve the correct balance between the daily requirement of electrical energy consumption by the loads and the daily production of solar-powered electrical energy (Rifai, et al., 2015). Therefore, at outset, it is very important to ascertain daily desirable solar-powered electrical energy and the total peak power of solar generators (Table 3). This net metering system is a bit different from the traditional solar powering system and is connected to the national grid and supplies power to the national ring main during the daytime and reversely operated the electricity meter which is fixed by the Sri Lanka electricity board. Then, while BWRO planting is operating, the same electricity meter is running in the correct direction and deducts the amount that was supplied to the national grid.

*E. Total power requirement for BWRO plant*

- i. Power requirement of high-pressure pump = 2.2 kW
- ii. Power requirement of feed Pump = 1.0 kW
- iii. Power requirement of dosing Pump
- iv. and Control Panel = 0.8 kW
- v. Total Power Requirement = 4.0 kW

Considering the total power requirement of the BWRO application, a 5 kW solar panel was incorporated into the Net Metering System (Filippini, et al., 2019).

Table 3. Mean Monthly Solar Radiation in Sri Lanka [8]

Month	Mean Monthly Solar Radiation (kWh/m <sup>2</sup> ,day)
January	5.35
February	5.5
March	5.7
April	6.0
May	5.0
June	4.9
July	4.6
August	4.8
September	4.6
October	4.5
November	5.0
December	5.25

*F. Test Procedure*

The function of the BWRO was demarcated into two processes such as pre-treatment and reverse osmosis operations. As per the preliminary step, a pre-treatment procedure was conducted to remove turbidity, and muddiness and improve the efficiency of coagulation (McMordie, et al., 2013). Accordingly, two numbers solar-powered net metering systems were fixed with BWRO plants at Vavuniya (Irrattaperilakulam) and Madawachchiya Town (Mithreepala Senanayake Central College). The other three BWRO plants were connected to National Grid Power Supply. Subsequently, reverse osmosis operation began through a control panel. Only single-mode operation is comprised of the control panel including the operation of high-pressure and low-pressure safety cut-outs. Both the feed

water pump and high-pressure pump were operated simultaneously to avoid developing a vacuum inside the PPR pipes and both sand and carbon filters. The feed water is flowing through the sand filter and the active carbon filter as a pre-treatment process (Raju & Ravinder, 2018). Then, water is flowing through the cartridge filter up to the high-pressure pump. Eventually, water is pressured up to 10 bar by a high-pressure pump and allowing water to flow through both membranes and collect the product water into a 1000 L tank and permit reject water collection to another 1,000 L tank. Then, the reject water tank is connected to feed water through a mixture, which can regulate the feedwater conductivity automatically or manually. In addition, whenever product water flow is declining badly, the cleaning cycle starts automatically and cuts off the high-pressure pump and backwashes the membranes, and cleans. Recovery ratio calculation was carried out for six months and obtained the mean value. Subsequently, daily water consumption and monthly electricity bills were checked for six months and obtained a mean value.

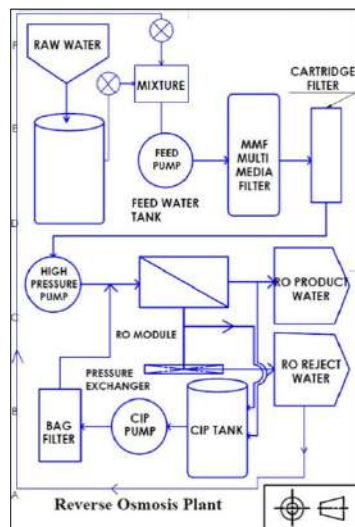


Figure 3. The Schematic of the Brackish Water Reverse Osmosis Plant was developed by Sri Lanka Navy

### G. Operation and Routine Maintenance

Many BWRO plants functioning in Sri Lanka are distributed with no form of verified technical documentation, thus questioning their efficacy and efficiency for a sustainable operation (Indika, et al., 2021). Therefore, SLN introduced a trainer-trainee course for BWRO plant operators with a proper set of guidelines to avoid occurrences of regular defects and stoppages to maintain a continued supply of safe drinking water for the affected community in December 2015. Further, SLN operators are engineering mechanics in the profession and very sound in technical operations and maintenance of the BWRO plants. Moreover, SLN adopted an administrative method to gather monthly operation parameters, maintenance details, and water consumption named 'monthly return of BWRO plants' in Annex 'A' to this report. In addition, workshop facilities have been established in Welisara Navy Camp, SLNS Padukabaya, SLNS Mahanaga, and SLNS Barana to handle any emergency breakdowns without difficulties and make the BWRO plants operational to supply safe drinking water around the clock.

### H. Membrane Cleaning Mechanism

This mechanism was designed and developed locally with the utilization of practical experience gathered during my BWRO research. In this design, a 4-bar pressure pump is fixed with membrane housing through a 10-bar pressure gauge, using PVC pipes, and then, fixed with a 20 L stock tank which is filled with the detergent mixture. Subsequently, a clogged membrane is installed with housing, and operate the system with 1 bar pressure then regulate pressure from time to time, at least 4 hours.



Figure 4. Membrane Cleaning Mechanism

### 3. Results and Discussion

Physicochemical water quality parameters of all five locations were tested through ITI and indicated (Supplementary Table 2).

Table 5. Comparison Average product water parameters in five selected locations

Location	Water Input (L)	Recovery (L)	Recovery Ratio (%)
Vavuniya	1000	756	75.6
SLNS Pandukabaya (Poneewa)	1000	751	75.1
Madawachchiya	1000	758	75.8
Dutuwewa	1000	755	75.5
Kadawathrabe wa	1000	746	74.6

SLS-Sri Lanka Standard

Table 6: Recovery ratio of all five locations

Parameters	Product water	SLS Requirement
Colour Hazen units (max)	10	15
Turbidity NTU (max)	0.88	2
pH at 25 <sup>o</sup> C	7.2	6.5 - 8.5
Electrical Conductivity S/m	163	
Chloride (as Cl) mg/l	14.5	250
Total Alkalinity (as CaCO <sub>3</sub> ) mg/l	50	200
Total Dissolved Solids mg/l	48	500
Nitrate (as NO <sub>3</sub> <sup>-</sup> ) mg/l	8.1	50
Nitrite (as NO <sub>2</sub> ) mg/l	0.012	3
Fluoride (as F) mg/l	0.04	1.0
Total Phosphates (as PO <sub>4</sub> ) mg/l	0.45	2.0
Sulfate (as SO <sub>4</sub> ) mg/l	1	250
Total iron (as Fe) mg/l	0.1	0.3
Magnesium (as Mg) mg/l	0.001	0.1

BWRO design was purely dependent on the following Feedwater parameters such as TDS, Total Hardness, Calcium, Magnesium, Arsenic, and Cadmium are critical factors that are considered during the designing of a suitable BWRO plant. The permissible levels of TDS, Total Hardness, Calcium, Magnesium, Arsenic, and Cadmium contents offered water as per SLS 614 and exiting levels of those feed water quality parameters in five selected locations (Vauniya

(Irrattaperilakulam), Sri Lanka Naval Ship Pandukabaya (SLNS) (Poneewa), Madawachchiya Town (Mithreepala Central College), Dutuwewa village and Kadawthrabewa village were shown in figure 6.

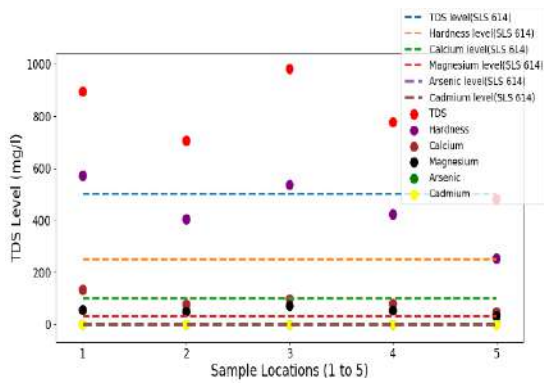


Figure 6. Feedwater quality parameters (solid lines) of BWRO plant operated in Vavuniya (Irrattaperilakulam), Sri Lanka Naval Ship Pandukabaya (SLNS) (Poneewa), Madawachchiya town (Mithreepala Central College), Dutuwewa village, and Kadawthrabewa village. Values of Total Dissolved Solids (TDS) and level of magnesium in product water were shown in red and black lines. Dash lines indicate the permissible levels as per the Sri Lankan standard 614 (SLS 614).

More importantly, analysis of feed water quality revealed that the values of TDS at locations 1 and 4 were above the permissible limit except at location 5. Further, the value of total hardness at all five locations (locations 1-5) was above the permissible limit. The calcium content of feed water at Vavuniya (Irrattaperilakulam) is higher than the permissible value but the Calcium content of feed water in other four locations (Sri Lanka Naval Ship Pandukabaya (Poneewa), Madawachchiya Town (Mithreepala Senanayake Central College), Dutuwewa Village, and Kadawthrabewa Village) are below the permissible value of SLS 614. The magnesium content of feed water in all five locations is greater than the permissible value of SLS 614. The level of Arsenic and Cadmium was not

detected in all samples except location 4. Though the amount of Arsenic level in location 4 was within the limits of SLS 614, however Cadmium level was not detected in this sample.

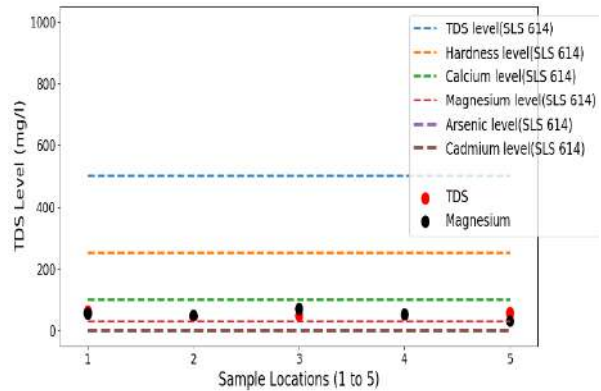


Figure 7. Product Water Parameters (solid lines) in Vavuniya (Irrattaperilakulam), Sri Lanka Naval Ship Pandukabaya (SLNS) (Poneewa), Madawachchiya Town (Mithreepala Central College), Dutuwewa village, and Kadawthrabewa village. Values of Total Dissolved Solids (TDS) and level of Magnesium in product water were shown in red and black lines. Dash lines indicate the permissible levels as per the Sri Lankan Standard 614 (SLS 614).

Most of the imported BWRO plants have been encompassed with positive displacement high-pressure pumps, and they can be pressurized up to 25 bar. Further, the flow rate remains constant with a variation in pressure (Purcell & Silvaggio, 1997). Though, their operating pressure of them was always maintained at less than 12 bar at Naval Bases, NPC due to good quality feed water inputs. Considering the above facts, 15 bars multistage centrifugal high-pressure pump was chosen in this novel BWRO application to bring down the manufacturing cost [Supplementary Table 1].

In this study, different configurations of electrically driven BWRO systems have been tested however, it was realized that the recovery can be improved by up to 75% but with high

electrical energy consumption (Qiu & Davies, 2012). In the global context, brackish water desalination plants are powered by solar with battery banks and are a bit expensive affair (Mahmoud, 2003). Therefore, to make the process economically feasible, a solar-powered net metering system was incorporated into this novel design. Further, a cost comparison between SLN the novel design of a solar-powered BWRO plant, and an imported electrically driven BWRO plant with a similar capacity revealed that the SLN-manufactured novel design of solar-powered BWRO plant was 7-fold cheaper over the use of electrically driven imported BWRO plants. Application of the novel design of solar-powered BWRO operation in Vavuniya (Irrattaperilakulam) and Madawachchiya Town (Mithreepala Central College) in Sri Lanka, a drastic reduction in the cost of electricity was achieved compared to the other three locations where electrically driven BWRO plants operated [Supplementary Table 3]. Further, the production cost of purified water was reduced and the payback period for the net metering system was approximately 7 years and six months. In addition, product water recovery is improved by up to 75% [Table 6].

However, in the Sri Lankan context, it has been recognized that most of the BWRO plants contained membranes in parallel to the applications and the recovery ratio is an average of 39% and membrane lifetime is limited to one year or a little more as per the operator's skill (Indika, et al., 2021). Therefore, this novel BWRO plant has been configured with the automated mixture (sets of valves) which facilitates the measurement of conductivity and TDS of reject water, then induct as feed water into the pre-treatment process. Subsequently, the stage array membrane fixing method was incorporated with a novel application and enhanced the product water recovery up to 75% and meets the mandatory requirement of the United States Environmental Protection Agency. In addition, it

shows that the membrane lifetime is enhanced to 2 years and a little more.

SLN operators are manning BWRO plants around the clock and are ready to supply safe drinking water for consumers at any given time. Further, they are providing 20 L for family and maintaining records daily basis. Subsequently, SLN BWRO operators are carrying out daily backwashing 100% and ensuring all the operating parameters are within specified limits. Therefore, regular defects and membrane clogging are not taking place compared to CBO-operated BWRO plants (Indika, et al., 2021). In addition, monthly returns are evident that the maintenance cost of these BWRO plants is very minimal (annually 135 USD), and issuing more than 5,000 L per day of safe drinking water to the CKDu-impacted community. Generally, membranes were replaced after 2 -3 years due to the fouling and scaling leading to low recovery. Then, the replacement of membranes was depending on feed water quality, the efficiency of the pre-treatment process, and best practices such as avoiding lower pressure operation below standard value by operators. Further, an improvised membrane cleaning method is adopted by SLN experts and enhances the lifetime by one year. Cartridge filters were replaced once every six months. However, it was experienced that the cartridge filters were become dark brown colour after operating the BWRO plant for a few days especially in the dry season due to inorganic precipitants and clogging sediments such as manganese and oxides of iron in the feed water and then, washed by the operator and reused it. Though, regular cleaning of filters becomes vain after a few cleaning cycles and shows the requirement for replacement. Usually, the replacement period of the cartridge filter was depending on the efficacy of the sand filter, Carbone filter, and feed water quality. Consequently, skilled SLN operators adopted one method to wash sand and active Carbone and reused them, and enhanced the life of sand and Carbone filters [Table 5].

The operating pressure of the BWRO plant is one of the main and critical parameters which specify the existing condition of the membrane. The chemistry of the feed water is the key factor that fluctuates the pressure inside the membrane and also, and maintaining proper and standard pressure is somewhat challenging (Ahn, et al., 2008). Normally, all five BWRO plants were operated at 8 to 12 bar even in the direst season.

In this context, it is revealed that the essential minerals were rejected during this BWRO operation and become a major drawback of this application (Indika, et al., 2021). Therefore, the automated mixture is incorporated with this novel system, and the percentage of rejected water mixed up with product water and remineralization was adopted and then, avoid taking place any health-related issues among CKDu impacted community. In addition, SLN operators and repair teams are regularly carrying out water quality tests in both feed water and product water and maintaining the standards specified by SLS.

The novel design of the solar-powered BWRO plant can be manufactured locally at a low cost, and hence it would be the ideal replacement for imported BWRO plants to access high-quality drinking water for the farming community who could not have sufficient wealth to obtain safe drinking water on a payment basis (Dissanayake, et al., 2021). Subsequently, it is making the pathway to access safe drinking water for the impacted communities, which makes a huge impact on the prevention of prevailing CKDu among rural populations living in CKDu-impacted areas.

#### **4. Conclusion**

The solar-powered BWRO plant considerably reduced the government overheads to subsidize the water purification cost by up to 90% of the existing expenses with minimal GHG emissions. Further, introducing 15 bars multistage

centrifugal high-pressure pump is a viable solution to bring down the manufacturing cost with moderate power consumption. Moreover, the recovery ratio is enhanced up to 75%. In addition, using skilled operators and best practices would minimize defect occurrences and enhance the lifetime of the BWRO plant. Therefore, recommend integrating a net metering system for all BWRO plants to bring down government expenses. Further, PVC pipes with gauge  $10^3$  instead of PPR pipes in the BWRO system can be recommended to bring down the manufacturing cost.

#### **Reference**

- Ahn, J., Chung, W., Pinnau, I. & Guiver, M., 2008. Polysulfone/silica nanoparticle mixed-matrix membranes for gas separation. *Journal of Membrane Science*, Volume 314 (1), pp. 123-133.
- Dissanayake, M., 2020. Dissanayake, M.C., 2020. An Air Operated Domestic Brackish Water Reverse Osmosis Plant: Economically Sustainable Solution for Safe Drinking Water Supply for Chronic Kidney Disease of Unknown Etiology Affected Areas in Sri Lanka. X. *Journal of Water Resource* .
- Dissanayake, M., Ginige, R. & Fernando, K., 2021. Chronic Kidney Disease of Unknown Aetiology in Sri Lanka: An Implication of Optimizing Recovery Ratio of Brackish Water Reverse Osmosis Plant..
- Ezzeghni, U., 2018. Designing and optimizing 10,000 m<sup>3</sup>/day conventional SWRO desalination plant.
- Filippini, G., Al-Obaidi, M., Manenti, F. & Mu, 2019. Design and economic evaluation of solar-powered hybrid multi-effect and reverse osmosis system for seawater desalination. pp. 114-125.
- Indika, S. et al., 2021. Evaluation of Performance of Existing RO Drinking Water Stations in the

North Central Province Sri Lanka. Volume 11(6), p. 383.

International standards for drinking water, 2019. Leaving no, one behind. The United Nations world water development report,1963., s.l.: World Health Organization.

Jayasumana, C. et al., 2016. Reverse osmosis plant maintenance and efficacy in chronic kidney disease endemic region in Sri Lanka. Environmental health and preventive medicine. Volume 21(6), pp. 591-596.

Knops, F., Van Hoof, S., Futselaar, H. & Broens, S., 2007. Economic evaluation of a new ultrafiltration membrane for pretreatment of seawater reverse osmosis. Desalination. Volume 203(1-3), pp. 300-306.

Mahmoud, M., 2003. Solar electric powered reverse osmosis water desalination system for the rural village, Al Maleh: design and simulation. International Journal of Sustainable Energy, Volume 23(1-2), pp. 51-62.

McMordie, H., Stoughton, K., Wendel, E. & Duan, X., 2013. Reverse Osmosis Optimization (No. PNNL-22682). Pacific Northwest National Lab.(PNNL), Richland, WA (United States).

Purcell, J. & Silvaggio, J., 1997. A comparison of positive displacement and centrifugal pump applications. In Proceedings of the 14th international pump users' symposium. Texas A&M University. Turbomachinery Laboratories.. s.l., s.n.

Qiu, T. & Davies, P., 2012. Comparison of configurations for high-recovery inland desalination systems. Volume 4(3), pp. 690-706.

Raju, Y. & Ravinder, R., 2018. Reverse Osmosis Plant Design and Evaluation-A Case Study. International Journal of Latest Trends in Engineering and Technology IJLTET, Volume 10(3).

Ranasinghe, A., Kumara , G. & Karunarathna, R., 2019. The incidence, prevalence, and trends of

Chronic Kidney Disease and Chronic Kidney Disease of uncertain etiology (CKDu) in the North Central Province of Sri Lanka: an analysis of 30,566 patients. p338., Volume 20, p. 338.

Rifai, S. et al., 2015. Off-Grid Development of Sustainable Energy Resources for Ecotourism Facilities in Kalpitya Peninsula Sri Lanka..

Wanasinghe, W., Gunarathna, M. & Herath, 2018. Drinking Water Quality on Chronic Kidney Disease of Unknown Etiology (CKDu) in Ulagalla Cascade, Sri Lanka.Sabaragamuwa Uni.. Volume 16(1), pp. 17-27.

### Author Biography



Cmde (E) MCP Dissanayake, CEng (India) is currently performing as the Head of Department (MarineEngineering) and holds 2 patents for his research papers published so far. He is an inventor and published 06 No's publications on Brackish Water Reverse Osmosis application, Fan Boat Building and Oscillation Water Column, Ocean Wave Energy Converter. He was the Director in Research & Development at Sri Lanka Navy and has received commendations on number of occasions from the Commander of the Navy, HE the President of Sri Lanka for his innovation. Further, he was awarded with prestigious, Japanese, Sri Lanka Technical Award for his own developed low-cost Reverse Osmosis Plant, to eliminate Chronic Kidney Disease from Sri Lanka. Moreover, he has vast exposure on marine diesel engines and possesses a Master's degree in Marine Engineering from Australian Maritime College, University of Tasmania, Australia.

Supplementary Table 1. Comparison of Positive Displacement Pump Vs Centrifugal Pump

Feature	Positive Displacement Pump	Centrifugal Pump
Mechanism	Develop pressure by generating flow	Develop flow by generating pressure
Performance	Flow rate remains constant with a variation in pressure	Flow rate contrasts with a variation in pressure
Viscosity	Flow rate quickly inclines with an increment of viscosity	Flow rate quickly decline with an incline of viscosity
Efficiency	Efficiency is very minimally affected by pressure (High)	Optimum efficiency at a specific pressure and decreased efficiency as per variation of pressure (low to moderate)
Power Consumption	High	Moderate
Cost	High	Low

Supplementary Table 2. Physicochemical water quality parameters of feed water in five villages

Test	Requirement (Maximum)	Method	Results					L. O. D.	E.U.% (k=2)
			Vauniyawa	SLNS Pandukabaya	Mada wchc hiya Twon	Dutu wewa	Kadawathrebe		
Colour	15 Hazen units (max)	APHA 2120 B	ND	ND	ND	ND	ND	5	
Odor	Unobjectionable	CML 1	UnOb:	UnOb:	UnOb:	UnOb:	UnOb:		
Turbidity	2 NTU (max)	APHA 2130 B	ND	ND	ND	ND	ND	1.0	
pH at 25°C	6.5 - 8.5	APHA 4500 H+B	7.33	7.48	7.27	7.47	7.95		
Chloride (as Cl)	250 mg/l	APHA 4500 Cl- B	104	71	138	89	36		4
Total Alkalinity (as CaCO <sub>3</sub> )	200 mg/l	APHA 2320 B	510	403	498	438	358		4
Free Ammonia (as NH <sub>3</sub> )	0.06 mg/l	SLS 614:2013,	ND	ND	ND	ND	ND	0.02	



Albuminoidal Ammonia (as NH <sub>3</sub> )	1.15 mg/l	Appendix A	0.06	0.08	0.08	0.1	0.16		
Nitrate (as NO <sub>3</sub> <sup>-</sup> )	50 mg/l	APHA 4500-NO <sub>3</sub> <sup>-</sup> B	13.1	19.0	18.6	8.7	11.6		
		CML/MM /02/02/019/V1.2							
Nitrite (as NO <sub>2</sub> )	3 mg/l	APHA 4500 - NO <sub>2</sub> <sup>-</sup> B	ND	0.05	0.03	ND	ND	0.03	14
Fluoride (as F)	1.0 mg/l	APHA 4500 - FC	0.8	1.2	0.97	0.87	1.1	0.10	6
Total Phosphates (as PO <sub>4</sub> )	2.0 mg/l	APHA 4500 - P B & C	ND	ND	ND	ND	ND	1	
Total Dissolved Solids	500 mg/l	APHA 2540 C	896	707	981	777	481		
Total Hardness (as CaCO <sub>3</sub> )	250 mg/l	APHA 2340 C	572	403	537	423	253		4
Sulfate (as SO <sub>4</sub> )	250 mg/l	Modified APHA 4500 SO <sub>4</sub> <sup>2-</sup> E	60	45	75	50	25		
Calcium (as Ca)	100 mg/l	APHA 3500 Ca - B	133	78	96	80	47		
Magnesium (as Mg)	30 mg/l	APHA 3500 Mg - B	57	50.0	72	54	32		
Cyanide (as CN)	0.5 mg/l	CML 18	ND	ND	ND	ND	ND	0.05	
Sodium (as Na)	200 mg/l	APHA 3125 B	59.3	63.3	87.4	60.0	75.9		
Total Iron (as Fe)	0.3 mg/l		ND	ND	ND	ND	ND	0.01	
Copper (as Cu)	1.0 mg/l		ND	ND	ND	ND	ND	0.01	
Manganese (as Mn)	0.1 mg/l		0.003	0.003	0.14	0.002	0.006		

Zinc (as Zn)	3.0 mg/l		0.03	ND	ND	ND	ND	0.01	6.3
Aluminum (as Al)	2.0 mg/l		ND	0.01	ND	ND	ND	0.01	
Chromium (as Cr)	0.05 mg/l		ND	ND	ND	ND	ND	0.01	
Nickel (as Ni)	0.02 mg/l		ND	ND	ND	ND	ND	0.01	
Arsenic (as As)	0.01 mg/l		ND	ND	ND	0.002	ND	0.01	2.6
Cadmium (as Cd)	0.003 mg/l		ND	ND	ND	ND	ND	0.01	
Lead (as Pb)	0.01 mg/l		ND	ND	ND	0.002	0.002	0.01	
Selenium (as Se)	0.01 mg/l		ND	ND	ND	ND	ND	0.01	
Mercury (as Hg)	0.001 mg/l		ND	ND	ND	ND	ND	0.01	
Chemical Oxygen Demand (COD)	10 mg/l	APHA 5220 D	ND	ND	ND	ND	ND	5	4
Phenolic compounds (as C <sub>6</sub> H <sub>5</sub> OH)	0.001 mg/l	APHA 5530 B & D	ND	ND	ND	ND	ND	0.5	
Oil & Grease	0.2 mg/l	APHA 5520 B	ND	ND	ND	ND	ND	2	

Supplementary Table 3. Cost comparison of the monthly electrical bill among five locations

Srl. No	Location	Plant Cost (US\$)	Solar Powering Cost (US\$)	Total Cost (US\$)	Daily Water Consumption (L),	Monthly Electrical Bill (US\$)
1	Vavuniya (Irrataperilakulam)	3,169	4,850	8,019	2,660	1
2	Madawachchiya Town (Mithreepala Senanayake Central College)	3,169	4,850	8,019	2,800	1
3	Sri Lanka Naval Ship Pandukabaya (SLNS) (Poneewa)	3,169		3,169	2,600	55
4	Dutuwewa Village	3,169		3,169	2,500	52

# Design and Development of an Autonomous Underwater Vehicle (AUV): For Rip Current Data Collection and Shallow Water Explorations

MCP Dissanayake<sup>1#</sup>, NVL De Silva<sup>1</sup> and RDMHM Ariyaratne<sup>1</sup>

<sup>1</sup>Department of Marine Engineering, Faculty of Engineering, General Sir John Kotelawala Defence University, Sri Lanka

#dissanayakemcp@kdu.ac.lk

**Abstract:** *Autonomous Underwater Vehicle is an emerging trend in the modern maritime scenario. Though there are various developed designs, researchers are keen on developing more maneuverable, stable and endurance structures with improved capabilities. Based on utilization, AUVs can be divided into two major categories; Deep-water operated and shallow-water operated. The purpose of the AUV designed and developed in our study is two-fold; this can be utilized for rip current data collection and shallow water exploration operations. However, the project is planned under two phases and this paper only describes the design and constructional aspects of the vessel with improved stability, maneuverability and lighting capability. On achievement of the full design, it will enable precise rip current data collection and conduct shallow-water exploration operations in both sea and freshwater streams with an online video streaming facility. In the present context, such operations are undertaken in presence of a diver and our new design eliminates the need of a diver.*

**Keywords:** *Autonomous Underwater Vehicles (AUV), maneuverability, stability, endurance, rip current data collection, shallow water explorations*

## 1. Introduction

Autonomous Underwater Vehicles (AUVs) and “Remotely Operated Underwater vehicles (ROV)” are two different kinds of unmanned underwater robotic applications. Generally, ROV is operated from the surface, through a wired

connection and restricted its maneuverability. However, AUV is a bit different from ROV and when it assigns a task, it collects data and come back to the original position with high maneuverability and using narrow complex pathways (Blidberg, 2001). In addition, the underwater research community is focused on manufacturing materials, adopting new technologies, fixing with advanced sensors, utilization of Computational Fluid Dynamics (CFD) simulations, and advanced batteries to produce very reliable AUV in this juncture (Aras, et al., 2009). AUV is an emerging research field that maintains an economy of effort during large-scale and long-term underwater data collection without risking human divers. A significant amount of theoretical, experimental, and CFD simulation has been carried out in the field of AUV over the last few decades, especially in the area of underwater and hydrography (Kim, et al., 2015). AUV is comprised of three major components such as propulsion system, controlled system, and navigation system. Present-day context, it is revealed that many universities are researching AUV to optimize existing capabilities of control systems and endurance.

Once reviewing earlier studies, a technical team of the Department of Marine Engineering, Faculty of Engineering, General Sir John Kotelawala Defence University designed an AUV with limited capabilities for Rip current data collection and shallow water explorations. The complete project is undertaken under two

phases; (1) design and develop an AUV with adequate maneuvering and lighting capability, and (2) develop an advanced control system to collect Rip current data and deploy it for shallow water exploration missions (Engle & MacMahon, 2002). Accordingly, this paper describes phase 1 of the AUV project; firstly, it describes the basic design of KDU AUV (version 1) and then it explains the detailed records of trials and performances of AUV.

## 2. Design and Developmnet

At the start of the project, the requirement of rip current data collection and robust shallow water exploration is identified and then the capabilities of AUV are defined. The pressure rise with the depth of the sea and the upsurge of strong external force is the major factors taken into consideration in designing the AUV structure. Accordingly, based on the findings of previous studies and a thorough analysis of material strengths to build the AUV hull is chosen, which is characterized to withstand high pressures, strong corrosion-resistant and light in weight. The AUV construction project is undertaken under three stages; (1) design and development of mechanical structure, (2) the basic control system for maneuvering and lighting, and (3) GRP (Glass Reinforced Plastics) structure. Initial drawings of AUV were made using Solid Works software, and principle dimensions are determined with stability calculations and trial and error. Then, decided to design a remote operating system to navigate the AUV to achieve the expected shallow-water exploration. In addition, the maximum submerged depth was decided to have 1m for AUV KDU (version 1).

### A. Hull

The AUV KDU (version 1) is comprised of a 22 cm diameter PVC pipe as the middle part of the spherical body and GRP nobs are fitted with either side of the PVC pipe to minimize water resistance during forward movement and to get

the standard shape of the AUV (Alvarez, et al., 2009). Further, components of the hull are easily detachable and maintainable. The PVC hull and anticorrosive marine paints applied on the hull provides complete hull protection against corrosion. Watertight integrity and dryness inside the hull are of paramount importance in AUV operation, which is achieved by simple mechanical fastenings.



Figure 1. Construction of AUV hull by PVC pipe

### B. Hull Resistance

Conventionally, the total hull resistance is comprised of friction, waveform and wave resistance components. The friction resistance is mainly depends upon the wetted surface area, speed and length of the vessel, and density of the operating fluid. Since AUV (Version I) is a partially submerged vessel, the residuary resistance contribute to the total resistance of the vessel, as it is applied for a displacement hull vessel. Considering above aspects, the hull of the AUV was designed and built in such a way to minimize friction, experiencing minimal hull resistance.

### C. Propulsion

A three-baled propeller is fitted with an electrically driven motor to propel the vessel. The propulsion mechanism is positioned in a way to minimize noise interference with other electronic components and propeller-to-hull interactions. Therefore, avoids unwanted

impacts on the hydrodynamics of AUV. With this propulsion system, the speed of the vessel can be varied by a wireless remote controller, overriding the function of a conventional AUV and optimizing its capabilities in rough sea conditions. Figure 2 and Figure 3 depicts the preliminary stages of construction of AUV.



Figure 2. Preliminary stages of construction of AUV

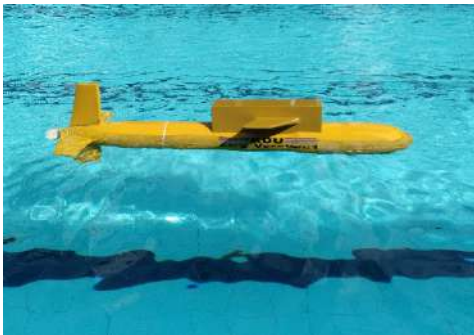


Figure 3. Developing of the propulsion system and testing at KDU Swimming Pool

#### *D. Stability and Submerging*

The AUV used for the rip data collection and shallow water exploration should be able to dive deep in order to change the submerged depth. Such capability can be achieved with ballasting or thrusters. However, AUV KDU (version 1) is designed and developed to partially submerge on the water surface as the main objective of this development phase of the project is to improve the maneuverability of the vessel. Accordingly the volume of the vessel remains constant, which provides space to install equipment for rip

current data acquisition system and further improvements which enhances diving capabilities and maneuverability. Though KDU version 1 does not use ballasting or thruster utilization in this operation to dive a consistent weight of 50 maintains a fixed draft from the beginning of the operation and enough to meet the focused requirement. Figure 4 depicts the efforts taken by the designing team to determine the actual drafting condition after theoretical calculations, pertaining to maintenance of above stated draft.

Further, the vessel is designed with four static hull stabilizers at the amidship of the hull and the tail of the vessel, which adds extra stability to the vessel achieving

neutrally equilibrium condition even in extreme wave conditions. The constructed vessel was tested at sea and KDU swimming pool under varying wave conditions to ensure safe operations in both sea and freshwater conditions.



Figure 4. Preliminary stability testing at KDU lake.

#### *E. Rudders*

The improved maneuverability is one of the main concerns in the development of KDU AUV (version 1). With identified loopholes in previous designs, KDU AUV (version 1) is designed with two GRP-made spade type rudders, which are capable to generate adequate

lift to maneuver the vessel even against strong wave conditions. Further, improved response to the command is another cause of improved maneuverability of our design. These rudders are operated with linear actuators and capable of changing its course as per the given command by the rudder control system. However, the fixed planes provide stability to the vessel.



Figure 5: Rudder testing at hydrodynamics laboratory, KDU

#### F. Powering

AUV is powered by 12V sealed batteries. There are three major sections to be powered by batteries such as propulsion, control system, and high-intensity light.

Therefore, the batteries are parallel connected and current flow between batteries is avoided using protective devices. More importantly, components and essential equipment are selected to draw minimum power to enhance endurance in order to complete the focus mission comfortably.

#### G. Lighting

KDU AUV (version 1) is equipped with 12V waterproof light to provide illumination required for shallow-water exploration (Leathermen & Leatherman, 2017). For the version I, we have used a basic light considering the cost-benefit and it is installed at the forward underwater surface of the vessel with a fixed mounting.



Figure 6. Illumination device

### 3. Results and Discussion

As discussed in the previous section, the objective of phase I of the KDU AUV (version 1) development project is to design and develop the vessel with improved maneuverability and lighting capability to conduct shallow exploration missions. The capability of rip current data collection and online video streaming facility for shallow water explorations will be added during the second phase of the development project. Accordingly, our model's maneuverability and illumination capability were tested at sea and lake under various lighting conditions.

#### A. Testing at sea

The model was tested for its performance at the Colombo harbour in day and night light. During testing, predefined performance parameters of the model were tested with the assistance of a diver. During testing, the model has operated at various locations of the harbour with different wave conditions. Subsequently, the following average data was recorded;

Table 1. Performance data during testing at sea in the daylight

Performance parameter	Performance
Depth	Surface submerged
Average Speed	2.0 Knots
Turning circle radius	3.0 m

Speed drop during turning	Negligible
Illumination	
Up to 5 m	Clearly visible
5 - 8 m	Clearly visible
8 - 10 m	Clearly visible
10-12 m	Visible
Endurance	5 hours
Max. remote operation	50 meters

Table 2. Performance data during testing at sea under the night light

Performance parameter	Performance
Depth	Surface submerged
Average Speed	2.2 Knots
Turning circle radius	3.0 m
Speed drop during turning	Negligible
Illumination	
Up to 5 m	Clearly visible
5 - 8 m	Visible
8 - 10 m	Visible. But objects are unidentifiable
10-12 m	Not visible
Endurance	5 hours
Max. remote operation	50 meters

### B. Testing in the lake

The performance of the model in freshwater is tested at the KDU lake and the following data are recorded.

Table 3. Performance data during testing at the lake in the daylight

Performance parameter	Performance
Depth	Surface submerged

Average Speed	2.4 Knots
Turning circle radius	3.0 m
Speed drop during turning	Negligible
Illumination	
Up to 5 m	Clearly visible
5 - 8 m	Clearly visible
8 - 10 m	Visible
10-12 m	Objects are unidentifiable
Endurance	5 hours
Max. remote operation	50 meters

Table 4. Performance data during testing at the lake in the nightlight

Performance parameter	Performance
Depth	Surface submerged
Average Speed	2.5 Knots
Turning circle radius	3.0 m
Speed drop during turning	Negligible
Illumination	
Up to 5 m	Clearly visible
5 - 8 m	Clearly visible
8 - 10 m	Objects are unidentifiable
10-12 m	Not visible
Endurance	5 hours
Max. remote operation	50 meters

The recorded data reveals that the developed model is capable to provide adequate lighting for the video recording during shallow-water exploration. Further, it's maneuverable enough to conduct such operations with minimized water currents.

#### 4. Conclusion

AUV is an emerging trend in underwater research. AUVs are utilized for numerous ocean-based applications, thus the need for AUVs with improved capabilities is demanding. The model designed and developed during this study is the successful outcome of the first phase of the AUV project which is intended to use for rip current data collection and shallow-water exploration. The developed model is a redesign of the existing AUV model with new modifications to improve identified loopholes. The PVC hull structure of the model eliminates corrosion damages experienced when using steel AUVs, and further, powerful maneuvering capability eliminates drag due to water current which is a common issue in AUVs. More importantly, sea trial results have proven it's fitness in terms of stability and maneuvering to utilize for rip current data collection, which will be developed through equipping an improved control mechanism. Further, test results have proven the best results of its illumination capability in order to utilize for shallow water explorations and thus, our model will be further developed by introducing a modern online video streaming facility during next development stage.

#### References

- Alvarez, A., Bertram, V. & Gualdesi, L., 2009. Hull hydrodynamic optimization of autonomous underwater vehicles operating at snorkeling depth. *Ocean Engineering*, 36(1), pp. 105-112.
- Aras, M., Kasdirin, H., Jamaluddin, M. & Ba, 2009. Design and development of an autonomous underwater vehicle (AUV-FKEUTeM). In *Proceedings of MUCEET2009 Malaysian Technical Universities Conference on Engineering and Technology*. Malaysia.
- Blidberg, D., 2001. The development of autonomous underwater vehicles (AUV); a brief summary.. Volume 4, No.01.

Engle, J. & MacMahon, J., 2002. *Formulation of a Rip Current Predictive Index Using Rescue Data*, Florida: Department of Civil and Coastal Engineering, University of Florida..

Kim, H. et al., 2015. Free running simulation of an Autonomous Underwater Vehicle undergoing a straight line manoeuvre via Computational Fluid Dynamics.. *Pacific International Maritime Conference*, Sydney, s.n.

Leathermen, B. & Leatherman, P., 2017. Techniques for Detecting and Measuring Rip Currents. *International Journal of Earth Science and Geophysics*, Volume 33, pp. 1228-1234.

#### Acknowledgment

The authors would like to acknowledge (General Sir John Kotelawala Defence University) for guidance and kind assistance throughout this research project

#### Author Biography



Cmde (E) MCP Dissanayake, CEng (India) is currently performing as the Head of Department (Marine Engineering) and holds 2 patents for his research papers published so far. He is an inventor and published 06 No's publications on Brackish Water Reverse Osmosis application, Fan Boat Building and Oscillation Water Column, Ocean Wave Energy Converter. He was the Director in Research & Development at Sri Lanka Navy and has received commendations on number of occasions from the Commander of the Navy, HE the President of Sri Lanka for his innovation. Further, he was awarded with prestigious, Japanese, Sri Lanka Technical Award for his own developed low-cost Reverse Osmosis Plant, to eliminate Chronic Kidney Disease from



Sri Lanka. Moreover, he has vast exposure on marine diesel engines and possesses a Master's degree in Marine Engineering from Australian Maritime College, University of Tasmania, Australia.



Viraj De Silva is a Marine Engineer in Sri Lanka Navy and presently serving as a Senior Lecturer (GR II) attached to the Department of Marine Engineering, Faculty of Engineering, KDU. He earned his BSc (DS) MarEng from KDU, MSc in MarEng from Naval University of

Engineering, China and MBA(MoT) from University of Moratuwa



LCdr (E) RDMHM Ariyaratne is presently serving as a lecturer in the Department of Marine Engineering, Faculty of Engineering, KDU and possesses a BSc in Marine Engineering from General Sir John Kotelawala Defence University, with a 1st class merit. He is a Chartered Engineer (India) and an associate member of Institute of Engineers Sri Lanka (IESL)

# Indigenously Designed Addressable Bilge Alarm System for Naval Vessels

M Karunanayake<sup>1#</sup>, S Nanayakkara<sup>1</sup> and A Bamunusungha Aarachchi<sup>1</sup>

<sup>1</sup>Sri Lanka Navy, Sri Lanka

#chathurkamahiraj@gmail.com

**Abstract:** *The primary purpose of an Addressable Bilge Alarm Panel is to provide an early warning of the bilge level of a vessel so that the personal, equipment and valuable resources can be protected and action is taken to remove bilges as soon as possible, all according to a predetermined plan. This study presents aspects of the bilge alarm system onboard Sri Lanka Naval Ship (SLNS) Sagara, by analyzing the existing system based on automation and advanced microcontroller programming using Raspberry Pi3, and ATMEGA 328P microcontrollers. The designed system is an addressable type bilge alarm system that communicates in serial RS 485. The novelty of the designed system are the own data protocol used in RS 485 communication, voice command of specific bilge location and the self designed advanced graphical user interfaces (GUI). In the simulation process, the bilge alarms may be raised automatically by a bilge sensor or manually by a person operating a test button. This response indicates the exact location of the ship on the given blueprint of the touch panel and provides an automatic warning alarm of the bilge location through the ship fitted General Alarming system. The study covers the designing process, implementation, microcontroller and Touch Panel programming, simulation process, testing and commissioning process. The designed system was installed onboard and tested for several months under different sea conditions by experienced Senior Electrical Engineers and Marine Engineers of SLN, then the system was commissioned on 03<sup>rd</sup> February 2022.*

**Keywords:** *Bilge alarm, communication protocol, GUI*

## 1. Introduction

A ship either being a merchant or war, the bilge alarm system plays an enormous role to protect the ship by confirming its stability and reducing the risk of marine casualties. It helps to identify any leakages of water, oil or any types of liquid in underwater compartments whether from onboard fitted machinery or ingress water from the sea. To identify the bilges compartment of the ships, reserved with risk markings are fitted with floater or level activated sensors. These sensors are activated with the bilges crossed to their permissible limit and give sensing data to the designed integrated system. The Officer Of the Watch (OOW) on the Bridge, officer in the Machinery Control Station (Engine Room) and Damage Control Headquarters (DCHQ) of the ship will immediately identify and activate the preventive actions such as bilge pumps operation, emergency repair party initiatives, etc.

The overview of the GUI is displayed in figure 1. Specific bilge locations are plotted on the blueprint of the specific ship such that any bilge status is clearly visible in an emergency. Meantime, an audible alarm specifying the relevant bilge location is activated through the ship's broadcast system so that ship's crew gets aware of the bilge location remotely.



Figure 2. Bilge Alarm GUI

## 2. Literature Review

International regulations have been imposed to confirm the water tight integrity of a ship. Standards for bilge alarms and de-flooding have been introduced through such regulations as Safety of Life at Sea (SOLAS), UK Statutory Instruments etc. Procedures have been mentioned to implement in a flooding situation.

As per UK Statutory Instruments (Regulations, 2021) have been imposed in 2021 for cargo ship bilge alarms. It is stated that a bilge alarm may be risen within 30 seconds upon detection of a high bilge state by a sensor.

Regulations related to the pumping of flooded compartments have been listed under SOLAS by the International Maritime Organization (IMO) (SOLAS, 1997) . All parameters related to bilge main, pumps etc have been elaborated in the regulation.

Studies have been conducted by different parties to calculate the risk factors according to the flooding level and risk severity of a ship (Liu, et al., 2021). Many researchers have applied fuzzy reasoning to logically express the risk analysis of flooding.

## 3. Implementation

The study was carried out to introduce a novel design with an indigenous server client communication protocol with advanced

monitoring and alarm facilities. The overall functional diagram is described in figure 2.

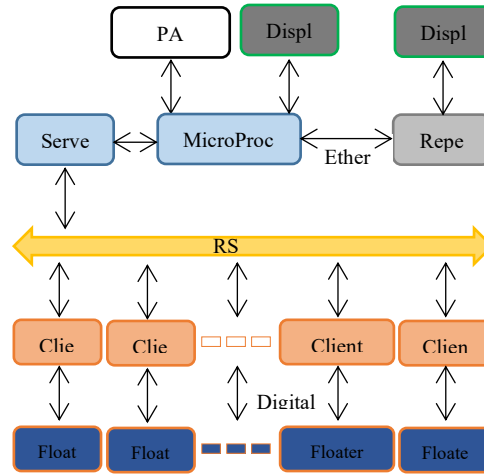


Figure 2. Functional Block Diagram

### A. The Server

server is designed to be the heart of the overall functioning of the system. Main processing, communication establishment and execution of audio files will be handled by the server. The layout of the server is elaborated in figure 3. A printed circuit board (PCB) shown in figure 4 has been self designed to cater to the server functions.

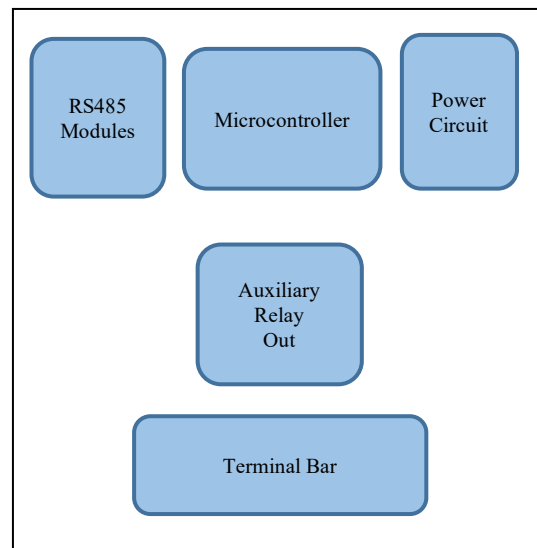


Figure 3. Server Layout



Figure 4. Server PCB

### B. Client (Slave Device)

There are 06 Nos. of clients in the designed system which is feasible to be extended up to 31 Nos. Individual floater switches are integrated into the relevant client to indicate bilge high/ low state. Following bilge locations of the ship have been installed with the clients.

- i. After Steering Post
- ii. Engine Room
- iii. Auxiliary Engine Room
- iv. Harbor Diesel Alternator Room
- v. After Baggage Room
- vi. Forward Baggage Room

Each client will be responsible for communicating with the server to send the real time bilge status of each floater. A self designed PCB shown in figure 5 has been used for the client's purpose.

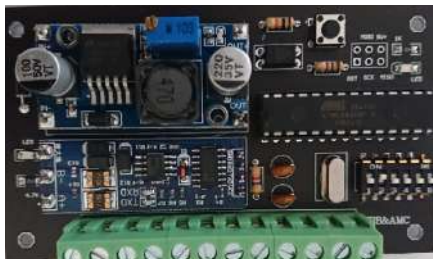


Figure 5. Client PCB

### C. The Communication Protocol

An indigenous communication protocol has been introduced using RS 485 serial communication. Each client has been assigned both physical and software addresses as their ID. The physical address is to be set with the aid of dip switches shown in figure 5. The software address has been set in the program. Both addresses will be matched by the server for data transfer during serial communication.

A data array has been formed by the client in the following form shown in figure 6.



Figure 6. Client Data Format

The server will send a request to each client with the client ID. The corresponding client will respond to the server with the real time bilge status. In every loop, each client will be called by the server. Then, the above data stack will be appended by the server as in figure 7. Any malfunction of a client will be notified on the GUI as a communication error.

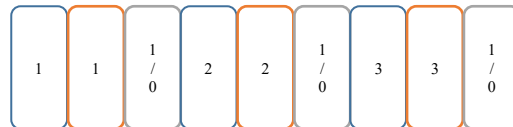


Figure 7. Appended Data Array

Thus appended data array corresponding to the number of clients will be transferred serially to the Raspberry Pi microprocessor shown in figure 3.

#### D. Graphical User Interface

The GUI has been designed for the server and repeater panels to demonstrate the bilge locations as shown in figure 1. In order to indicate the specific location, the appended data array has been split again by the microprocessor and mapped on the GUI as a low/high alarm state.

#### E. Main Monitoring Panel

The main monitoring panel shown in figure 8 consists of the server, Raspberry Pi microprocessor and touch screen display (configured in Raspbian operating system) with GUI and has been installed either in the machinery control room or the DCHQ. Further, GUI is created based on JavaScript programming language and an executable file is generated for easy access through the touch screen panel to simulate the bilge indications.



Figure 8. Main Monitoring Panel

#### F. RepeaterPanel

A repeater panel shown in figure 9 has been introduced and installed on the bridge of the ship for remote monitoring of the bilge status. A similar GUI has been modeled into the repeater panel. The latter communicates with the main monitoring panel through Ethernet communication. The system has been designed as user friendly such that a healthy connection between the two panels is indicated on each monitoring panel.



Figure 9. Repeater Panel

#### 4. Performances

Specific fixed address for each client and allocated for every bilge compartment. The facility has been provided to the end user to manually test each client by pressing a test button arranged in each client device. Simultaneously, the bilge alarm warning on the GUIs of the main monitoring display and the repeater panel was checked along with the vocal alarm of the specific location through the ship's broadcast system. The following additional indications have been provided on the GUIs for user friendly fault identification.

- i. Slave (Client) Communication Error (On main monitoring display)
- ii. Repeater Connecting (On main monitoring display)
- iii. Repeater Connected (On main monitoring display)
- iv. Master Connecting (On repeater display)
- v. Master Connected (On repeater display)

The system was thus tested for performance and fault tolerance, then commissioned on 03<sup>rd</sup> February 2022 onboard Sri Lanka Navy Ship Sagara.

## 5. Conclusion and Future Work

A study has been conducted to introduce an indigenously designed and developed addressable bilge alarm system for Sri Lanka Naval vessels. Self designed monitoring and advanced communication methods have been introduced to monitor the risk of bilges inside vulnerable compartments in a ship. Self designed PCBs, communication protocol based on RS 485, GUIs and vocal alarms have been put forward as the novel outputs of the design. The addressable bilge alarm system has been tested and proven to the suitability in a marine environment.

The design can be extendable up to 31 Nos. of Clients (Slave devices). Further, this study can be continued with fuzzy reasoning to calculate the risk likelihood and risk severity of flooding for a given compartment. Risk likelihood may be based on the location, draft of the compartment, type of machinery available in the compartment etc.

### References

Liu, Z. et al., 2021. An Improved Failure Risk Assessment Method for Bilge System of the Large Luxury Cruise Ship under Fire Accident Conditions. *Journal of Marine Science and Engineering*, Volume 9(9), p. 957.

Regulations, 2021. The Merchant Shipping Cargo Ship (Bilge Alarm), <https://www.legislation.gov.uk/ukxi/2021/592/made>.

SOLAS, 1997. , consolidated text of the International Convention for the Safety of Life at Sea, 1974, and its Protocol of 1978, London

### Acknowledgment

Authors were supported by the Sri Lanka Navy.

### Author Biography



Mihiraj Karunanayake received the BSc. (Hons). Degree in Electrical & Electronic Engineering from General Sir John Kotelawala Defence University, Ratmalana, Sri Lanka in 2016. He is a current student of MSc. in Artificial Intelligence at University of Moratuwa, Sri Lanka. He has published two conference research papers. He is currently employed as a research engineer at Electrical New Design Center (East) of the Sri Lanka Navy. His current research interests are Embedded Systems, Artificial Intelligence and Marine Control Systems.



Savindu Nanayakkara received the BSc. (Hons). Degree in Electrical & Electronic Engineering from General Sir John Kotelawala Defence University, Ratmalana, Sri Lanka in 2017. He is reading his MSc. in Artificial Intelligence at University of Moratuwa, Sri Lanka. He is currently employed as a research engineer at Electrical New Design Center (East) of the Sri Lanka Navy. His current research interests are Marine Control Systems, Embedded Systems, Unmanned Aerial vehicles (UAVs) and Radio Frequency Machine Learning Systems (RFMLS).



Akila Bamunusinghe Arachchi received a B.Tech Degree in Electrical and Electronics Engineering from Jawaharlal Nehru University, New Delhi, India in 2012. Since 2014, he has engaged in many research and development (R&D) activities in the Electrical and Electronic fields. He has published a conference research paper and is currently employed as a research engineer at the Electrical New Design Center (East) of the Sri Lanka Navy as a Senior Electrical and Electronic Engineer. His current research interests are Automation solutions for various marine control systems and training simulators for beginners.

# Thermographic Inspection System for Surface Coating Defects on Aircraft Fuselage

WPMY Thilakarathna<sup>1#</sup>, AA Ziyad<sup>1</sup>, ND Wijesinha<sup>1</sup>, KVP Dhammika<sup>2</sup> and GMSM Gaspe<sup>1</sup>

<sup>1</sup>Department of Mechanical Engineering, Faculty of Engineering, KDU

<sup>2</sup>Department of Electrical, Electronic and Telecommunication Engineering, Faculty of Engineering, KDU

#thilakarathnamy@kdu.ac.lk

**Abstract:** The aircraft outer shell is coated with a corrosion-resistant layer because its alloy does not possess sufficient intrinsic resistance to wear and corrosion. Impacts by small particles or large objects such as bird strikes can lead to damage to the coated surface inducing surface defects. Micro cracks initiated due to surface damages create stress concentration zones which could lead to catastrophic failure of the aircraft due to fatigue crack formation. Therefore, the importance of regular inspection of surface coating is highlighted. Visual inspection is widely used for surface damage identification but, manual procedures with the bare eye are time-consuming and lead to human errors. Effective automation of the inspection can be considered a viable solution. The aim of this project was to develop an automated inspection system based on non-contact, non-destructive Infrared Thermography to identify defects on an aircraft's surface coating. The system developed was a two-axis gantry attached to a four-wheel structure equipped with a tiltable thermal camera assembly and a control panel. The inspection method follows the sequence; Firstly, thermal image capturing. Next, image processing and identifying the defect area. Thirdly, giving a signal to the operator if a defect is present. The system was tested on a significant dataset and its capability of detecting surface defects on an aircraft's coating was demonstrated. The results suggest an automated thermographic inspection system

for surface coating defects on aircraft fuselage can successfully replace visual inspection leading to a 9.25 % increase in efficiency and minimizing its inherent disadvantages.

**Keywords:** Thermographic Inspection, Aircraft Defect Detection, Image Processing

## 1. Introduction

The outer coating of an aircraft is expected to have a prolonged life whilst enduring extreme conditions to ensure the integrity of the aircraft structure. Wear/damage of the coatings due to the impact of bird strikes initiate surface defects which can induce serious structural failure with time. Thus, the detection of coating defects became a prime importance in aeronautical applications and it's understood that regular inspections on coatings must be carried out through in-service monitoring to ensure satisfactory lifespan of aircraft surface structure (Sause, 2021).

In the field of engineering, Non-Destructive Testing (NDT) is the most common technology that used to detect and evaluate flaws in materials: cracks, defects or variations in structural properties of materials. Traditional NDT methods involve visual inspections, radiography, ultrasonic testing (UT), magnetic particle testing, penetration testing, eddy current testing etc (Dwivedi, Vishwakarma

and Soni, 2018). Out of which, visual inspection is the most popular method that used to identify abnormalities in aircraft structure, but it creates greater maintenance downtimes and human errors (Stamm et al., 2021). Especially, it is not applicable for complex and sensitive aircraft structural inspections like identifying coating defects.

Infrared Thermography (IRT) is a popular solution which has emerged in recent years to address complex NDT problems in aviation industry. However, in the conventional method of thermographic inspection also involves the operator continuously monitoring the aircraft surface manually, through a view finder of the thermal imaging equipment to identify the abnormalities produced in the thermal image. In this manual thermographic inspection method, the operator requires sufficient expertise and is under continuous pressure to accurately identify and take the required action of confirming a surface defect (Srajbr, Bräutigam and Dillenz, 2012).

The aim of this project is to elaborate an innovative method for identification of aircraft coating defects based on Infrared Thermography whilst reducing the burdens of visual inspection method. This paper describes designing, fabricating and testing a scaled down automated system which can identify surface defects on an aircraft's fuselage coatings using non-contact, non-destructive Infrared Thermographic inspection.

## **2. State of the Art**

In the Aerospace industry, NDT techniques are used to detect the presence of abnormalities in aircraft structures. Review of NDT methods for composite materials by Gholizadeh (2016) provides an overview of basic types of NDT methods that are used in the Aerospace (Aero) Industry: Visual Inspection, UT, Radiography, IRT, Vibration Methods, Shearography and XCT. Out of which Infrared thermography is a revolutionary method that used to analyse flaws in materials in the Aero industry. IRT refers to a non-contact NDT method where

thermal information obtained from a specimen is analyzed and produced an image of temperature variation of the specimen as output.

Some literatures explicitly discuss the use of IRT in Aero Industry. Yang et al (2019) has presented an IRT based Crack Detection method of steel sheets using Convolutional Neural Networks (CNN). Shang et al (2007) developed a climbing robot with a scanning arm to detect loose rivets in aircraft fuselage through thermal imaging. Another IRT application was In-plane heatwave thermography inspection technique for fasteners in aircraft fuselage by Stamm et al (2021). Cramer and Winfree (2006) from NASA studied the application of IRT inspection techniques to the space shuttle thermal protection system. Accordingly, there were various NDT techniques that have been used by NASA in the examination of the Reinforced Carbon-Carbon (RCC) panels in space shuttles, but they found thermography is the most effective inspection alternative to other methods. NASA is currently using the commercial infrared thermography system called EchoTherm for RCC Inspections.

Eddazi and Belattar (2018) have proposed a method to evaluate Aircraft Fuselage corrosion resulted from chemical reactions by using IRT and Finite Element Method. In that work, simulations were based on changes in heat flux and thickness of corrosion that determine the degree of detectability of the IRT method with the analysis of resulted temperature differences. Srajbr, Bräutigam and Dillenz (2012) proposed an induction excited thermography for fatigue crack detection in the aluminum skin of the Boeing 737. In their project, eddy current testing was intended to be replaced by an automated thermographic sensor positioned on a robot which offers non-contact extensive testing of structures by a defect selective visualization of induction heating irregularities.



However, according to the journal article Damage Detection Systems for Aerospace by Sause (2021), it's important to understand the defect types in order to implement defect detection systems to produce the desired structural integrity. Thus, basic types of aircraft structural material include metals, composites, coatings, and adhesively bonded and welded joints. Out of which coatings (thin or thick film) in aircraft surface is there to reduce the effect of corrosion/wear that can cause serious safety effects. According to the journal article of Structural Defect Types by Faisal et al (2021), wear/damage of the coated surface due to the impact of small sand particles or large objects such as bird strikes and indentations of the structure during the handling process are the most common reasons of inducing surface defects. That article emphasizes the importance of preventive and remedial inspection methods on aircraft surface coatings to rectify any unexpected defects.

Although the most common NDT method of identifying surface defects is visual inspection, Stamm et al (2021) states that the manual visual inspection performed with the naked eye has inevitable drawbacks whereas its outcome is subjective to individual inspector and time consuming. A review on NDT by Dwivedi, Vishwakarma and Soni (2018) reveals that visual inspection is not suitable to detect small flaws on surfaces like coating scratches which were mentioned above.

The proposed automated thermographic inspection system for aircraft fuselage coating defects detection aims to fulfill the drawbacks in visual inspection by replacing it with Infrared Thermography.

### **3. Methodology**

Based on the identified research gap, a methodology for developing the thermographic inspection system was formulated. The proposed system was a rover with a double-axis gantry attachment for scanning the aircraft in an aircraft hangar.

Three major parts of the system were (1) the Driving Trolley, (2) the Camera Lifting and Tilting Mechanism and (3) the Controlling Mechanism. The reference aircraft for the inspection system design was the PT-06 Aircraft accessed through the Air Support Wing (ASW) - Ratmalana, Sri Lanka.

#### *A. Conceptual Design*

Concept generation of the project involved the integration of a design table (Table 1) with a concise rating table based on fragmented 7 sub parts of the main system: (1) Thermal Camera (2) Lifting Mechanism (3) Lifting actuators (4) Controller for Thermal Imaging and Processing (5) Camera Tilting Mechanism (6) Power source (7) Defect Detection Indicator. The Design Table was based on the extensive Literature Review done under the aforementioned categorization.

The range of applicable technologies for each part was identified and integrated to form 4 design concepts. The selected sub-parts were individually analyzed based on their unique advantages and disadvantages by giving scores according to specific weighted design attributes : (1) Thermal Camera – Resolution, Field of View (2) Lifting Mechanism – Stability (3) Lifting Actuators – Torque applicability, complexity (4) Controller for Image Processing – Processing Capability, Availability (5) Camera Tilting Mechanism – Area Coverage , Weight (6) Power source – Energi Density, Weight (8) Defect Detection Indicator – Visibility , Understandability. Cost was primary selection attribute for all the sub parts. Completed rating table opened a path for determining the quantitative best design using total weighted score and the selected design was Design 2 which had the total weighted score of 77.75.

Table 1. Design Table

Sub Parts	Design 1	Design 2	Design 3	Design 4
Thermal Camera	FLIR A35	FLIR Lepton 3	Adafruit	FLUKE flexcam
Lifting Mechanism	Crane	Linear Drive	Linear Drive	Hydraulic Scissor lift
Lifting actuators	Hydraulic Piston	Electric Motor	Electric Motor	Hydraulic Piston
Controller for Imaging Processing	Intelligent Global Controller	Raspi	Arduino MEGA 2560	PC
Camera Tilting Mechanism	Platform Pan/Tilt	Pan and Tilt	Solid Mount	Motor on Motor Mount
Power Source	Lithium Battery	Tether	Lithium Battery	Lead Acid Battery
Defect Detection Indicator	Display	Display, LEDs, alarm	Alarm	Display

*B. Design Considerations*

1) *Rover and Lifting Mechanism:* A Trolley with wheels was selected for the rover. Trolley proportions were based on the PT6 aircraft used for testing, total area coverage for one static placement of the system and total weight of mounting components. The respective calculations were done accordingly.

To capture the thermal images of the focus area, the lifting mechanism was needed to be embedded in the system which can mount and carry the camera for scanning the surface.

Two-axis gantry consist with two linear drives was the selected method for the lifting mechanism. One unit of linear drive consists of a ball screw, guide rails, linear bearings, end mounts and guide mount. Based on pre-load dynamic torque calculations, selected two linear drives were ball screw SFU 1605 and SFU 1204. As shown in Figure 1, a linear static stress analysis was carried out using SOLIDWORKS Simulation software by applying relevant stiffness data in order to confirm the rigidity of the selected vertical ball screw SFU 1605.

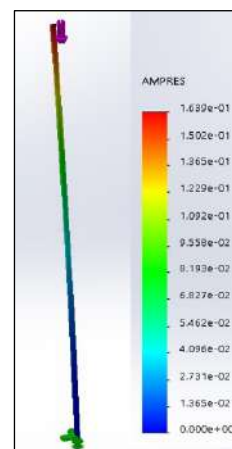


Figure 1. Stress Analysis Diagram for Vertical Ball Screw

Two linear drives were decided to be driven by stepper motors and to estimate the power requirements for both forward and backward movements, respective calculations were done by using torque requirements based on dynamic loading conditions. For Horizontal ball screw drive torque and back drive torque, calculations were done by equation (1) and for vertical linear drive it was done by equation (2).

$$T_h = (S_L P \mu) / (2\pi E_{ff}) \tag{1}$$

where : P = Applied Dynamic Load (N)

S<sub>L</sub> = Lead of Screw (m)

μ = Coefficient of sliding friction

E<sub>ff</sub> = Ball screw efficiency (90%)

$$T_v = (J + (mr^2)/e) \times a/r + r/e \times mg$$

(2)

where : m = Mass of the load and the nut

J = Moment of inertia

a = Upward acceleration

r = Transmission ratio of lead

screw (5mm/rev)

e = Fractional efficiency of Lead Screw (90%)

$T_h$  (forward) = 0.001Nm

$T_h$  (backward) = 0.00015Nm

$T_v$  (forward) = 3.1Nm

$T_v$  (backward) = 0.031Nm

Nema 23 and Nema 17 stepper motors were selected based on above calculated drive torque requirements and the respective power requirements were 16.88W and 7.8 mW.

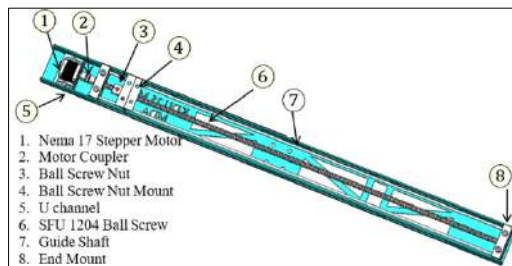


Figure 2. Design of Horizontal Linear Drive

## 2) Thermal Camera and Tilting Mechanism:

Based on the extensive comparison done in the design table FLIR Lepton Thermal camera was identified as the most economical and accurate thermal camera for this application. From lepton series, FLIR Lepton 3 was selected as per the required specifications of compact size, resolution of 160 (h) x 120 (v) active pixels and shutter capability for image capturing. Since the camera setup was needed to be attached to the horizontal ball screw nut, a camera mount was designed for Lepton 3 camera. To capture the thermal image effectively, the camera must be turned to face the aircraft surface with optimal depth of field

(DOF) which is 30 cm. Thus, a servo-controlled tilt mechanism was designed with IR sensor which can detect the ideal DOF.

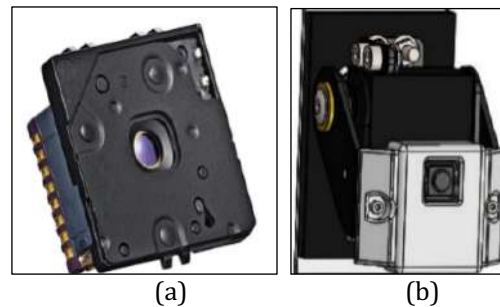


Figure 3. (a) FLIR Lepton 3 Thermal Camera  
(b) Tilting Mechanism Design

In designing stage, all the mechanical components: Trolley, Lifting Mechanism, Camera Setup and Tilting Mechanism were drawn part-wise using SolidWorks software. Respective components were assembled to get the visual representation of the final system given in the Figure 4.

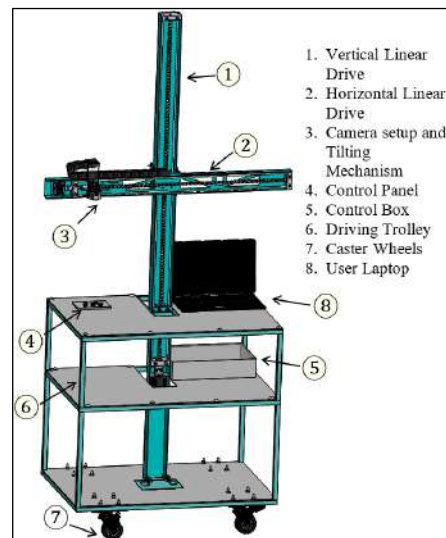


Figure 4. Final Design of the Mechanical Systems

## C. Fabrication

Fabrication of the project was fragmented into 3 sub-assemblies: Trolley, Lifting mechanism with horizontal and vertical linear drives, Tilting mechanism with Camera setup. Starting

with trolley fabrication, skeleton of the trolley was fabricated using 19 x 19 x 1.4 mm steel box bars welded together. Plywood planks were fixed to the skeleton as shelves with plastic toggles using 6mm drilled holes. To drive the trolley, pair of locked caster wheels and universal cater wheels were used.

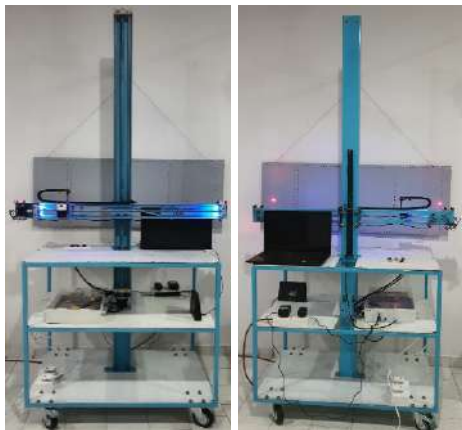


Figure 5. Finalized System

Next, fabrication of the lifting mechanism was initiated part by part. For one linear drive, there were 8 parts as shown in Figure 2. According to the dimensional requirement, ball screw was needed to be modified by using lathe machine and end mounts made out of Teflon were lathed and drilled to place bearings and guide rails. For motor mounts and the ball screw nut mount, 5 mm steel metal sheets were laser cut and bent in 90 degrees with metal bending machine. The whole linear drive setup was mounted on an U channel made out of 2 mm thick steel metal sheet and the guide rails were 6 mm and 8 mm stainless steel rods. Finally, the fabricated components of lifting mechanism together with camera setup were assembled to the trolley for the completion of the inspection system (Figure 5).

#### D. Image Processing

1) *Configuration of Thermal Camera and Controller:* The microcontroller for image processing was selected under 4 main factors: power and storage capacity, compatibility with thermal camera and reliability. Thus,

Raspberry Pi 4 model B (Raspi) was selected as the suitable controller for image capturing and processing system. The circuitry was integrated with Lepton 3 Thermal Camera, PureThermal 2 I/O board, Raspi and 5V 3A power supply as shown in Figure 6. VNC Viewer was used as the method of accessing the Raspi remotely. Configuration of Raspi was done to operate the thermal camera Lepton 3 for testing the thermal images captured, verifying the applicability of it.

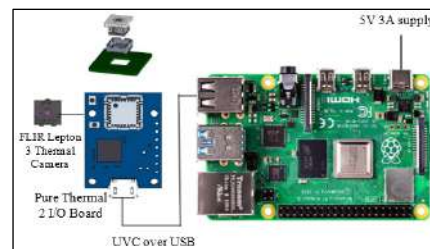


Figure 6. Connection Diagram of Image Capturing System

There were two viewing softwares of using the Lepton 3 interfaced to a Pure-Thermal 2 I/O board on a Raspi called GetThermal and Parabilis thermal. Although the GetThermal software was the Purethermal 2 proprietary software its dependency on OpenGL driver presumably brought upon indistinguishable errors when executing GetThermal. Therefore, Parabilis thermal was used since the functionality was same even though proprietary software was not used. Parabilis thermal can only allow recording of a video of the thermal view in HDF5 format but the proposed system requires image capturing as the project aims to fully automate the process of defect detection. Therefore, Parabilis Thermal was used to create the dataset of 'defect' and 'no defect' images by recording a video and later isolation of individual frames were done through the post processing script of Parabilis Thermal.

Before initiating the image capturing, required calculations were done to find the field of view of an image captured by thermal camera using specifications of the Lepton 3. Thus, with 30

cm ideal DOF, horizontal and vertical field of views were 31.9 cm and 28.5 cm respectively.

2) *Thermal Imaging and Image Processing:* Lepton 3 camera was used to capture 70 thermal images containing 44 images of defects and 26 images with no defects by using a fuselage panel removed from an aircraft of Sri Lankan Airforce. The conditions were simulated based upon operating the equipment on an aircraft immediately after landing whilst maintaining the surface temperature of the aircraft above 36°C. To obtain the required heat of 39°C test piece was heated by a heat gun. The defects were simulated by impacting the test piece using a sharp metal rod to demonstrate a bird strike on the aircraft. To capture the videos in HDF5 format, RecordIR script of Parabilis Thermal software was used and PostProcessIR script was used to separate frames in the video to be saved as images in PNG format.

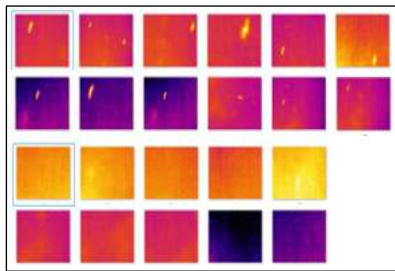


Figure 7. Part of source dataset of thermal images

70 images were flipped and mirrored to make a dataset of 560 8-bit images (Figure 7) and those RGB images were converted to gray scale (Figure 8) by using python script to perform the image manipulations using the Pillow library.

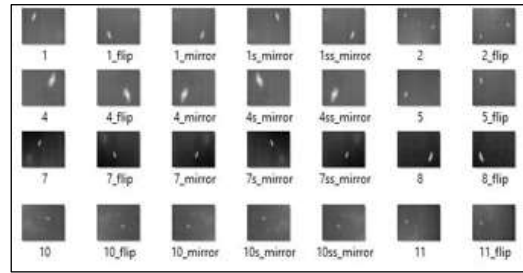


Figure 8. Part of dataset after manipulation and gray scaling

Since the thresholding was selected as the segmentation method for this system, the cv2.threshold() function within the OpenCV library was used to perform thresholding on the images. Thresholding involves analyzing the image at the pixel level to separate background from foreground. As thresholding binarizes an image, the grayscale image was converted to a binary image making the pixels either 0 or the maximum i.e 255 (maxval). The gray scaled thermal image can be defined as a function  $f(x, y)$  whereas the threshold image  $g(x, y)$  can be defined as follows:

T= Adequate Threshold value

$$g(x, y) = \begin{cases} \blacksquare(maxval) & \text{if } f(x, y) \geq T \\ 0 & \text{otherwise} \end{cases}$$

Two thresholding methods based on grayscale histograms were considered – Otsu’s method and Triangle method. Otsu’s method computes an optimum value for ‘T’ assuming that the image consists of two classes, the background and the foreground represented by a bimodal grayscale histogram. It computes a global threshold by minimizing the weighted variance between the two classes. In the triangle method a line is constructed between the peak and the far-end of the histogram. The threshold is the greatest distance (dmax) between the line and the histogram. Triangle method was selected as it clearly isolated the defect than Otsu’s method which produce more images with noise causing incomplete separation of the defect area. Figure 9 shows the histogram that resulted from defective image after triangle thresholding and the basis for calculating the threshold value.

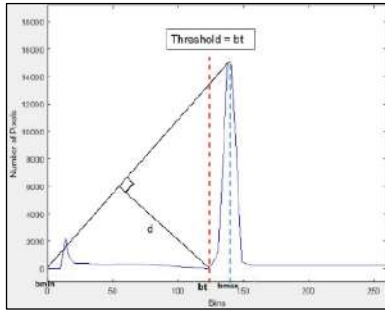


Figure 9. Histogram resulted from Triangle Thresholding

For filtering, 5 most frequently used image filters in image pre-processing: Mean, Gaussian, Median, Conservative and Image Arithmetic filters were explored. As per the comparison, it was observed that the Mean, Gaussian, Median and Conservative filters tend to merge both defect areas and non-defect areas. From the Image Arithmetic matrix addition or subtraction the brightness and contrast of the image was manipulated. Subtraction arithmetic filter was chosen to be used as it reduces the brightness, resulting in defects with higher pixel intensities being distinguished. It was applied before the thresholding function because when triangle thresholding is applied, the defect area will be unclear since the contrastive strength of the image is low.

Final script was formulated incorporating grayscale conversion, subtraction arithmetic filtering, triangle thresholding and an if conditional active pixel counting to obtain a defect judgement regarding an image that is captured by the thermal camera. Respective sequence of defect identification process is mentioned in Figure 12.

### E. Control System

Control system had 2 subsystems which were controlled by two different controllers: Raspberry Pi to control the image capturing and processing, Arduino MEGA 2560 for controlling lifting and tilting mechanism (Figure 10). Operation of image processing system controlled by Raspi was according to the explanation given in the previous section.

Controller 2: Arduino Mega was for controlling lifting and tilting mechanism. Since the lifting mechanism was with two ball screws driven by stepper motors Nema 17 and 23, the respective coding was needed to be done after setting the circuitry. Circuitry of one linear drive was with set of components: Stepper motor and driver, SMPS controlled by Arduino.

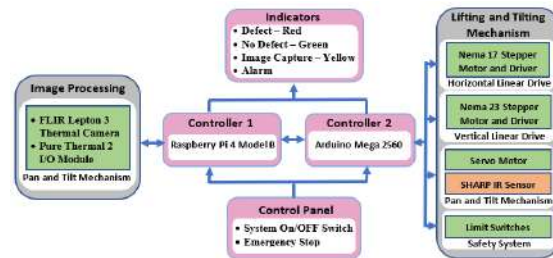


Figure 10. Structure of the Control System

Prior to commence the programming of lifting mechanism controlling section, step count calculations of stepper motor were done correlating with the camera's field of view (FOV). Based on the calculations, FOV of Lepton 3 was 31.9 x 28.5 cm when camera is placed 30 cm (DOF) perpendicular to the capturing surface. Stepper motor coupled with horizontal linear drive was to stop in each 29.5 cm linear movement to capture images as horizontal field of view (HFOV) is 31 cm. Thus, vertical linear drive stops at every 26 cm (VFOV) distance movement. With those decided values, the step count per run was calculated and programming for combination of two linear drives was conducted. In this system the total area coverage per run was 135 x 120 cm<sup>2</sup> and it was divided to 20 squares of 31 x 26 cm which covers per take when the camera is set up 30 cm distance perpendicular to the test surface. Figure 11 shows the area coverage and the graphical view of lifting mechanism moving algorithm.

Camera Pan/tilt mechanism with servo motor MG955 attached to the horizontal linear drive was also controlled by Arduino. According to the controlling algorithm when the horizontal linear drive stopped to take the image, servo motor rotated and IR sensor attached to it was

used to identify the ideal perpendicular distance (30 cm) with curvy aircraft surface before image capturing.

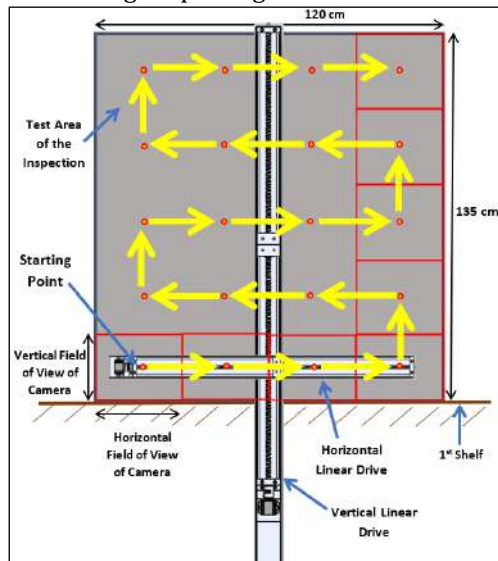


Figure 11. Area coverage and graphical view of lifting mechanism movement

Explaining the overall algorithm of the control system, after accurate positioning of the equipment using laser beams, to start the operation of the testing equipment “Start” button was there to press and then start signal is read by the Raspi, communicating it to the Arduino by using Serial Communication. With the continuous start signal given from Raspi, Arduino take action on the operation of lifting and pan/tilt mechanism by initiating the servo motor for the tilt setup and the stepper motors for linear drives appropriately according to specified functions in code. When the specified number of steps has reached in the horizontal operation stepper motor, a delay will be initiated on further movements of the camera whilst the Arduino sends a signal to the Raspi to initiate the camera capture python script and it’s indicated by yellow LED. After the camera capture script is initiated, the image is processed and judged for defects. If there is no defect, the Raspi sends a serial command to the Arduino as “No Defect” and if condition continues the Arduino operation appropriately for the “No Defect” command. Simultaneously, the Raspi lights a green LED to

indicate the operator of no defect. However, if it’s determined that there is a defect, then the Raspi send the serial command “Defect” and it’s indicated by red LED and alarm. This process (Figure 12) follows on a loop till the end of the total test area leading to the re-positioning of the equipment by the operator and continuing the process.

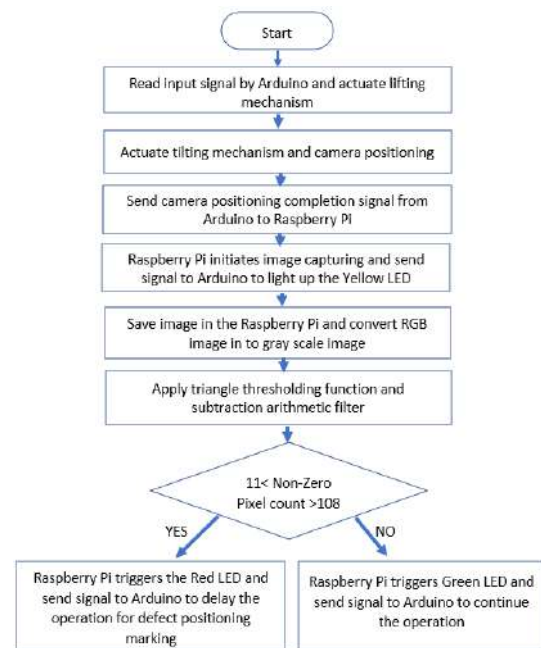


Figure 12. Control Flow

#### 4. Results and Discussion

The main aim of this project was to develop a prototype of an automated system that can test for surface coating defects on a aircraft fuselage using non-contact, non-destructive IRT inspection and relieve the uncertainty in manual inspections. During the project completion, equipment was segmented by its main components and segment wise testing was done after fabrication prior to finalizing the system.

Especially considering the image processing system, different conditions that the thermal camera would possibly encounter such as low light, high exposure, shadow on surface and abstract angle conditions was explored whilst testing. A stock camera image with defect was

analyzed using same conditions to justify the use of the thermal camera instead of a normal camera for the equipment.

As aforementioned, during image processing stage, two types of threshold segmentation methods were compared to confirm the system applicability. It was observed that the Triangle method was better than the Otsu's method in dealing with effectively defining the foreground to the defect area since it brought less amount of noise to the foreground. Following results shows the comparison of two thresholding methods and noise appearance.

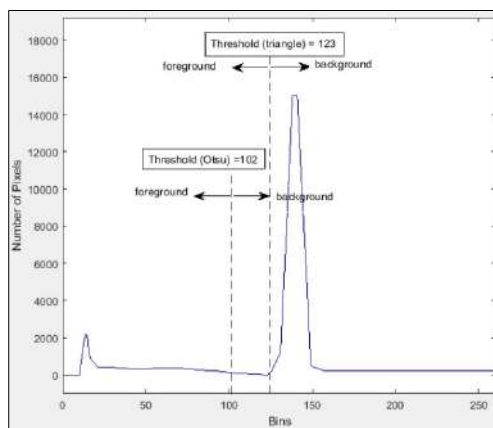
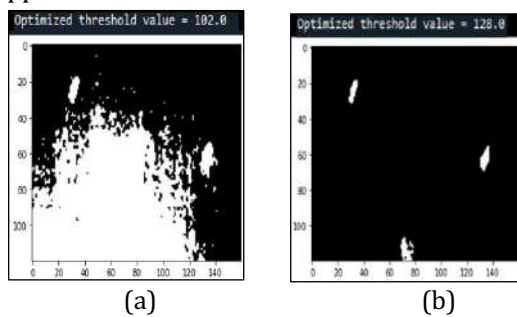


Figure 13. (a) Otsu's thresholding method (b) Triangle thresholding method (c) Comparison of Otsu's method vs Triangle Method

As per the results, for the selected defective image thresholding values for Otsu and Triangle method were 102 and 128 respectively (Figure 12). Respective histogram clearly emphasize the separation of background and foreground.

According to the results obtained after analyzing all the source data set underwent triangle thresholding it was determined that the pixel count range of defect images is between 11 to 108 non-zero pixels (Figure 13). Results inferred that a defect will be present for images with non-zero pixel counts above 11 and below 108. Further research is to be done for the integration of machine learning algorithm to create a self-learning system that can identify the region of non-zero pixel range.

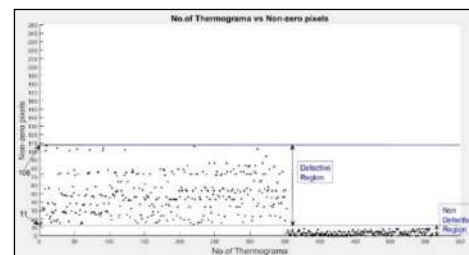


Figure 14. No. of Thermograms vs Non-zero pixels

For this inspection system, the total area coverage per one static placement of the system was 16,200 cm<sup>2</sup> and the total time taken for the inspection procedure for one static placement of the system was 18 mins and 55 secs whereas the manual inspection took 20 mins and 40 secs increasing the overall efficiency by 9.25%. Hence, the estimated inspection time for the total area coverage of PT 6 aircraft is 5 hrs and 42 mins. Further research is required to analyze the applicability of this system for surface defect inspections of large-scale aircraft.

## 5. Conclusion

The prototype of a thermographic inspection system for surface defects on aircraft was developed to introduce a novel concept to surface coating defect detection and to overcome the drawbacks of the existing manual inspection methods. As identified in the methodology, the worker involvement and the total time required for manual inspection were reduced by automating the camera lifting and tilting mechanism and due to the



embedded image processing system with an automated defect indication mechanism. Research continued improving the image processing system with a machine learning algorithm and further research needs to be done to improve the system design, with an automated navigation system and IOT-based indication system, to obtain zero worker involvement in the inspection procedure. As the experimental results confirmed the functionality of the prototype, it can be concluded that the Thermographic Inspection System for surface defects on aircraft is ready for further research in commercializing the equipment, building its accuracy, and showcasing it to the world.

## References

- Gholizadeh, S. (2016) 'A review of non-destructive testing methods of composite materials', *Procedia Structural Integrity*, 1, pp. 50–57. doi:10.1016/j.prostr.2016.02.008.
- Yang, J. et al. (2019) 'Infrared Thermal Imaging-Based Crack Detection Using Deep Learning', *IEEE Access*, 7, pp. 182060./ACCESS.2019.
- Shang, J. et al. (2007) 'Design of a climbing robot for inspecting aircraft wings and fuselage', *Industrial Robot*, 34(6), pp. 495–502.
- Stamm, M. et al. (2021) 'In-plane heatwave thermography as digital inspection technique for fasteners in aircraft fuselage panels', *Applied Sciences (Switzerland)*, 11(1), pp. 1–19. doi:10.3390/app11010132.
- Cramer, K.E. and Winfree, W.P. (2006) 'The Application of Principal Component Analysis Using Fixed Eigenvectors to the Infrared Thermographic Inspection of the Space Shuttle Thermal Protection System', (July). doi:10.21611/qirt.2006.002.
- Dwivedi, S.K., Vishwakarma, M. and Soni, P.A. (2018) 'Advances and Researches on Non Destructive Testing: A Review', *Materials Today: Proceedings*, 5(2), pp. 3690–3698. doi:10.1016/j.matpr.2017.11.620.
- Eddazi, A. and Belattar, S. (2018) 'Nondestructive testing evaluation of aircraft fuselage corrosion by infrared thermography and finite element method', *Proceedings - 2017 14th International Conference on Computer Graphics, Imaging and Visualization, CGiV 2017*, pp. 56–61. doi:10.1109/CGiV.2017.13.
- Faisal, N. et al. (2021) 'Defect Types', *Springer Aerospace Technology*, pp. 15–72. doi:10.1007/978-3-030-72192-3\_3/FIGURES/57.
- Gholizadeh, S. (2016) 'A review of non-destructive testing methods of composite materials', *Procedia Structural Integrity*, 1, pp. 50–57. doi:10.1016/j.prostr.2016.02.008.
- Sause, M.G.R. (2021) *Structural Health Monitoring Damage Detection Systems for Aerospace*.
- Shang, J. et al. (2007) 'Design of a climbing robot for inspecting aircraft wings and fuselage', *Industrial Robot*, 34(6), pp. 495–502. doi:10.1108/01439910710832093.
- Srajbr, C., Bräutigam, K. and Dillenz, A. (2012) 'Crack Detection at Aluminum Fuselages by Induction Excited Thermography', (November 2012), pp. 3–8.
- Stamm, M. et al. (2021) 'In-plane heatwave thermography as digital inspection technique for fasteners in aircraft fuselage panels', *Applied Sciences (Switzerland)*, 11(1), pp. 1–19. doi:10.3390/app11010132.
- Yang, J. et al. (2019) 'Infrared Thermal Imaging-Based Crack Detection Using Deep Learning', *IEEE Access*, 7, pp. 182060–182077. doi:10.1109/ACCESS.2019.2958264.

## Author Biography



WPMY Thilakarathna completed the undergraduate academic programme in the field of Mechatronics Engineering from KDU and waiting for the graduation. Currently working as a Temporary Instructor at KDU. Her research interest includes mechanical designing, control systems and robotics.



AA Ziyad completed the undergraduate academic programme in the field of Mechatronics Engineering from KDU and waiting for the graduation. Currently working as an Executive Automation Engineer at MAS Holdings, Sri Lanka. His research interest include machine designing , automobile and robotics.



ND Wijesinha completed the undergraduate academic programme in the field of Mechatronics Engineering from KDU and waiting for the graduation. Currently working as an Executive Automation Engineer at MAS Holdings, Sri Lanka. Her research interest include machine designing and automobile.



Col KVP Dhammika, Commanding Officer Cyber 12<sup>th</sup> Signal Corps Cyber Security Regiment of Sri Lanka Army and the Visiting Senior Lecturer at Faculty of Engineering, KDU. He obtained bachelor degree in Electronic Engineering from KDU

and M.Phil in Electronic and Telecommunication Engineering from the University of Moratuwa Sri Lanka, MSc in Military Technology Degree from Pune University India.



GSM Gaspe received the bachelors degree in Science and Technology specialized in Mechatronics from Uva Wellassa University of Sri Lanka in 2013. She has completed Masters in Applied Electronics at the University of Colombo in 2019. Currently, she is working as a lecturer at Faculty of Engineering, KDU. Her current research areas includes Intelligent Control Systems.

# Estimation of Lift Hysteresis of an Airfoil in low speed flow

WARD Jayathilake<sup>1</sup> and JI Abeygoonewardene<sup>1#</sup>

<sup>1</sup>Kotelawala Defence University, Ratmalana, Sri Lanka

#jabeygoonewardene@kdu.ac.lk

**Abstract:** A phenomenon called hysteresis leads to a difference in separation and reattachment angles of an airfoil at angles of attack near and above stall. This is an airfoil than expected for a given angle of attack when recovering from a stall. This leads to asymmetric flow parameters around a body even when the boundaries remain symmetric. Empirical results for lift and pressure coefficients were obtained for a two-dimensional Clark Y-14 at low speeds. The lift characteristics of the airfoil was observed while varying angle of attack and Reynold's number. It was seen that the extent of the lift hysteresis largely depends on Reynold's number. Further experiments and Computational Fluid Dynamics (CFD) simulations will be conducted in order to determine occurs when there is a difference in the lift distribution of the relationship of the effective body of the stalled airfoil and the presence of hysteresis loops.

**Keywords:** Coefficient of pressure, Lift hysteresis, Lift curve, Flow separation, Stall

## 1. Introduction

It is commonly assumed that symmetric boundary conditions produce symmetric flows. However, this is often far from the real case. A flow that has large regions of separation will result in asymmetries in the instantaneous as well as mean flow, even when the boundaries remain symmetric. This leads to hysteresis, in which the forces and moments on a body depend on the time history of the attitude. This phenomenon is often observed during flow visualization of bodies such as aircraft models in wind tunnels (Barlow, et al., 1999). In case of airfoils, this is due to

the fact that when the angle of attack is increased beyond its stalling angle, the flow does not reattach at the same angle when the angle of attack is lowered again. In other words, an airfoil does not recover from a stall following the same variation of flow parameters it underwent before it was stalled. The difference between the separation and reattachment angles is defined as the size of the hysteresis loop (Morris, et al., 2020). From an aerodynamic point of view, hysteresis is the existence of multiple values for lift, drag and moment coefficients for a given angle of attack instead of a single value. Aerodynamic hysteresis is of two types: namely, static and dynamic hysteresis (Williams, et al., 2015). Static hysteresis also termed as conventional hysteresis is the results that are obtained when the readings are taken under quasi static conditions which is by slowly pitching the airfoil until stalled and pitching it back down slowly while dynamic hysteresis is seen when the airfoil is under motion. There are various factors that affect the extent and the formation of the hysteresis loops in the aerodynamic coefficients such as the Reynolds number (Brunner, et al., 2021), Turbulence intensity (Hoffmann, 1991), effective body of the airfoil (Landman, 2001), type of separation formed (Marchman, 1987) and the boundary layer transition (Mueller, 1985) and/or separation on the airfoil (Timmer, 2008), (Traub, 2016). In a study conducted on a symmetrical NACA 0012 airfoil at a Reynolds number (Re) of 475000, Morris et al found an agreement with the hypothesis that the reattachment angle of

the stalled airfoil is the stalling angle of the associated effective body.

A majority of the available work has concentrated on analysing the static and dynamic hysteresis on symmetric airfoils. The present study aims at estimating the extent of static lift hysteresis on an asymmetric Clark Y-14 airfoil in low-speed flows, while analysing the parameters affecting the same and determining relationship of the effective body of the airfoil and the occurrence of hysteresis loops in stall hysteresis.

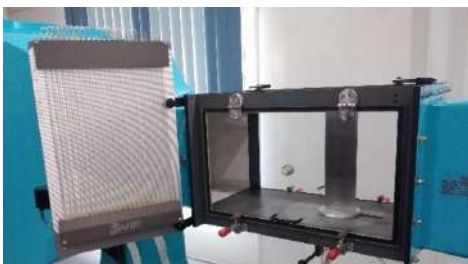


Figure 1. Wind tunnel apparatus

## 2. Methodology and Experimental Design

The preliminary stage of the methodology consists of deriving experimental results for a Clark Y-14 airfoil. The experiment is conducted in the Aerolab educational wind tunnel at Kotelawala Defence University which is capable of simulating low speed flows in the range of 4.5 to 64 m/s, having a test section dimension of 30.5 cm × 30.5 cm × 30.5 cm. The pressure wing, resembling a Clark Y-14 airfoil having a chord of 8.9 cm, has 18 flush mounted taps which render pressure readings via a multi-tube liquid manometer.

Appropriate range of Reynold's number ( $Re$ ) was selected for the experiment considering the limitations of the wind tunnel ranging from 60941 to 204155. The experiments were carried out by varying the fan speed of the wind tunnel from 400 to 1200 rpm (revolutions per minute) in increments of 100 rpm to bring about the change in the Reynold's number as depicted in table 1.

Table 1. Corresponding Reynolds number for fan speed

Fan speed, rpm	Reynolds number
400	60941
500	79224
600	91412
700	112742
800	134072
900	146260
1000	164543
1100	182825
1200	204155

The experiment was conducted at standard sea level conditions. The pressure readings for the upper and the lower surface was tabulated by varying the angle of attack (AoA) in 1 degree intervals and the lift coefficient ( $C_L$ ) for the pitch up and the pitch down was calculated using the student version of MATLAB software. Thereby the lift curve and coefficient of pressure ( $C_p$ ) variations for each setting were obtained.

## 3. Results

The variation of the coefficient of pressure ( $C_p$ ) for some angles of attack for the forward and backward stroke (pitch up and pitch down) for different flow speeds are given below. Since the flow speed is the only parameter varied, it therefore shows the dependence with change in Reynold's number. Figures 2 to 10 depict the  $C_p$  plotted against  $x/c$  (the distance along the chord/length of the chord).

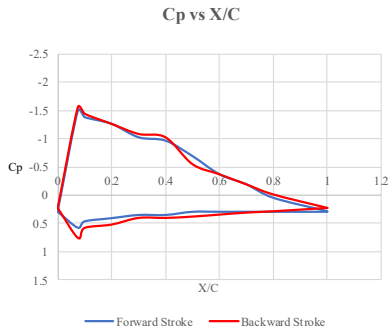


Figure 2. Cp vs x/c for Re = 112742 at 5°

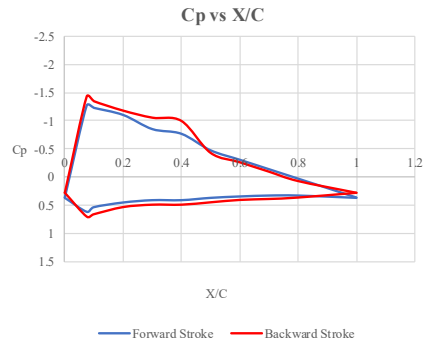


Figure 5. Cp vs x/c for Re = 134072 at 5°

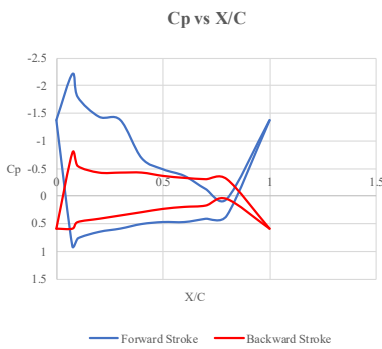


Figure 3. Cp vs X/C for Re = 112742 at 10°

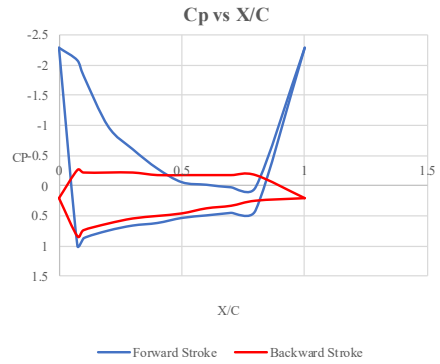


Figure 6. Cp vs x/c for Re = 134072 at 15°

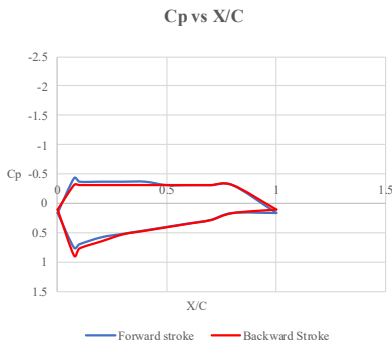


Figure 4. Cp vs x/c at Re = 112742 at 15°

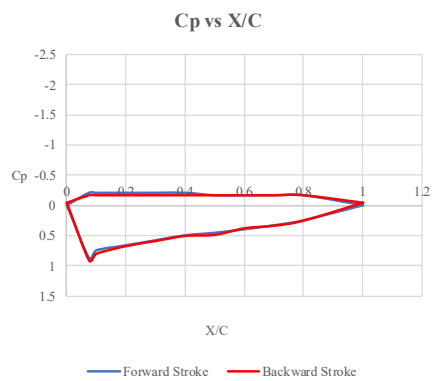


Figure 7. Cp vs x/c for Re = 134072 at 18°

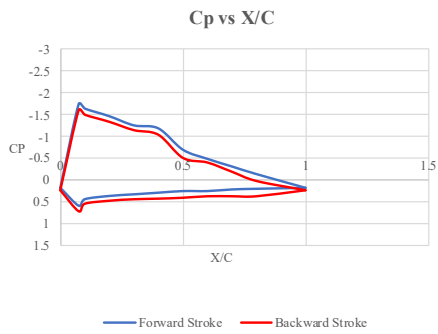


Figure 8. Cp vs x/c for Re = 146260 at 5°

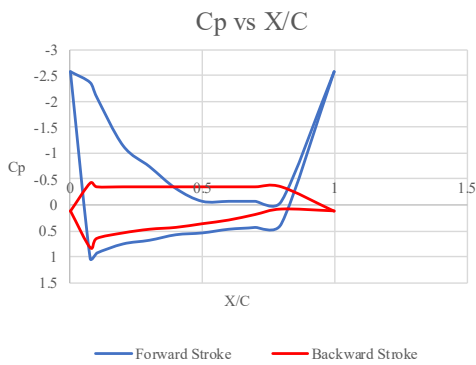


Figure 9. Cp vs x/c for Re = 146260 at 15°

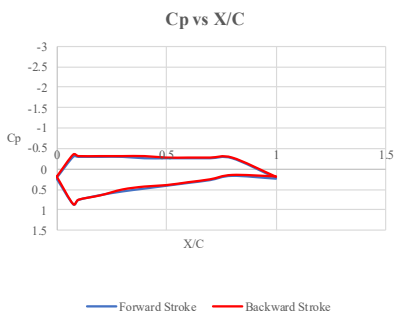


Figure 10. Cp vs x/c for Re = 146260 at 18°

The plotted lift curves (lift coefficients vs the AOA) with the aid of the MATLAB software for different Reynolds numbers are given in figures 11 to 15.

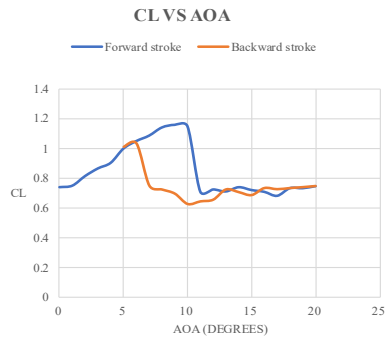


Figure 11. Figure Lift curve for Re = 91412 for forward and backward stroke

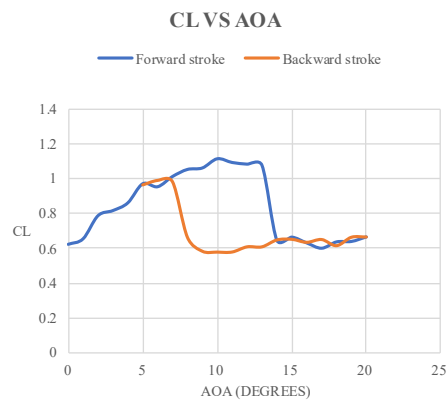


Figure 12. Lift curve for Re = 112742 for forward and backward stroke

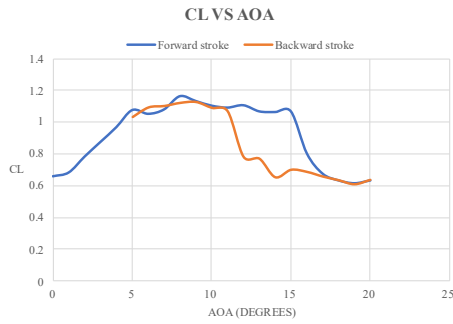


Figure 13. Lift curve for Re = 134072 for forward and backward stroke

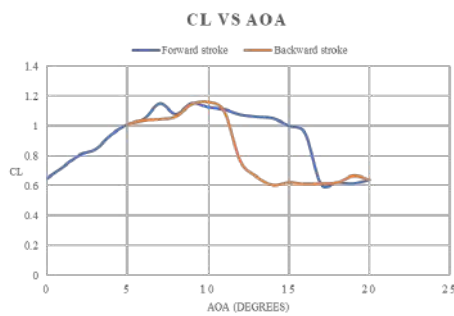


Figure 14. Lift curve for Re = 146260 for forward and backward stroke

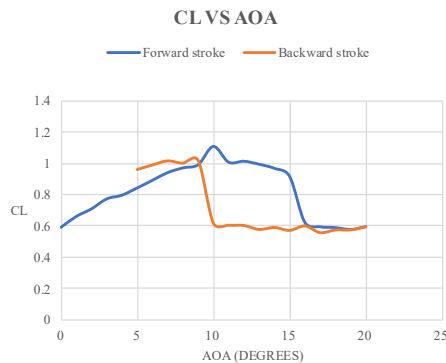


Figure 15. Lift curve for Re= 164543 for forward and backward stroke

#### 4. Discussion

The present study focused on the experimental results derived via a two-dimensional airfoil for low speeds. It was observed that at very low speeds, no

significant hysteresis loop is created. The lift coefficient variations at low angles of attack (5 degrees) for varied Reynold's numbers are almost identical for the forward and backward strokes. Further, there are no signs of flow separation.

As angle of attack and Reynold's number increases (as shown in figures 3, 6 and 9), it is evident that the presence of a significant hysteresis loop as the difference between separation and reattachment are more prominent. Further, the lower surface of the airfoil displays a rather similar trend in its pressure coefficient variation for both the forward and backward stroke. The upper surface on the other hand, shows significant deviations. This maybe a result of the higher level of separation on the upper surface due to increased camber. The upper surface pressure coefficient reaches a maximum closer to the leading edge during the forward stroke, while it drastically decreases during the backward stroke. The pressure distribution on the upper surface during the backward stroke also shows a constant value, indicating that large scale flow separation has occurred (Russel, 1979).

Considering the variation of lift coefficient, the clockwise hysteresis loop is observed (figures 11 to 15). The extent of the loop increases with Reynolds number before it starts to decrease again. Table 2 depicts the extent of the hysteresis loops obtained for different Reynolds numbers.

Table 2. Extent of the hysteresis loop with Reynolds number

Reynolds number	Extent of hysteresis loop	Presence of hysteresis loop
60941	negligible	-
79224	negligible	-
91412	6° - 11°	4°
112742	7° -14°	6°
134072	9° -16°	7°
146260	11° -17°	5°
164543	11° -17°	5°

The results render that the hysteresis loop is prominent at an angle of attack of 7° at a Reynold's number 134072. The stalling angles of attack of the Clark Y-14 airfoil derived through experimental results are given in table 3. The stalling angle of attack peaks around 16°.

Table 3. Variation of stalling angle with Reynolds number

Reynolds number	stalling angle
91412	above 10°
112742	above 13°
134072	above 15°
146260	above 16°
164543	above 16°

From the above results it can be concluded that the Reynold's number plays an important part in determining the existence of hysteresis loop of an airfoil. At very low Reynolds numbers, no significant hysteresis loops were detected. With the increase of the Reynolds numbers the extent of the hysteresis loops continued to increase until 134072 and slightly decrease for Reynolds number of 146260 and 164543. Also, the stalling angle also has a positive relationship with the Reynolds number. When the Reynold's number was increased the stalling angle continued to rise with an exception at Reynolds number of 164543.

The accuracy of the empirical results derived maybe compromised to a certain extent due to common factors affecting results obtained during wind tunnel testing. Buoyancy effect, solid and wake blockage in the test section and errors associated with reading liquid heights of the manometer tubes cannot be neglected. Thus, a comprehensive validation of the results through numerical simulations is necessary.

## 5. Future Work

The second intended stage of the methodology to be followed will involve validating of the experimental results using computational fluid dynamic simulations. Further the effective body of the stalled Clark Y-14 airfoil will be isolated and modelled in order to obtain its lift curve, so as to investigate the relationship between the effective body and hysteresis loop of the airfoil.

The work will be continued to examine the lift hysteresis of a three-dimensional airfoil to better understand the parameters affecting the phenomenon. The experimental results will be validated using CFD simulations considering both the two dimensional and three-dimensional airfoils. The effective body of the stalled Clark Y-14 airfoil is to be modelled in order to determine the relationship between the effective body and the hysteresis loops present. While the work here li. mited only to low-speed flows, further examination can be made in flows in the higher subsonic or even transonic regimes.

## 6. Conclusion

The hysteresis loop of a two-dimensional asymmetric airfoil was observed in low-speed flows by varying parameters of angle of attack and Reynold's number. It was found that Reynold's number and angle of attack are primary parameters that have an impact on the occurrence of static lift hysteresis and the size of the hysteresis loop is significant at particular Reynolds number at low speeds for the Clark Y 14 airfoil.

## References

- Brunner, C., Kiefer, J., Hansen, M., Hultmark, M., (2021). Study of Reynolds number effects on the aerodynamics of a moderately thick airfoil using a high-pressure wind tunnel. *Experiments in Fluids*, 62(8).
- Hoffmann, J., (1991). Effects of freestream turbulence on the performance characteristics of an airfoil. *AIAA Journal*, 29(9), pp.1353-1354.



Landman, D., Britcher, C., (2001). Experimental Investigation of Multielement Airfoil Lift Hysteresis due to Flap Rigging. *Journal of Aircraft*, 38(4), pp.703-708.

Marchman, J., Sumantran, V., Schaefer, C., (1987). Acoustic and turbulence influences on stall hysteresis. *AIAA Journal*, 25(1), pp.50-51.

Morris, W., Zenker, C., Ingraham, J., Wolfenbarger, T., (2020). A Theory of Stall Hysteresis - Why the reattachment angle is less than the separation stall angle. *AIAA Scitech 2020 Forum*.

Mueller, T., (1985). The influence of laminar separation and transition on low Reynolds number airfoil hysteresis. *Journal of Aircraft*, 22(9), pp.763-770.

Rae, W., Pope, A., Barlow, J., (1999). *Low speed wind tunnel testing*. New York: Wiley.

Timmer, W., (2008). Two-Dimensional Low-Reynolds Number Wind Tunnel Results for Airfoil NACA 0018. *Wind Engineering*, 32(6), pp.525-537.

Traub, L., (2016). Semi-Empirical Prediction of Airfoil Hysteresis. *Aerospace*, 3(2), p.9.

Williams, D., An, X., Iliev, S., King, R., Reißner, F., (2015). Dynamic hysteresis control of lift on a pitching wing. *Experiments in Fluids*, 56(5).



JI Abeygoonewardene is a Senior Lecturer in Aeronautical Engineering at the Faculty of Engineering of General Sir John Kotelawala Defence University, Sri Lanka.

### Author Biography



WARD Jayathilake is an undergraduate at the Department of Aeronautical Engineering at the Faculty of Engineering of General Sir John Kotelawala Defence

University, Sri Lanka.

# An analysis of the impact of technical communication on aviation risk mitigation in the context of aircraft maintenance operations in Sri Lanka

SCM Bandara<sup>1</sup>, KMGMB Samarkoon<sup>1</sup> and WTS Rodrigo<sup>1#</sup>

<sup>1</sup>Department of Aeronautical Engineering, General Sir John Kotelawala Defence University  
Sri Lanka

#thusith.rodrido@kdu.ac.lk

**Abstract:** Aviation safety plays a vital role in the airline industry including aircraft maintenance operations. The equilibrium between safety and productivity is inversely proportionate as additional efforts on safety have an inverse impact on operational efficiency. Therefore, a major attribute that decides the operational effectiveness of an aircraft maintenance establishment is decided on how effectively it can handle the equilibrium between safety and productivity. Accordingly, this paper empirically evaluates the impact of technical

communication on aviation safety through the theoretical framework of aviation safety management in the context of commercial aircraft maintenance operations in Sri Lanka. A conceptual framework is formulated with independent variables addressing written and verbal communication, information

**Keywords:** technical communication, risk mitigation aviation safety management, written and verbal communication, employee engagement.

## 1. Introduction

### 1. Background of the Study

Effective safety management plays a vital role in the Airline industry including aircraft maintenance operations as it handles the delicate equilibrium between safety and operational productivity. Generally, aviation safety management is based on four main pillars, namely safety policy, safety risk management (SRM), safety assurance, and safety promotion (Chatzi et al., 2019). Even though there is a significant amount of research on the impact of safety policy, management, and risk assurance there is a severe dearth of literature evaluating the safety promotion's impact on overall aviation safety. The scope of safety promotion directly communication (EL Hajjar and Alkhanaizi, 2018). Technical communication generally includes verbal and written communication methods used in assessing and interpreting technical data keeping and maintenance of documentation, transferring and continuation

connects with technical communication and training aspects (Andrei, 2011). Especially in the context of the Sri Lankan commercial aircraft maintenance industry, a huge scarcity is observed in technical research to prove the sustainable impact of technical communication on aviation safety. Hence, this paper is focused on addressing this long prevalent research gap through an empirical analysis.

Aircraft maintenance is a highly human-intensive process where the productivity and effectiveness of work transferring through shift work, faultfinding, rectifications, inspections, work supervision, and quality assurance is fundamentally based on effective technical

of work logs in between shifts, and maintaining the other relevant documentation in the form of the necessary information, and maintenance records (Taylor and Thomas, 2003). Especially in the context of Sri Lankan aviation, the Civil Aviation Authority of Sri Lanka (CAASL) has

specifically highlighted the essentiality of standardization of technical communication through proper SMS practices to enhance the safety of the working environment through

## 2. Problem Statement

Technical communication directly affects aviation safety through written and verbal communication lapses, misunderstandings, language problems, pronunciation, misinterpretations, etc. The situation is more complicated when considering the dynamic environments of Flightline maintenance and base maintenance activities where the

## 3. Research Questions

1. Does written & verbal communication with significant impact on aviation safety?
2. Does the level and quality of technical information understanding by the aircraft maintenance staff affects aviation safety?
3. Does the level of employee engagement related to aviation safety enhancements in aircraft maintenance operations?

## 4. Objectives

1. To evaluate the impact of written and verbal communications on overall technical communication in aircraft maintenance operations.
2. To evaluate the relationship between technical information understanding and aviation safety risk mitigation.
3. To evaluate the impact of technical employee engagement on effective technical communication.
4. To ascertain the overall impact of technical communication towards risk mitigation in aircraft maintenance operations.

## 2. Literature Review

### 1. Theoretical Background

proper record keeping, supervision, and auditing on the communication process(CAASL, 2015).

fluctuating maintenance demand is to be fulfilled with limited resources without compensating the quality and standards. Also, the employee engagement of technical staff in ensuring effective communication significantly differs from person to person depending on their attributes. Against this backdrop, technical communication problems could endanger the safety of the aircraft while significantly reducing the aircraft maintenance operational productivity.

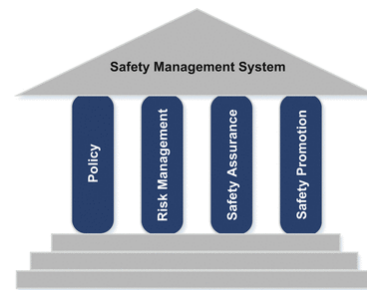


Figure 1: Four pillars of aviation safety management

According to the International Civil Aviation Organization (ICAO) definition, Aviation safety management systems (SMS) has four pillars; safety policy, safety assurance, safety risk management, and safety promotion. According to the ICAO, safety promotion focuses on safety communication and training (Andrei, 2011). Safety promotion ensures that aviation personnel training and competent to perform their duties and engage in a two-way communication of safety issues between the organization's maintenance management and operational personnel. To implement safety promotion in the aviation industry, mitigating risks in aircraft maintenance operations can be considered a crucial factor in terms of line maintenance and base maintenance. So, it is important to improve communication factors for risk mitigation (Study, 2017).

## 2. Written/verbal Communication,

The main mode of technical communication can be considered written and verbal communication. In Safety communication, make proper written and verbal communication systems for all organization members, and assist in the implementation of the safety management system. The language used in aviation-related subjects such as vocabulary, and aviation-related abbreviations understanding helps to maintain communication standards. Using communication equipment is important when attending verbal communication during aircraft maintenance activities (Parohinog and Meesri, 2015).

## 3. Information Understanding

A proper understanding of information especially in terms of technical documentation is highly important in maintenance operations. The technical staff should strictly refer to maintenance manuals, technical documentation, and other related regulatory documentation when discharging their daily duties. Here, misinterpretations, language problems, technical knowledge problems, vocabulary issues, and fundamental language problems can contribute significantly to safe operation (Yudoko and Purboyo, 2017). On the other hand, the language competencies of different technicians might impact their level of understanding of the instructions. Also, when information is overloaded, it might be leading to confusion.

In addition, information understanding on clear communication, understanding the situational hazards and getting action regarding the safety issues affect to optimize the safety performance. Supervised and advised the employees regarding proper safety procedures related to informational understanding. Making an own system of self-learning lessons at the working time and language proficiency assists in the improvement of informational understanding and help to maintain a low accident& incident rate (Alsamadani *et al.*, 2013).

## 4. Employee Engagement

In every industry employee engagement is significantly related to organizational performance and safety. The employee's qualifications, attitudes, behaviors, and accident & incident reporting skills improved work environment safety. Employee engagement and feedback systems positively increase the safety aspects of the organization (Alsamadani *et al.*, 2013).

### 1. Methodology

This research is designed as an empirical hypothetic deductive study conducted through a statistical analysis of the responses provided by the respondents who were carefully selected to represent the aircraft maintenance technical population in Sri Lanka(Mendonca and Carney, 2017). The sampling frame used in this study was distributed to the line and base maintenance employees in Sri Lankan aviation organizations. The independent and the dependent variables were carefully selected through literature and with the qualitative responses received through a set of structured interviews as indicated in Figure 2.

#### 1. Conceptual Framework

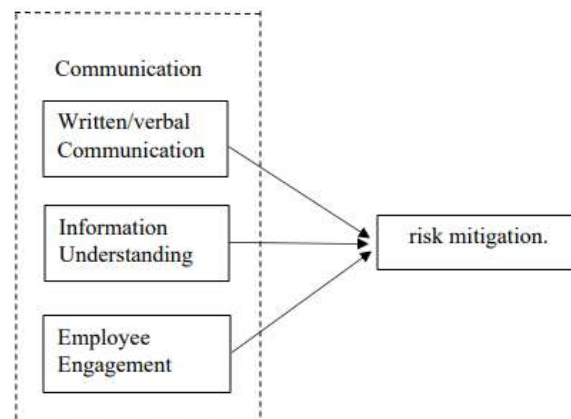


Figure 2: Conceptual Framework

Based on the above conceptual framework, the following hypothesis was developed to be tested statistically through the collected data from a carefully modulated questionnaire. The following three alternate hypotheses were formulated along with the related null

hypothesis. Collected data online through a google sheet with permissions of government and private organizations.

**H1:** Written & verbal communication has a positive impact on risk mitigation.

**H1n:** Written & verbal communication has no impact on risk mitigation.

**H2:** Information understanding has a positive impact on safety risk mitigation.

**H2n:** Information understanding has no impact on risk safety mitigation.

**H3:** Employ engagement has a positive impact on safety risk mitigation.

**H3n:** Employ engagement has no impact on safety risk mitigation.

The empirical responses were accurately captured through a Likert scale of one to five where one represents highly unsatisfactory and five represents a highly satisfactory level. The sample of the study was distributed among 160 employees. A random stratified sampling method was used to collect the data because of the difficulties of collecting data on an island-wide scale. The collected data were analyzed statistically using IBM SPSS Software.

#### 2. Operationalization of the variables

In terms of operationalization of the independent and dependent variables following indicators were examined through the questionnaire.

Table 1: Operationalization of variables

Variable /Indicator	
<i>Written/Verbal communication</i>	
i.	Language proficiency
ii.	Referring technical manuals
iii.	Updating technical documents
iv.	Use of communication equipment
<i>Information understanding</i>	
i.	Understanding briefings & debriefing information

ii.	Understanding of maintenance documents content
iii.	Conducting maintenance meetings
iv.	Knowledge sharing among employees
<i>Employee engagement</i>	
i.	Use of written and verbal feedback systems
ii.	Occupational health & safety
iii.	Employee's abilities & skills in communication
iv.	Corrective & preventive actions via communication
<i>Risk mitigation</i>	
i.	Record incidents & accidents
ii.	Analyze reported accidents & incidents
iii.	Safety audits & informal inspection

## 4. Analysis and Results

### 1. Normality

Checking the information is normally distributed by Skewness and Kurtosis. For Skewness, the agreed value should be within -1 to + 1 and for Kurtosis, should be within the range of -3 to + 3 (Mishra *et al.*, 2019).

Table 2: Normality Test

	Skewness	Std. Error of Skewness	Kurtosis	Std. Error of Kurtosis
Risk mitigation	-.074	.199	.129	.396
Written/verbal communication	-.018	.199	-.019	.396
Information understanding	.132	.199	-.197	.396
Employee engagement & feedback	-.564	.199	.509	.396

### 2. Validity

Kaiser-Meyer-Olkin (KMO) method was used

to determine the validity of data and typically KMO should be between 0-1. If the value of the Kaiser-Meyer-Olkin (KMO) which is a Measure of Sampling Adequacy is obtained as 0.913 and as it is closer to 1 indicates that the data collected is acceptable (Kingdom *et al.*, 2015).

### 3. Multicollinearity Test

Multicollinearity considers an identical linear relationship between two or more of the input variables. Regression analysis and subsequent results can be influenced by this situation (Daoud, 2018). The tolerance value must usually be greater than 0.1 and VIF should be less than 5 (Shrestha, 2020).

Table 3: Multicollinearity Test

variables	Collinearity Statistics	
	Tolerance	VIF
Written/verbal communication	.541	1.849
Information understanding	.445	2.249
Employee engagement & feedback	.674	1.485

### 4. Correlation

Pearson's correlation coefficient is generally used as a measurement to determine the correlation. If there is a coefficient (r) range between -1 to +1 it is considered a proper correlated relation. To test whether there is an adequate relationship between dependent and independent variables. Significance value can also be used as a measure to take a hypothesis decision (Zhang and Wang, 2018)

Table 4: Correlation Test

Hypothesis	Pearson Correlation	Decision
H1	.523	Hypothesis accepted
H2	.607	Hypothesis accepted
H3	.522	Hypothesis accepted

### 5. Regression

Regression is a mathematical method used to analyze variables' relationships. If there is a situation where there is more than one independent variable multiple regression is carried out (Plotts, 2011). Here the linear relationship between independent variables and risk mitigation (dependent variable) was analyzed. According to the analysis, the R-value indicates a positive relationship with the dependent variable of risk mitigation due to the R-value being 0.728.

Table 5: ANOVA

Model	Sum of Squares	df	Mean Square	F	Sig.
Regression	27.384	6	4.564	28.445	.000 <sup>b</sup>
Residual	22.624	141	.160		
Total	50.008	147			

According to the above table, it can be concluded that the overall regression model is a good fit for the data where  $F(6,141) = 26.576$  and  $p < 0.0005$ . Therefore, by considering the overall significance level given in the ANOVA table it could be concluded that this study is statistically significant. And the following regression equation is formulated where written and verbal communication is denoted by (WVC), information understanding is denoted by (IU), and employee engagement is denoted by (EEF).

Risk mitigation = 0.205 + 0.486 (WVC) + 0.188 (IU) + 0.214 (EEF)

Table 6: Coefficients

Model	Unstandardized Coefficients		Standardized Coefficients	t	Sig.
	B	Std. Error	Beta		
(Constant)	0.205	.356		.576	.565
WVC	.486	.110	.061	.787	.433
IU	.188	.093	.170	2.007	.047
EEF	.414	.079	.187	2.714	.007

### 5. Discussion

It is observed that all three hypotheses were accepted through the statistical results derived. This is a clear indication that the conceptual framework derived through the careful observation of previous literature and qualitative inputs derived from industry experts are highly acceptable and applicable in the Sri Lankan aviation context. Moreover, both the correlation analysis and coefficients are focused in a similar direction which again is a clear indication of the accuracy level of the research conducted.

According to the statistic findings, the following points are significant. The initial hypothesis H1 which considered the relationship between written and verbal communication for safety risk mitigation indicates that strong positive relationship (Krivonos, 2007) where the coefficient for correlation of Pearson is 0.523. Hence it can be clearly stated that there is a

positive relationship between written and verbal communication toward risk mitigation.

When considering the second hypothesis H2 on information understanding it also indicates a positive impact on risk mitigation (Endsley and M. Robertson, 2000) and it is evident that situation awareness and information understanding assist to improve employee working performance and reduce accidents and incidents. According to this study coefficient for correlation of Pearson is 0.607 for information understanding. Therefore, it can also be stated that there is a positive relationship between information understanding towards risk mitigation. In terms of the third hypothesis H3, which refers to employee engagement & feedback has a positive impact on risk mitigation toward safety promotion. Baxter, Lauren (Baxter, 2013) establishes that supportive leadership and employee engagement assist to risk mitigation in the working environment. According to this study coefficient for correlation of Pearson is 0.522 for employee engagement.

### 6. Conclusion and Recommendation

The findings of this research present very important facts to concern ensuring of safety through efficient technical communication methods. The first hypothesis indicating a high positive correlation highlights that language proficiency, clear focus, and training on how to refer to the technical manuals have a significant impact on safety. Hence, it is very important to take measures to develop the technical communication competency of the aircraft maintenance staff especially focusing on language competency and technical literacy. In addition, the results highlight the importance of giving proper training for the handling of communication equipment, especially in flight line operations. Also, the result supports the argument that there should be a proper auditing process to check the reliability of updating technical documentation as it is based on the individual communication competency of the technical staff.

In terms of correlation, the next positively supported hypothesis is employee engagement. This supports the establishment of strong feedback systems on employee operational engagement to be conducted by the management. In addition, this relationship also highlights the importance of emphasizing more on occupational health and safety in aircraft maintenance operations. The empirical results clearly show that employees are concerned about their safety and an effective communication method should be established to get positive feedback on their occupational health and safety concerns. In addition, the results strongly support the timely communication of corrective and preventive maintenance information to the technical staff accurately. Here more emphasis should be paid to documents like service bulletins(SBs), manufacturing instructions and airworthiness directives(ADs) to be correctly communicated to the ground-level staff.

Out of the three variables, information understanding is the one that shows a lesser impact on aviation safety. However, as it is positively related to proper conducting of technical briefings and debriefings, timely conduct of maintenance meetings and technical knowledge sharing needs to be emphasized. Here the reason for the lesser significance obtained on this specific variable in the empirical response might be due to the reason that these practices are already well established in an aircraft maintenance environment. So that there is less need to re-emphasize those facts compared to the other two variables.

Hence, in conclusion, it is understood that technical communication has a very significant impact on risk mitigation and aviation safety, especially in the context of aircraft maintenance. Therefore, it is to be emphasized that written and verbal communication place a very vital role in enhancing the standards of technical communication. The other most important area to be concerned about is employee engagement in effective feedback systems. Lastly, it is revealed that relatively

lesser emphasis could be paid to information understanding purely because such systems are effective in operation in the present context.

When evaluating the main limitations of this study, the difficulty in collecting information from stakeholders representing the entire industry in Sri Lanka was a challenge. In addition, with the vital role of safety, it is the path to understand that other aviation stakeholders like pilots, logisticians, air traffic controllers, and ground handlers also need a significant role to play in this research domain where their responses were not collected. Therefore, it is strongly suggested that in future research more emphasis could be paid to these areas and special focus can be paid to effective methods of improving written and verbal communication through the usage of new technology.

The KDU IRC 2022 makes the international stage for graduates and undergraduate students in Sri Lanka. This will be a huge opportunity to succeed in their future goals through innovations to the world. Specially KDU IRC 2022 is the best path for aeronautical engineering researchers with a highlighted category.

## References

Ahmad, A. I. H. and Adamu, M. (2014) 'The Relationship Between Training Effectiveness and Employee Performance: Mediating Role of Work Environment', *Asian Academic Research Journal of Social Sciences & Humanities*, 1(21), pp. 230-247.

Alsamadani, R. *et al.* (2013) 'Construction Management and Economics Measuring and modelling safety communication in small work crews in the US using social network analysis Measuring and modelling safety communication in small work crews in the US using social network analysis', (January 2015), pp. 37-41. doi: 10.1080/01446193.2012.685486.

Andrei, F. (2011) *Safety Management Manual, ICAO Doc 9859 AN/474, Incas Bulletin*. doi:



10.13111/2066-8201.2011.3.1.17.

Baxter, L. E. (2013) 'Supportive Leadership, Employee Engagement and Occupational Safety: A Field Study', 12, p. 77. Available at: [http://trace.tennessee.edu/utk\\_graddiss/2556](http://trace.tennessee.edu/utk_graddiss/2556)

.CAASL (2015) 'CIVIL AVIATION AUTHORITY State Safety Programme Policy and Procedures Manual Second Edition -2015 State Safety Programme Policy and Procedures Manual'.

Chatzi, A. V *et al.* (2019) 'The Unexplored Link between Communication and Trust in Aviation Maintenance Practice', pp. 1-18.

Daoud, J. I. (2018) 'Multicollinearity and Regression Analysis', *Journal of Physics: Conference Series*, 949(1). doi: 10.1088/1742-6596/949/1/012009.

Datta, P. P., Srivastava, A. and Roy, R. (2013) 'A simulation study on maintainer resource utilization of a fast jet aircraft maintenance line under availability contract', *Computers in Industry*, 64(5), pp. 543-555. doi: 10.1016/j.compind.2013.02.011.

Endsley, M. R. and M. Robertson, M. (2000) 'Situation awareness in aircraft maintenance teams', *International Journal of Industrial Ergonomics*, 26(2), pp. 301-325. doi: 10.1016/S0169-8141(99)00073-6.

EL Hajjar, S. T. and Alkhanaizi, M. S. (2018) 'Exploring the Factors That Affect Employee Training Effectiveness: A Case Study in Bahrain', *SAGE Open*, 8(2). doi: 10.1177/2158244018783033.

Kingdom, U. *et al.* (2015) 'Impact of non-technical dimensions of service quality on the satisfaction, loyalty, and the willingness to pay more: a cross-national research on gsm operators', 2I(11), pp. 1-16.

Krivosos, P. D. (2007) 'Communication in Aviation Safety: Lessons Learned and Lessons Required', (June), pp. 1-35. Available at: [http://asasi.org/papers/2007/Communication\\_in\\_Aviation\\_Safety\\_Paul\\_Krivosos.pdf](http://asasi.org/papers/2007/Communication_in_Aviation_Safety_Paul_Krivosos.pdf).

McCulloch, P. *et al.* (2009) 'The effects of aviation-style non-technical skills training on technical performance and outcome in the operating theatre', *Quality and Safety in Health Care*, 18(2), pp. 109-115. doi: 10.1136/qshc.2008.032045.

McDonald, N. *et al.* (2000) 'Safety management systems and safety culture in aircraft maintenance organisations', 34.

Mendonca, F. A. C. and Carney, T. Q. (2017) 'A Safety Management Model for FAR 141 Approved Flight Schools A Safety Management Model for FAR 141 Approved Flight Schools', (May). doi: 10.7771/2159-6670.1144.

Mishra, P. *et al.* (2019) 'Descriptive statistics and normality tests for statistical data', *Annals of Cardiac Anaesthesia*, 22(1), pp. 67-72. doi: 10.4103/aca.ACA\_157\_18.

Parohinog, D. and Meesri, C. (2015) *ICAO-Based Needs Assessment in Thailand's Aviation Industry: A Basis for Designing a Blended Learning Program*, *Procedia - Social and Behavioral Sciences*. Elsevier B.V. doi: 10.1016/j.sbspro.2015.11.202.

Plotts, T. (2011) 'A Multiple Regression Analysis of Factors Concerning Superintendent Longevity and Continuity Relative to Student Achievement (Doctoral Dissertation)', pp. 1-132.

Robson, A. L. *et al.* (2010) 'A systematic review of the effectiveness of training & education for the protection of workers', (January).

Shrestha, N. (2020) 'Detecting Multicollinearity in Regression Analysis', *American Journal of Applied Mathematics and Statistics*, 8(2), pp. 39-42. doi: 10.12691/ajams-8-2-1.

Siddiqui, M. H., Iqbal, A. and Manarvi, I. A. (2012) 'Maintenance resource management: A key process initiative to reduce human factors in aviation maintenance', *IEEE Aerospace Conference Proceedings*, (March). doi: 10.1109/AERO.2012.6187379.

Study, C. (2017) 'Aviation Risk Management Strategies', (January).

Taylor, J. C. and Thomas, R. L. (2003) 'Written Communication Practices As Impacted By a Maintenance Resource Management Training Intervention', *Journal of Air Transportation*, 8(1), pp. 69–90.

Teperi, A. (2010) 'Learning at air navigation services after initial training', 22(6), pp. 335–359. doi: 10.1108/13665621011063469.

Yudoko, G. and Purboyo, H. (2017) 'ScienceDirect ScienceDirect Developing a

Conceptual Model of Organizational Safety Risk: Case Studies of Aircraft Maintenance Organizations in Indonesia', *Transportation Research Procedia*, 25, pp. 136–148. doi: 10.1016/j.trpro.2017.05.386.

Zhang, L. and Wang, Y. (2018) 'Research on Prevention Strategies of General Aviation Flight Accidents Based on Regression Analysis Method', 147(Ncce), pp. 32–37. doi: 10.2991/ncce-18.2018.7.

### **Acknowledgment**

We would like to express our deepest appreciation to our supervisor Dr. WTS Rodrigo, who motivated, advised, and encouraged us regarding our research. Without his guidance and continuing help, this dissertation would not have been

possible. And also, we would like to extend our sincere gratitude to the department of aeronautical engineering and all the academic and non-academic personnel who have helped us all along.

### **Author Biography**



Dr. WTS Rodrigo  
Senior Lecturer  
Department of Aeronautical Engineering  
General Sir John Kotelawala Defence University  
Colombo, Sri Lanka



SCM Bandara  
Undergraduate in Engineering  
Department of Aeronautical Engineering  
General Sir John Kotelawala Defence University  
Colombo, Sri Lanka



KMGMB Samarakoon  
Undergraduate in Engineering  
Department of Aeronautical Engineering  
General Sir John Kotelawala Defence  
University Colombo, Sri Lanka

# An empirical analysis of the impact of aircraft maintenance technical training on risk mitigation in the Sri Lankan aviation industry

SCM Bandara<sup>1</sup>, KMGMBWB Samarkoon<sup>1</sup> and WTS Rodrigo<sup>1#</sup>

<sup>1</sup>Department of Aeronautical Engineering  
General Sir John Kotelawala Defence University, Colombo, Sri Lanka

#thusith.rodrigo@kdu.ac.lk

**Abstract:** The operational efficiency of aircraft maintenance activities is pivoted on the equilibrium between safety and productivity. Against this backdrop, aviation safety management systems play a vital role in ensuring safe operations while enhancing operational efficiency. Out of the main four pillars of safety management systems, safety promotion and to be specific technical training and its impact on risk mitigation are analyzed in this paper through an empirical study. A conceptual framework with the independent variables covering initial training, continuous training, and the availability of training infrastructure is evaluated against the impact on risk mitigation. This addresses a very specific research gap, especially in the context of the Sri Lankan commercial aviation sector where the

relationship between technical training and aviation safety is very rarely researched. The research is conducted in the form of a hypothetic deductive study based on the empirical responses of aircraft maintenance field stakeholders evaluated through statistical analysis. The outcome of the research reveals some important points as all three hypotheses are positively supported and highlight the importance of qualitative improvement of initial training and continuous training. Meanwhile, it also highlights the importance of expanding the training infrastructure to cater to the increasing technical manpower demand.

**Keywords:** Aviation Safety Management System, safety promotion, technical training, Continuous training, risk mitigation.

## 1. Introduction

### 1. Background of the Study

Importance of technical training both initial and the job is of very high importance to ensure safe operations in all aircraft maintenance endeavors. Even though the umbrella word training is used in most literature, it needs to be critically evaluated in detail. especially in the context of aviation safety management systems, the prominence of technical training is emphasized through the main aspect of safety promotion. A safety management system consists of Risk management, Safety promotion, Safety assurance, and Safety policy. Especially in the context of Sri Lankan aviation safety

promotion is given a very minimum emphasis. Safety is an essential phase of a civil aviation organization's survival and development. Aircraft maintenance can take as a far-reaching accountable factor for the safe operation of the aircraft. The accepted SMS model is credible to reduce hazards and risks, but it is difficult to directly link safety performance and risk mitigation. However, identified through training and education. Organization development gains effective competency in maintaining leadership for health and safety. (Mcdonald *et al.*, 2000). Aviation training design assists to enhance communication skills, safe working techniques, and developing situational awareness among employees (Chatzi *et al.*, 2019). Aviation safety training and education is

an essential factor to enhance safety performance. Safety promotion includes training and education and safety communication. Training and education should consist of initial job-oriented training, continuous training, and recurrent training (Andrei, 2011).

Management leadership capabilities and knowledge-sharing behavior directly affect the performance of the organization and safe working conditions. Considering the training schedule, training environment & facilities, and management review. (Alkhanaizi, 2018). Proper training on written and verbal communication, the use of communication equipment, and language proficiency is important for safe maintenance activities (Thomas, 2003). When considering the Sri Lankan aviation industry, SMS implementations are used to maintain a safe working environment and risk mitigation. So, risk assessment, hazard identification, maintaining safe data quality, record keeping, advanced safety training, improving occupational health and safety, and continuous monitoring are given a high priority by the civil aviation authority Sri Lanka within the SMS implementation framework (CAASL, 2015).

## *2. Problem Statement*

Training and education directly affect risk mitigation through safety promotion because of factors of low consideration of training and education, training capacity, lack of training knowledge, training experience problems, lack of training concurrency, etc. The safety management system is considered a systematic approach to managing safety. Training and education failures directly affect aviation safety because of the lack of updates on safety promotion. Aircraft maintenance, in-flight activities, maintenance manual referring, data records, correct procedures, and many more sectors are affected by effective technical training and education. Without proper training and education aircraft safety will entirely collapse. All modern commercial aircraft and associated equipment are highly complicated

and any person who performs maintenance activities on them needs to have in-depth exposure and training without which it will endanger both the safety of the aircraft and the passengers who are flying on board.

Aviation safety management systems (SMS) have four main pillars; safety policy, safety assurance, safety risk management, and safety promotion. Safety promotion ensures that aviation personnel is trained and competent to perform their duties and engage in a two-way communication of safety issues between the organization's management and operational personnel. To implement safety promotion in the aviation industry, mitigating risks in aircraft maintenance operations can be considered an important factor in terms of line maintenance and base maintenance. According to the ICAO, safety promotion focuses on two elements as training & education and safety communication (Andrei, 2011). So, it is important to improve training & education to mitigate the risks. Aviation risk management considers the knowledge and education of employees, Training on hazard identification and using PPE, Occurrence reporting, resources management, concern about OSH, and information understanding (Study, 2017). Therefore, considering these backgrounds researchers tend to investigate, how can these factors affect improving safety promotion towards risk mitigation in the aviation industry.

## *3. Research Questions*

1. Does continuous training impact aviation safety?
2. Does the level and quality of Initial Training by the aircraft maintenance staff affects aviation safety?
3. Does the level and quality of Training resources available by the aircraft maintenance staff affects aviation safety?

## *D. Objectives*

1. To evaluate the impact of continuous training on overall Training & education in aircraft maintenance.

2 To evaluate the relationship between initial training and Training & education in aircraft maintenance.

3. To evaluate the impact of Training resources availability towards Training & education in aircraft maintenance.

4. To ascertain the overall impact of Training & education towards risk mitigation in the craft maintenance operations.

## **2. Literature Review**

### *1. Theoretical Background*

Safety is the most important phase in the aviation industry. The national transportation safety committee of Indonesia assures that 60% of accidents and incidents occur from human factors and 34% occur from technical problems and the rest happened due to environmental problems (Yudoko and Purboyo, 2017). For safety management systems and safety performance in the aviation industry, a self-regulatory model was introduced to improve the safety of organizational aspects. The SMS should identify and reduce safety hazards by maintaining a proper level of safety risk controls. To suggest an SMS model for federal aviation regulations 141 approved flight schools have the potential to allow safety enhancement through a well-structured management system to control risk in operations. The SMS model develop based on ICAO and FAA concepts and adheres to their safety protocols. This model includes processes to initiate responsibilities and accountabilities for safety, evaluate associated risks and identify safety hazards. Safety communication and safety training & education are initial factors for risk mitigation. One of the most significant causes of accidents is still deficiencies in the training of technical personnel. Hence improving the training of technical personnel is an effective way to increase the safety of the organization (Mendonca, 2017).

2. Initial Training, continuous training, and training resources availability perspective on safety promotion.

An adequate level of initial training helps to enhance the safety of the working environment; This initial training is a supportive path to getting experience and improvement of work reliability and safety in the organization (Teperi, 2010). A proper training procedure improves employees' knowledge about all areas of safety-related activities in the organization. Training conduct for the use of personal safety equipment, maintenance safety, corrective actions, emergency precautions, responsibilities of own job areas, and how to behave in a safe work environment is most important because the final expectation of these pieces of training is risk mitigation in the working environment (McCulloch et al., 2009). Workplace productivity and standard of maintenance also depend on continuous training. Providing effective continuous training to all employees ensures better performance of the organization. To improve performances, aircraft maintenance organizations have to maintain continuous training & monitoring, updates about new manuals, and updates about new technology (Robson et al., 2010). In resource availability, the different kind of rescues and tools are important to conduct basic maintenance activities. Aircraft maintenance safety depends on the availability of technical and human resources. Aviation is the most functioning industry in the world because of that day to day updating with new procedures, tools, technology, and technical resources, and maintaining resources is very important. Maintenance resources management training also helps to enhance the performance and safety of the organization. To improve the training availability of qualified persons for training, allocating sufficient time and resources for training is also important (Datta, Srivastava and Roy, 2013).

## **3. Methodology**

This research is conducted by using the quantitative method and the study is a cross-sectional analysis. The research is based on the deductive approach which is concerned with building up hypotheses relevant to an existing

theory of aviation safety management systems. The sampling frame used in this study was distributed to the line and base maintenance employees in Sri Lankan aviation organizations. This study considered independent variables such as initial training, continuous training, and training resources availability. Risk mitigation is considered a dependent variable. According to the variables, the conceptual framework was developed to link safety promotion and risk mitigation. The necessary data for the execution of the study was gathered through a Likert scale questionnaire by creating a google form. The sample of the study was distributed among 160 employees. The random stratified sampling method was used to collect the data because of the difficulties of collecting data island-wide. The parameter became the training and education of the statistic of maintenance employees in the Sri Lankan Airlines Engineering, Fits Aviation, and Sri Lanka Airforce. The questionnaire is based on considered variables and contains eight sections. The data which was collected from questionnaires were analyzed statistically using IBM SPSS Software to examine the impact of initial training, continuous training, training resources availability, written/verbal communication, information understanding, employee engagement & feedback towards risk mitigation.

**1. Conceptual Framework**

By referring to the SMS model for federal aviation regulations 141 approved flight schools (Mendonca and Carney, 2017) developed the conceptual framework to link safety promotion and risk mitigation. training and education are categorized as initial training, continuous training, and training resources availability. The research will be discussed under six hypotheses.

H1: Initial training has a positive impact on risk mitigation towards safety promotion.

H1n: Initial training has no impact on risk mitigation towards safety promotion.

H2: Continuous training has a positive impact on risk mitigation towards safety promotion.

H2n: Continuous training has no impact on risk mitigation towards safety promotion.

H3: Training resource availability has a positive impact on risk mitigation towards safety promotion.

H3n: Training resource availability has no impact on risk mitigation towards safety promotion.

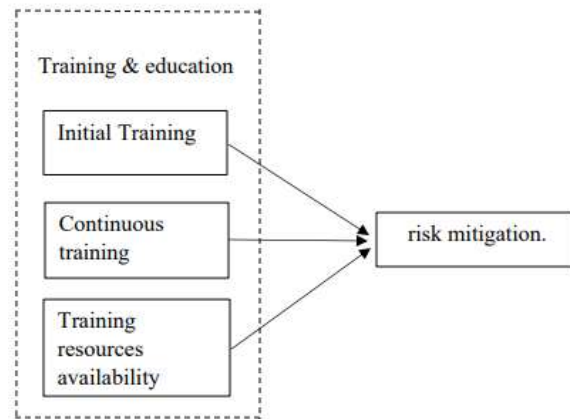


Figure 1: Conceptual Framework

**4. Results**

**1. Normality**

Checking the information is normally distributed by Skewness and Kurtosis. For Skewness, the agreed value should be within -1 to + 1 and for Kurtosis, should be within the range of -3 to + 3 (Mishra *et al.*, 2019).

Table 1: Normality Test

	Skewness	Std. Error of Skewness	Kurtosis	Std. Error of Kurtosis
Risk mitigation	-.074	.199	.129	.396
Initial Training	-.205	.199	-.543	.396
Continuous Training	-.102	.199	.019	.396

Training resources availability	-.499	.199	-.141	.396
---------------------------------	-------	------	-------	------

## 2. Validity

Kaiser-Meyer-Olkin (KMO) use to determine the validity of data and typically KMO should be between 0-1. If the value of the KMO is closer to 1 indicates that the data collected is acceptable (Kingdom *et al.*, 2015).

Table 2: KMO Test

Kaiser-Meyer-Olkin Measure of Sampling Adequacy	0.913
---	-------

## 3. Multicollinearity Test

Multicollinearity considers an identical linear relationship between two or more of the input variables. Regression analysis and subsequent results can be influenced by this situation (Daoud, 2018). The tolerance value must usually be greater than 0.1 and VIF should be less than 5 (Shrestha, 2020).

Table 3: Multicollinearity Test

variables	Collinearity Statistics	
	Tolerance	VIF
Initial Training	.430	2.327
Continuous Training	.437	2.287
Training resources availability	.530	1.886

## 4. Correlation

Pearson's correlation coefficient is generally used as a measurement to determine the correlation. If there is a coefficient (r) range between -1 to +1 it is considered a proper correlated relation. To test whether there is an adequate relationship between dependent and independent variables. Significance value can also be used as a measure to take a hypothesis decision (Zhang and Wang, 2018).

Table 4: Correlation Test

Hypothesis	Pearson Correlation	Sig. (2-tailed)	Decision
H1	.655	.000	Not Rejected
H2	.606	.000	Not Rejected
H3	.524	.000	Not Rejected

## 5. Regression

Regression is a mathematical method used to analyze variables relationships. If there is a situation where there are more than one independent variable multiple regression is carried out (Plotts, 2011). Here the linear relationship between independent variables and risk mitigation (dependent variable) has been analyzed.

Table 5: Model Summary

Model	R	R Square	Adjusted R Square	Std. Error of the Estimate
1	.740 <sup>a</sup>	.548	.528	.400

According to the above model summary, the R-value indicates a positive relationship with the dependent variable of risk mitigation due to the R-value being 0.728.

Table 6: ANOVA

Model	Sum of Squares	df	Mean Square	F	Sig.
Regression	27.384	6	4.564	28.445	.000 <sup>b</sup>
Residual	22.624	141	.160		
Total	50.008	147			

According to the above table, it can be concluded that the overall regression model is a good fit for the data where  $F(6,141) = 26.576$

and  $p < 0.0005$ . Therefore, by considering the overall significance level given in the ANOVA table which is .000 can be concluded that this study is statistically significant.

Table 7: Coefficients<sup>a</sup>

Model	Unstandardized Coefficients		Standardized Coefficients	t	Sig.
	B	Std. Error	Beta		
(Constant)	0.205	.356		.576	.565
IT	.243	.076	.277	3.209	.002
CT	.158	.083	.162	1.988	.049
TRA	.072	.084	.067	.856	.393

According to the unstandardized coefficients (B) values in the above table the regression equation can be derived which indicates, that change in one unit in independent variables affects the increase of risk mitigation as per the unstandardized coefficients B values. The equation can be derived as follows,

$$\text{Risk mitigation} = 0.205 + 0.243 (\text{IT}) + 0.158 (\text{CT}) + 0.072 (\text{TRA})$$

## 5. Discussion

The hypotheses suggested by the researchers based on the conceptual framework will be contributed to the discussion of the study. So mainly focus of this research is to analyze the relationship between safety promotion and risk mitigation. It can be done through training & education and communication channels related to safety promotion. Training & education effectiveness were analyzed through three channels initial training, continuous training, and training resources availability. Results of the normality test Skewness and Kurtosis values are within the good range as in the mid,

near to zero (+1,-1 & +3,-3) and it shows good results in normality. When considering the first hypothesis that initial training has a positive impact on risk mitigation towards safety promotion, research carried out by Ahmad and Muhammad (Ahmad and Adamu, 2014) has proven that training effect employee performance and risk mitigation. According to this study, findings revealed that initial training has a positive relationship with risk mitigation. The linear relationship between initial training and risk mitigation was found significant value (P) less than 0.01. According to findings the coefficient for correlation of Pearson is 0.655 also indicates the linear relationship.

The second hypothesis that considered continuous training has a positive impact on risk mitigation towards safety promotion, research carried out by Robson, Stephenson, and Carol (Robson *et al.*, 2010) found that continuous training and enhance knowledge assist to improve safe working conditions. According to this study, for an appropriate correlated relationship, the coefficient should range from -1 to + 1. According to findings the coefficient for correlation of Pearson is 0.606. Therefore it can be concluded that there is a positive relationship between continuous training and risk mitigation.

Referring to the third hypothesis training resource availability has a positive impact on risk mitigation towards safety promotion, according to the previous findings of Siddiqui, Habibullah, and Iqbal (Siddiqui, Iqbal, and Manarvi, 2012) establish that maintenance resources management assists to maintain safe work environment. According to this study, findings revealed that training resource availability has a positive relationship with risk mitigation. The linear relationship between training resources availability and risk mitigation was found significant value (p) less than 0.01. According to findings the coefficient for correlation of Pearson is 0.524 also indicates the linear relationship. But according to the regression, there is only a marginal contribution of training resources availability towards risk mitigation.



## 6. Conclusion

This study specifically examined the factors that impact safety promotion toward risk mitigation. The initial training, continuous training, and training resources availability were the variables that were used as affecting factors during this research and after the study, the researchers verified that all the above factors have a significant impact on safety promotion improvement towards risk mitigation. The findings confirm that the initial training, continuous training, and training resources availability, have a positive impact on risk mitigation in the aviation industry. According to our findings initial training highly affected safety promotion towards risk mitigation. So, to mitigate risk in an organization safety promotion improvement is very important. But training resource availability has only a marginal contribution towards risk mitigation.

As recommendations, the results of this research could be served as a foundation for further research on safety promotion evaluation in the aviation industry. Training resource availability areas have to be significantly improved for risk mitigation. When considering the initial training aspects can improve hazard identification training, use of personal protective equipment training, and human factor training for technicians and engineers. Continuous training is also an important factor in enhancing safety. Engaging continuous training of safety procedures in maintenance activities, and updating employees about new manuals and technology have to be improved. Training resource availability enhancement and the development of innovative training systems are also essential. Maintaining better learning & working environment and engaging qualified persons for training activities are necessary factors. Providing training course materials and training program evaluation by management assists to improve the training performance.

When considering the limitations of the study, the data were collected from just aviation-

related organizations and selected only aviation-related employees. Also, only consider the line maintenance and base maintenance trades for data collection. The study was based on quantitative data and further research may be carried out by embedding qualitative data gathered through interviews and focused group discussions for in-depth analysis. The result of this study paper could be served as a foundation for further research on enhancing safety culture through training & education.

## References

- Andrei, F. (2011) *Safety Management Manual, ICAO Doc 9859 AN/474, Incas Bulletin*. doi: 10.13111/2066-8201.2011.3.1.17.
- Baxter, L. E. (2013) 'Supportive Leadership, Employee Engagement and Occupational Safety: A Field Study', 12, p. 77. Available at: [http://trace.tennessee.edu/utk\\_graddiss/2556](http://trace.tennessee.edu/utk_graddiss/2556).
- CAASL (2015) 'CIVIL AVIATION AUTHORITY State Safety Programme Policy and Procedures Manual Second Edition -2015 State Safety Programme Policy and Procedures Manual'.
- Datta, P. P., Srivastava, A. and Roy, R. (2013) 'A simulation study on maintainer resource utilization of a fast jet aircraft maintenance line under availability contract', *Computers in Industry*, 64(5), pp. 543-555. doi: 10.1016/j.compind.2013.02.011.
- Endsley, M. R. and M. Robertson, M. (2000) 'Situation awareness in aircraft maintenance teams', *International Journal of Industrial Ergonomics*, 26(2), pp. 301-325. doi: 10.1016/S0169-8141(99)00073-6.
- Kingdom, U. *et al.* (2015) 'Impact of non-technical dimensions of service quality on the satisfaction, loyalty, and the willingness to pay more: a cross-national research on gsm operators', 21(11), pp. 1-16.
- Krivosos, P. D. (2007) 'Communication in Aviation Safety: Lessons Learned and Lessons Required', (June), pp. 1-35. Available at: [http://asasi.org/papers/2007/Communication\\_in\\_Aviation\\_Safety\\_Paul\\_Krivosos.pdf](http://asasi.org/papers/2007/Communication_in_Aviation_Safety_Paul_Krivosos.pdf).

- McCulloch, P. *et al.* (2009) 'The effects of aviation-style non-technical skills training on technical performance and outcome in the operating theatre', *Quality and Safety in Health Care*, 18(2), pp. 109–115. doi: 10.1136/qshc.2008.032045.
- Mcdonald, N. *et al.* (2000) 'Safety management systems and safety culture in aircraft maintenance organisations', 34.
- Mendonca, F. A. C. and Carney, T. Q. (2017) 'A Safety Management Model for FAR 141 Approved Flight Schools A Safety Management Model for FAR 141 Approved Flight Schools', (May). doi: 10.7771/2159-6670.1144.
- Mishra, P. *et al.* (2019) 'Descriptive statistics and normality tests for statistical data', *Annals of Cardiac Anaesthesia*, 22(1), pp. 67–72. doi: 10.4103/aca.ACA\_157\_18.
- Parohinog, D. and Meesri, C. (2015) *ICAO-Based Needs Assessment in Thailand's Aviation Industry: A Basis for Designing a Blended Learning Program*, *Procedia - Social and Behavioral Sciences*. Elsevier B.V. doi: 10.1016/j.sbspro.2015.11.202.
- Robson, A. L. *et al.* (2010) 'A systematic review of the effectiveness of training & education for the protection of workers', (January).
- Shrestha, N. (2020) 'Detecting Multicollinearity in Regression Analysis', *American Journal of Applied Mathematics and Statistics*, 8(2), pp. 39–42. doi: 10.12691/ajams-8-2-1.
- Siddiqui, M. H., Iqbal, A. and Manarvi, I. A. (2012) 'Maintenance resource management: A key process initiative to reduce human factors in aviation maintenance', *IEEE Aerospace Conference Proceedings*, (March). doi: 10.1109/AERO.2012.6187379.
- Taylor, J. C. and Thomas, R. L. (2003) 'Written Communication Practices As Impacted By a Maintenance Resource Management Training Intervention', *Journal of Air Transportation*, 8(1), pp. 69–90.
- Teperi, A. (2010) 'Learning at air navigation services after initial training', 22(6), pp. 335–359. doi: 10.1108/13665621011063469.
- Yudoko, G. and Purboyo, H. (2017) 'ScienceDirect ScienceDirect Developing a Conceptual Model of Organizational Safety Risk: Case Studies of Aircraft Maintenance Organizations in Indonesia', *Transportation Research Procedia*, 25, pp. 136–148. doi: 10.1016/j.trpro.2017.05.386.
- Zhang, L. and Wang, Y. (2018) 'Research on Prevention Strategies of General Aviation Flight Accidents Based on Regression Analysis Method', 147(Ncce), pp. 32–37. doi: 10.2991/ncce-18.2018.7.

### Acknowledgment

We would like to express our deepest appreciation to our supervisor Dr. WTS Rodrigo, who motivated, advised, and encouraged us regarding our research. Without his guidance and continuing help, this dissertation would not have been possible. And also, we would like to extend our sincere gratitude to the department of aeronautical engineering and all the academic and non-academic personnel who have helped us all along.

## Author Biography



Dr. WTS Rodrigo  
Senior Lecturer  
Department of Aeronautical Engineering  
General Sir John Kotelawala Defence  
University Colombo, Sri Lanka



SCM Bandara  
Undergraduate in Engineering  
Department of Aeronautical Engineering  
General Sir John Kotelawala Defence University  
Colombo, Sri Lanka



KMGWB Samarakoon  
Undergraduate in Engineering  
Department of Aeronautical Engineering  
General Sir John Kotelawala Defence  
University Colombo, Sri Lanka

# Predicting the Freezing of Gait in Parkinson's patients based on Machine Learning and Wearable Sensors: A review

MDVAG Jayawardena<sup>1#</sup>, PPCR Karunasekara<sup>1</sup> and YVND Sirisena<sup>2</sup>

<sup>1</sup>Department of Electrical, Electronic and Telecommunication Engineering, Faculty of Engineering, General Sir John Kotelawala Defence University, Ratmalana, Sri Lanka.

<sup>2</sup>North Central Teaching Hospital, Ragama, Sri Lanka

#varsha.anarkali@gmail.com

**Abstract:** Freezing of Gait (FoG) is a common incapacitating complication in Parkinson's patients, which will temporarily hinder the forward progression and will prevent them from re-initiating their normal gait. This can lead to potentially fatal falls and severely affect the quality of life of the patient. Due to characteristic changes in their gait, FoG can be identified by using wearable sensors such as pressure sensors, Inertial Measurement Units (IMU), and Electroencephalogram (EEG) electrodes. Classification models that run on machine learning algorithms have been frequently used. Prediction of FoG would be highly useful for the patients since this identifies the changes in their gait preceding the event and the patient can be notified. This will allow them to overcome FoG. This systematic review identifies the best sensors, sensor placements, predictive algorithms, and the limitations of the existing prediction systems. Out of all the methods reviewed, combinations of plantar pressure sensors placed on the insoles and IMUs placed on the shank produced the highest accuracies with a specificity of 91.6%. The best algorithm was identified as Convolutional Neural Networks.

**Keywords:** Freezing of Gait, Prediction, Machine learning, Wearable sensors

## 1. Introduction

Freezing of Gait (FoG) is identified as a common debilitating neurological complication in patients with Parkinson's Disease (PD), where they are temporarily unable to continue the progression of their normal gait, due to being fixated in a single position (Shalin et al., 2020a) (Mazilu et al.,

2015). Despite the patients' efforts, their motion becomes hindered, and their feet will appear to be "magnetized" or "glued" to the surface and are unable to re-initiate the normal gait. This is also termed "Paroxysmal Akinesia" (Chen et al., 2021). The quality of life of 20-80% of Parkinson's patients will be hindered due to the Freezing of Gait (Parakkal Unni et al., 2020a).

It has been observed in a study containing 6629 PD patients that 47% of the sample exhibited symptoms of FoG frequently and 28% of the population exhibited these symptoms daily (Mazilu et al., 2015). 2 out of 3 of the late-stage PD patients will experience FoG (Handojoseno et al., 2014). The severity of this condition lies with the falls resulting from this. This is because the patient will attempt to move forwards by "unfreezing" themselves, and the inability to do so will fixate them despite their efforts. Their upper body momentum will propel them forwards, resulting in a potentially dangerous fall, which could even lead to the death of the patient. 60% of the patients diagnosed with PD will experience falls caused by the FoG. (Chen et al., 2021). No cure has yet been identified to treat the FoG. Pharmaceutical therapy such as Dopamine and Leva-Dopa and treatments such as Deep Brain Stimulation (DBS) will help to alleviate the symptoms (Huang et al., 2018). Nonetheless, chemical-based therapies and DBS does not work for all patients and some patients will develop a resistance to these treatments. This emphasizes the need for drug-free therapy (Mazilu et al., 2015) (Naghavi and Wade, 2019a)

Apart from an individual's physical well-being, their psychological well-being can also be affected by the FoG. The patient will have to live their life with a constant fear of falling, which will further impede their mobility. This will lead to a characteristic change in their gaits, such as trembling of the feet and making shuffling steps, and a reduction in the step length. Due to the patient's hesitancy to move, they will experience secondary health problems such as osteoporosis and constipation (Prasad et al., 2018). Mental health problems such as anxiety could also arise due to FoG. The patients will also be highly dependent on assistance when performing their day-to-day activities, thus, will lose their sense of independence (Reches et al., 2020). This will not only be inconvenient to the patient but will be a burden for the caretakers as well. The reluctance to move out of their retreat will result in reduced amounts of social interactions, which could lead to potential social isolation, and thereby depression. This highlights the severity of FoG and the need for this issue to be addressed (Mazilu et al., 2015).

Detection of FoG can be beneficial to the patients since this will help them overcome the event and re-initiate their normal gait. Abnormal changes in the gait will be detected to identify events of FoG. After the event is detected, FoG episodes can be overcome by either changing the original path of motion, by auditory stimulations such as humming or using metronomes, or by making high steps. Current clinical modes of detection are done using video-recorded data of their gait and performing an offline analysis process. This will not be highly beneficial to the patient since they cannot be monitored continuously. (Rahman et al., 2008) (Tips to Overcome "Freezing" | ParkinsonsDisease.net, 2017).

Increasingly engineering-based solutions such as using wearable sensors are used for the detection of FoG. EEG (Electroencephalogram) and EMG (Electromyography) electrodes, skin conductance sensors, pressure sensors, and Inertial Measurement Units are commonly

used since they can be easily and comfortably worn by the patient for a long period, enabling continuous patient monitoring. They are better than motion capture systems since they work in real-time and are easy to set up. To identify and analyze the swift changes in the Gait characteristics during FoG, machine learning algorithms such as Support Vector Machines, Neural Networks, and Decision Trees have been developed (Pardoel, 2021a) (Aich et al., 2018a) (Palmerini et al., 2017a).

Prior to the occurrence of FoG, a progressive deterioration of the spatial-temporal gait patterns of individuals is observed (Borzi et al., 2021). This enables early detection or prediction of this event. Predictive systems are more desirable than detection systems since they identify FoG a time window ahead of its occurrence, thereby addressing the latency issue associated with detection systems. Detection of the event will not allow sufficient time for the patient to respond and overcome FoG. Individuals can independently identify FoG events during their medication "OFF" stage, so the use of detection systems will be limited. Prediction systems paired with preemptive cueing will notify the patient well ahead of the event. The predictive systems will use gait characteristics during a time window ahead of the event, known as "Pre-FoG", for analysis. Together with the FoG and Non-FoG gait characteristics, Pre-FoG data will be used in the identification of characteristic motor changes in PD patients before the Freezing of Gait (Mazilu et al., 2015) (Pardoel, 2021a). Thus, the analysis and development of FoG predictive systems would be highly beneficial to PD patients. Therefore, the aim of this literature review is to explore and analyze the methods of predicting FoG. This review will focus on the existing FoG predictive systems, that use wearable sensor hardware systems and predictive software developed based on machine learning algorithms. An analysis will also be done on the accuracy and feasibility of the systems developed.

## 2. Methodology

This review takes a systematic approach to analyze the existing literature. (Wright, 2007) (Aromataris and Pearson, 2014). The scope of the review was initially identified as the existing predictive technologies of Freezing of Gait in Parkinson's patients, that followed engineering-based approaches. The area of interest was studied by exploring peer-reviewed articles and scientific journals based on this topic. The databases Google Scholar, Science Direct, PubMed, and Research Gate were used to obtain the relevant literature. The keywords used for this quest, along with their synonyms, were recorded as "Freezing of Gait", "Parkinson's Disease", "Machine learning", "Prediction", "Detection", "Wearable sensors", and "Predictive algorithms". Using Boolean operators such as "And" and "Or", the keywords were combined to scale down the search results. This yielded combinations such as "Prediction of Freezing of Gait and Machine learning", "Detection or Prediction of Freezing of Gait", "Prediction algorithms and Freezing of Gait", "Parkinson's disease and Machine learning" and "Wearable sensors and Freezing of Gait".

The search results were refined by scanning the titles and the abstracts of the research articles and the latest and the most relevant literature was given priority. The duplicate articles were discarded. Following the process of screening, the literature was completely examined to identify those that used only wearable sensors and machine learning. To refine the eligible articles, 9 characteristics were observed: the number of patients used in the experiment, their age ranges, the freeze-inducing activities performed, types of sensors used, the sensor placements, number of trials for each activity, features extracted, the algorithms used for the classification process and the results obtained. A table was compiled consisting of the references for each article and the criteria observed (Table 1). Finally, the data obtained were used to develop a critical analysis of the literature that was reviewed.

Table 1. Summary of the literature.

Reference	No. of patients	Age	Activities	Sensor, Algorithms, Results
(Chen et al., 2021)	24	males- 62.827 ± 8.82, Female 69.20 ± 5.89	gait initiation, 360- and 180-degree turns and walking through crowded halls and narrow corridors	IMU sensor, Random forest algorithm, Hit rate of 68%
(Shalin et al., 2020)	5	67-80 years	walking in a freeze-inducing path, 90/180 degree turns	plantar pressure sensors, CNN classifier, Sensitivity- 82.3%, Specificity- 94.2%
(Mazilu et al., 2015)	11	68.9 ± 10.2	180 and 360-degree turns, walking on a straight line and through narrow corridors	9 IMUs, IR sensors, ECG and SCR electrodes, patient-specific cross-validation, 71.3% prediction accuracy
((Borzi et al., 2021)	11	73 ± 7	7m Timed Up and Go Test (TUG)	2 IMUs, Decision Trees and Support Vector Machines, sensitivity-84.1%, specificity -85.9%

Source: Author

### 3. Results

256 research articles were obtained from the initial search from all the databases collectively. The screening process yielded 21 articles on prediction and 50 articles on the detection of FoG. Only 22 articles that satisfied the eligibility criteria were used to compile the review. 5 review articles and 2 theses were used in the review process as well. Only the key findings for the 4 articles, with the highest number of citations, were presented in Table 1, due to space constraints. The following sections will present the results of the literature review.

#### A. Sensor types and Placements

Table 2 summarizes the types of sensors used, parameters measured, the common sensor placements, and the highest reported prediction accuracy when for different sensors.

Table 2. Summary of the types of sensors used

Sensor	Parameter	Placements	Accuracy (%)	References
Inertial Measurement Units (IMU)- Accelerometers, Gyroscopes, Magnetometers	Acceleration, angular motion, fluctuations of the magnetic field	Shin, shank, thigh, lower back, ankles, above the knee, hip	85.5	(Mazilu et al., no date b) (Chen et al., 2021) (Borzi et al., 2021) (Shalin, 2021) (Naghavi and Wade, 2019b) (Assam and Seidl, 2014)(Aich et al., 2018b) (Palmerini et al., 2017b)(Pardoel et al., 2021)(Yuan and Chakraborty, 2020) (Pardoel, 2021b)

Pressure sensors	Pressure	Plantar pressure sensors placed as an insole in shoes	92.0	(Shalin et al., 2021) (Pardoel et al., 2021)
Force plate	Ground reaction force	Beneath the feet	Not provided	(Parakkal Unni et al., 2020b)
EEG electrodes	Electrical activity -brain	Motor control region - Brain	72	(Naghavi, Miller and Wade, 2019b)(Handojoseno et al., 2018b)
ECG electrodes	Electrical activity -heart	Chest	71.3	(Mazilu et al., 2015)
Skin conductance sensors	Electrical conductance-skin	Index and middle fingers, wrist	71.3	(Mazilu et al., 2015)

Source: Author

Some of the commonly used sensors are displayed in Figure 1.



Figure 1. Types of sensors used

Sources: A) A pressure sensor insole B) 2 IMUs worn as bands on the shank (Shalin et al., 2020a) C) An ECG electrode placed on the chest and a Skin conductance electrode worn on the wrist (Mazilu et al., 2015)

Figure 2 depicts some of the common sensor locations.

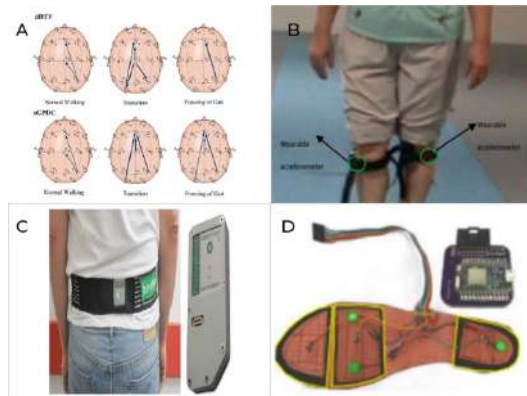


Figure 2. Sensor placements

Sources: A) EEG electrodes placed on the motor regions of the brain (Handojoseno et al., 2014) B) Accelerometers placed on the shank (Aich et al., 2018a) C) An IMU worn as a band on the waist (Weiss et al., 2013) D) 3 pressure sensors placed in an insole (Prado et al., 2020)

### C. Feature Extraction

Features are measurable quantitative data extracted from the manipulation of raw sensor data. Some of the commonly used time domain features are Mean, Standard deviation, angular velocity, angular jerk, and foot velocity (Mazilu et al., 2015) (Pardoel, 2021a) (Handojoseno et al., 2013b) (Naghavi, Miller and Wade, 2019a) (Borzi et al., 2021) (Shalin et al., 2020a). Some of the commonly used frequency domain features are spectral density and the power of the signal obtained from Fourier Transform and Approximation and Detail Coefficients obtained from Wavelet Transform (Pardoel, 2021a) (Naghavi and Wade, 2019a) (Handojoseno et al., 2013a) (Mazilu et al., 2015) (Borzi et al., 2021).

### D. Algorithms

Implementations of the commonly used algorithms are done through:

1) *Supervised pattern classification*: Uses labeled data to develop the classification model and categorizes the data into training and testing groups. Labeled training data is used to develop the classification model and

unlabelled testing data is used to validate the model (Mazilu et al., 2015) (Borzi et al., 2021).

2) *Unsupervised pattern classification*: Yields better results for prediction rather than the supervised models. Uses unlabelled data, thus this will eliminate the subjective biases. The model itself will perform the labeling process and cluster the data into freezing and non-freezing groups (Mazilu et al., 2015) (Borzi et al., 2021).

3) *Semi-supervised pattern classification*: This is a composite of the supervised and unsupervised models, so uses the advantages of both methods. A major portion of the unlabelled data and a minor portion of the labeled data is used for the development of this classifier. This eliminated the need for laborious labeling processes and allows the development of generalized and subject-specific models too. The highest reported sensitivity and specificity using this classifier were 95.9% and 95.6% respectively (Mazilu et al., 2015) (Borzi et al., 2021).

A few of the commonly used algorithms are:

1) *Neural Networks*: Convolutional Neural networks allow independent identification of spatial patterns and are favorable since feature extraction is not a necessity for this algorithm. They develop images using the data and work on pattern recognition principles. Minor disadvantages of this model are its complexity and time consumption. Sensitivities and specificities of 98.8% and 95.1% have been reported using this algorithm (Shalin et al., 2021) (Pardoel, 2021a).

2) *Decision Trees*: The observed studies used a binary classification tree method. This method prevents overfitting of the data and exhibits greater transparency in comparison with the other algorithms. Compares the data with a threshold and categorizes it along the nodes. Uses boosting techniques such as Logistic, Adaptive, and Robust boosting to enhance the performance. Can produce sensitivities and specificities of 83.8% and 82.1% (Pardoel, 2021a).



3) *Support Vector Machines*: Based on principles of binary or multiclass classification and classifies the data by constructing a hyperplane. The planes and the classes are given the maximum disparity and new data points are classified based on their positions on the plane. Can yield sensitivities as high as 89.2% (Pardoel, 2021a) (Borzì et al., 2021) (Naghavi and Wade, 2019a) (Handojoseno et al., 2013b).

#### 4. Discussion

The findings of the review will be summarized, discussed, and analyzed in-depth in this section. Prediction of FoG is identified as the detection of FoG during a period preceding its incidence and warning them using preemptive signaling. Most recent studies focused on prediction algorithms since they assist Parkinson's patients in overcoming FoG more effectively than detection systems. Thus, this review will mainly focus on the results obtained pertaining to the prediction of FoG.

##### A. Sensor types

The variations in the gait of a PD patient will result in fluctuations in the kinetics and the kinematics during and prior to the event (Parakkal Unni et al., 2020a). These can be effectively captured by wearable sensors. Different physiological parameters respond to FoG in different ways, thus different types of sensors will capture different characteristics of FoG, depending on the type of data that it collects. Increasingly, multimodal sensors have been used for the detection and prediction of FoG, since all the variations cannot be captured by a single type of sensor. (Shalin et al., 2020a). This also maximizes the chance of identifying the event, by compensating for the patient-specific differences. Figure 1 and Table 2 refer to the commonly used types of sensors.

It is evident that IMUs were the most widely used sensors and pressure sensors yielded the highest accuracy out of all the sensors reviewed. IMUs are lightweight and compact devices that could be easily accessed and worn on the patient's body, with minimal

inconvenience. This makes IMUs preferable compared to the other wearable sensors. They are usually combinations of accelerometers, gyroscopes, and magnetometers. Accelerometer data were more commonly used in comparison with other IMU data. Pressure sensors are among those that emerged recently, and these sensors yielded the highest reported prediction accuracy. They are more comfortable to be worn on the body and are less intrusive. All pressure sensors observed were used as plantar pressure sensors on the insole of the shoe. Thus, pressure sensors can capture data more conveniently from the patients, with greater accuracy. Pairing pressure sensors with IMUs yielded the highest reported sensitivity (78.0%) and specificity (91.6%), in comparison with single sensors, and multimodal sensors produced the best overall performance. (Shalin et al., 2021) (Pardoel, 2021a). To analyze the use of other sensors like force plates, EEG electrodes, ECG electrodes, and skin conductance sensors, limited literature was available.

##### A. Sensor Placements

Several studies compared the best sensor placements for the IMUs, which produced a greater prediction accuracy compared to EEG, ECG, and skin conductance electrodes. Figure 2 and Table 3 depict the common sensor placements. Wearable accelerometers that were sported on the shank and the thigh yielded the highest prediction rates, which were 95.7 and 96.7 respectively (Naghavi and Wade, 2019a) (Assam and Seidl, 2014). Sensors which were worn on the waist were unable to capture a large portion of FoG data since it is distal from the lower body that is mostly affected by FoG. It was only able to capture 5.1% of the FoG data. Out of all the sensor positions reviewed, it was evident that the shank was the optimal sensor location due to the highest prediction accuracy and the least patient dependency. Plantar pressure sensors were not used as single pressure units, but multiple sensors were used to capture point pressure data. Most of the studies using

pressure sensors used the commercial F-Scan sensing system, which had 3.9 sensors per cm<sup>2</sup>, and yielded sensitivities of 82.1% and specificities of 89.5% (Pardoel, 2021a). One study used 3 pressure sensors placed on the metatarsals, calcaneus, and phalanges. This yielded a mean sensitivity of 96% and a mean specificity of 99.6% (Prado et al., 2020). Thus, individual pressure sensing cells can capture more accurate FoG data, in comparison with the commercial F-Scan system. All the systems placed sensors on the left and right regions of the body, and no detectable differences between the data recorded from the 2 regions were identified (Palmerini et al., 2017a).

### *C. Feature Extraction*

Features that exhibit characteristic differences in the gait patterns of FoG, Non-FoG, and Pre-FoG events should be used in the prediction of FoG. Threshold-based detection methods are less complex, so they can be processed faster (Pardoel, 2021a). This allows threshold-based classification methods to be used in the real-time prediction of FoG. It has been identified that frequency domain data allows the mapping of minute changes in the Pre-FoG windows. Time domain features allow distinct differences to be observed between the gait patterns. By performing a time-frequency analysis of the data, using the optimum number of parameters, the best results can be obtained (Pardoel et al., 2019) (Shalin et al., 2020b).

### *D. Algorithms*

Predictive systems were mostly based on 3 class classification techniques, since the FoG, Non-FoG, and Pre-FoG classes have to be taken into consideration. Subject-specific models yield greater prediction accuracies as opposed to models that are generalized for the whole population. However, limited data is available to generate models specific to each individual, therefore generalized models are more desirable. All the studies used for the review used machine learning models to classify the data and produce predictions. (Mazilu et al., 2015). The algorithms that yielded the best

performances were identified as Convolutional Neural Networks, Adaptive Boosted Decision Trees, Support Vector Machines, and Random Forests (Pardoel, 2021a).

### *E. Limitations*

Most of the existing predictive systems have not focused on producing real-time results and are based on offline processing techniques. Without real-time analysis, feedback cannot be provided to the patient with a minimal time delay, thereby making the existing systems less useful. FoG manifests in different ways for different PD patients, therefore generalized models are less effective. The feasibility of the existing systems cannot be guaranteed due to patient-specific differences. This poses a risk of incorrect classification and classification metrics, thereby producing incorrect validations for the model (Pardoel et al., 2019) (Palmerini et al., 2017a).

## **5. Conclusion**

review, the need for an accurate FoG prediction system has been identified, which was to address the latency issues posed by the detection system. This will be more useful for the patients to overcome events of FoG. Out of the literature reviewed, the best wearable sensors were identified as multimodal sensors that used Plantar pressure sensors and Inertial Measurement Units, with the sensitivities and specificities reported as 78.0% and 91.6%. The optimal sensor placements for the IMU were identified as the shank and for the plantar pressure sensors, the positions of calcaneus, metatarsals, and phalanges yielded a greater accuracy. Classification models that used time-frequency domain features were better than individual time or frequency domain features since they combined the advantages of the two domains. The best classification algorithm out of the commonly used ones was identified as the Convolutional Neural Networks, with the highest reported sensitivity of 98.8%. A degree of personalization could be added by incorporating semi-supervised classification techniques. Thus, a system based on plantar

pressure sensors and Inertial Measurement Units would open a promising avenue for the prediction of Freezing of Gait.

## References

Aich, S. et al. (2018a) "A validation study of freezing of gait (FoG) detection and machine-learning-based FoG prediction using estimated gait characteristics with a wearable accelerometer," *Sensors* (Switzerland), 18(10). Available at: [HYPERLINK "https://doi.org/10.3390/s18103287"](https://doi.org/10.3390/s18103287)<https://doi.org/10.3390/s18103287>.

Aromataris, E. and Pearson, A. (2014) "The systematic review: an overview," *The American journal of nursing*, 114(3), pp. 53–58. doi: 10.1097/01.NAJ.0000444496.24228.2c.

Assam, R. and Seidl, T. (2014) "Prediction of freezing of gait from parkinson's disease movement time series using conditional random fields," in *Proceedings of the 3rd ACM SIGSPATIAL International Workshop on the Use of GIS in Public Health, HealthGIS 2014 - In Conjunction with the 22nd ACM SIGSPATIAL International Conference on Advances in Geographic Information Systems, ACM GIS 2014*. Association for Computing Machinery, pp. 11–20. Available at: <https://doi.org/10.1145/2676629.2676630>.

Barry, E. et al. (2014) "Is the Timed Up and Go test a useful predictor of risk of falls in community dwelling older adults: A systematic review and meta- analysis," *BMC Geriatrics*, 14(1). Available at: <https://doi.org/10.1186/1471-2318-14-14>.

Borzi, L. et al. (2021) "Prediction of freezing of gait in parkinson's disease using wearables and machine learning," *Sensors* (Switzerland), 21(2), pp. 1–19. Available at: <https://doi.org/10.3390/s21020614>.

Chen, Z. et al. (2021) "Prediction of Freezing of Gait in Parkinson's Disease Using a Random Forest Model Based on an Orthogonal Experimental Design: A Pilot Study," *Frontiers in Human Neuroscience*, 15. Available at:

<https://doi.org/10.3389/fnhum.2021.636414>  
..

Handojoseno, A.M.A. et al. (2013a) "Using EEG spatial correlation, cross frequency energy, and wavelet coefficients for the prediction of Freezing of Gait in Parkinson's Disease patients," in *Proceedings of the Annual International Conference of the IEEE Engineering in Medicine and Biology Society, EMBS. Institute of Electrical and Electronics Engineers Inc.*, pp. 4263–4266. Available at: <https://doi.org/10.1109/EMBC.2013.6610487>.

Handojoseno, A.M.A. et al. (2018a) "Prediction of freezing of gait in patients with Parkinson's disease using EEG signals," in *Studies in Health Technology and Informatics*. IOS Press, pp. 124–131. Available at: <https://doi.org/10.3233/978-1-61499-845-7-124>.

Huang, C., Chu, H., Zhang, Y., & Wang, X. (2018). *Deep Brain Stimulation to Alleviate Freezing of Gait and Cognitive Dysfunction in Parkinson's Disease: Update on Current Research and Future Perspectives*. *Frontiers in Neuroscience*, 12(FEB). <https://doi.org/10.3389/FNINS.2018.00029>

Mazilu, S. et al. (2015) *Prediction of Freezing of Gait in Parkinson's from Physiological Wearables: An Exploratory Study*, *IEEE JOURNAL OF BIOMEDICAL AND HEALTH INFORMATICS*. Available at: [www.shimmer-research.com](http://www.shimmer-research.com).

Naghavi, N., Miller, A. and Wade, E. (2019a) "Towards real-time prediction of freezing of gait in patients with parkinson's disease: Addressing the class imbalance problem," *Sensors* (Switzerland), 19(18). Available at: <https://doi.org/10.3390/s19183898>.

Palmerini, L. et al. (2017a) "Identification of characteristic motor patterns preceding freezing of gait in Parkinson's disease using wearable sensors," *Frontiers in Neurology*, 8(AUG). Available at: <https://doi.org/10.3389/fneur.2017.00394>.

- Parakkal Unni, M. et al. (2020a) "Data-Driven Prediction of Freezing of Gait Events From Stepping Data," *Frontiers in Medical Technology*, 2. Available at: <https://doi.org/10.3389/fmedt.2020.581264>.
- Pardoel, S. et al. (2019) "Wearable-sensor-based detection and prediction of freezing of gait in parkinson's disease: A review," *Sensors (Switzerland)*. MDPI AG. Available at: <https://doi.org/10.3390/s19235141>.
- Prado, A., Kwei, K., Vanegas-Arroyave, N., & Agrawal, S. K. (2020). Identification of Freezing of Gait in Parkinson's Patients Using Instrumented Shoes and Artificial Neural Networks. *Proceedings of the IEEE RAS and EMBS International Conference on Biomedical Robotics and Biomechatronics, 2020-November*, 68-73. <https://doi.org/10.1109/BIOROB49111.2020.9224357>
- Prasad, S., Lenka, A., Stezin, A., Naduthota, R. M., Jha, M., Yadav, R., & Pal, P. K. (2018). A Comparative Study of Early and Late Onset Freezing of Gait in Parkinson's Disease. *Annals of Indian Academy of Neurology*, 21(4), 256. [https://doi.org/10.4103/AIAN.AIAN\\_459\\_17](https://doi.org/10.4103/AIAN.AIAN_459_17)
- Rahman, S. et al. (2008) "The factors that induce or overcome freezing of gait in Parkinson's disease," *Behavioural Neurology*, 19, pp. 127-136.
- Reches, T., Dagan, M., Herman, T., Gazit, E., Gouskova, N. A., Giladi, N., Manor, B., & Hausdorff, J. M. (2020). Using wearable sensors and machine learning to automatically detect freezing of gait during a fog-provoking test. *Sensors (Switzerland)*, 20(16), 1-16. <https://doi.org/10.3390/s20164474>
- Shalin, G. et al. (2020a) "Prediction of Freezing of Gait in Parkinson's Disease from Foot Plantar-Pressure Arrays using a Convolutional Neural Network," in *Proceedings of the Annual International Conference of the IEEE Engineering in Medicine and Biology Society, EMBS. Institute of Electrical and Electronics Engineers Inc.*, pp. 244-247. Available at: <https://doi.org/10.1109/EMBC44109.2020.9176382>.
- Shalin, G. (2021) Prediction and Detection of Freezing of Gait in Parkinson's Disease using Plantar Pressure Data.
- Tiedemann, A. et al. (2008) "The comparative ability of eight functional mobility tests for predicting falls in community-dwelling older people," *Age and Ageing*, 37(4), pp. 430-435. Available at: <https://doi.org/10.1093/AGEING/AFN100>.
- "Tips to overcome 'freezing'" (2017) *Parkinsonsdisease.net*, 24 March. Available at: <https://parkinsonsdisease.net/living-with-pd/overcoming-freeze> (Accessed: July 15, 2022).
- Weiss, A. et al. (2013) "Does the evaluation of gait quality during daily life provide insight into fall risk? A novel approach using 3-day accelerometer recordings," *Neurorehabilitation and neural repair*, 27(8), pp. 742-752. Available at: <https://doi.org/10.1177/1545968313491004>.
- Wright, R. W. et al. (2007) "How to write a systematic review," *Clinical orthopaedics and related research*, 455, pp. 23-29. doi: 10.1097/BLO.0b013e31802c9098.
- Yuan, A.M. and Chakraborty, S. (2020) "A Study of Deep Learning for Predicting Freeze of Gait in Patients with Parkinson's Disease," in *Proceedings - 19th IEEE International Conference on Machine Learning and Applications, ICMLA 2020. Institute of Electrical and Electronics Engineers Inc.*, pp. 1324-1331. Available at: <https://doi.org/10.1109/ICMLA51294.2020.00207>.

### Author Biography



Varsha Jayawardena is currently a final year Biomedical Engineering Undergraduate at the Faculty of Engineering of

General Sir John Kotelawala Defence University. Her final year research is based on the Prediction of Freezing of Gait in Parkinson's patients using wearable sensors.



Dr. PPCR Karunasekara is a senior lecturer of the Biomedical Engineering degree program at the Department of Electrical, Electronic, and Telecommunication Engineering at General Sir John Kotelawala

Defence University, Sri Lanka. Her research interests include Neural Engineering, Biomechanics, and Rehabilitation Engineering.



Dr. Darshana Sirisena (MBBS, MD (Col.)) is a consultant Neurologist with a special interest in Movement disorders. He is currently the president of the Association of Sri Lankan Neurologists.

# Local Binary Pattern based features for Prostate Cancer Detection

KAI Harsha<sup>1#</sup>, MB Rathnayaka<sup>2,3</sup> and DK Hewadikaram<sup>1</sup>

<sup>1</sup>General Sir John Kotelawala Defence University, Ratmalana, Sri Lanka

<sup>2</sup>University of Colombo, Colombo

<sup>3</sup>Utsouthwestern, University of Texas, Texas, USA

#harsha99indu@gmail.com

**Abstract:** Prostate cancer is one of the most common cancers in males and one of the significant causes of cancer mortality. Most prostate malignancies are presently diagnosed based on an increased PSA level, despite this biomarker having only limited accuracy. Prostate cancer differs from most other cancers because it is frequently multifocal and does not appear as a single spherical mass. The illness progresses at different rates, and it is frequently asymptomatic until it has gone to late stages. Multi-parametric MRI (mpMRI) has advanced dramatically in the last 20 years, as has the treatment of localised prostate cancer. As a result, this research aims to develop an algorithm to identify features based on the Local Binary Pattern (LBP) based histogram and Grey Level Run Length Matrix (GLRLM) characteristics of mpMRI images, to improve detection rate and accuracy of prostate cancer diagnosis. Local binary patterns are texture descriptors that have been effectively employed as image descriptors in various applications. Images were gathered from a public image database to complete this work. The operator is applied to the selected region of interest (ROI) to generate the LBP image. Texture pattern probability was summarised into a histogram, and second-order statistics were obtained using the GLRLM operator. The statistical significance of the eleven characteristics was determined using an independent two-sample t-test using four features from the histogram and seven features from the GLRLM operator. The suggested approach yielded three favourable outcomes in the research, which can be utilised to identify malignant tumours from benign tumours. The positive results include the first-

order statistics standard deviation and kurtosis and the second-order statistic Run Length Non-uniformity (RLN).

**Keywords:** Prostate cancer diagnosis, LBP, GLRLM

## 1. Introduction

Prostate cancer is the second most common cancer among men, and men with prostate cancer face death at a higher rate than their estimated frequency, as shown in Figure 1. Because prostate cancer is typically multifocal and does not show as a single spherical mass, it is different from most other tumours. The disease advances at varying speeds, and it is typically asymptomatic until it is advanced. According to the Global Cancer Observatory, the incidence and mortality rate of prostate cancer is expected to drastically increase (see Figure 2). Prostate cancer usually has no symptoms in its early stages, but it may be detected by screening, even if it is latent in the body. Physicians have an interesting but difficult task in identifying prostate cancer accurately. In today's medical world, there is a clear link between high prostate-specific-antigen (PSA) findings and prostate cancer diagnosis. Despite its low sensitivity and specificity for identifying prostate cancer, the PSA test remains one of the best conventional indicators for early identification of prostate cancer (Etzioni *et al.*, 2002; Catalona and Loeb, 2005; Mitchell *et al.*, 2005; Schröder and Roobol, 2009).

Current methods have the unintended consequence of over-diagnosing low-risk illnesses while under-diagnosing high-risk

cancers. In those with high PSA levels, histological confirmation is required, which is usually obtained by random transrectal ultrasonography (TRUS) guided prostate biopsy. This approach, on the other hand, provides false-negative outcomes. As a result of these false results, there is a growing understanding of the potential benefits of employing imaging tools to guide biopsy, allowing for better diagnosis of larger tumours that are more likely to be clinically important.

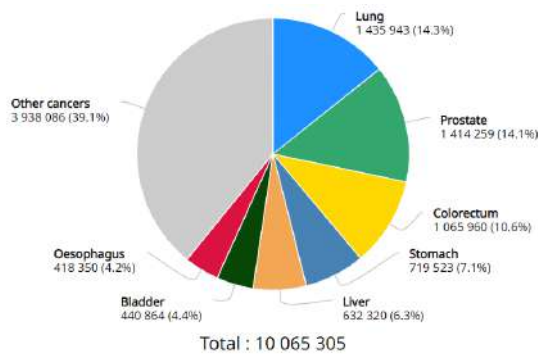


Figure 1. Estimated number of new cases in 2020, worldwide, males, in all ages

Source: GLOBOCAN 2020

#### A. Multi-parametric Magnetic Resonance Imaging (mpMRI)

The spectrum of available imaging modalities is always growing in response to changes in treatment choices, scientific developments, and technology advancements. One of the earliest imaging modalities to be employed was computed tomography (CT). CT has been replaced by alternative imaging methods such as endorectal, transrectal, ultrasonography for diagnosis and localised staging, and magnetic resonance imaging (MRI) at various institutions since it cannot identify intrinsic prostate cancer.

Among all imaging modalities, mpMRI has emerged as the most efficient and well-established approach for identifying and staging cancers inside the prostate gland (Hricak *et al.*, 2007; Fuchsjager *et al.*, 2008; Seitz *et al.*, 2009; Dinh *et al.*, 2016). mpMRI

paired with image-guided biopsy has better-assessed parameters such as the size, location, and staging of distinct lesions inside the prostate than the blood PSA screening test. A mpMRI imaging combines anatomical T2-weighted images with other imaging techniques such as diffusion-weighted (DW) imaging, dynamic contrast-enhanced imaging (DCE), and magnetic resonance spectroscopic imaging (MRSI). T2 weighted MRI imaging aid in the rapid identification of different portions of the prostate, such as the peripheral zone, transition zone, and other structures such as the prostatic capsule, prostatic urethra, and seminal vesicles. Because of their superior resolution, T2 weighted images are also better at identifying the anatomic interactions of the tumour with crucial structures such as the prostatic capsule and neurovascular bundles (Weinreb *et al.*, 2009; Turkbey *et al.*, 2016).

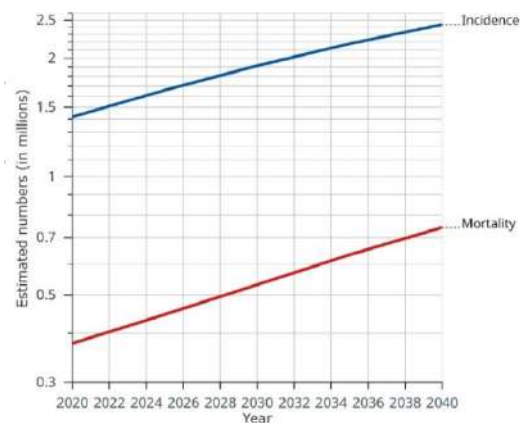


Figure 2. Estimated numbers from 2020 to 2040, age (0-85+)

Source: CANCER TOMORROW | IARC

#### B. Local Binary Pattern (LBP)

Texture analysis is critical in the field of pattern recognition and classification (Haralick, Dinstein and Shanmugam, 1973; Feng *et al.*, 2015). Initially, classification methods focused mostly on textural image statistical data. The local binary pattern (LBP) was established by Ojala *et al.* as a texture descriptor for describing 2D textures in grey images (Ojala, Pietikäinen and Harwood, 1996; Ojala *et al.*, 2001). Due to its ease of implementation, quick calculation, and high

efficiency, LBP has already been extensively researched and used in a variety of fields. The importance of using the word “Local” is that the LBP value is continuously computed by examining the pixel characteristic of its surrounding called the neighbourhood. It is explained in the following content how this property can be expressed solely using the numbers “0” and “1,” resulting in a 0-1 pattern, which is why the name “Binary Pattern” is used. The centre pixel of the image is obtained by comparing the pixel value to its neighbours. By thresholding each image pixel in the neighbourhood with the pixel value of the centre pixel, a binary value is obtained for each image pixel. A binary pattern may be made out of this binary code by reading the values clockwise or anticlockwise. This process is shown in Figure 3. It is important to remember to maintain the exact starting pixel location and the direction throughout the calculation. Each binary pattern is then converted into a decimal value.

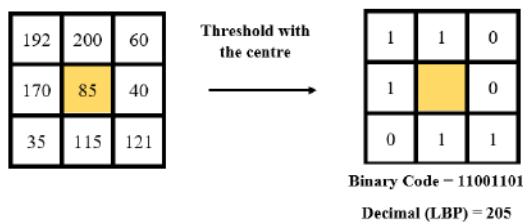


Figure 3. Basic LBP Operator

The LBP code generated is used for classification or segmentation features. As a result, a histogram based on the frequency of binary patterns is constructed. The histogram developed depicts the distribution of local micropatterns such as edges, spots, and flat areas throughout the whole image. Furthermore, while expressing an image, it is critical to keep the spatial information of the pixels in mind.

### B. Gray Level Run Length Matrix (GLRLM)

The grey-level run-length matrix (GLRLM) is a matrix that may be used to create texture characteristics for texture analysis of a given ROI. The texture is characterised as grey

intensity pixels stretching out from the reference pixels in a specific direction. A grey level run collects pixels with the same grey level score scattered over the ROI in a particular sequence collinearly. The GLRLM is a two-dimensional matrix with each element representing the number of elements  $j$  in the direction and the intensity  $I$ . Horizontal ( $0^\circ$ ), anti-diagonal ( $45^\circ$ ), vertical ( $90^\circ$ ), and diagonal ( $135^\circ$ ) are the four primary orientations that are usually considered in an application (see Figure 4).

Galloway initially proposed the run-length method for statistical texture analysis in 1975 (Galloway, 1975). Since then, various applications have been developed based on features created from this technique, including content-based image retrieval, image segmentation, object classification, and many others. Galloway presented five features for classifying the identical set of terrain samples investigated by Haralick (Haralick, Dinstein and Shanmugam, 1973), and the results were auspicious. Long Runs Emphasis (LRE), Short Runs Emphasis (SRE), Gray Level Non-uniformity (GLN), Run Length Non-uniformity (RLN), and Run Percentage (RP) are the features. Chu et al. developed two additional features that employ the grey level distribution of runs instead and are proven to be highly helpful in classification after observing the symmetrical roles played by grey levels and run-length (Chu, Sehgal and Greenleaf, 1990). These two features are said to be analogical to LRE and SRE. In this research, these seven features were extracted from the LBP image of the selected ROI, expecting better classification results. Table 1 lists the features and their computation.



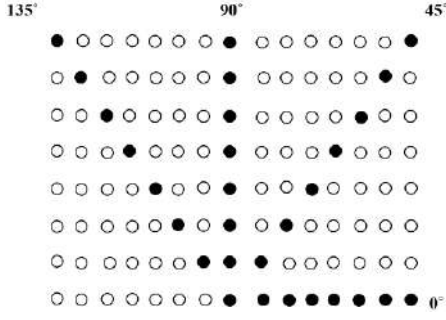


Figure 4. Four main directions of GLRLM computation

### C. The Cancer Imaging Archive (TCIA)

TCIA is a public-access service that de-identifies and makes a large collection of cancer-related medical images accessible to the public. The information is organized into "collections," which are collections of images from various patients that are linked by a common disease, imaging modality, or research topic. TCIA's principal radiological imaging file format is DICOM. Images are complemented by supporting data such as patient outcomes, treatment information, genomes, and expert assessments when they are available.

## 2. Methodology

### Image Database: PROSTATEx Image Collection

"PROSTATEX" image collection is a collection of MRI studies performed on the prostate from the past study carried out by Litjens et al (Geert Litjens *et al.*, 2017). The collection contains T2-weighted, DCE, DW and proton density-weighted (PD-W) imaging used in research (K *et al.*, 2013; Litjens *et al.*, 2014; Geert Litjens *et al.*, 2017). Litjens et al. obtained a total of 165 subsequent studies with prostate cancer (187 lesions) and 183 patients without prostate cancer for a total of 348 trials of 347 individuals to test the CAD system outlined in the research. A pathologist assessed the biopsy specimens, and the results were utilised as the actual truth. With a score per modality and a point marker, the radiologist identified regions of suspicion. A

biopsy was taken if an area was suspected of being cancerous. According to the PI-RADS recommendations for prostate MRI acquisition, all images were taken without the involvement of an endorectal coil. In the subsequent phases, prostate segmentation is necessary to lower the complexity of the detection problem for the classifiers. The segmentation was done using an atlas-based technique. DICOM encoding is used to deliver the obtained MR images. A single study with numerous DICOM images is created for each subject. The DICOM images are divided into several series, each of which contains several instances. Two separate CSV files were used to present the study findings and DICOM image details, named ProstateX-Findings and ProstateX-Images respectively.

Table 1. GLRLM features

Feature
Short Run Emphasis (SRE) = $\frac{1}{n} \sum_{i,j} \frac{p(i,j)}{j^2} \dots (1)$
Long Run Emphasis (LRE) = $\frac{1}{n} \sum_{i,j} j^2 p(i,j) \dots (2)$
Grey Level Non-uniformity (GLN) = $\frac{1}{n} \sum_i (\sum_j p(i,j))^2 \dots (3)$
Run Percentage (RP) = $\sum_{i,j} \frac{n}{p(i,j)} \dots (4)$
Run Length Non-uniformity (RLN) = $\frac{1}{n} \sum_i (\sum_j p(i,j))^2 \dots (5)$
Low Grey Level Run Emphasis (LGRE) = $\frac{1}{n} \sum_{i,j} \frac{p(i,j)}{i^n} \dots (6)$
High Grey Level Run Emphasis (HGRE) = $\frac{1}{n} \sum_{i,j} i^2 p(i,j) \dots (7)$

### A. MRI Image Selection

The images were categorised into training and test sets. The training set included 204 subjects, and the test set included 140 subjects.

From the ProstateX-Findings.csv file, patients with only a fid value of 1 were selected. This means that the patient has only one lesion. Selected patients were then further categorised into ‘True’ and ‘False’ categories using the parameter ‘ClinSig’ in the ProstateX-Findings.csv file. For each of the classified patients, T2-weighted Turbo Spin Echo images from the transversal plane were selected to further proceed in the study. This categorisation process resulted in 76 False and 33 True patient data. The images have been cropped to facilitate image analysis efforts and lessen the detection process’s complexity. It was done with the use of an atlas-based segmentation method. The cropped images were of BMP file format. Figure 5(a) and (b) shows the DICOM images of True and False patients from the transversal plane, while Figure 5(c) and (d) depicts the selected cropped images.

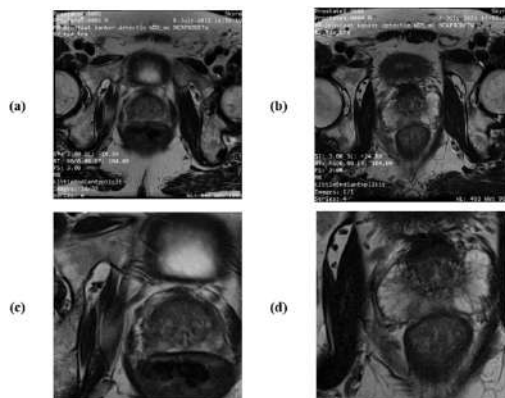


Figure 5. MRI images of the transversal plane. DICOM image of (a) False patient and (b) True patient. Cropped image of (c) False patient and (d) True patient

### B. Algorithm Implementation

LBP and GLRLM were proposed to implement the detection algorithm in this research work. To compute the first-order and second-order statistics, the algorithm was built using the MATLAB (2021a) platform with an experimental environment of Windows 11 system and 11th Gen Intel(R) Core (TM) i5

processor 2.40 GHz. The algorithm’s phase structure is made up of stages, each of which serves a different purpose. The flow diagram of the algorithms is depicted in Figure 6.

1) Algorithm 1: LBP + Histogram Features: The MRI images were collected from the database POSTATEX Image Collection, and the initial stage in this algorithm is to read them. The second step is to use manual ROI selection to mask out the prostate gland, shown in Figure 7. The function ‘roipoly’ was used to construct the mask as a binary image for manual ROI selection, setting pixels inside the ROI to 1 and pixels outside the ROI to 0.

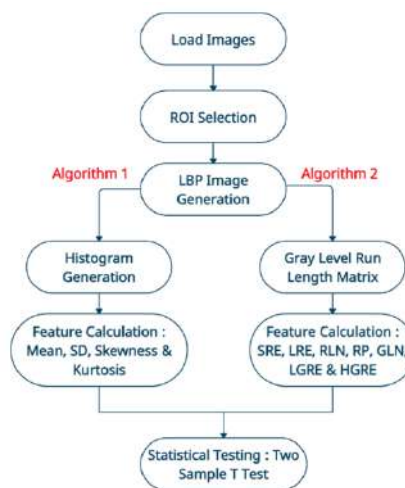


Figure 6. Flow diagram of the proposed algorithms

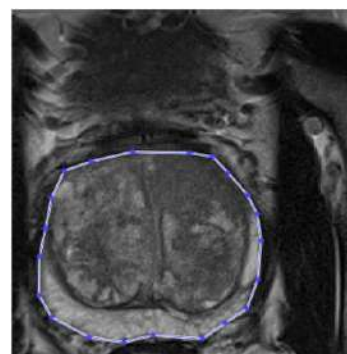


Figure 7. Manual ROI selection of the prostate gland

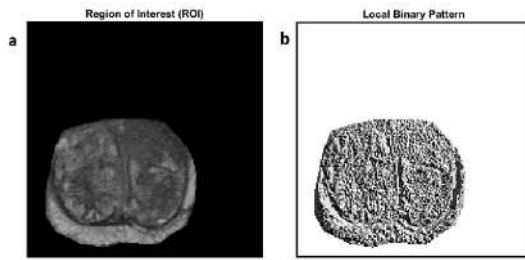


Figure 8. Region of Interest and LBP Image (a) Region of Interest (b) LBP image of the ROI

The next step is to create the LBP image from the chosen ROI, one of the most critical steps. The LBP image was generated using a MATLAB script. Figure 8 shows the ROI selected and the LBP image generated. The histogram of the ROI's LBP image was created after the ROI's LBP image was produced. To accomplish so, the mask's pixels outside the ROI set to 0 were first transformed to NaN (Not a Number) format. The background pixels were then assigned to NaN by scalar multiplying the mask with the LBP image. Then using the functions 'unique' and 'accumarray', the grey values and their frequencies of the LBP image was determined. Finally, using the function "bar", the histogram was generated (see Figure 9). determined. Four first-order statistics were calculated using the histogram: mean, skewness, standard deviation, and kurtosis. These features were calculated for both True and False patients, and the results were tabulated.

2) Algorithm 2: LBP + GLRLM Features: Manual ROI selection and LBP image creation utilised the same MATLAB script as for algorithm 1. A user-defined function named 'glrlm' was constructed with reference to a preprogramed script to produce the GLRLM matrix (Elferink, 2021). The newly defined process computed the seven features. The features are SRE, LRE, RLN, RP, GLN, LGRE and HGRE. For statistical testing, the seven features were computed for both True and False patients and tabulated.

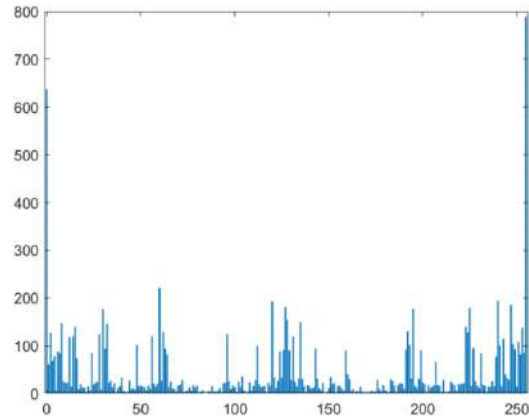


Figure 9. Histogram generated out of an LBP image.

3) Statistical Testing: In the field of research, one is interested in deriving conclusions about a population, yet it is typically impractical or impossible to examine the entire population. Because the goal is frequently to predict the future performance of the proposed system, prototype, or algorithm under similar or different conditions, statistical inference is critical to having rigorous and appropriate tests. The two-sample t-test performed the hypothesis testing of this study. The two-sample independent t-test used in this study confirms if the mean of a normally distributed numerical outcome variable varies between the two separate groups. The variables of the test were the histogram and GLRLM features of True and False patients. The two-sample t-test was conducted at a 5% confidence level. The algorithm was programmed to return whether the null hypothesis was rejected or not along with the p-value. The MATLAB script uses the variable "h", which produces "0" if accepted null hypothesis. If not, the algorithm indicates the null hypothesis was rejected by returning "1". The p-value in a t-test is the chance of finding a test statistic that is as severe as, or more extreme than, the observed value. Small p values cast doubt on the validity of the null hypothesis.

### 3. Results

To diagnose prostate cancer patients, the purpose of this study was to find any LBP-

based features that can classify benign and malignant tumours. The algorithm calculates four first-order and seven second-order statistics using True and False patient image data. A histogram feature provided first-order statistics, whereas GLRLM provided second-order statistics. Next, by carrying out a two-sample T-test, the aim was to confirm which of the statistics were better at classifying the patients as healthy and cancerous. Table 2 summarises the results obtained from the t-test for first-order statistics. The features mean and skewness gave a result of “0”, indicating the acceptance of the null hypothesis. This result concludes no significant difference in the two populations at a 5% confidence interval. In contrast, the features SD and kurtosis produced a result of “1”, indicating the rejection of the null hypothesis. This observed result concludes that these two features would better identify benign tumours from malignant tumours.

Table 2: Results of the two-sample t-test of the histogram features

Feature	h	Accept/ Reject	p
Mean	0	Accept	0.1898
SD	1	Reject	7.5079e-04
Skewness	0	Accept	0.0794
Kurtosis	1	Reject	0.0300

Table 3 summarises the results of the two-sample t-test. The features SRE, LRE, GLN, RP, LGRE and HGRE gave a result of “0”, indicating the acceptance of the null hypothesis. This result concludes no significant difference in the two populations at a 5% confidence interval. On the contrary, for the feature RLN, the result was “1”, indicating the rejection of the null hypothesis. This observed result concludes that this feature would be better at identifying benign tumours from malignant tumours.

Table 3. Results of the two-sample t-test of the GLRLM features

Feature	h	Accept Reject	p
SRE	0	Accept	0.4730
LRE	0	Accept	0.1099
GLN	0	Accept	0.0567
RP	0	Accept	0.0270
RLN	1	Reject	0.0207
LGRE	0	Accept	0.0614
HGRE	0	Accept	0.0578

#### 4. Discussion

Texture characteristics from mpMRI images have previously been promoted as predictive biomarkers in prostate cancer. The suggested method generated first-order and second-order statistics to reveal LBP-based features to detect prostate tumours using mpMRI images. Eleven LBP texture features were assessed in the study. The researcher found three statistically significant ( $P < 0.05$ ) features using a statistical evaluation approach. They were: first-order statistics SD (B-14.5611, M-16.5000), Kurtosis (B-54.5794, M-39.0421) and second-order statistic feature GLRLM-based RLN (B-5193.4605, M-4361.7848). The results obtained depict that the benign and malignant tumours can be distinguished using these three features. Future developments make it possible to improve algorithms for automatic detection of prostate cancer using the identified positive features. Assessed other features: Mean, Skewness, SRE, LRE, GLN, RP, LGRE and HGRE showed no statistical difference between the two categories. These negative results indicated that benign and malignant tumours could not be distinguished using these eight features.

GLRLM-based RLN has been effectively used in many cancer detection algorithms. A. Kunimatsu et al. (2018) used MRI image-based texture analysis to compare and elucidate

Primary Central Nervous System Lymphoma (PCNSL) and Glioblastoma (GBM) (Kunimatsu *et al.*, 2018). This research estimated first-order and second-order features using grey level co-occurrence matrix (GLCM), GLRLM, grey level size zone matrix, and multiple grey level size zone matrix. Out of all features computed, RP were the most effective texture characteristics for indicating differences between GBM and PCNSL. Unlike SD and kurtosis, this feature's unit of measurement has no physical explanation. As a result, more research needs to be conducted to support the use of this measure in clinical practice. The extraction of unique and robust textural primitives has a significant impact. If feature extraction does not lead to better texture representation, the intended results of the study shall not be attained. The demand for practical texture analysis and representation approaches grows, notably in medical image analysis, face recognition, biometrics, aerial imagery analysis, and content-based image retrieval. The LBP method was established by Ojala *et al.* The invariance of LBP to monotonic greyscale shift, modest computing complexity, and ease of implementation are its most notable features. For improved texture detection in ultrasound images of the liver, K. Aggarwal *et al.* (2016) used a modified LBP with the OTSU approach (Aggarwal, Bhamrah and Ryait, 2016). There were positive findings in identifying cirrhosis in the liver.

There are certain limitations to this research. Despite the fact that the chosen criteria resulted in an improved malignant patient diagnosis for the current dataset, malignant image misclassifications continue, which needs to be better understood. For patients with prostate cancer, tumour heterogeneity contributes as the main reason for mislabelling the images in the patient's image set. Although the patient's biopsy indicates that the tumour is malignant, and images reveal malignant characteristics, other images may have most or all benign features due to the tumour's possible heterogeneity. The second limitation of this study is having a limited dataset of

benign and malignant prostate images, among which the number of benign images was greater than the number of malignant tumour images. In machine learning, small datasets can lead to the overfitting of models. As a result of an imbalanced dataset including fewer cancer image samples than benign image samples, the classifier will be biased toward the benign class and misclassify malignant labelled images. A possible suggestion to overcome this issue would be the synthetic minority oversampling technique. Another major limitation was the time constraint. With the lack of time, it was not possible to carry out the classification and validation process of the algorithm. Finally, a final constraint is the usage of 2D images rather than 3D images. For many of the same feature extraction methods employed in this work, other research comparing 2D and 3D MRI in cancer image analysis show that 3D imaging delivers higher classification performance than 2D pictures (Chen *et al.*, 2007; Arai, Herdiyeni and Okumura, 2012; Ortiz-Ramon *et al.*, 2017).

## 5. Conclusion

Pre-processing, ROI selection, feature extraction, and classification are the main stages that are usually followed in the medical image processing procedure. An approach for determining the optimum feature extraction method for categorising medical images is suggested in this study. This study aims to identify any histogram and GLRLM based features using LBP images and classify malignant and benign tumours of the prostate. Features were extracted from the LBP image using a histogram and the GLRLM operator for feature extraction. The study resulted in four histogram features and seven GLRLM features. Out of the eleven features, the study identified three positive features. Statistical testing confirmed a significant difference in the features between benign and malignant tumours. This research was conducted under limitations, such as imbalance and small image dataset, time constraint, and image misclassification.

Although the outcome of this prostate cancer detection method is positive, there is potential for development in the future. Due to time restrictions, it was impossible to carry out several other objectives to improve the research study. A real clinical analysis should be performed as the images were obtained from an open-access platform. The suggested algorithm's code could be enhanced and automated to categorise images by training classifiers. Along with improvement, the code needs to be cleaned up to improve performance. Future advancements might also involve using 3D volumetric images since 3D texture characteristics have been essential to better discrimination in machine learning systems. The proposed algorithm can also be compared with other image classification techniques such as LBP variants, GLCM and other techniques.

## References

- Aggarwal, K; Bhamrah, M S and Ryait, H S (2016): The identification of liver cirrhosis with modified LBP grayscale and Otsu binarization, *SpringerPlus*, 5(1). Available at: <https://doi.org/10.1186/s40064-016-1970-6>.
- Arai, K; Herdiyeni, Y and Okumura, H (2012): Comparison of 2D and 3D Local Binary Pattern in Lung Cancer Diagnosis, *International Journal of Advanced Computer Science and Applications*, 3(4). Available at: <https://doi.org/10.14569/ijacsa.2012.030416>.
- Candefjord, S; Ramser, K and Lindahl, O A (2009): Technologies for localization and diagnosis of prostate cancer, *Journal of Medical Engineering and Technology*, 33(8), pp. 585–603. Available at: <https://doi.org/10.3109/03091900903111966>.
- Catalona, W J and Loeb, S (2005): The PSA era is not over for prostate cancer, *European Urology*, 48(4), pp. 541–545. Available at: <https://doi.org/10.1016/j.eururo.2005.07.014>.
- Chen, W; Giger, M L; Li, H; Bick, U and Newstead, G M (2007): Volumetric texture analysis of breast lesions on contrast-enhanced magnetic resonance images, *Magnetic Resonance in Medicine*, 58(3), pp. 562–571. Available at: <https://doi.org/10.1002/mrm.21347>.
- Chu, A; Sehgal, CM and Greenleaf, J F (1990): Use of gray value distribution of run lengths for texture analysis, *Pattern Recognition Letters*, 11(6), pp. 415–419. Available at: [https://doi.org/10.1016/0167-8655\(90\)90112-F](https://doi.org/10.1016/0167-8655(90)90112-F).
- Dinh, C V; Steenberg, P; Ghobadi, G; Heijmink, S W T J P; Pos, F J; Haustermans, K and van der Heide, U A (2016): Magnetic resonance imaging for prostate cancer radiotherapy, *Physica Medica*, 32(3), pp. 446–451. Available at: <https://doi.org/10.1016/j.ejmp.2016.01.484>.
- Elferink, W O (2021): *Gray Level Run Length Image Statistics, MATLAB Central File Exchange*. Available at: <https://www.mathworks.com/matlabcentral/fileexchange/52640-gray-level-run-length-image-statistics> [Accessed: 8 November 2021].
- Etzioni, R; Penson, D F; Legler, J M; di Tommaso, D; Boer, R; Gann, P H and Feuer, E J (2002): Overdiagnosis due to prostate-specific antigen screening: Lessons from U.S. prostate cancer incidence trends, *Journal of the National Cancer Institute*, 94(13), pp. 981–990. Available at: <https://doi.org/10.1093/jnci/94.13.981>.
- Feng, J; Dong, Y; Liang, L and Pu, J (2015): Dominant – Completed Local Binary Pattern for Texture Classification, (August), pp. 233–238.
- Fuchsjager, M; Shukla-Dave, A; Akin, O; Barentsz, J and Hriack, H (2008): Prostate cancer imaging, *Acta Radiologica*, 49(1), pp. 107–120. Available at: <https://doi.org/10.1080/02841850701545821>.
- Galloway, M M (1975): Texture analysis using gray level run lengths, *Computer Graphics and*

- Image Processing*, 4(2), pp. 172–179. Available at: [https://doi.org/10.1016/s0146-664x\(75\)80008-6](https://doi.org/10.1016/s0146-664x(75)80008-6).
- Litjens, G; Debats, O; Barentsz, J; Karssemeijer, N and Huisman, H (2017): *ProstateX Challenge data*, *The Cancer Imaging Archive*. Available at: <https://doi.org/https://doi.org/10.7937/K9T CIA.2017.MURS5CL>.
- Haralick, R M; Dinstein, I and Shanmugam, K (1973): Textural Features for Image Classification, *IEEE Transactions on Systems, Man and Cybernetics*, SMC-3(6), pp. 610–621. Available at: <https://doi.org/10.1109/TSMC.1973.4309314>.
- Hricak, H; Choyke, P L; Eberhardt, S C; Leibel, S A and Scardino, P T (2007): Imaging prostate cancer: A multidisciplinary perspective, *Radiology*, 243(1), pp. 28–53. Available at: <https://doi.org/10.1148/radiol.2431030580>.
- Clark, K; Vendt, B; Smith, K; Freymann, J; Kirby, J; Koppel, P; Moore, S; Phillips, S; Maffitt, D; Pringle, M; Tarbox, L and Prior, F (2013): The Cancer Imaging Archive (TCIA): Maintaining and Operating a Public Information Repository, *Journal of Digital Imaging*, 26(6), pp. 1045–1057. Available at: <https://doi.org/https://doi.org/10.1007/s10278-013-9622-7>.
- Kunimatsu, A; Kunimatsu, N; Kamiya, K; Watadani, T; Mori, H and Abe, O (2018): Comparison between glioblastoma and primary central nervous system lymphoma using MR image-based texture analysis, *Magnetic Resonance in Medical Sciences*, 17(1), pp. 50–57. Available at: <https://doi.org/10.2463/mrms.mp.2017-0044>.
- Litjens, G; Debats, O; Barentsz, J; Karssemeijer, N and Huisman, H (2014): Computer-aided detection of prostate cancer in MRI, *IEEE Transactions on Medical Imaging*, 33(5), pp. 1083–1092. Available at: <https://doi.org/10.1109/TMI.2014.2303821>.
- Mitchell, R E; Shah, J B; Desai, M; Goluboff, E T; Katz, A E; Petrylak, D P; Olsson, C A; Benson, M C and McKiernan, J M (2005): 948: Has Pre-Operative PSA Lost the Ability to Predict Biochemical Failure after Radical Retropubic Prostatectomy?, *Journal of Urology*, 173(4S), pp. 256–257. Available at: [https://doi.org/10.1016/s0022-5347\(18\)35104-8](https://doi.org/10.1016/s0022-5347(18)35104-8).
- Ojala, T; Valkealahti, K; Oja, E and Pietikäinen, M (2001): Texture discrimination with multidimensional distributions of signed gray-level differences, *Pattern Recognition*, 34(3), pp. 727–739. Available at: [https://doi.org/https://doi.org/10.1016/S0031-3203\(00\)00010-8](https://doi.org/https://doi.org/10.1016/S0031-3203(00)00010-8).
- Ojala, T, Pietikäinen, M and Harwood, D (1996): A comparative study of texture measures with classification based on featured distributions, *Pattern Recognition*, 29(1), pp. 51–59. Available at: [https://doi.org/https://doi.org/10.1016/0031-3203\(95\)00067-4](https://doi.org/https://doi.org/10.1016/0031-3203(95)00067-4).
- Ortiz-Ramon, R; Larroza, A; Arana, E and Moratal, D (2017): 'A radiomics evaluation of 2D and 3D MRI texture features to classify brain metastases from lung cancer and melanoma', *Proceedings of the Annual International Conference of the IEEE Engineering in Medicine and Biology Society, EMBS*. Institute of Electrical and Electronics Engineers Inc., pp. 493–496. Available at: <https://doi.org/10.1109/EMBC.2017.8036869>.
- Schröder, F H and Roobol, M J (2009): Defining the optimal prostate-specific antigen threshold for the diagnosis of prostate cancer, *Current Opinion in Urology*, 19(3), pp. 227–231. Available at: <https://doi.org/10.1097/MOU.0b013e328329a2d0>.
- Seitz, M; Osman, M and Choyke, P L (2009): Functional Magnetic Resonance Imaging in Prostate Cancer, *European Urology*, 55(4), pp. 801–814. Available at: <https://doi.org/10.1016/j.eururo.2009.01.027>.

Turkbey, B; Brown, A M; Sankineni, S; Wood, B J; Pinto, P A and Choyke, P L (2016): Multiparametric prostate magnetic resonance imaging in the evaluation of prostate cancer, *CA: A Cancer Journal for Clinicians*, 66(4), pp. 326–336. Available at: <https://doi.org/10.3322/caac.21333>.

Weinreb, J C; Blume, J D; Coakley, F V; Wheeler, T M; Cormack, J B.; Sotito, C K; Cho, H; Kawashima, A; Tempny-Afdhal, C M; Macura, K J.; Rosen, M; Gerst, S R and Kurhanewicz, J (2009): Prostate cancer: Sextant localization at MR imaging and MR spectroscopic imaging before prostatectomy - Results of ACRIN prospective multi-institutional clinicopathologic study, *Radiology*, 251(1), pp. 122–133. Available at: <https://doi.org/10.1148/radiol.2511080409>.

### Acknowledgment

First and foremost, I want to express my gratitude to my supervisor, Mr EHADK Hewadikaram, and co-supervisor, Mr RMUKGMS Bandara, for their assistance throughout this research. Next, I owe a huge debt of gratitude to Mr WLPK Wijesinghe, lecturer at Department of Electrical, Electronic and Telecommunication, General Sir John Kotelawala Defence University, for giving me really helpful comments and supporting me to correct myself during this research. I would also like to thank the Cancer Imaging Archive (TCIA) for making the PROSTATEx Challenge image collection available to the public. I thank Global Cancer Observatory and IARC Publications for making the global statistics available for research work.

### Author Biography



KAI Harsha holds a BSc (Hons) in Biomedical Engineering from General Sir John Kotelawala Defence University, expecting to graduate in the Year 2022. Currently, she is following a MSc in Biomedical Engineering from General Sir John Kotelawala Defence University.



Dr. Rathnayaka received his B.Sc. in physical science, M.Sc. in Medical Physics, and Ph.D. in Bio-Medical Imaging Physics, from the University of Colombo, Sri Lanka. Currently he is a Post-Doctoral Fellow at Utsouthwestern, University of Texas, USA.



Mr. EHADK Hewadikaram is a senior lecturer in physics, Department of Electrical, Electronics and Telecommunication Engineering at General Sir John Kotelawala Defence university. After his graduation from University of Colombo, he completed an MSc in physics at Central Michigan University, USA and MPhil (Medical Physics), University of Colombo. His research interests are ultrasound, nuclear medicine, radiation protection and medical imaging.



# Methods of measuring CSF Pressure: A Review

HSH Perera<sup>1#</sup> and EHAD Hewadikaram<sup>1</sup>

<sup>1</sup>Department of Electrical, Electronic and Telecommunication Engineering, Faculty of Engineering,  
General Sir John Kotelawala Defence University, Sri Lanka

#hshperera99@gmail.com

**Abstract:** Cerebrospinal fluid pressure is considered as one of the key diagnostic parameters to identify different pathological conditions related to the central nervous system. Different clinical methods have been used to measure the intracranial pressure (ICP) inside the craniospinal compartment of the brain. But most of those invasive methods pose a significant risk for the patients. Hence, CSF pressure is measured during Lumbar Puncture procedure as an indication to the ICP. The main aim of this review is to study and analyse the different methods of measuring CSF pressure specially during Lumbar Puncture procedure. But there is a limited literature regarding modern advanced methods of measuring CSF pressure during LP. Hence, this review emphasizes on the existing methods and peer review literature that focus on different methods of measuring CSF pressure.

**Keywords:** Lumbar Puncture, CSF Pressure, Intracranial Pressure

## 1. Introduction

In human body, it is important to keep different parameters under normal range to maintain the homeostasis. Cerebrospinal fluid, also known as CSF, is one such important parameter that plays a major role in the nervous system including the brain. Thus, different neurological conditions can occur due to any abnormality in CSF pressure, composition, and the CSF flow.

Cerebrospinal fluid is a crystal-clear fluid that surrounds and bathes the brain and spinal cord protecting the central nervous system. Mainly, cerebrospinal fluid gives mechanical and immunological protection for the nervous system (CSF leak Association, 2017). It also

acts as a buffer in central nervous system (CNS) while giving a hydromechanical protection for the neuraxis (Sakka, Coll and Chazal, 2011). CSF further aids in regulating the electrolyte balance and eliminating the produced catabolites. Hence, CSF is important in regulating the neuronal functioning by maintaining and developing the homeostasis of the interstitial fluid (Sakka, Coll and Chazal, 2011).

According to existing literature, the mean density of cerebrospinal fluid is  $1.00059 \pm 0.00020 \text{ gml}^{-1}$  and hence it is considered as slightly thicker than the water (Lui, Polis and Cicutti, 1998). For healthy conditions, the CSF appears as a colorless fluid that is similar to the water. But due to various abnormalities in the body, CSF can appear in turbid or in a different color. Thus, CSF has become a main diagnostic key to identify different abnormalities and diseases within the body, specially related to central nervous system. CSF, extracted from the body, is hence tested in medical laboratories for diagnostic purposes.

Cerebrospinal fluid has a dynamic pressure which is caused due to the secretion of CSF, absorption, circulation and its resistance to flow. For a healthy individual, around 125-150ml CSF volume is present in the body at a time, where the 25ml of CSF volume is present in the brain ventricles and around 125ml CSF volume in subarachnoid spaces as an average (Sakka, Coll and Chazal, 2011), (CSF leak Association, 2017). Further, roughly around 400ml to 600ml Cerebrospinal fluid is secreted per day for a healthy adult (Telano and Baker, 2020). According to existing literature, approximately about 20ml of CSF is produced for each hour and the Cerebrospinal fluid

secretion is majorly done by choroid plexuses in brain which contributes for around 60% - 70% secretion of the total CSF volume (Doherty and Forbes, 2014). Reabsorption of Cerebrospinal fluid is mainly done by Cranial and spinal arachnoid villi at a rate of about 0.35 ml/min (CSF leak Association, 2017). Depending on the pressure, the absorption of CSF by villous also adapts its filtration rate according to the cerebrospinal fluid pressure where the whole process is considered as a dynamic process. The dynamic circulation of CSF also affects cerebral homeostasis. It consists of a dynamic circulation which flows a pulsatile flow that is followed by systolic pulse wave. Despite that, respiratory waves, the posture and physical efforts of the individual jugular venous pressure also affects the dynamic flow of CSF (Sakka, Coll and Chazal, 2011). For normal conditions, Cerebrospinal fluid is renewed about 4-5 times per day for a young individual and this turnover rate can be changed when aging leading to various neurodegenerative diseases (Telano and Baker, 2020). Hence, Cerebrospinal fluid pressure is considered as one of the key indicators for several neurological conditions.

The cerebrospinal fluid pressure in the body can be measured in two main ways.

1. *By inserting a needle into subarachnoid space in spine to measure the opening pressure during lumbar puncture procedure.*
2. *By inserting a needle into ventricle of the brain as a part of Intra Cranial Pressure (ICP) directly using a pressure sensor (Muhamed et al., 2014)*

In addition, different non-invasive procedures are being developed to measure the CSF pressure using different technologies which are still in research levels. In clinical practice, the CSF pressure is measured widely by obtaining the opening pressure when conducting a lumbar puncture procedure via a CVP manometer.

## 2. Methodology

Literature review plays a vital role in academic field that enables to conduct a deeper study and analysis in different research areas. To conduct the review, the specific research topic and the research scope was first identified and analysed. Using online and offline data bases including Google scholar, ResearchGate, ScienceDirect etc, Peer reviewed articles, research papers, journal articles were selected to study the research area in depth about methods of measuring CSF pressure highlighting the pressure measurements during Lumbar Puncture procedure. Mainly, Lumbar Puncture, CSF Pressure measurement, Intracranial Pressure etc were identified as the key words that were used to collect the related paper articles. Out of 55 paper results obtained, abstracts were read, and the number of citations were considered to collect the most suitable and related papers for the review, avoiding any duplicates. The selected papers were studied in depth to conduct a better analysis of the study, focusing the CSF pressure measurement methods related to Lumbar Puncture procedure.

## 3. Literature Review

Different comparisons have been done to evaluate the effectiveness of the main two methods of measuring the CSF pressure. Specially, studies have done to estimate the accuracy of measuring the intracranial pressure via LP procedure. In one of the studies, a brain tissue sensor that was located in the right ventricle anterior roof and a lumbar space transducer were used to conduct the comparison between the two methods (Lenfeldt et al., 2007).

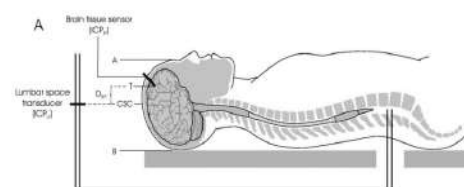


Figure 1. Set up of measuring ICP using Brain tissue sensor and lumbar space transducer

Source: (Lenfeldt et al., 2007)

As per the results, the total mean and the standard derivation of the difference between the two pressures, measured in brain tissue and lumbar space was  $10 \pm 29$  mmH<sub>2</sub>O. Further, the results have shown that the corresponding individual mean were similar, and the standard derivation was similar as well. (Lenfeldt et al., 2007)

#### A. Intra cranial pressure measurement using invasive methods

Intra Cranial Pressure also known as ICP is mainly measured using different invasive methods that are accurate but can pose a high risk for the patients. Some of the methods are Intra Cranial Pressure measured using implantable ICP sensors, ventricular catheters etc (Evensen and Eide, 2020). Among them, intraventricular or intraparenchymal catheters are widely used as a golden clinical standard of measuring ICP (Xu et al., 2016). In addition to that, biocompatible and implantable telemetric ICP sensors have been introduced, that enables to obtain mean ICP of the patients using an external receiver (Evensen and Eide, 2020).

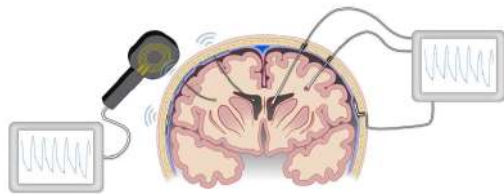


Figure 2. Different methods of ICP monitoring

Source: (Evensen and Eide, 2020)

The existing dedicated implantable ICP sensors include Fibre optic Camino ICP sensors, Strain gauge Codman micro sensors, Pneumatic sensors etc (Evensen and Eide, 2020). Fibre optic Camino ICP sensors serves as an advanced and novel platform that enables multimodality neuromonitoring where in Strain gauge Codman micro sensors, diffuse piezoelectric string gauges are included in transducer to measure ICP. In contrast, in Pneumatic sensors, the distal end of the probe contains a balloon to measure the pressure of the surrounding tissue in brain (Harary, Dolmans and Gormley, 2018).

Pulsatile ICP monitoring is also one of the novel approaches that is practiced in very limited facilities. This method enables to study and analyse the ICP pressure changes that occurs during each cardiac cycle. Hence, the resultant output can be obtained as a wave or pulse ICP pressure graph.

In most of the scenarios, a hole is made in skull to insert the sensor or transducer into brain parenchyma. Depending on the requirement and availability, the duration of the pressure monitoring and the most suitable method is selected along with the sensor type. These invasive methods are highly complex, expensive, and mostly done in intensive care units under aseptic conditions and some of the methods are limited to highly advanced health care Centres. Also, they pose a greater risk for infections to the patients compared to other methods.

#### B. CSF pressure measurement during Lumbar puncture

Lumbar Puncture, also known as LP procedure, is considered as one of the widely spread methods of measuring the CSF pressure. It was initially explained by Dr. Heinrich Irenäus Quincke in 1890s (Bø and Lundqvist, 2020). Compared to other methods of measuring Intra Cranial Pressure, it is considered as a simple, less invasive method performed using minimal equipment that can be used to measure the ICP (Muhammed et al., 2014).

During the Lumbar puncture procedure, cerebrospinal fluid volume is extracted to perform laboratory tests to diagnose different neurological disease conditions aiding doctors to determine further treatment and therapeutic procedures. Mainly these laboratory tests are performed related to cell counts, protein levels, glucose levels, cultures and microscopic examination. In addition to that, the opening pressure is measured during lumbar puncture as an indirect measurement depending on the requirement.

Usually, LP procedure is performed by a neurologist where the procedure is invasive

and should be done under aseptic conditions to avoid any infections and negative impacts to the patients. To perform the Lumbar puncture procedure, the patient can be either positioned in lateral recumbent position or sitting position, also known as upright position. But mostly, this procedure is done in lateral recumbent position, with patient's neck bent in full flexion and knees bent in full flexion up to the chest to provide the maximum lumbar spine flexion (Sternbach, 1985). Further, during the procedure, the patient must keep still without any physical movement because the positioning and the physical activity can affect the final readings of the overall procedure leading to inaccurate diagnosis.

This normal range of CSF pressure can be changed due to different reasons including age, weight, gender, positioning different health conditions etc. For an example, the pressure values for normal conditions can be ranged up to 25cmH<sub>2</sub>O for overweight adults even in healthy conditions (Doherty and Forbes, 2014). Moreover, for children, the CSF pressure values are higher than the adults which lies between 3mmHg-7.7mmHg (A. Artru, n.d.). For a healthy individual, the opening pressure of lumbar puncture procedure in lateral recumbent position lies around 6-20cmH<sub>2</sub>O. If the patient is seated while obtaining the opening pressure readings, normal pressure values lie between 20-30cm H<sub>2</sub>O (Muhamed et al., 2014). According to the literature, if the opening pressure is higher than 25cmH<sub>2</sub>O, it is considered as an elevated intracranial pressure (Mogambery, Moodley and Connolly, 2018).

Lumbar puncture procedure is performed on the patient's back where a 22 Gauge lumbar puncture needle is inserted to the body pierces skin to enter the subarachnoid space below the cauda equina (Greenlee, 2021). Then after removing the stylet of the needle, the device is attached to the needle.

Currently, Cerebrospinal fluid pressure is mainly measured via 2 medical devices.

1. C.V.P manometer
2. Compass Lumbar Puncture

1). *C.V.P manometer*: During LP procedures, CSF pressure is widely measured using C.V.P. manometer, also known as central venous pressure manometer. This device has been using to measure CSF pressure from many years ago, but yet, most of the doctors around the world, still use water column manometer for pressure LP measurements. The device is simple and mainly consists of a 3-way stop cock that connects to the needle and a uniform tube as the fluid column. The pressure range that can be measured using CVP manometer lies between (-3) cmH<sub>2</sub>O to 30cmH<sub>2</sub>O. Once the manometer is attached to the needle, CSF enter to the manometer and the level of filling can be identified with the aid of red marker inside of the manometer floating on the CSF. The length of the fluid column in the manometer is measured as the opening pressure of the procedure.



Figure 3. Linear regression between spinal manometer and IVGS when measuring opening CSF pressure

For accurate results, whole apparatus including puncture site, needle and the 3-way stop cock of the manometer should be in line while the water column manometer should be placed perpendicular to the needle.

The mechanism of the CVP manometer is simple and similar to a U-tube that is based on basic physics. Once the cerebrospinal fluid enters the manometer, due to the CSF pressure inside of the body, the fluid rises inside of the CVP manometer. After a certain period of time,

the equilibrium point occurs where the pressure exerted by the fluid column in the manometer gets equal to the CSF pressure inside of the patient's body. At this point, the final reading is considered as the CSF pressure in water centimeters. where the pressure exerted by the fluid Column is given by,

$$P = h\rho g \quad (1)$$

$P$  = cerebrospinal fluid pressure during LP

$h$  = height of the CSF fluid column

$\rho$  = density of the CSF

$g$  = gravitational acceleration

Since the density of the cerebrospinal fluid is approximately similar to water, the final measurement of the manometer is read in water centimeters.

Despite that, in resource limited healthcare facilities, intravenous giving sets (IVGS) is also used as an alternative to the CVP manometer where the cost of IVG set is approximately 30 times lesser than the CVP manometer (Mogambery, Moodley and Connolly, 2018).



Figure 4. A. CSF opening pressure measure using IVGS,

B. CSF opening pressure measure using spinal manometer

Source: (Mogambery, Moodley and Connolly, 2018)

According to research done using 100 patients by applying both CVP manometer and the IVGS, the results have shown that when identifying the normal CSF readings and the elevated CSF pressure, the agreement between the CVP manometer and the intravenous giving set is 75% (Mogambery, Moodley and Connolly, 2018). The linear regression of the

two devices when measuring the opening CSF pressure depicts a better correlation despite where the IVGS underestimates the CSF opening pressure. The research further emphasizes that the 25cmH<sub>2</sub>O of the CVP manometer is denoted by 19cmH<sub>2</sub>O in the IVGS. Thus, the CSF pressure measured by intravenous giving set should be considered as elevated ICP. Therefore, CVP pressure measurements using IVGS is discouraged in clinical practice. (Mogambery, Moodley and Connolly, 2018)

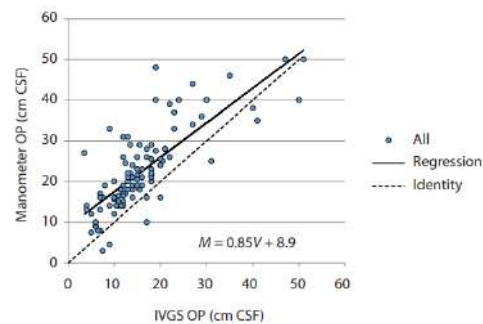


Figure 5. Linear regression between spinal manometer and IVGS when measuring opening CSF pressure

Source: (Mogambery, Moodley and Connolly, 2018)

2). *Compass lumbar puncture*: Compass lumbar puncture is considered as a novel medical device which is compact and single use medical tool that enables digital pressure measuring of CSF. It is known as one of the simplest methods to measure cerebrospinal fluid pressure during LP procedure. Yet, it is only used in limited healthcare facilities in the world.

The device mainly consists of 3 parts. (biomedical, n.d.)

1. Pressure transducer.
2. Integrated pre-programmed diagnostic computer.
3. Liquid crystal display (LCD).

The CSF pressure is measured via the sensor and then convert the pressure into an electrical signal displaying the resultant output value in the LCD display in water centimeters (cmH<sub>2</sub>O). Compared to the water column manometer, compass lumbar puncture device is very fast and user friendly. But there is very limited literature regarding the specific components and mechanisms used in the device.



Figure 6. Compass Lumbar Puncture device

Source: (Biomedical, 2022)

According to a study done by the Department of Anesthesiology, Westchester Medical Center, New York, USA; 27 patients with Lumbar Puncture indications were used for the comparison of fluid manometer and compass lumbar puncture (Sekhri, Parikh and Weber, 2019). They have identified a significant time gap between the two devices to acquire the resultant readings where the compass lumbar puncture was very time-efficient compared to the CVP manometer.

The results show that there is strong correlation between the opening pressures and the closing pressures, but the resultant readings of the compass lumbar puncture were always high compared to the water column manometer. (Sekhri, Parikh and Weber, 2019)

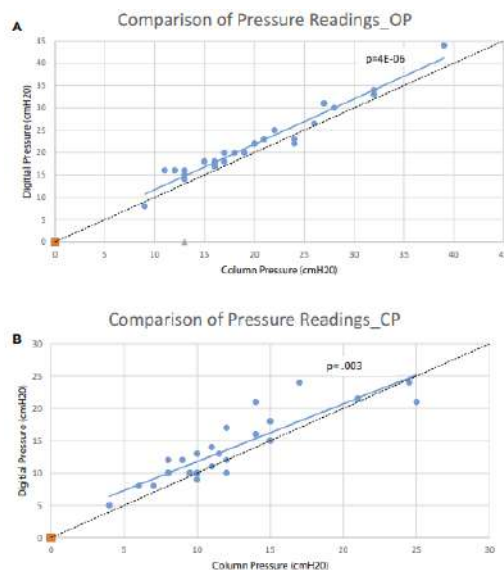


Figure 7. Linear regression of readings taken by compass Lumbar puncture device and CVP manometer,

A. Comparison between two devices for opening CSF pressure, B. comparison for closing CSF pressure

Source: (Sekhri, Parikh and Weber, 2019)

#### 4. Discussion

ICP pressure has been one of the critical parameters to investigate pathological conditions related to nervous system and further used for therapeutic purposes as well. The invasive methods of measuring ICP in brain via ventricular catheters and implants are considered as complex methods which contains a higher accuracy, but those methods can pose a higher risk and different other complications to the patients. Hence, unless there a necessity, in all most all the clinical scenarios, the ICP is measured via CSF pressure during an LP. This practice is routinely performed using a water column manometer which is one of the simplest methods to investigate Intra cranial pressure. But this method is considered as a time consuming and a cumbersome procedure for physicians where the manual stability is requited during the procedure for accurate results.

According to the literature, the use of compass lumbar puncture in clinical scenario is limited even though it overcomes most of the difficulties of the existing method specially when measuring CSF of infants and kids. The device is highly time efficient compared to manometer and addressed the issues when measuring the closing pressure of the Lumbar puncture. Yet, the accuracy of the device is +/- 3cmH<sub>2</sub>O (Biomedical, 2022) and the whole device should be discarded per patient along with included pressure sensor and LCD display. Thus, it creates an unnecessary waste more than the CVP manometer.

Despite these methods, different structural and functional non-invasive methods of measuring ICP is still conducted under research levels. The research under structural modalities is mainly conducted using CT (Computed Tomography), MRI (Magnetic Resonance Imaging), OCT (optical coherence tomography), ocular ultrasound etc and the functional facilities are studied using TCD, (transcranial Doppler ultrasound, VEP (visual evoked potentials), near-infrared spectroscopy (NIRS) etc (Xu et al., 2016). Even though some methods including ocular ultrasound shows positive results in detecting elevated ICP, the overall reliability and the expected outcomes are still being studied.

## 5. Conclusion

The paper addresses different methods of measuring cerebrospinal fluid during Lumbar Puncture procedure. Even in a modern sophisticated world with advanced technologies applied in healthcare sector; water column manometer is widely being used in most of the countries for the CSF pressure measurement during LP which has been using even many years ago. However, Compass Lumbar puncture device addresses most of the difficulties and limitations of the existing fluid manometer but clinical differences may occur. Hence, the literature emphasizes that physicians should be careful when using the compass lumbar device for all the cases instead of the CVP manometer. In conclusion,

it can be seen that the healthcare sector lacks an advanced, accurate, reusable user-friendly device to measure cerebrospinal fluid pressure overcoming the difficulties and limitations of the existing devices.

## References

A. Artru, A. (n.d.). Cerebrospinal Fluid - an overview | ScienceDirect Topics. [online] [www.sciencedirect.com](http://www.sciencedirect.com). Available at: <https://www.sciencedirect.com/topics/medicine-and-dentistry/cerebrospinal-fluid> [Accessed 12 June. 2022].

Biomedical, M. (2022). Compass™ Lumbar Puncture | Manualzz. [online] [manualzz.com](http://manualzz.com). Available at: <https://manualzz.com/doc/27568562/compass%E2%84%A2-lumbar-puncture> [Accessed 13 Jul. 2022].

biomedical, M. (n.d.). Compass Lumbar Puncture - Mirador Biomedical now part of Centurion Medical Products. [online] [www.miradorbiomedical.com](http://www.miradorbiomedical.com). Available at: <http://www.miradorbiomedical.com/products/compass-lumbar-puncture> [Accessed 10 Jul. 2022].

Bø, S.H. and Lundqvist, C. (2020). Cerebrospinal fluid opening pressure in clinical practice – a prospective study. *Journal of Neurology*, [online] 267(12), pp.3696–3701. doi:10.1007/s00415-020-10075-3.

CSF leak Association (2017). CSF LEAK ASSOCIATION Measuring Opening Pressure and Intracranial Pressure (ICP). [online] Available at: <https://csfleak.info/docs/FactsheetsLeaflets/CSF-Leak-Association-Factsheet-Measuring-Opening-Pressure-and-Intracranial-Pressure-ICP-24-August-2017.pdf>.

Doherty, C.M. and Forbes, R.B. (2014). Diagnostic Lumbar Puncture. *The Ulster Medical Journal*, [online] 83(2), pp.93–102. Available at: <https://pubmed.ncbi.nlm.nih.gov/25075138/>.

- Evensen, K.B. and Eide, P.K. (2020). Measuring intracranial pressure by invasive, less invasive or non-invasive means: limitations and avenues for improvement. *Fluids and Barriers of the CNS*, 17(1). doi:10.1186/s12987-020-00195-3.
- Greenlee, J.E. (2021). How To Do Lumbar Puncture - Neurologic Disorders. [online] MSD Manual Professional Edition. Available at: <https://www.msmanuals.com/professional/neurologic-disorders/how-to-do-lumbar-puncture/how-to-do-lumbar-puncture>.
- Harary, M., Dolmans, R.G. and Gormley, W. (2018). Intracranial Pressure Monitoring—Review and Avenues for Development. *Sensors*, 18(2), p.465. doi:10.3390/s18020465.
- Lenfeldt, N., Koskinen, L.-O. .D., Bergenheim, A.T., Malm, J. and Eklund, A. (2007). CSF pressure assessed by lumbar puncture agrees with intracranial pressure. *Neurology*, 68(2), pp.155–158. doi:10.1212/01.wnl.0000250270.54587.71.
- Lui, A.C., Polis, T.Z. and Cicutti, N.J. (1998). Densities of cerebrospinal fluid and spinal anaesthetic solutions in surgical patients at body temperature. *Canadian Journal of Anaesthesia = Journal Canadien D'anesthésie*, [online] 45(4), pp.297–303. doi:10.1007/BF03012018.
- Mogambery, T.A., Moodley, A. and Connolly, C. (2018). Is the intravenous giving set a reliable alternative to the spinal manometer in measuring cerebrospinal fluid opening pressure? *South African Medical Journal = Suid-Afrikaanse Tydskrif Vir Geneeskunde*, [online] 108(10), pp.865–869. doi:10.7196/SAMJ.2018.v108i10.13176.
- Muhamed, M., Padmanabha, S., Philip, J. and Shantaram, M. (2014). BEDSIDE MONITORING OF CSF PRESSURE. undefined. [online] Available at: <https://www.semanticscholar.org/paper/BEDSIDE-MONITORING-OF-CSF-PRESSURE-Muhamed-Padmanabha/bec0ebf88d2c9ae5867bb7c2ed7dbd64ee9d3bf5> [Accessed 10 Jul. 2022].
- Sakka, L., Coll, G. and Chazal, J. (2011). Anatomy and physiology of cerebrospinal fluid. *European Annals of Otorhinolaryngology, Head and Neck Diseases*, 128(6), pp.309–316. doi:10.1016/j.anorl.2011.03.002.
- Sekhri, N.K., Parikh, S. and Weber, G.M. (2019). Comparison Of Digital Manometer And Water Column Manometer Pressures Measurements During Lumbar Puncture. *Medical Devices: Evidence and Research*, Volume 12, pp.451–458. doi:10.2147/mder.s225757.
- Sternbach, G. (1985). Lumbar puncture. *The Journal of Emergency Medicine*, 2(3), pp.199–203. doi:10.1016/0736-4679(85)90397-x.
- Telano, L.N. and Baker, S. (2020). Physiology, Cerebral Spinal Fluid (CSF). [online] PubMed. Available at: <https://www.ncbi.nlm.nih.gov/books/NBK519007/>.
- Xu, W., Gerety, P., Aleman, T., Swanson, J. and Taylor, J. (2016). Noninvasive methods of detecting increased intracranial pressure. *Child's Nervous System*, 32(8), pp.1371–1386. doi:10.1007/s00381-016-3143-x.

### Acknowledgment

Authors would like to thank Dr.Amali Dalpadatu and Dr.Chryshanth Dalpadatu for the extended support and guidance.

### Author Biography



Sithumini Perera is currently a Biomedical Engineering undergraduate in the Department of Electrical, Electronic and Telecommunication

Engineering of the Faculty of Engineering at General Sir John Kotelawala Defence University, Sri Lanka.





Dulitha K Hewadikaram is currently a Senior Lecturer in the Department of Electrical, Electronic and Telecommunication Engineering of the Faculty of Engineering at General Sir John Kotelawala Defence University.

# Ceramic Tile Waste as Fine Aggregate for Marine Concrete Modules In Sri Lanka

SU Liyanage<sup>1</sup>, IGN Anuradha<sup>2</sup>, SN Gangabadaarchchi<sup>1</sup>, RY Galagedara<sup>1</sup>, RU Halwathura<sup>1</sup> and PBTP Kumara<sup>3#</sup>

<sup>1</sup> Department of Civil Engineering, University of Moratuwa, Sri Lanka

<sup>2</sup> Department of Quantity Surveying, Sri Lanka Institute of Information Technology, Sri Lanka

<sup>3</sup> Department of Oceanography and Marine Geology University of Ruhuna, Sri Lanka

#samudikaumayanga@gmail.com

**Abstract:** Construction waste has a major impact on the environment. Reusing and recycling this waste can reduce the extraction of raw materials and help waste management. Therefore, this study was focused on ceramic tile waste which is released in the squaring process of tile manufacturing, and to develop a design to protect the coastal area as an end product. A mixed design based on BS 5328 with M15 targeted strength was achieved with the use of cement, water, and aggregates, where fine aggregates were replaced with ceramic tile waste in 25%, 50%, 75%, and 100%. XRD test was conducted to test the constituents of ceramic tile waste. Results indicated that a higher compressive strength was achieved when the replacement was at 25%. No heavy metals were detected in the XRD test. This study concludes that the optimum percentage and the water/cement ratio would be 25% of fine aggregates replaced with ceramic tile waste with a 0.5 W/C ratio. Two designs were introduced and samples were deployed in Polhena beach, Sri Lanka. The growth of corals on the designed structure indicated the appropriateness of the material and the structure of conserving corals.

**Keywords:** Ceramic tile waste, Corals, Marine conservation, Mix designs, Waste management

## 1. Introduction

All around the world is consuming an abundance of raw materials for their day-to-day construction works (Anuradha & Halwatura, 2020). Simultaneously, massive construction waste is also generated by creating numerous issues in management. From environmental, industrial, and sanitation, waste minimization is a significant area that needs to be vigilantly focused on (Elmahgary, et al., 2018). Therefore, the reuse and recycling of construction and demolition waste receive a high priority. This decreases the mismanagement of virgin raw materials and resolves the waste disposal problem leading to the availability of more land by averting the waste disposal sites. Not only that but also, but air and water pollution, deforestation, illicit mining of river beds for materials, and fossil fuel consumption, are also minimized through proper waste management (Bansal & Mishra, 2016). Furthermore, the reuse of waste gives aid in terms of energy, mostly when the waste of kiln industries such as ceramic industry or roof tile industry where high endothermic decomposition reactions occurred, consequently recovering the energy assimilated during the manufacturing stage. The ceramic tile industry has prevailed all around the world and Figure -1 portrays the variation of tile production as per the area.

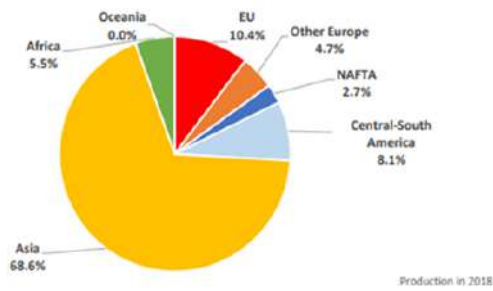


Figure 1. : World tile production by geographical area in 2018 (Ekop, 2016)

The Ball clay, Kaolin, Quartz, Feldspar, Silica, and Dolomite are used for the production of ceramic tiles and they can be easily found in Sri Lanka (Liyanage & Ranasinghe, 2019). The production of these tiles follows five main steps, raw material extraction, grinding and mixing the extracted materials, granulating by spray drying, pressing, firing, and finally polishing and glazing [4]. Due to the increment in infrastructure development in recent years, Sri Lanka has focused on using natural aggregates and waste reduction techniques (Deiyagala, et al., 2017). Currently, manufacturers are disposing the ceramic tile waste to fill the low lands and abandoned mines. Although ceramic tile waste is generated before the kiln process is reused, waste that is generated after the kiln process has become a real threat as it is disposed to the environment (refer to Figure 2).



Figure 2. Production and waste generation process of ceramic tiles.

Moreover, ceramic tile wastes are generated not only within the ceramic tile processing but

also within the construction stage of the floor and the demolition stage.

Most importantly, ceramic tile wastes reason for the pollution of groundwater, air, and soil. Further, these ceramic tile wastes are stored as heaps at disposal sites. Assessed values show that approximately 30% of the daily production of the ceramic industry turns into waste and there is no form of recycling for the ceramic waste (Tabak, et al., 2016). Moreover, annually nearly 250,000 tons of tiles are dilapidated, whereas 100 million tiles are used for maintenance work (Topçu & Canbaz, 2007). Nevertheless, ceramic tile waste is, hard, durable, and highly resilient to physical, biological, chemical, and degradation processes (Bansal & Mishra, 2016). Waste ceramic tiles reason only the presence of pollution. Owing to these reasons ceramic industries are trying to find answers for the disposal of tons of ceramic tile wastes. In the meantime, conventional fine aggregate (sand) reserves are draining fast as they use for numerous construction works. Due to the post-war construction boom of Sri Lanka, these two issues are significantly posed. Even though ceramic tile waste generates prolonged negative effects on the environment, only a limited number of studies have been conducted in Sri Lanka to develop alternative construction materials from ceramic tile waste (Tabak, et al., 2016).

Sri Lanka is an island surrounded by the Indian Ocean. Sri Lankan coastal area was rich with corals a few decades back and currently reducing rapidly due to various human activities. During the 26 years of civil war (1983-2009) tourism has been focused on the southern area rather than the Northern side. Therefore, the physical damage to the southern area is a bit higher. This has affected negatively the corals too. The coral cover on the southern beaches is being deteriorated at an increasing speed. The corals need ideal conditions and a very long time for their regrowth, but this has not been provided for the corals on the Southern coast. Thus, various precautions are adopted to protect corals as

well as to plant them. Placing concrete sections is one of the methods to grow coral but they are not effective as the design of the concrete section is not very suit for the Sri Lankan coastal conditions. Therefore, it is necessary to come up with suitable designs for the concrete sections. Further, if it is possible to develop these suitably designed structures for coral plantation with concrete which is developed through ceramic tile waste, it would be ideal as it supports nature in two ways. But, no studies have been conducted related to this, and therefore, this research aimed to develop suitably designed structures for Sri Lankan coastal areas with concrete manufactured through ceramic tile waste. Therefore, two objectives were implemented to achieve the above aim (1) To develop a mixed design as a partial replacement for the fine aggregate of concrete and (2) To design and test the suitability of marine conservation modules constructed from the developed mixed design.

## 2. Materials and Methods

### A. Material

Commercially accessible Ordinary Portland Cement following BS 12 [10] was used in testing. The coarse aggregate, size of between 20mm and 4.75mm was considered for the study. The fine aggregate used in the experiment was a mix of natural sand and ceramic tile waste. The ceramic tile waste was obtained from the wet squaring waste plant of Royal Ceramic Lanka (PLC), Horana, Sri Lanka.

The sieve analysis test confirmed that the major part of the fine aggregate is the powder passing through the 125 µm filter with a weight of 75g of the selected sample. Preliminary investigations were directed on the aggregates following BS 882 to determine their suitability. The water used for mixing and curing specimens was drinking quality water.

Table 1. Selected mixed design ratios

Mix designs	Materials			
	Cement	Fine Aggregates		Coarse Aggregates
		Ceramic Tile Waste	Natural Sand	
M1	1	0.5	1.5	4
M2	1	1	1	4
M3	1	1.5	0.5	4
M4	1	2	0	4
M5-Stand	1	0	2	4

### B. Methodology

A mixed design based on BS 5328 with M15 (Anon., 1990) was achieved with the use of cement, water, and aggregates. There the fine aggregates were replaced with varying percentages of ceramic tile waste at 25%, 50%, 75%, and 100%. In each mix, nine (9) 150mm x 150 mm x 150 mm sized concrete cubes were produced as the total was 45 cubes. The water to cement ratio was varied from 0.5 - 1.1 to achieve the required workability yet no admixtures were used for the mixing. Then the materials were mixed within a mechanical mixer. The slump test was performed Mix designs Materials Cement Fine Aggregates Coarse Ceramic Aggregates Tile Waste Natural Sand M1 1 0.5 1.5 4 M2 1 1 1 4 M3 1 1.5 0.5 4 M4 1 2 0 4 M5-Stand 1 0 2 4 according to the BS EN 12350-2 (Anon., p. 2009) for the prepared concrete before the molds are filled with concrete for the cube test. The cast specimens (cubes) were covered with polythene only to be removed from the mold when it was up to 24 hours and cured in water until their testing age of 28 days (Refer to Figure 3). The compressive strength was tested using a universal compression testing machine.

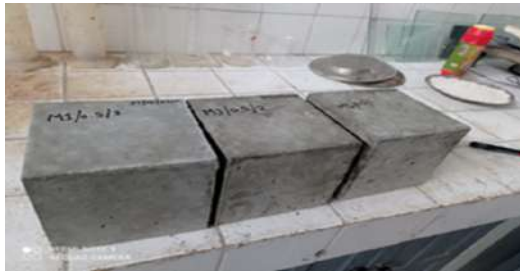


Figure 3. Prepared test samples before curing

An XRD test was conducted for the ceramic tile waste. This was mainly to understand the constituents of the ceramic tile waste (refer to Table 2) as well as to check the presence of heavy metals and other harmful chemical constituents which would have a negative effect on the coastal area.

Table 2. Composition of ceramic tile waste

Constituent	Clay	Na-Feldspar	Talc	K-Feldspar	Cyclone dust	Filter dust	Sudge
LOI	7.99	0.97	7.20	0.48	4.24	4.47	4.0
SiO <sub>2</sub>	66.1	66.4	47.2	71.29	64.45	63.3	65.4
Al <sub>2</sub> O <sub>3</sub>	19.5	19.0	7.22	15.51	19.25	20.2	18.8
Fe <sub>2</sub> O <sub>3</sub>	1.66	0.75	7.13	0.54	3.07	2.76	2.10
TiO <sub>2</sub>	1.95	0.41	0.15	0.07	1.16	1.04	0.74
CaO	0.06	0.60	0.35	0.47	0.81	0.74	2.80
MgO	0.05	0.12	30.2	0.00	1.87	2.19	2.99
K <sub>2</sub> O	0.52	0.32	0.13	7.71	1.28	1.24	1.57
Na <sub>2</sub> O	0.03	10.9	0.03	3.41	2.70	2.97	2.57
MnO <sub>2</sub>	0.03	0.03	0.11	0.03	0.04	0.04	0.03
P <sub>2</sub> O <sub>5</sub>	0.00	0.03	0.00	0.00	0.57	0.47	0.46
Cl <sup>-</sup>	0.16	0.06	0.05	0.08	0.00	0.00	0.00
SO <sub>4</sub> <sup>-</sup>	1.44	0.18	0.99	0.08	0.00	0.00	0.00
Total	99.7	99.8	99.9	99.67	99.44	99.5	99.58

Source: (El-Fadaly, et al., 2010)

An appropriate design was developed for a coral hub considering the environmental issues, easy handling, applicability, and adaptability to the marine environment.

### 3. Results and Discussion

Figure 4 displays the X-ray diffraction (XRD) analysis of the ceramic tile waste. The XRD indicates that the main peaks were noticed between 2-theta values of 20° and 30° which designates the existence of Silicon Dioxide (SiO<sub>2</sub>). Results indicate that there are no heavy metals present in the ceramic tile waste.

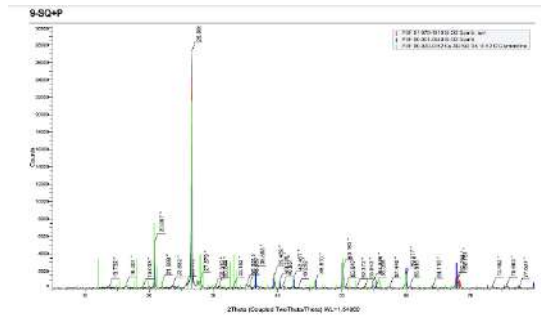
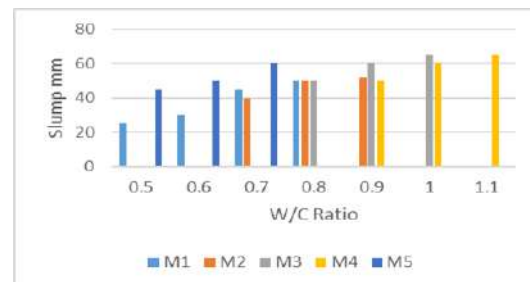


Figure 4. XRD results of ceramic tile waste.

### Figure 5. Slump test analysis

The slump test was conducted using the selected sample concrete mixers. Most of the concrete mixes had zero workability for 0.5 – 0.7 water-cement ratios. According to Figure 5, M1 is the only mixed design with ceramic waste that shows a slump value of 0.5 water-



cement ratios. M5 shows the conventional concrete without ceramic waste. So, the workability is higher in low water-cement ratios. Ceramic waste concrete shows workability for higher water-cement ratios which indicates this concrete needs more water to get a slump. In M1 the ceramic dust has only been used for 25%. In M2 where the dust is 50% increased there is no workability in a 0.5 W/C ratio. But in 0.7w/c workability was appropriate. The experiment has done without using any kind of admixture. In M1 the ceramic dust has only been used for 25%. In M2 where the dust is 50% increased there is no workability in a 0.5 W/C ratio. But in 0.7w/c workability was suitable. The experiment has done without using any kind of admixture. Figure 6 demonstrates conducting the slump test in the laboratory.



Figure 6. Conducting Slump test in the lab

Figure 7 demonstrates the variation of compressive strength against the w/c ratio with different compositions (25%, 50%, 75%, and 100%) of fine aggregate replacements in 28 days of curing age.

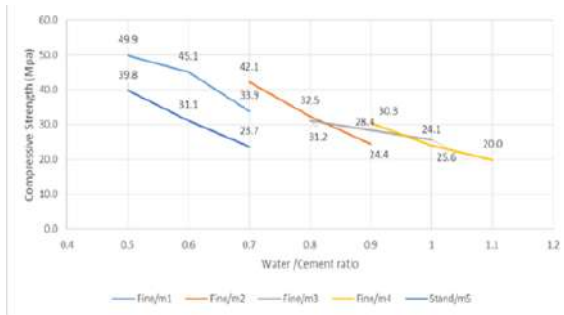


Figure 7. Variation of compressive strength against the w/c ratios

There the water to cement ratio (w/c) was increased with the increment of ceramic tile waste proportion. The test results show that using ceramic tile waste as fine aggregate replacements increases the compressive strength of concrete compared to the compressive strength of normal concrete. It can be identified that the highest compressive strength was obtained when the natural sand was replaced by 25% (M1) from the ceramic tile waste having a value of 49.9 MPa with a W/C ratio of 0.5.

So M1 mix design was chosen for the final product design.

As the next step, two designs were introduced from the newly developed concrete.

1. Design A - This structure was developed to conserve the corals. When the structure is deployed, the corals can be grown on the structure. (Refer to Figure 8)
2. Design B - This structure was introduced to build a walking path where people can walk without harming the corals. This also creates a breeding environment for fish. (Refer to Figure 9)

Structures are designed to be attached to existing infrastructure, while others sit independently on the substrate underneath or adjacent to infrastructure. Figure 8 shows the developed coral hub design.

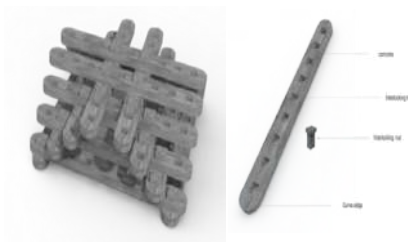


Figure 8. Structure of Design A

These single modules or structures with multiple modules can be used as new infrastructure or added to existing structures. Most importantly, single modules can be modified to hang on aquatic infrastructure. Figure 9 represents the design developed for the building of the walking path.

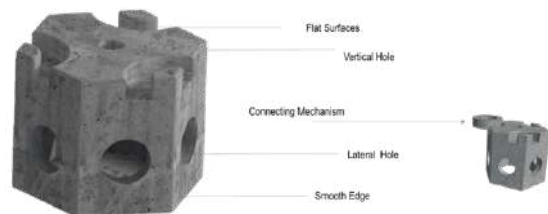




Figure 9. Structure of Design B

These modules can be attached to the infrastructure and anchored to the substrate to provide additional stability in high-energy environments such as tidal waters, storm, and flood conditions.

To assess the suitability of these designs, prepared samples were deployed in Polhena beach, Sri Lanka. Polhena is a well-known beach that includes coral reefs and reef lagoons. Many local and foreign visitors visit Polhena as the area is blessed with immaculate stretches of coral reefs, enriched with high biodiversity (refer to Figure 10).

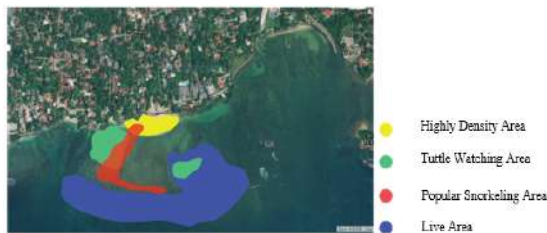


Figure 10. Selected study area, Polhena Beach, Sri Lanka

Most importantly, lots of coral reefs and reef lagoons in this beach have been damaged due to these visitors and the fishermen in the area. Therefore, the purpose of these developed designs was to replant the corals.

The deployed samples and designs A & B were checked after 2 months, 6 months, 1 year, and 2 years (refer to Figure 11-18) for the growth of corals. It was identified that even without planting the corals on the structure, they have grown confirming the appropriateness of the product.



Figure 11. After deploying the samples to the research area, coral development was observed after 2 months



Figure 12. After deploying the samples to the research area, coral development was observed after 2 months



Figure 13 Puff fish choosing Marine Condo as its habitat



Figure 14. Design B after 1 year of deploying



Figure 15. Coral development after 2 years of Design B



Figure 16. Design A after 3 days of deploying the sample



Figure 17. Design A after 1 year of deploying the sample



Figure 18. Development of corals on Design A after 2 years of deploying the sample.

#### 4. Conclusion

Ceramic tile factories in Sri Lanka produce waste products such as ceramic powder, ceramic glaze, and sludge and there is no mechanism to deal with that waste locally. Every factory had been made an effort to provide a better solution, but there arises a requirement of a common solution to dispose of these wastes. This is not only important for countries like Europe, India, China who are the giant in the manufacturing field of ceramic but also for Sri Lanka which is an island where there aren't many factories are situated and this is being a very severe problem in the long run because this ceramic waste will decay for many years and will not be added to the environment. Tile fragments were not considered in this study. The main focus has been on squaring and polishing waste. To simulate the interest, to re-use the ceramic waste, it should be cheaper to re-use than dispose of. Tile pieces are often used after a process of remaking. But due to the powdery nature of tile-squaring, it can be used to manufacture other products profitably. Although there are advanced techniques for waste management in the world, those are not properly utilized in Sri Lanka Reusing the maximum amount of waste without damaging the quality of the tile can prevent the wastage and by utilizing other waste in more suitable industries,

we can maximize the use of natural resources as well as protect the environment XRD testing can make it clear that it does not contain any harmful substance for the environment and organisms. Durability, strength, and heat resistant properties of this ceramic powder make it ideal for producing economically important products. According to many other study references, these are being used in concrete mixing. 50 Also, the amount of waste removed from dry squaring is subtle.

The compressive strength of concrete increased with tile waste content in the concrete and decreased with the increased water/ cement ratio of the concrete. The



workability of concrete decreases with an increase in tile waste content in the concrete.

The highest compressive strength was obtained when the fine aggregate mixture was 1:3, ceramic tile waste: natural sand and the water/cement ratio is 0.5. This ceramic waste has the potential to cover a large area of production in addition to this, for further experiments, some field investigations are being carried out to use this waste for the growth of marine organisms. Within a short period of two months, we could observe a variety of algae appeared on it. These optimum values were used in producing the designed blocks. After observing the results, it can be seen that the structure wasn't moved yet corals have grown on covered the deployed structure. The product has blended with the environment preserving marine life.

## References

Anon., n.d. *BS 5328 Part 2:1990, Methods for specifying concrete mixes.*, s.l.: s.n.

Anon., n.d. *BS EN 12350 Part 2:2009 Testing fresh concrete: slump test.*, London: s.n.

Anuradha, I. & Halwatura, R., 2020. *Life Cycle Embodied Carbon Assessment of Roofing Materials.* s.l., s.n.

Bansal, A. & Mishra, G. B. S., 2016. Recycling and reuse of construction and demolition waste: sustainable approach. *ICSBE*, Issue 129, p. 6.

Deiyagala, D. et al., 2017. Engineering and Economic Viability of Using Crushed Construction Waste in the Production of Concrete and Mortar. *ENGINEER; The Institution of Engineers, Sri Lanka*, L(03), pp. 41-53.

El-Fadaly, E., Bakr, I. M. & Breka, M. A., 2010. Recycling of Ceramic Industry Wastes in Floor Tiles Recipes. *Journal of American Science*, pp. 241-247.

Ekop, O. A. H. a. I. E., 2016. Compressive Strength Characteristics of Tile Waste

Concrete. *International Journal of Engineering Sciences & Research Technology*, pp. 268-273.

Elmahgary, M. G., Amin, S. K., Sadek, M. A. & Abadir, M. F., 2018. Waste Minimisation of Ceramic Wall Tiles. *Chemical Engineering Transactions*, Volume 70, p. 6.

Liyanage, S. & Ranasinghe, D. W., n.d. *Identification of the possibility to reuse the ceramics glazed tile waste as an Eco friendly raw material for the manufacturing industry in Sri Lanka.* 2019, University of Moratuwa, Sri Lanka.

Tabak, Y. et al., 2016. *Ceramic tile waste as a waste management solution for concrete.* s.l., s.n., p. 9.

Topçu, B. & Canbaz, M., 2007. Utilization of Crushed Tile As Aggregate in Concrete. *Iranian Journal of Science & Technology, Transaction B, Engineering*, 31( The Islamic Republic of Iran), pp. 561-565.

## Abbreviations and specific symbols

XRD - X-ray diffraction analysis

W/C ratio - Water /Cement Ratio

## Acknowledgment

I would like to express my deep gratitude to our research supervisors, for their patient guidance, enthusiastic encouragement and useful critiques of this research work.

I would also like to extend my thanks to the technicians of the laboratory of the civil engineering department for their help in offering me the resources in this research paper.

# Identifications of Pathways for Phosphorus-based Product Recovery from Sewage Sludge using Multi-Criteria Decision Analysis for Sri Lankan Context

KA Lakshan<sup>1</sup> and MAS Preethika<sup>1#</sup>

<sup>1</sup>University of Peradeniya, Sri Lanka

# akilalakshan123@gmail.com

**Abstract:** *This study was carried out to inspect the suitability of 5 methods to produce phosphorus-based products using sewage sludge as an alternative to the rock phosphate demand to produce phosphate fertilizers. The considered methods are supercritical water gasification of sewage sludge, struvite precipitation, thermochemical treatment of sewage sludge, wet chemical treatment of sewage sludge and electro dialysis of sewage sludge. These methods are compared with each other to determine best method using 11 different criteria selected in Sri Lankan context. The comparison was carried out using a multi-criteria decision making (MCDM) technique called TOPSIS under 3 different scenarios which assigned different values to the criteria in environmental, economical and fertilizer suitability aspects. An analysis was carried out regarding results of the MCDM to determine the best method and struvite precipitation was selected as the best method in Sri Lankan context to recover the phosphorus in wastewater.*

**Keywords:** *phosphorus, wastewater, multiple criteria decision making, sludge processing*

## 1. Introduction

Phosphorus is a key component in agriculture. It has to be supplied to cultivations in the form of fertilizers. Phosphorus fertilizers are manufactured using rock phosphate and due to the heavy consumption, rock phosphate reservoirs are depleting in a remarkable rate. According to researches, a half of global rock phosphate reservoirs would deplete within next fifty years (Egle, Rechberger and Zessner,

2015; Cieřlik and Konieczka, 2017). Therefore, the search has been widened to find alternatives to rock phosphate and municipal wastewater has been identified as a viable source of phosphorus.

Several methods have been developed to extract phosphorus from wastewater and most of them use the residue of the wastewater treatment process which is called the sewage sludge. The sewage sludge is treated in various methods achieve the maximum extraction of phosphorus. These methods vary from each other in many aspects. Some of them are phosphorus yield, treatment cost, power requirement, carbon footprint, form of the recovered phosphorus and etc. therefore, these methods have to be evaluated using a universal list of criteria to find the method that suits best under a predetermined set of aspects. A literature review was carried out to find necessary data regarding the selected methods of phosphorus extraction. A number of methods have been developed for the objective and some of them are chemical hydrolysis, supercritical water gasification, struvite precipitation, bioleaching of sewage sludge, thermo-reductive treatment, thermochemical treatment, wet chemical treatment and electro dialysis of sewage sludge (Guedes et al., 2014; Egle, Rechberger and Zessner, 2015; Cieřlik and Konieczka, 2017; Shiba and Ntuli, 2017; Amrullah and Matsumura, 2018; Gorazda et al., 2018; Semerci, Kunt and Calli, 2019). This study is carried out to check the viability of these methods for Sri Lanka as a sustainable solution for fertilizer crisis.

Eleven criteria have been selected for the evaluation and they have been selected considering the sustainable development goals published by United Nations in 'The 2030 agenda for sustainable development'. A number of MCDM tools and techniques were under consideration for the analysis and some of them were namely PROMETHEE, ELECTRE, DEXI, TOPSIS and etc. (Pohekar and Ramachandran, 2004; Huang, Keisler and Linkov, 2011). TOPSIS was selected as the MCDM technique for the study due to its versatility and applicability in the subject of waste management (Karimi et al., 2011; Yahya et al., 2020). After the mathematical analysis of collected data, they were interpreted graphically as well as numerically to obtain the desired results.

## 2. Materials and Methods

### *Methods to recover phosphorus*

Five methods were selected to recover phosphorus. They are supercritical water gasification (SCWG), struvite precipitation, thermochemical treatment of sewage sludge, wet chemical treatment of sewage sludge and electro dialysis of sewage sludge. The mentioned methods vary from each other in many aspects and they are discussed in the following section.

In the process of supercritical water gasification, dewatered sewage sludge is dried to reduce the water content further. The drying has to be done for 2 hours at 110 °C (Weijin et al., 2019). Then the dried sewage sludge is allowed to cool in air. Then the sludge is mixed with deionized water to acquire optimal solubility and concentration of soluble matter for the gasification process (Weijin et al., 2019). After that, formed slurry is sent into the gasification chamber where the temperature and pressure is maintained at 500 °C and 37 MPa respectively and it is kept in there for about 15 minutes (Weijin et al., 2019). The residue in the chamber after the completion of gasification is collected and it is left to cool. Then sulfuric acid is added to the

residue at a solid-liquid ratio of 1:1000 (Acelas et al., 2014). The pH value of the medium is maintained at 2 to ensure the maximum yield of phosphorus as phosphoric acid and it is collected as the product in this process (Acelas et al., 2014). In the process of SCWG, no specific method is used to remove heavy metals from the sewage sludge and this has an impact on the environment.

In the process of struvite precipitation, first of all dewatered sewage sludge is leached using sulfuric acid and the ratio is 100 ml of 1M sulfuric acid for 1g of sewage sludge (Shiba and Ntuli, 2017). Then it is left to settle for 2 hours (Shiba and Ntuli, 2017) and then it has to be filtered. The leachate has to be treated to remove heavy metal content and this is done using Bentonite (Egle et al., 2016; Shiba and Ntuli, 2017; Li et al., 2019). Then magnesium and nitrogen have to be added externally to precipitate struvite which is  $Mg.NH_4.PO_4$  and magnesium and nitrogen are added as magnesium chloride and ammonium hydroxide respectively (Cieřlik and Konieczka, 2017; Shiba and Ntuli, 2017).

In the process of thermochemical treatment, dewatered sewage sludge is incinerated in a muffle furnace at a temperature of 800 - 1000 °C for two hours (Yang et al., 2019). Then the ash is grinded and sieved. Then magnesium chloride is added to the sieved ash as 10g of magnesium chloride per 1kg of ash (Yang et al., 2019) and then the mixture is incinerated again in a muffle furnace again at a temperature of 800 - 1000 °C for two hours to remove heavy metals (Yang et al., 2019). Then again the residue is grinded and sieved to get magnesium phosphate as the product (Jeon and Kim, 2018; Yang et al., 2019). Residue after sieving is again sent to the grinder. This is a costly and complex process compared to other processes. Two incinerations produce a considerable amount of flue gas while second incineration removes heavy metals as chlorides. Even though this is a costly process, it has a high phosphorus yield.

Wet chemical treatment of sewage sludge is another method recover phosphorus from sewage sludge which seems to be suitable for Sri Lanka. In this process, sewage sludge is incinerated in a muffle furnace at a temperature of 800 - 1000 0C for two hours (Yang et al., 2019) and then it is treated with sulfuric acid as 300-500 g of acid per 1kg of ash(Liang et al., 2019). Then the solution is filtered to separate the leachate and the leachate is treated using bentonite to remove heavy metal contamination. After that the leachate is mixed with magnesium chloride and ammonium hydroxide with a molar ratio of 1:1:1 (Liang et al., 2019) to precipitate Struvite (Liang et al., 2019).

In the process of electrodialysis, sewage sludge is incinerated to obtain sewage sludge ash. Sludge is incinerated at a temperature of 800 – 1000 0C for two hours (Guedes et al., 2014). Then it is mixed with 0.08 M sulfuric acid at a mass: volume ratio of 1:10 (Guedes et al., 2014). An electrodialysis cell with two platinum coated electrodes, a stirrer and 0.01 M sodium nitrate mixed with nitric acid at 1:1 ratio has been selected for the experiment (Guedes et al., 2014). Nitric acid is used to fix the pH value at 2 (Guedes et al., 2014). Then the solution is electrolyzed for 14 days with a current of 199 mA (Guedes et al., 2014) and phosphoric acid is the final product of the process.

#### A. Evaluated criteria

Eleven criteria have been selected according to the UN’s sustainable development goals and weights have been assigned to the selected criteria according to the considered scenario. Table 1 shows the list of criteria along with assigned weights. Assignment of the weights for the respective criteria was carried out by considering their importance for the respective scenario. The baseline weight was taken as 1 and it was changed increasing or decreasing according to the scenario. This was done to obtain a better impact from each criterion on various situations.

Table 1- Selected criteria and their weights

Criterion	Equal weight	Environment conservation	Profitability	Fertilizer applicability
P yield	1	0.5	1.7	0.8
Cost to treat 1g of SS	1	0.5	1.7	0.3
Estimated income per 1g of SS	1	0.5	1.7	0.3
Energy consumption	1	1.5	1.3	0.3
Carbon footprint	1	1.8	0.3	0.2
Approximate time for 1 batch	1	0.2	1.3	0.3
Fertilizer suitability	1	1.3	1.0	1.5
Heavy metal content	1	1.4	0.5	1.2
Chance of mechanical failure	1	0.2	1.0	0.1
Noise impact	1	1.0	0.2	0.1
Technical complexity	1	0.2	0.7	0.1

#### B. Technique of order of preference by similarity to ideal solution (TOPSIS)

TOPSIS has been selected as the tool for the Multi-Criteria Decision Analysis technique. In TOPSIS, the calculations are carried out as shown below and the ranking is done according to the performance scores obtained.

Normalization of matrix.

Table 2- Decision matrix

<b>Criteria</b>	<b>Supercritical water gasification</b>	<b>Precipitation</b>	<b>Incineration with chloride</b>	<b>Wet chemical treatment</b>	<b>Electrodialysis</b>
P yield (mg/1g SS)	32.3	20.4	33.32	29.92	23.7
Cost to treat 1g of SS (LKR)	27.35	2.86	106.10	51.03	49.80
Estimated income per 1g of SS (LKR)	0.005	0.000003	0.02	0.000004	0.004
Energy consumption (kWh/1g SS)	4.68	0.37	10.68	5.18	4.56
Carbon footprint (kg CO <sub>2</sub> / 1g SS)	3.32	0.26	8.68	4.78	4.33
Approximate time for 1 batch (hr)	12	7	5	9	336
Fertilizer suitability (5- max 1- least)	1	5	3	5	1
Heavy metal content (1- high 0-low)	1	0	0	0	0
Chance of mechanical failure (3- high 2- medium 1- low)	2	1	3	2	1
Noise impact (2-high 1- medium 0- low)	1	0	2	1	1
Technical complexity (2-high 1- medium 0- low)	2	0	2	1	1

$$\bar{X}_{ij} = \frac{X_{ij}}{\sqrt{\sum_1^j X_{ij}^2}}$$

where,

$\bar{X}_{ij}$ = Normalized value of ith criterion of jth method.

$X_{ij}$ = Value of ith criterion of jth method.

Calculation of Euclidian distances

Two parameters named as ideal best value and ideal worst value is extracted from the matrix after normalizing and weighing. If the considered criterion affects positively on the analysis (i.e profit), the highest value in the row is taken as ideal best value ( $V_{ij}^+$ ) and the lowest value in the row is taken as ideal worst value ( $V_{ij}^-$ ). If the considered criterion's effect is negative (i.e cost), lowest value in the row is taken as ideal best value and the highest value in row is taken as the ideal worst value.

After selecting ideal values, respective Euclidean distances are calculated according to following equations.

$$S_j^+ = \sqrt{\sum_1^i (V_{i1} - V_i^+)^2}$$

$$S_j^- = \sqrt{\sum_1^i (V_{i1} - V_i^-)^2}$$

where,

$S_j^+$  - positive Euclidean distance

$S_j^-$  - negative Euclidean distance

Calculation of performance score,

$$P_j = \frac{S_j^-}{S_j^+ + S_j^-}$$

### C. Collected data

Table 2 shows all the data collected through a literature survey and necessary calculations.

## 3. Results and Discussion

### A. Results of TOPSIS

Figure 1 shows the normalized matrix of collected data which provides an idea of the behavior of the selected methods of phosphorus recovery.

Figure 2 shows the performance score variation obtained from the TOPSIS analysis.

### B. Discussion

As shown in Figure 2, struvite precipitation provides better results over other 4 methods in each scenario. When the environment friendly scenario is considered, precipitation is advantageous over other 4 methods due to negligible energy consumption, noise impact, carbon footprint and heavy metal removal. Due to those reasons, struvite precipitation outperforms other methods in environment friendly scenario. It outperforms other methods in profitability and fertilizer applicability too. However, in those scenarios, precipitation does not show a massive margin.

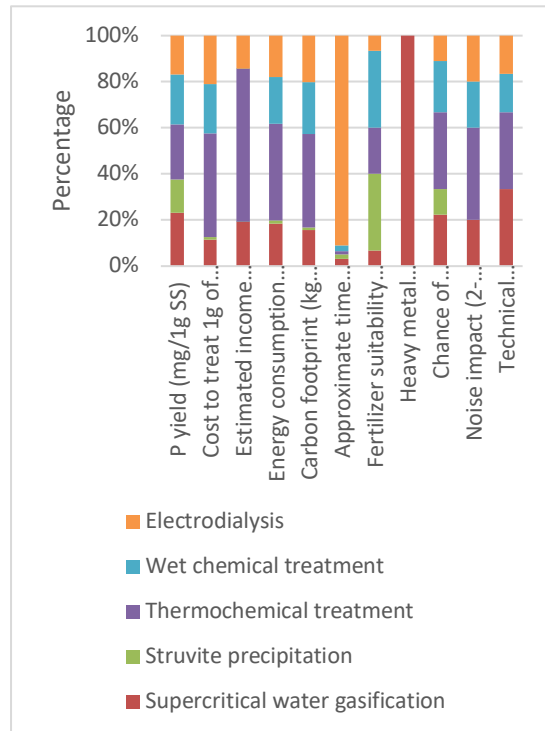


Figure 1- Performance scores comparison

When it comes to fertilizer applicability, precipitation is on par with wet chemical treatment. According to fig. 2, precipitation slightly outperforms other methods in terms of profitability. Even though the expected income per 1g of sewage sludge is very small, this method has the upper hand due negligible cost and power consumption alongside with lower chance of mechanical failures.

When the process of supercritical water gasification is considered, that it provides a strong performance score only in the profitability scenario. When it comes to profitability, SCWG is the second-best option after precipitation. This happens due to the low cost of operation, relatively low energy consumption and relatively high phosphorus yield. The effect of these criteria can be seen from fig. 1.

SCWG underperforms badly in other 3 scenarios while producing worst performance score in the fertilizer applicability scenario. This happens due to the formation of phosphoric acid as the product of process. Phosphoric acid is not used as a fertilizer but it is used to manufacture fertilizers. Therefore, this could be useful if plans are laid to manufacture phosphorus fertilizers using phosphoric acid. When it comes to environment friendly scenario, SCWG can be seen at the bottom position. This happens due to the heavy metal contamination and the energy consumption.

Thermochemical treatment stands at the third place when it comes to the equal weight scenario while underperforms on environment friendly scenario. This happens due to the high-power consumption, high carbon footprint and high noise impact. Even fig. 1 shows that thermochemical treatment has a higher impact on environment related criteria.

When it comes to profitability and fertilizer applicability, thermochemical treatment sits in a strong position. This happens due to high phosphorus yield, high income per 1g of sewage sludge, low time of operation and low

heavy metal content. Thermochemical treatment provides magnesium phosphate as the final product. This is used as a fertilizer (Li et al., 2018; Luo et al., 2020) and therefore thermochemical treatment gets placed into a stronger position compare to electro dialysis and SCWG.

When wet chemical treatment is considered, it becomes a strong competitor for struvite precipitation when it comes to fertilizer applicability. This happens due to the heavy metal removal and the production of struvite as the final product. According to fig. 2, wet chemical treatment sits only behind precipitation when it comes to equal weight scenario and environment friendly scenario. Wet chemical treatment outperforms SCWG, thermochemical treatment and electro dialysis in the environment friendly scenario due to substantially lower energy consumption, carbon footprint and noise impact.

When the terms of profitability are considered, wet chemical treatment underperforms due to the lower income, higher chance of mechanical failures and moderate cost, energy consumption and technical complexity.

When electro dialysis is considered, according to fig. 2 the process underperforms in terms of profitability. Major reason for this is the high operating time. Longer operating period has erased the benefit of having moderate cost, phosphorus yield, energy consumption and lower chance of mechanical failure. Electro dialysis sits on 4th place not only in the fertilizer applicability scenario, but also in the unbiased analysis. Even though electro dialysis produces phosphoric acid as the final product, it has gained a significant lead from SCWG in terms of fertilizer applicability due to the removal of heavy metals. Electro dialysis has proved to be a competitor in terms of environment friendly scenario. It sits on the 3rd place after precipitation and wet chemical treatment due to lower noise impact, carbon footprint, energy consumption and heavy metal removal.

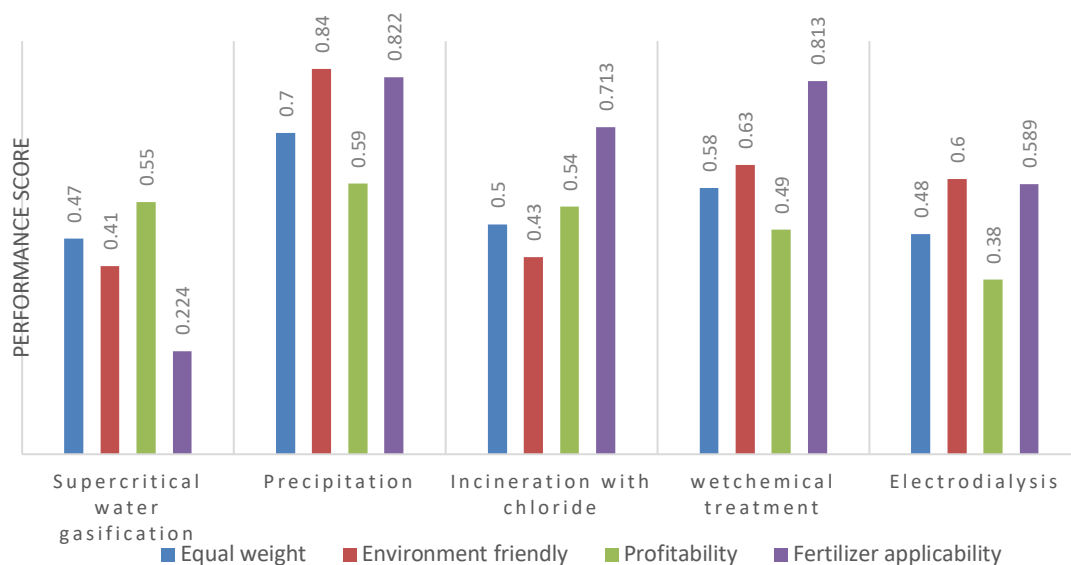


Figure 2- Normalized matrix of data

#### 4. Conclusion

Five methods which were selected from a pool of methods to recover phosphorus from sewage sludge formed during the wastewater treatment process were evaluated using a multi-criteria decision analysis technique to determine the most suitable method to Sri Lanka. 11 criteria were selected according to the sustainable development goals imposed by UN and the analysis was carried out using TOPSIS multicriteria decision-making technique.

Analysis was done considering 4 different scenarios where the weights of the criteria were changed according to the scenario and the results were generated for the comparison to choose the method which is most suitable for Sri Lanka. According to the results, struvite precipitation stood above all other methods in each scenario. This happens due to low energy consumption, heavy metal removal during the process, zero emission of flue gases, relatively low use of machinery and the formation of struvite as the final product.

Even though precipitation stands as the most suitable method, more studies are essential since the requirement of land, uses of alternative products such as phosphoric acid

are not included in the multi-criteria analysis. Inclusion of those parameters might provide a more accurate result when it comes to real world feasibility assessment.

After considering results, it is fair to say that the research hypothesis, which is most suitable and feasible method to recover phosphorus fertilizer from sewage sludge which is generated in municipal wastewater treatment plants in Sri Lanka can be selected by considering multiple criteria, is true and acceptable.

#### References

- Acelas, N. Y. et al. (2014) 'Supercritical water gasification of sewage sludge: Gas production and phosphorus recovery', *Bioresource Technology*, 174, pp. 167–175. doi: 10.1016/j.biortech.2014.10.003.
- Amrullah, A. and Matsumura, Y. (2018) 'Supercritical water gasification of sewage sludge in continuous reactor', *Bioresource Technology*, 249(October 2017), pp. 276–283. doi: 10.1016/j.biortech.2017.10.002.
- Cieřlik, B. and Konieczka, P. (2017) 'A review of phosphorus recovery methods at various steps of wastewater treatment and sewage sludge management. The concept of "no solid



- waste generation" and analytical methods', *Journal of Cleaner Production*, 142, pp. 1728–1740. doi: 10.1016/j.jclepro.2016.11.116.
- Egle, L. et al. (2016) 'Phosphorus recovery from municipal wastewater: An integrated comparative technological, environmental and economic assessment of P recovery technologies', *Science of the Total Environment*, 571, pp. 522–542. doi: 10.1016/j.scitotenv.2016.07.019.
- Egle, L., Rechberger, H. and Zessner, M. (2015) 'Overview and description of technologies for recovering phosphorus from municipal wastewater', *Resources, Conservation and Recycling*, 105, pp. 325–346. doi: 10.1016/j.resconrec.2015.09.016.
- Gorazda, K. et al. (2018) 'Sewage sludge as a fuel and raw material for phosphorus recovery: Combined process of gasification and P extraction', *Waste Management*, 73, pp. 404–415. doi: 10.1016/j.wasman.2017.10.032.
- Guedes, P. et al. (2014) 'Phosphorus recovery from sewage sludge ash through an electro-dialytic process', *Waste Management*, 34(5), pp. 886–892. doi: 10.1016/j.wasman.2014.02.021.
- Huang, I. B., Keisler, J. and Linkov, I. (2011) 'Multi-criteria decision analysis in environmental sciences: Ten years of applications and trends', *Science of the Total Environment*, 409(19), pp. 3578–3594. doi: 10.1016/j.scitotenv.2011.06.022.
- Jeon, S. and Kim, D. J. (2018) 'Enhanced phosphorus bioavailability and heavy metal removal from sewage sludge ash through thermochemical treatment with chlorine donors', *Journal of Industrial and Engineering Chemistry*, 58, pp. 216–221. doi: 10.1016/j.jiec.2017.09.028.
- Karimi, A. et al. (2011) 'Using of the fuzzy TOPSIS and fuzzy AHP methods for wastewater treatment process selection', *International journal of academic research*, 3(1), pp. 737–745.
- Li, L. et al. (2019) 'Characterization of phosphorus species distribution in waste activated sludge after anaerobic digestion and chemical precipitation with Fe<sup>3+</sup> and Mg<sup>2+</sup>', *Chemical Engineering Journal*, 373(May), pp. 1279–1285. doi: 10.1016/j.cej.2019.05.146.
- Li, Y. et al. (2018) 'Performance of phosphogypsum and calcium magnesium phosphate fertilizer for nitrogen conservation in pig manure composting', *Bioresource Technology*, 250, pp. 53–59. doi: 10.1016/j.biortech.2017.07.172.
- Liang, S. et al. (2019) 'A comparison between sulfuric acid and oxalic acid leaching with subsequent purification and precipitation for phosphorus recovery from sewage sludge incineration ash', *Water Research*, 159, pp. 242–251. doi: 10.1016/j.watres.2019.05.022.
- Luo, W. et al. (2020) 'Mitigation of Cd accumulation in rice with water management and calcium-magnesium phosphate fertilizer in field environment', *Environmental Geochemistry and Health*, 42(11), pp. 3877–3886. doi: 10.1007/s10653-020-00648-6.
- Pohekar, S. D. and Ramachandran, M. (2004) 'Application of multi-criteria decision making to sustainable energy planning - A review', *Renewable and Sustainable Energy Reviews*, 8(4), pp. 365–381. doi: 10.1016/j.rser.2003.12.007.
- Semerçi, N., Kunt, B. and Calli, B. (2019) 'Phosphorus recovery from sewage sludge ash with bioleaching and electro-dialysis', *International Biodeterioration and Biodegradation*, 144(March), p. 104739. doi: 10.1016/j.ibiod.2019.104739.
- Shiba, N. C. and Ntuli, F. (2017) 'Extraction and precipitation of phosphorus from sewage sludge', *Waste Management*, 60, pp. 191–200. doi: 10.1016/j.wasman.2016.07.031.
- Weijin, G. et al. (2019) 'Hydrogen production and phosphorus recovery via supercritical water gasification of sewage sludge in a batch reactor', *Waste Management*, 96, pp. 198–205. doi: 10.1016/j.wasman.2019.07.023.

Yahya, M. N. et al. (2020) 'Evaluation of wastewater treatment technologies using tophis', *Desalination and Water Treatment*, 177(May), pp. 416–422. doi: 10.5004/dwt.2020.25172.

Yang, F. et al. (2019) 'Phosphorus recovery from sewage sludge via incineration with chlorine-based additives', *Waste Management*, 95, pp. 644–651. doi: 10.1016/j.wasman.2019.06.029.

### **Acknowledgment**

I would like to thank the department of chemical and process engineering of University of Peradeniya for the support which was shown during a period of pandemic for the success of this desk research.

### **Author Biography**



K.A. Lakshan is an undergraduate from engineering faculty of University of Peradeniya with research interests in the fields of wastewater processing, sludge processing, extractions and simulations. He is a self motivated researcher, learner and a career driven person.



M.A.S. Preethika is a Lecturer at the Department of Chemical & Process Engineering, University of Peradeniya. Her research interests include sustainable wastewater treatment, nutrient recovery, life cycle assessment, and multi-criteria decision making. She has published many articles in peer reviewed journals and holds an h-index of 14. She enjoys travelling to new places to admire the beauty of nature.

# Genetic Algorithm-based Path Planning for an Unmanned Aerial Vehicle Considering Energy Consumption and Payload

HDI Piyumini<sup>1#</sup> and CH Hsu<sup>2</sup>

<sup>1</sup>Department of Mechanical Engineering, General Sir John Kotelawala Defence University, Sri Lanka

<sup>2</sup>Department of Mechanical Engineering, National Kaohsiung University of Science and Technology, Taiwan

#piyuminihdi@kdu.ac.lk

**Abstract:** *Unmanned Aerial Vehicles (UAVs), more commonly known as drones, have a wide range of applications spread across various industries. Drones are plagued with several challenges concerning their limited battery life and payload. Until researchers come up with a much more advanced and long-lasting battery solution, drones must use the most optimum path for delivery, which will increase battery efficiency and reduce overheads. This study analyses the battery energy consumption, velocity, and flight time of the quadcopter for varying payloads and develops a suitable mathematical relationship for path planning problem formulation. This paper proposes a Genetic algorithm -based path optimization to obtain the most energy optimal path for the drone carrying a certain payload for a set of specified destinations.*

**Keywords:** *Path planning, Unmanned Aerial Vehicle, Genetic Algorithm, Energy Consumption, Simulation, Payload*

## 1. Introduction

Despite its many advantages, a significant drawback in using an Unmanned Aerial Vehicle (UAV) or a drone is its battery life limitation and payload. The limited power supply restricts the drone's flight duration. Researchers have invested a considerable effort to minimize the weight of the rotorcrafts by adopting improvements. As payload is a crucial factor affecting the drone's flight duration, lack of sufficient battery power brings out a worse scenario of drone malfunction or drone crash before the

completion of delivery. Until researchers develop a much more advanced long-lasting battery solution, research on optimizing routes and battery consumption has become an exciting area.

Much existing literature has not considered the case of drone failure before it completes the journey due to the loss of battery power. As most researchers used commercially available drones for their research, they have determined the energy consumption by considering the Battery Consumption Rate (BCR) of the drone (Yacef et al., 2017; Torabbeigi et al., 2020). In contrast to these, this paper considers the battery power, energy consumption, and varying payloads to formulate the optimization problem. The contributions of this paper are as follows:

- i. An energy model is derived from the power consumption and the flight time of a LiPo battery used by a custom-made drone for different payloads. Here, path is planned by considering payload as a significant factor affecting the drone's energy consumption.
- ii. A Genetic Algorithm (GA) approach is used to search for the optimal energy-efficient path.
- iii. The operation is visualized using a Python-based simulation.

## 2. Literature Review

Many researchers presented several approaches to analysing the range and endurance of battery-powered quadrotors. Traub (2011) has examined and validated (Traub, 2013) the effect of battery

discharge rate and the voltage drop on its adequate capacity. An experiment (Abdilla et al., 2015) to validate the endurance model for LiPo battery-powered UAV was conducted to characterize the consumption of power of rotorcrafts. Kim and his team (2018) proposed a robust method to find the most optimal flight schedule considering uncertain battery duration. Morbidi and his team (2016) addressed UAVs' battery power limitation by determining the minimum energy paths by utilizing the electrical model of a BLDC motor for a commercial quadrotor.

The rising issue of determining energy-optimal paths for a drone considering the power and payload has not received the related literature's required attention. Several path planning approaches have been studied by many researchers worldwide, considering the state-of-health of the battery (Schacht-Rodríguez et al., 2018), the coverage and resolution (Di Franco and Buttazzo, 2015), and wind condition (Yacef et al., 2020). The paper presented by Torabbeigi and his team (2020) claims that the payload is a linear function of the battery consumption rate using linear regression.

Algorithms such as Greedy (Ahmed et al., 2016), Particle Swarm Optimisation (PSO) (Huang et al., 2016), Dijkstra algorithm (Bekhti et al., 2017), Bellman-Ford algorithm (Samar and Kamal, 2012), and Genetic Algorithm (GA) (Shivgan and Don, 2020; Bagherian and Alos, 2015) are among the most used algorithms for UAV path planning. When these researchers compared their results with different algorithms for the same conditions, GA has provided a more accurate solution. According to Bagherian and Alos (2015), GA provides a much better solution to the problem, even with more calculations.

## 3. Methodology

### C. Hardware Setup

The drone used in this experiment is an X-shaped quadcopter. The Carbon fiber frame holds four Gemfan 9047 Carbon Nylon CW/CCW propellers, four brushless DC motors, and four multirotor brushless electronic speed controllers. The system is powered by a three-cell 11.1V LiPo (5C) Battery. The flight controller used in the study is Radiolink Mini Pix V1.0, which includes a processor, barometer, accelerometer, and compass. Flight control is achieved by the communication between the hand-held Transmitter (TX) and the receiver (RX) attached to the flight controller. The radio transmitter is a Flysky FS i6X model joystick controller, and the receiver is a Flysky FS iA6B 2.4 GHz 6 channel receiver.



Figure 2. Drone used in this experiment

The Ground Control Station (GCS) used for this study is the Mission Planner for Radiolink 1.3.50, an open-source platform. The ground control station can create different missions via a flight plan. Once this mission is loaded, the quadcopter flies according to the given commands autonomously. An image captured while the drone was on air is shown in Fig. 1.

### D. Experimental Data Analysis

Two experiments were performed to obtain the data required for the research at the open-space playground of Sirindhorn International Institute of Technology, Thailand. Gathered data was used to study the relationship of battery life, flight time, and velocity to an added payload to the drone's existing weight.

The first experiment was performed to understand the LiPo battery's behaviour with the drone's flight time. The quadcopter's battery consumption was measured during hovering mode (or "altitude hold mode" in Mission Planner). As there is a translational lift, the power consumption is relatively higher in hovering mode. Compared to hovering mode at the corresponding mass, vertical, and/or translational flight indicated the minimum difference, leading to the adoption of hovering as the nominal flight mode (Abdilla et al., 2015). The required experimental data was read from the flight data screen in Mission Planner using a radio connection with a baud rate of 57600.

In the first experiment, the battery voltage, power, and current consumption were recorded and plotted against the flight time for varying payloads. The experiment was conducted for a total weight ranging from 1.174 kg (net weight of the drone) to 1.674 kg (maximum weight the drone can withstand). The experiment was repeated by adding 50 g weight in each trial and aborted when the drone cannot take off any further or is hovering unstably. A total number of eleven (11) tests were performed.

The LiPo cell used for the experiment has a nominal voltage of 3.7 V. The battery has three cells in series, which accounts for a voltage of 11.1 V. The battery was discharged following the 80% rule, i.e., the battery should never be discharged down past 80% of its full capacity to prevent any damage. At 80% charge, the LiPo cell provided an approximate open-circuit voltage of 3.73-3.75 V. With this battery voltage, the maximum flight time without a payload for the drone was 620 s, and the maximum flight time with a payload of 500 g was 210 s. Low battery voltage was detected using a BX100 battery voltage buzzer. By observing the R squared value of the regression models, the following Eq. (1) was obtained, which showed that there is a linear relationship (according to Eq. (2)) between the battery voltage ( $B_v$ ) and the flight time ( $t$ ).

$$B_v = -0.0056t + 12.172 \quad (1)$$

The above equation is in the form of

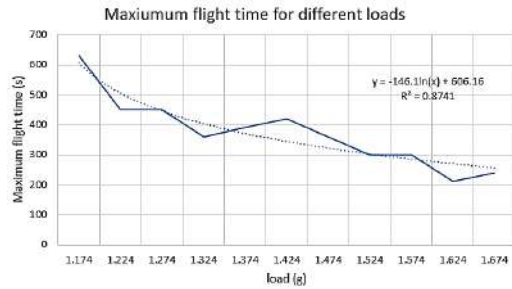
$$B_v = \alpha t + \beta \quad (2)$$

where  $\alpha$  is the slope and  $\beta$  is the intercept.

### E. Experimental Results

Using the data from the experiments, another analysis was performed to study how the flight time varies with increasing load. Due to the drone's additional power to lift the payload, the flight time showed a reducing pattern with an increasing load ( $w$ ), as shown in Fig. 2.

Figure 2. Variation of maximum flight time of



the drone with the total load of the drone

Here, the continuous line shows the experimental values while the dotted line represents the best fit curve. For the plot, the logarithmic fit showed the best R squared value of 0.8741. Therefore, it was concluded that the load  $w$  and the flight time  $t_{max}$  of the drone have a logarithmic relationship shown by the Eq. (3).

$$t_{max} = -146.1 \ln(w) + 606.16 \quad (3)$$

To obtain the data required to find the relationship between drone velocity ( $v$ ), power ( $p$ ), and load ( $w$ ), the UAV was flown in a straight line with a constant distance of 50 m and maintaining an altitude of 10 m. The data was gathered for payloads varying from 50 g to 500 g. The constant distance and the flying altitude were set using the Mission Planner software.

The results showed that the drone's velocity remained at an average value of  $3.23 \text{ ms}^{-1}$  for every different weight attached. This is mainly due to the electronic speed controller's function connected to the drone that supplies the adequate instantaneous current to maintain a constant velocity. The following graph in Fig.3 shows the relationship between the load and the drone velocity.

The average velocity remained unchanged with varying loads. However, when considering power variation with flight time for all the weights added, it was observed that the power consumption has increased with every added payload. The weight limit of the drone depends on the thrust produced by the motors.

The variation of power consumption with payload is given by the Eq (4).

$$p = 0.1288w - 27.303 \quad (4)$$

The trendline for velocity variation is given by,

$$v = 0.0003w + 2.794 \quad (5)$$

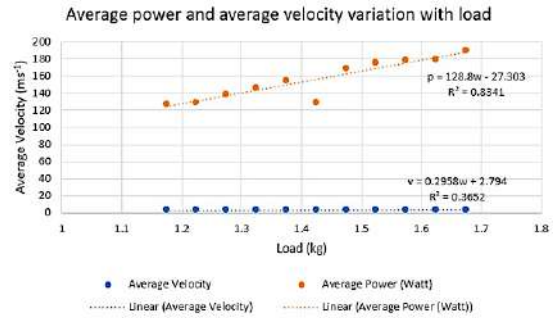


Figure 3. Variation of average velocity and the average power with a varying total load

In addition to this, the maximum distance for each flight was obtained by multiplying the corresponding velocity with the flight time.

#### F. Determining the Energy Consumption of the Drone

As energy consumption depends on the drone speed, the energy consumption model must consider the different flight stages, including acceleration, deceleration, and hovering. The energy consumption at different speeds and distances can be calculated by the Eq. (6).

$$E((v, d)) = \int_0^{t1} P_a dt + \int_{t1}^{t2} P_v dt + \int_{t2}^{t3} P_d dt \quad (6)$$

Here,  $P_a$  denotes the power consumed during acceleration,  $P_v$  denotes power consumed when the drone is flying with uniform velocity  $v$ ,  $P_d$  denotes the power consumed during deceleration,  $d$  is the distance traveled, and  $t1, t2$ , and  $t3$  is the time duration of the acceleration phase, constant speed flight phase, and deceleration phase, respectively. The particular current draw and the battery voltage data were obtained from the first experiment. The consumed power was then derived by multiplying the absorbed current by the supply voltage for each payload. The corresponding power consumption was plotted in a graph for every flight. The energy consumed by the total flight was calculated by obtaining the area under the curve, according to Eq. (7).

$$E_w = \int_{t=0}^{t=T} P(t) dt \quad (7)$$

In the Eq (7),  $E_w$  represents the energy

added weights. This was considered as an energy loss. The energy consumption for different loads was plotted in the graph, and the best fit's eligibility was observed. The fit with

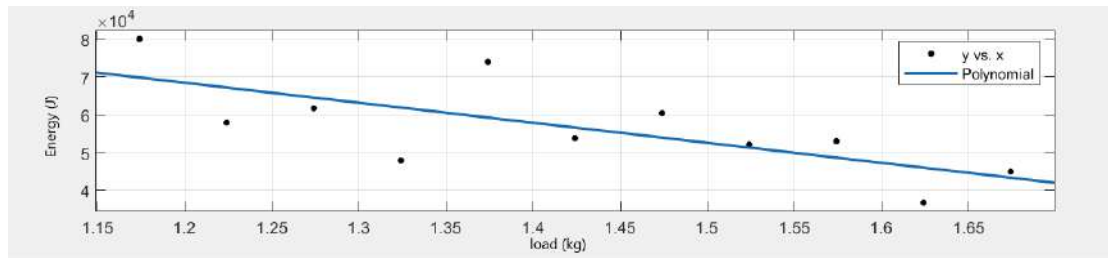


Figure 4. Energy consumption of the drone with varying load

consumed by a drone with a weight  $w$ . Fig. 4 shows that the energy level has reduced with one (1) was selected as the most suitable energy model equation.

Since there were four types of fits with an R squared value of more than 50%, cross-validation was performed to check which fit is more likely to give out the closest value to the actual energy value. The average percentage error for linear fit, polynomial fit of degree 1, polynomial fit of degree 2, and polynomial fit of degree 3 was 46.8%, 2.14%, 19.63%, 26.3%, respectively. As the model with a one-degree polynomial provided a closer value, it was selected as the energy model of the problem.

The energy model for the above analysis is given by Eq. (8).

$$E = p_1 w + p_2 \quad (8)$$

Where  $E$  is the energy consumption in Joules and  $w$  is the payload in Kilograms.  $p_1$  and  $p_2$  are two coefficients provided as  $p_1 = -5.306 \times 10^4$  and  $p_2 = 1.321 \times 10^5$ .

### G. Path planning

The path planning approach in this research was conducted as a Travelling Salesman Problem (TSP) to minimize energy

the R squared value closest to

consumption. Given a set of random cities or locations and the travel cost between each site, the TSP can find the cheapest route to visit all the cities and return to the initial starting point. A Genetic Algorithm (GA) approach was used to evaluate the shortest path that the drone travel using optimized energy and distance using the derived energy model.

In the proposed GA, the initial population is the set of all possible traveling routes for the drone which is defined by user input. A solution or a route is characterised by a set of parameters (genes) which links together to form a solution (chromosome). In this case, the fitness value was calculated based on the energy consumed along the path drone takes. For selecting the parent, this research used the Elite selection method. As the objective is to minimize the energy consumption, the parent with a smaller fitness value used in GA to push the hypothesis towards an optimal solution. The swapping is selected, which corresponds to the higher energy efficient path. New offspring are created by applying a crossover operator to the parents.

```

1 : Input: No of waypoints, Weight of the drone, Population size,
velocity
2 : P = -128.8w-27.30
3 : E = P * (d/v)
4 : Initialize population
5 : function evaluate_function
6 : for i=1: n do
7 :     for j=1: n do
8 :          $d_{ij} = \sqrt{(x_i - x_j)^2 + (y_i - y_j)^2}$ 
9 :     end for
10: end for
11: return E, dij
12: end function
13: while iteration < num_Iter do
14:     for p=1:popul_size do
15:         for K=1:chrom_size do
16:             N(p,k),e(p,k) = evaluate
function
17:             D=D+d(p,k)
18:             E=E+e(p,k)
19:         end for
20:         Total D(P)=D
21:         Total E(P)=E
22:     end for
23: if iteration > num_Iter then
24:     break
25: else
26:     repeat total energy calculation using cross over and
mutation
27: end if
28: for P=10: 10: popul_size do
29:     Use Elite selection to find parents
30:     Apply crossover to find new solution
31:     save in temp_pop
32:     for k=1: size(temp_pop) do
33:         select previously separated solution
from temp_pop
34:         apply swapping mutation
35:         if solution is feasible then
36:             save it in new_pop
37:         end if
38:     end for
39:     update solution in pop
40: end for
41: maximum_energy=-53063.39459*(w/1000) + 132107.63396
42: if drone_energy<maximum energy
43:     Print maximum_energy, total energy, total distance,
drone energy, maximum_energy-drone_energy
44: else print maximum energy is not enough to complete path
45: end if

```

Figure 5. Pseudocode for the simulation program

New offspring are created by applying a crossover operator to the parents. The two-point crossover method was used in our study. This method uses two points randomly selected, and these points are applied to a pair of chromosomes

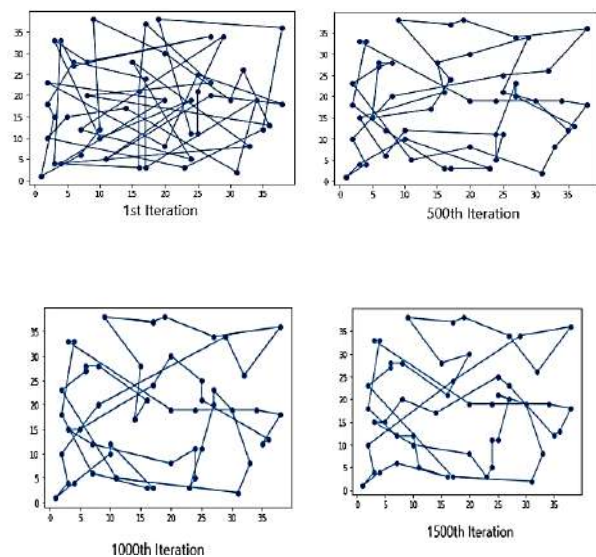
The two-point crossover method was used in our study. This method uses two points randomly selected, and these points are applied to a pair of chromosomes. Mutations are mechanism was used for mutation, which selects two or more random genes from a chromosome to be swapped. The mechanism selects two random positions on the chromosome and interchange the values. The

termination process determines when the GA process ends. Every iteration in the GA process brings out a better solution, but the progression starts to saturate when the improvements are minimal. The process is terminated when the solution becomes closer to the optimal.

The path planning process was simulated using Python 3.7 V based genetic library [17]. The computer used for this consisted of an Intel® Core™ i5-6200U CPU with a speed of 2.40 GHz. The system used a 64-bit Windows operating system with an x64 -based processor. The pseudocode for the program is provided in the Fig 5.

The first generation, also known as the initial population, generates several paths possible. This number (population size) is defined by the user in popul\_size, which is the set of all possible paths a drone can follow. The genetic algorithm process starts at this point. The initial population and selection algorithm is described in a class called GeneticAlgorithm. The primary role calls it for the GA process, which is initiated by the run function. The initial population is then sorted according to the fitness value in ascending order.

#### 4. Results





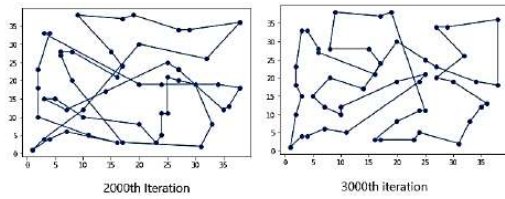


Figure 6. Simulation results for 50 waypoints with different iterations for 1374 g

The fitness value is generated by obtaining the sum of the

total energy ( $E(P)$ ) consumed by the drone when it is moving from one point to another for all the points and the total distance ( $D(P)$ ). Then the selection process is done using the elite selection model. The selection model sorts the initial population into sets of 10, and the set with the best fitness is considered as the new population. This new population is returned to the GA function. This set is subjected to mutation and crossover and calculates the fitness value again. This cycle is repeated until the best solution is obtained.

Results for path planning simulation were tested on several conditions. Tests were conducted for 50 waypoints, 20 waypoints, and 10 waypoints to observe the fitness value behaviour. The distance coordinates were chosen to be in the range of 0 m to 40 m, and the experiment was repeated for three selected weights (1174 g, 1374 g, 1424 g, and 1674 g). For each drone weight, five tests were conducted by changing the number of iterations.

The maximum energy calculated by the program for each given weight was close to the energy values for the tested payloads obtained using the Eq. (8). The results also showed the amount of energy consumed by the drone battery and the remaining energy. A sample simulation results for drone carrying a load of 1374 g with 50 waypoints with 3000 iterations is shown in Fig. 6.

Test simulations were conducted with a load of 1374 g for 10,20 and 50 waypoints to observe

the iteration at which the fitness value reaches a minimum. Results are shown in Table 1.

Table 1: Results of test simulation for 1374g.

No. of waypoints	Iteration at which the fitness value reaches minimum
10	60
20	100
50	3000

For 50 waypoints, as 1000 iterations were not enough to obtain an acceptable optimized solution, the no of iterations were increased to 3000. Then the fitness value started to stabilize at approximately 2000<sup>th</sup> iteration. Therefore, for higher number of waypoints, it is required to increase the number of iterations, which increases the number of generations to obtain an accepted fitness value.

The results in Table 1 were obtained only when the total distance travelled by the drone along the path generated is less than the maximum distance that the drone can travel with the available battery capacity. If the generated total distance is more than the drone's travel capacity, a message is displayed to show that the drone cannot cross the generated path.

## 5. Future Work

As an extension of this work, a real-time rescheduling based on real-time battery capacity reduction can be studied. An alternative flight path can be developed to minimize the unmet demand in a scenario where the remaining battery capacity falls below a threshold value due to temperature changes. As the drone's battery life is limited to approximately 10 minutes, new approaches such as battery swapping or autonomous battery recharging can be utilized at different depots on the map. These can be accounted to the path planning problem formulation for a much more realistic scenario. Furthermore,

this research can be conducted for higher loads to derive standard model for higher weight range.

## 6. Conclusion

Since long-lasting batteries for UAVs are still under research, this project has developed an optimized flight routing algorithm considering the available battery energy and the payload the drone can carry. Initially, data analysis on battery consumption, velocity, and flight time with the payload was conducted on a custom-made drone. The relationship between each parameter was developed, and an energy model was created. Using the developed energy model and relationships generated from the data analysis, the path planning algorithm was formulated and optimized. Then using a GA approach, the problem was simulated. The results obtained provided an energy-efficient path plan for each payload carried by the drone around a set of user-defined locations. This approach can be utilized for drones deployed in various industrial and domestic applications.

## References

- Abdilla, A., Richards, A. and Burrow, S., (2015), September. Endurance optimisation of battery-powered rotorcraft. In Conference Towards Autonomous Robotic Systems, 1-12. Springer, Cham.
- Ahmed, S., Mohamed, A., Harras, K., et al, (2016), April. Energy efficient path planning techniques for UAV-based systems with space discretization. In 2016 IEEE wireless communications and networking conference (1-6). IEEE.
- Bagherian, M. and Alos, A., (2015). 3D UAV trajectory planning using evolutionary algorithms: A comparison study. The Aeronautical Journal, 119(1220), 1271-1285.
- Bekhti, M., Achir, N., Boussetta, et al., (2017). Drone Package Delivery: A Heuristic approach for UAVs path planning and tracking. EAI endorsed transactions on Internet of Things, 3(9).
- Di Franco, C. and Buttazzo, G., (2015), April. Energy-aware coverage path planning of UAVs. In 2015 IEEE international conference on autonomous robot systems and competitions (111-117). IEEE.
- Huang, Y., Wang, H. and Yao, P., (2016). Energy-optimal path planning for solar-powered UAV with tracking moving ground target. Aerospace Science and Technology, 53, 241-251
- Kim, S.J., Lim, G.J. and Cho, J., (2018). Drone flight scheduling under uncertainty on battery duration and air temperature. Computers & Industrial Engineering, 117, 291-302.
- Morbidi, F., Cano, R. and Lara, D., (2016), May. Minimum-energy path generation for a quadrotor UAV. In 2016 IEEE International Conference on Robotics and Automation (ICRA), 1492-1498. IEEE.
- PyPI. (2022) "Geneticalgorithm," [Online]. Available: <https://pypi.org/project/geneticalgorithm/>. [Accessed: 15-March-2022].
- Samar, R. and Kamal, W.A., (2012). Optimal path computation for autonomous aerial vehicles. Cognitive Computation, 4(4), 515-525.
- Schacht-Rodríguez, R., Ponsart, J.C., García-Beltrán, C.D., et al, (2018). Path planning generation algorithm for a class of uav multirotor based on state of health of lithium polymer battery. Journal of Intelligent & Robotic Systems, 91(1), 115-131.
- Shivgan, R. and Dong, Z., (2020), May. Energy-efficient drone coverage path planning using genetic algorithm. In 2020 IEEE 21st International Conference on High Performance Switching and Routing (HPSR) (1-6). IEEE.
- Torabbeigi, M., Lim, G.J. and Kim, S.J., (2020). Drone delivery scheduling optimization considering payload-induced battery

consumption rates. *Journal of Intelligent & Robotic Systems*, 97(3), 471-487.

Traub, L.W., (2011). Range and endurance estimates for battery-powered aircraft. *Journal of Aircraft*, 48(2), 703-707.

Traub, L.W., (2013). Validation of endurance estimates for battery powered UAVs. *The Aeronautical Journal*, 117(1197), 1155-1166.

Yacef, F., Rizoug, N., Bouhali, O. et al., (2017), September. Optimization of energy consumption for quadrotor UAV. In *Proceedings of the International Micro Air Vehicle Conference and Flight Competition (IMAV)*, Toulouse, France, 18-21.

Yacef, F., Rizoug, N., Degaa, L. et al, (2020), June. Energy-efficiency path planning for quadrotor UAV under wind conditions. In *2020 7th International Conference on Control, Decision and Information Technologies (CoDIT)* (Vol. 1, 1133-1138). IEEE.

### **Acknowledgment**

The authors would like to thank the support provided by Sirindhorn International Institute of Technology, Thammasat University, Thailand.

### **Author Biography**



Ms. HDI Piyumini received her MSc in Engineering and Technology from Thammasat University, Thailand. She is currently serving as a Lecturer (probationary) in the Department of Mechanical Engineering, KDU.



Dr. CH Hsu received his PhD from Texas A&M University and he is currently serving as an academia in the Department of Mechanical Engineering, National Kaohsiung University of Science and Technology, Taiwan.

# Current Phasor Measuring Device for Three Phase Distribution Lines

RA Amarasinghe<sup>1#</sup>, MTTT Thanthirimalage<sup>1</sup>, WASSW Arachchi<sup>1</sup>, MGTR Amarasinghe<sup>1</sup>, JR Lucas<sup>1</sup> and N De Silva<sup>2</sup>

<sup>1</sup>General Sir John Kothelawala Defence University, Rathmalana, Sri Lanka

<sup>2</sup>Lanka Electricity Company (Pvt) Ltd, Colombo 6, Sri Lanka

#35-eng-119@kdu.ac.lk

**Abstract:** Protection and reliability are the most paramount considerations in the power system. Current measurement of distribution lines is essential for the power and quality evaluation purposes. The current measuring devices are used for controlling, monitoring and protection purposes. While the measurement of current at an end connected to a substation can be carried out without too much trouble, intermediate current measurements cannot be carried out with ease. Further instantaneous phase angle differences need to be measured to be able to evaluate power flow in distribution lines. Thus, at present power loss calculations are approximately carried out by the utility. So, the power quality analysis, switching operations and load transferring in distribution lines are not much accurate. The use of a flux concentrator and hall-effect sensor, with a filter, has demonstrated that a sinusoidal current waveform, with the correct phase angle, can be obtained. The use of the device on an existing line does not need disconnection, nor a separate earth connection to obtain the magnitude and phase angle of the current accurately. The data from the transducer is transmitted to the operator using radio signals rather than wi-fi.

**Keywords:** Current Phasor, Hall Effect Transducer, Magnetic Flux, Current Transformer, Zero Crossing Detection.

## 1. Introduction

With the necessity of a device to measure the current passing through the distribution lines, implementing of a portable as well as non-contact device, was taken into consideration. So, the utilities can have a rough idea about the amount of current passing and power flowing through the sections of lines. In medium voltage distribution lines, load transferring and switching operation are currently carried out approximately. The load balance is achieved by load transferring among feeders in distribution systems, as system losses are increased by the load imbalances. The load imbalance is solved by switching operations and switching operations are aimed at line and load dispatching operations. In power systems, the load flow is monitored to collect active and reactive power, to identify whether the load flow is exceeded. So, if there is any method to have a good idea about the amount of current passing through any point of the medium voltage distribution lines, it would be easy or an accurate system operation (Selva et al., 2015).

*A. The existing current measuring method in distribution lines and its drawbacks.*

Generally, Current Transformers are used to measure currents in conductors. Normally, to measure the current in a medium voltage distribution line, a pole should be erected, and a large current transformer should be installed. So, it takes more time. Another drawbacks of Current Transformers (CT) are

accuracy issues because of the droop, limitations of the duty factor and the inability to sense DC currents. CTs are used to measure Alternative Current (AC) currents. If the CT is operated without a load on the secondary, it will cause insulation breakdowns due to the high voltage. Moreover, the need to repair the CTs is not an easy task, and the testing equipment is expensive and time consuming (Karthick, 2015).

The present work has identified some research that has been carried out, and the methods developed in order to measure the current in distribution lines based in the Hall-effect.

### B. Hall effect based current measuring technique.

With the development of modern technology, there are various methods that can be used for current measuring in distribution lines (Chen, Guo and Ma, 2018). Nowadays, the Hall Effect sensor has become very attractive for current measuring purposes. By using hall sensors, the overall size of traditional CTs can be decreased. Hall Effect sensors can measure AC and DC currents without a supply interruption. The sensor is smaller in size compared to the CT, with noise-immunity, and less power consumption. It is also cost effective, has accuracy and linearity. Quick response ensures better performance of these Hall Effect based current measurement methods (Wu et al., 2021).

### C. Working principle.

The major relevant laws in electromagnetic fields are.

#### 1) Biot-Savart's law:

where,

B - Magnetic flux density

I - Current carrying in the cable.

$\mu_0$  - Permeability in the free space

r - Distance

$$B = (\mu_0 I) / 2R$$

(1)

The electrical and magnetic fields are coupled together to solve Maxwell's equation (Biot-Savart Law, no date).

2) Ampere's circuital law: The magnetic field surrounding a single current carrying conductor is given by the line integration of magnetic flux intensity, H round the path equal to the total current as given in equation 2.

$$\oint H \cdot dl = I$$

(2)

For a.c. fields, the measured value of B is averaged or rms value taken to obtain the rms current (Ampere's Law, no date).

3) Hall effect: When a magnetic field is applied at right angles to the current in a thin film, an electric field is generated which is mutually perpendicular to the current and the magnetic field and which is proportional to the product of current density and the magnetic induction (equation 3) (Hall Effect, no date).

$$V_H = IB / nqd$$

(3)

where,

$V_H$  - Hall voltage through the conductive plate

I - Current passing through the plate

B - Magnetic flux density

q - Magnitude of the charge carriers

n - Number of charge carriers per unit volume

d - Thickness of the sensor columns.

## 2. Methodology

### A. Selecting the Sensor Details

Initially, testing has been done using the 49E Hall Effect Transducer, but it was observed

that it saturates quickly due to its limited linear region and only provides a perfect sinusoidal wave within a small range of current (1-2A). Hence, the linear Hall Sensor DRV 5053 from Texas Instruments, shown in Figure 1 was selected to give a linear output with high sensitivity stability.



Figure 3: DRV 5053 Hall Effect Sensor (DRV5053 data sheet, product information and support | TI.com, 2017)

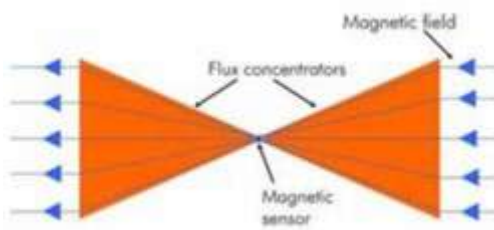


Figure 2: Magnetic Field Lines in Flux Concentrator ('Future Directions for Magnetic Sensors: HYBRID MATERIALS Achieving Better Sensitivity, Smaller Size, Lower Cost, & Lower Power Use', 2015)

### B. Constructing the flux concentrator

In this study, the current is measured using the magnetic flux generated when the current is passing through the conductor (Figure 2). A flux concentrator is used consisting with a hall effect transducer to convert the flux into a voltage signal.

### C. Testing the Hall Effect sensor

The flux concentrator in Figure 3 is a conically shape solid made of steel, and enhances the intensity of the magnetic field.



Figure 4: Flux Concentrator

In the analysis, the peak-peak voltage was obtained by giving different current values to the apparatus as given in table 1. The current is supplied through 30 turns of a coil to the device.

Table 1. Testing of Flux Concentrator

Step	Supply Current × Turns = Current (A)	Peak-Peak Voltage (mV)
1	1.0 A × 30 = 30 A	180
2	1.50 A × 30 = 45 A	200
3	2.5 A × 30 = 50 A	250



Figure 5: Testing the Sensor on Test Bench

The voltage from the transducer is converted to 0-5V range, as it is the sensing voltage of the Arduino. The input voltage is measured while giving maximum current. The Gain of the Amplifier is calculated from the peak-to-peak voltage as in equations 4 and 5.

$$V_{p-p} = 5 \times 2 = 10 \text{ V} \quad (4)$$

$$\text{Gain} \times 2 = V_{p-p} \quad (5)$$

#### D. Testing the Coupling Effect

When gathering flux from one conductor, there will be an effect from the flux generated by the other two conductors. Thus the flux measured is a function of three currents in three phasors as shown in the equation 6, 7 and 8.

$$\phi_a = f(i_a, i_b, i_c) \quad (6)$$

$$\phi_b = f(i_a, i_b, i_c) \quad (7)$$

$$\phi_c = f(i_a, i_b, i_c) \quad (8)$$

This magnetic field interference is caused by mutual and self-coupling. The self-coupling can be ignored if the mutual coupling is low. Both self and mutual coupling exist if the mutual coupling is high. To calculate the coupling factors, the equations are arranged in a matrix as shown in equation (9) (Zhang et al., 2022).

$$\begin{bmatrix} \phi_a \\ \phi_b \\ \phi_c \end{bmatrix} = \begin{bmatrix} K_{aa} & K_{ba} & K_{ca} \\ K_{ab} & K_{bb} & K_{cb} \\ K_{ca} & K_{cb} & K_{cc} \end{bmatrix} \begin{bmatrix} i_a \\ i_b \\ i_c \end{bmatrix} \quad (9)$$

However, it can be shown both theoretically as well as experimentally that a considerable coupling effect cannot be obtained from this Hall Effect based current measuring device.

#### E. Calculating the conductor currents

By solving the mutual transfer matrix of the matrix shown in equation 9, the currents passing through the three conductors  $i_a$ ,  $i_b$ ,  $i_c$  can be calculated. Since the interference is negligible, the error occurring due to coupling effect can be neglected.

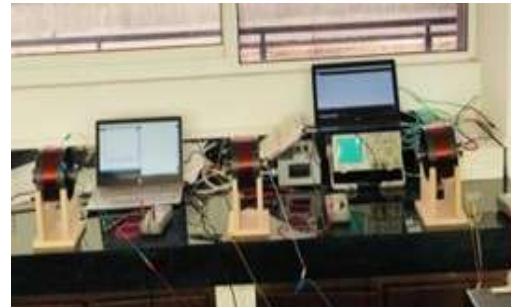


Figure 6: Testing the Coupling Factors

#### F. Circuit for obtaining measurements

1) The Signal conditioning circuit: Analog filters and an instrumentation amplifier are used to condition the analog signals before converting into digital signals. The higher harmonics starting from fifth are blocked by this circuit. The application of this circuit is for changing the input voltage and get the offset and the voltage reference of Analog to Digital Converter (ADC).

2) Op- amp rectification: Rectifiers measure the strength of the signal and convert the AC to DC. Diode and an operational amplifier can be used as the rectifier to get current flow in one direction.

### 3. Experimental Design

1) *Phase angle measurement*: Phase angles are obtained from the zero-crossing detection of current and voltage waveforms. The small signal which comes from the Hall effect sensor has a low amplitude with noise and it goes to the instrumentation amplifier through the low pass filter. The low-pass filter minimizes the noise and the signal interference. It improves signal to noise ratio and the accuracy. The filter is placed closer to the amplifier. The signal then goes to the rectifier bridge, and the waveform is rectified. Next, an opto-coupler passes the square shaped pulses to the micro controller.

Phase angle between the current and the voltage waveform is measured by Zero Crossing Detection (ZCD), as shown in Figure 6. The output from the ZCD is a square shaped waveform which goes through the RC series circuit. The time difference between the sine wave and thereference signal is detected by ZCD. If the input passes the zero and if it is in negative direction, Vout goes to positive saturation.

2) Designing and implementation the circuits:

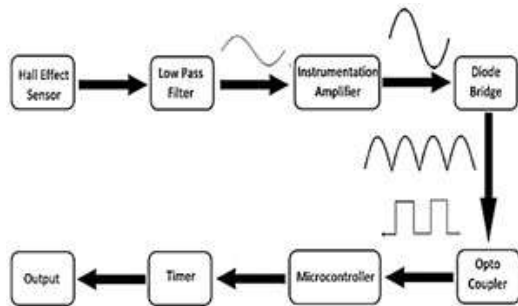


Figure 7: Measuring the phase angles

Implementing the first order low pass filter

The low pass filter is used to remove noise with a cut-off frequency chosen as 500Hz.

$$F \setminus C = 500Hz \tag{10}$$

The capacitor and the resistor are then chosen according to the cut-off frequency given in equation 11.

$$F = 1/2\pi RC \tag{11}$$

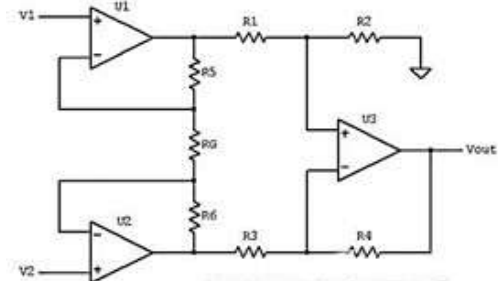
This gives the value as R = 21kΩ and C = 10nF.

Implementing the Instrumentation Amplifier

The LM 324 IC consisting of 4 op amps is used and saturates at VCC of 1.5 V. The instrumentation amplifier has a good sensitivity to dc offset errors due to the common mode. It increases the amplitude which comes from the sensor.

The resistors are selected as it is given gain of 6. The Gain of the instrumentation amplifier is calculated as in equation 12.

$$Gain(A_v) = V_0/(V_2 - V_1) = (1 + 2R_5)/R_g \times R_2/R_1 \tag{12}$$



3) Obtaining the zero crossings of the current:

Figure 8: Instrumental Amplifier Circuit

The Vo output is given to the full wave diode bridge connected to the opto-coupler. The output is obtained from the collector of the opto-coupler. When the AC sinusoidal wave crosses zero, the collector of the transistor goes high giving square shaped pulses at 0°, 180°, 360°... Since the amplitudes are changed with the current, this ZCD is complicated for the current measuring circuit than the Voltage measuring circuit.

4) Obtaining the voltage measurements: The current (i) is passed through a load (e.g: motor, water heater) to the test the apparatus. From the 230V AC waveform, 4.5V is obtained using a step-down transformer,. The signal is obtained by varying the voltage by a variac and given to Analog 1 pin of the Arduino.

5) Establishing the communication system: When utilities request the current phasor readings of a specific point, the server will transmit the relevant data to the utility. Ubidots is the dashboard which displays the data on computer screen. The dashboard is displayed as shown in the Figure 13.

4. Results

1) Coupling Effect Calculation: A considerable coupling effect was unable to be obtained from



this hall effect based current measuring device experimentally. Hence, the interference of the magnetic field of the conductors were calculated theoretically to check the reliability.

The apparatus was placed as in the same gap (0.7m) between the conductors in 11kV MV distribution lines as shown in the Figure 8.

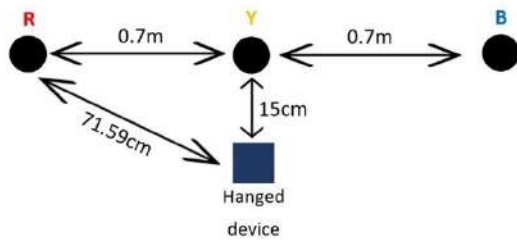


Figure 9: Arrangement of Three Conductors and the Device

From the equation (1),  $B = (\mu_0 I) / 2\pi R$ ; Tesla

A) Magnetic field strength from R or B conductor to the placed device,

$$\mu_0 = 4\pi \times 10^{-7} \text{ Hm}^{-1}$$

Permeability in copper medium;  $\mu = 1.25 \times 10^{-6} \text{ Hm}^{-1}$

$$B = (4\pi \times 10^{-7})(1.25 \times 10^{-6})200 / 2\pi(71.59 \times 10^{-2}) = 6.98 \times 10^{-11} \text{ T}$$

(Approximately 200A passes through 11kV distribution line)

B) Magnetic field strength from Y conductor to the placed device,

$$B = (4\pi \times 10^{-7})(1.25 \times 10^{-6})200 / 2\pi(15 \times 10^{-2}) = 33.33 \times 10^{-11} \text{ T}$$

Interference of Magnetic field strength from three conductors to place the device,

$$B = 2(6.98 \times 10^{-11}) + 33.33 \times 10^{-11} \text{ T} = 47.29 \times 10^{-11} \text{ T}$$

As the magnetic field strength is negligible, it was proved that, a considerable coupling effect cannot be obtained from this hall-effect based current measuring device experimentally as well as theoretically. Therefore, the magnetic field interference from other conductors can be neglected when measuring the current in one conductor. Hence, it's a significant improvement of this project.

2) *Obtaining Waveforms*: The signals which comes from the sensor is passed through an inverting instrumental amplifier to amplify the signal. The signal with the amplified signal is shown in the Figure 9.

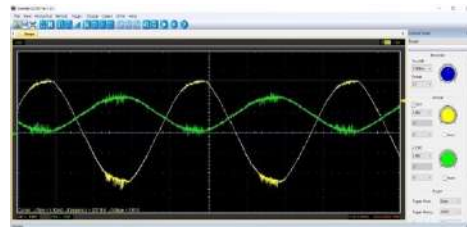


Figure 10: Current Waveform from the Sensor and the Amplified Waveform

When AC wave crosses zero crossings, the collector of the transistor in Opto-coupler goes high, thus gives poles 0-5V at 0°, 180°, 360° as shown in Figure 10.

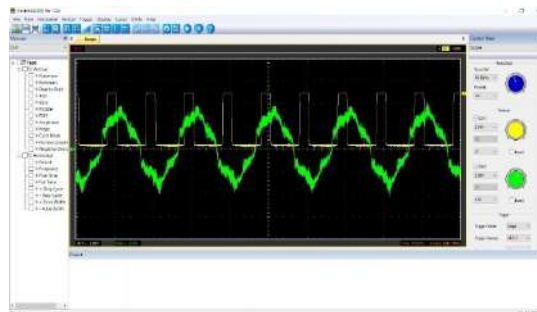


Figure 11: Zero Crossing Outputs from Opto-Coupler

The phase angle is measured from time shift of the current and the voltage waveforms. It is

obtained from the current and voltage zero crossing waves in Figure 11.

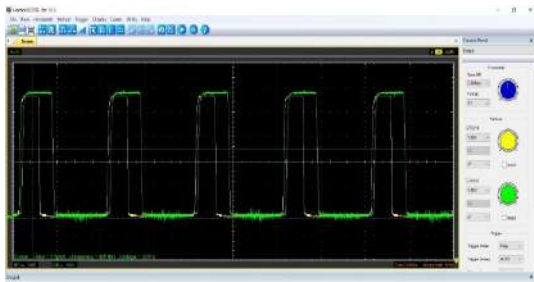


Figure 12: ZCD of current and voltage waveforms

The current measurements according to the Analog readings which come from the Hall sensor as Magnetic Flux are shown in this graph. This Graph proves the linearity of the Hall Sensor. Hence, it has been shown that results are accurate.

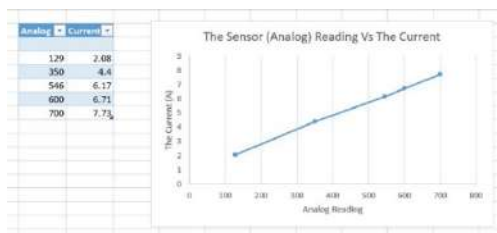


Figure 13: Graph of the Sensor (Analog) Reading vs the Current

The current, voltage, power, and power factor values are displayed on the Dashboard Application as per the utility's requirements is shown in the Figure 14.



Figure 14: Dashboard Application

Figure 15 shows the designed circuit. In particular the relevant parts of the circuit are labelled.

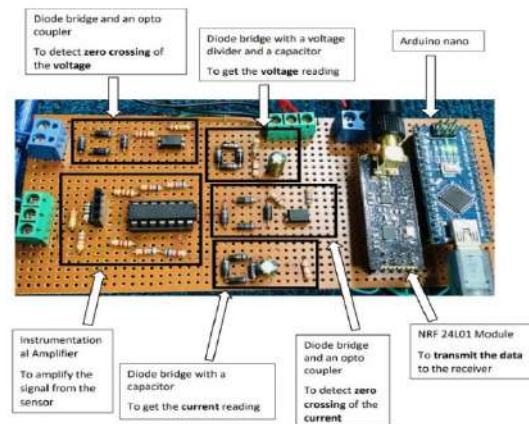


Figure 15: Designed Circuit



Figure 16: Fabricated Prototype

## 5. Discussion

This paper gives an effective solution for the current measuring purpose in distribution lines using hall effect sensor method. The research has demonstrated stable sinusoidal waveforms by using the Hall-Effect sensor with filters. The linearity of the sensor is used to compute the currents from magnetic flux considering the coupling effect. The low-pass filter is minimized the noises and it gives better output waveforms and also the signal conditioning circuit converts them to proper signals before processing. Therefore, the system accuracy will be high.

## 6. Conclusion

The proposed non-contact device can measure current phasors by hanging the device on the conductor. The readings are obtained from this device without disconnecting the power to that particular area. The coupling effect is considered when getting the magnetic flux readings. However, it was observed that a considerable coupling effect cannot be obtained from this hall effect based current measuring device experimentally as well as theoretically.

The proposed method can be improved by using more signal conditioning circuits to obtain more accurate and reliable data. Rechargeable batteries can be added to the device which can be charged from the induced conductor current according to the low power theories. To increase the data communication range, Lora modules can be used due to its high range.

Moreover, an apparatus for voltage measurement can be implemented. By placing a Copper plate parallel to the medium voltage distribution lines, the voltage can be obtained relative to the ground. So, it is like a capacitor between the ground and the copper plate. Then, the real time voltage data can be transmitted as the zero-crossing pulses.

## References

- Selva, K. T. et al. (2015) 'Non-contact Current Measurement in Power Transmission Lines', *Procedia Technology*. Elsevier B.V., 21, pp. 498–506. doi: 10.1016/j.protcy.2015.10.034.
- Karthick, S. (2015) 'Efficient Design of Hall-Effect Current Transformer for the Measurement and Protection of Power Systems', 3(16), pp. 1–6.
- Chen, K. L., Guo, Y. and Ma, X. (2018) 'Contactless voltage sensor for overhead transmission lines', *IET Generation, Transmission and Distribution*, 12(4), pp. 957–966. doi: 10.1049/iet-gtd.2017.1181.

Wu, J. et al. (2021) 'The study on the Mal-operation of the transformer current differential protection during external faults cause by CT saturation', *E3S Web of Conferences*, 260. doi: 10.1051/e3sconf/202126002016.

Biot-Savart Law (no date). Available at: <http://hyperphysics.phy-astr.gsu.edu/hbase/magnetic/Biosav.html>

Ampere's Law (no date). Available at: <http://hyperphysics.phy-astr.gsu.edu/hbase/magnetic/amplaw.html>.

Hall Effect (no date). Available at: <http://hyperphysics.phy-astr.gsu.edu/hbase/magnetic/Hall.html>.

DRV5053 data sheet, product information and support | TI.com (2017). Available at: <https://www.ti.com/product/DRV5053>.

'Future Directions for Magnetic Sensors: HYBRID MATERIALS Achieving Better Sensitivity, Smaller Size, Lower Cost, & Lower Power Use' (2015). Available at: [www.nist.gov/metallurgy](http://www.nist.gov/metallurgy).

Zhang, W. et al. (2022) 'Coupling Interference between Eddy Current Sensors for the Radial Displacement Measurement of a Cylindrical Target', *Sensors*, 22(12). doi: 10.3390/s22124375.

## Acknowledgment

We wish to pay our gratitude to the academic staff of the Faculty of Engineering, General Sir John Kotelawala Defence University as well as the staff of the Lanka Electricity Company Private Limited who extended their support to make this valuable opportunity for us to have this wide-ranging experience as undergraduates.

## Author Biography



Ravindi Amarasinghe is a highly motivated Electrical Engineer who completed Bsc (Hons) Engineering degree from General Sir John Kotelawala Defence University with innovative ideas and willingness to expand horizons in Engineering.



Thimas Amarasinghe, An Electrical Engineer who completed bachelor's degree (Hons) in Electrical and Electronics Engineering at General Sir John Kotelawala Defense University, Sri Lanka.



Thirangana Thanthirimalage is an Electrical Engineer who completed bachelor's degree (Hons) in Electrical and Electronics Engineering at General Sir John Kotelawala Defense University, Sri Lanka.



Prof J Rohan Lucas completed his PhD and MSc degrees from the University of Manchester in the UK and his BSc Engineering degree from the University of Ceylon. He is a Senior Lecturer at the General Sir John Kotelawala Defence University.



Subodha Sasanda is an Electrical Engineer who completed bachelor's degree (Hons) in Electrical and Electronics Engineering at General Sir John Kotelawala Defense University, Sri Lanka. The author's areas of specification include, high voltage, power systems and electrical installation.



Dr Narendra de Silva completed his PhD from the Heriot-Watt University in Edinburgh and his BSc Engineering degree from the University of Moratuwa Sri Lanka. He is the General Manager of Lanka Electricity Company Private Limited

# Analysis of the Behaviour of Improved Soil under Shallow Concrete Foundations

SYW Liyanage<sup>1</sup> and KHSM Sampath<sup>2#</sup>

<sup>1</sup> Department of Civil and Construction Engineering, University of Wolverhampton, Malabe, Sri Lanka

<sup>2</sup> Department of Civil Engineering, University of Moratuwa, Sri Lanka

# sampathkh@uom.lk

**Abstract:** As a step towards sustainability and environmental protection, use of waste material and by-products in construction activities is becoming a trend. Quarry dust is a waste product of stone crushing process, which can be effectively used as a shallow ground stabilizer. This research investigates the behaviour of improved soil under a shallow foundation, by adding various mix proportions of quarry dust to the natural weak soil. Further, based on the foundation stability analysis, determining an optimum proportion of soil + quarry dust mix is studied. This is done by numerically analysing the displacement, shear strength, stresses, strains, and safety factors of stabilized soil underneath a shallow foundation. The study confirms that mixing quarry dust with natural weak soil - layered under a shallow foundation can significantly improve the stability of the respective foundation. This is due to the improvement of soil shear strength parameters, i.e., cohesion and friction angle, which are used for the stability analysis in the numerical model – incorporating the Mohr-Coulomb failure criterion. Further, it can be concluded that the optimum quarry dust mix proportion that yields the highest factor of safety of the foundation is around 60% - 80%, in which further increase in quarry dust % can cause reduction in the stability, due to unbalanced effect of cohesion and friction angle of mixed soil. Overall, the study concludes that mixing quarry dust with natural weak soil can be considered as a better ground improvement technique; however, the optimum mix proportion has to be determined

after a careful analysis of the the specific soil types, ground conditions and the applied loads.

**Keywords:** Ground stabilization, Quarry dust, Shear strength, Shallow foundation

## 1. Introduction

In the field of Civil Engineering, in certain instances, it is necessary to deal with the improvement of soil, because the in-situ soil properties are not always adequate for the desired construction. The main objective of soil improvement is to improve the engineering performance of the ground and make use of it according to specific requirements. There are several techniques to improve soil, based on construction activity and the type of soil. Some of the most common improvement techniques are soil compaction, vibration methods, re-compression, consolidation, grouting and injection, chemical stabilization, soil reinforcement, use of geo textiles and geo membranes (Kumar and Birdar, 2014; Burland, 1990).

Out of these methods, stabilization of soil by mixing with a foreign material prior to foundation construction is quite important. This method is commonly used in the form of quarry dust, lime, cement, fly ash and sometimes by combining few of above-mentioned forms. These forms help to improve the shear strength of the soil, while increasing its bearing capacity and decreasing settlements, which are essential properties for

the stability of a foundation (Caraşca, 2016). The current research focuses on quarry dust as the mixing material to improve the characteristics of natural soil, in which the stability of shallow foundations lying on the improved sub soil layer is studied.

The main reason for choosing quarry dust as the mixing component is that it can be easily obtained through crushers and quarries because quarry dust is a by-product of crushing process (Soosan et al., 2001). The use of quarry dust instead of sand is healthy for the ecosystem, as well as it helps to reduce the cost in the construction field (Marr, 1999). Since the particle size of quarry dust is similar to that of sand, it yields more or less same improvements in mixed soil characteristics, but at a lower cost (Akter et al., 2018). Hence, by adding quarry dust to the natural soil at a certain mix proportion, it is possible to improve soil strength and compaction characteristics, and therefore guarantee the stability of the structures built on it (Onyelowe, 2010; Prakash and Rao, 2017)

In most cases, foundations are constructed using concrete, which in turn creates soil-concrete interfaces at boundaries. The shallow footings fail mainly due to the failure of the soil layer on which the footing is placed. When the load of the superstructure gets transferred to the soil below the footing, it is displaced from its position due to the shear failure of soil as well as ground settlements (Ramads et al., 2010). These types of failures can be duly taken care by improving the engineering properties of the weak soil. Although several studies are conducted on investigating the ground improvement techniques, the behaviour of a shallow foundation and the resultant stability variations on quarry dust - based stabilized soil are not much studied. This behaviour can be varied with different influential factors, especially the characteristics of the mixing material and the mixing proportions.

In this study, an extensive finite-element analysis is carried out using PLAXIS-2D

software to comprehensively analyse the stability of shallow foundations lying on improved soil. In fact, the study mainly focuses on the improvement of ground when the sub surface weak soil is mixed with different mix proportions of quarry dust. Important factors pertinent to shallow foundation stability such as total displacements, extreme principal strain, and shear strain, mean and deviatoric stresses and factor of safety values are analysed to assess the stability. Further, the optimum soil: quarry dust mix proportion that yields the highest factor of safety of the shallow foundation under given *in-situ* and loading conditions is assessed through the analysis.

## 2. Research Methodology

### A. Collection of Data

The collection of data for the numerical analysis is done through a rigorous literature review. Properties of quarry dust and natural soil used for the current analysis are tabulated in Table 1 and Table 2, respectively (Sridharan et al., 2006). The soil used for the analysis is basically a dried marine clayey soil as it has very less shear strength in its natural form. The failure criterion of the model was assessed with Mohr-Coulomb material model, which incorporates the cohesion and friction angle values to define the shear strength of soil. The respective shear strength parameters of stabilized soil with different quarry dust mix proportions used in the analysis are shown in Table 3 (Sridharan et al., 2006).

Table 1. Properties of chosen quarry dust sample (Sridharan et al., 2006)

Properties	Quarry Dust
Grain size distribution	
Coarse (2.0 - 4.75 mm) %	8.0
Medium (0.425 - 2.0 mm) %	34.1
Fine (0.75 - 0.425 mm) %	44.1

Silt size (0.002 – 0.075 mm)%	13.9
Clay size (< 0.002 mm)%	0
Uniformity coefficient ( $C_u$ )	11.1
Coefficient of curvature ( $C_c$ )	1.0
Specific gravity	2.80
Optimum Moisture Content (%)	12.6
Maximum Dry Density ( $kN/m^3$ )	19.1

Table 2. Properties of chosen soil type (Sridharan et al., 2006)

Properties	Soil Sample
Grain size distribution	
• Coarse (2.0 - 4.75 mm) %	0
• Medium (0.425 - 2.0 mm) %	5.1
• Fine (0.75 - 0.425 mm) %	23
• Silt size (0.002 – 0.075 mm)%	45
• Clay size (< 0.002 mm)%	21
Liquid limit (%)	73
Plastic limit (%)	36
Plasticity Index (%)	37
Shrinkage limit (%)	21
Specific gravity	2.62

Table 3. Shear strength characteristics of stabilized soil with different quarry dust mix proportions (Sridharan et al., 2006)

Quarry dust mix proportion (%)	Cohesion - C (kPa)	Friction Angle - $\phi$ (°)
0	20	15
20	18	19
40	15	26
60	13	30
80	11	35
100	6	43

### B. Finite Element Method (FEM)

The model designed in the study is a shallow foundation with 4 m width, sitting on a weak marine clay soil layer. The weak soil layer has a thickness of 2 m and laid on top of the bottom dense sand layer with a thickness of 5 m (see figure 1 (a)). The objective is to test the behaviour of foundation, when the top 2 m layer is improved with different quarry dust mix proportions. This is done by analysing total displacement, shear behaviour and factor of safety, in which the strength parameters of weak soil layer are varied with the experimental data given in section II (A). This will assist in analysing the effect of different quarry dust mix proportions on the stability of the foundation.

A 2-D plane-strain analysis was carried out, where the soil layers were modelled with Mohr-Coulomb material model, during which the cohesion and friction angle values of the topmost 2 m thick layer is systematically varied according to experimental data given in Table 3. This is to simulate the stabilized soil properties under different soil: quarry dust mix proportions. The shallow concrete foundation was modelled with a non-porous linear elastic model. In general, the numerical analysis was carried out as a sensitivity analysis, in which only the strength parameters of the top 2 m weak soil layer were varied, while all the other parameters are fixed. This enables the direct analysis and

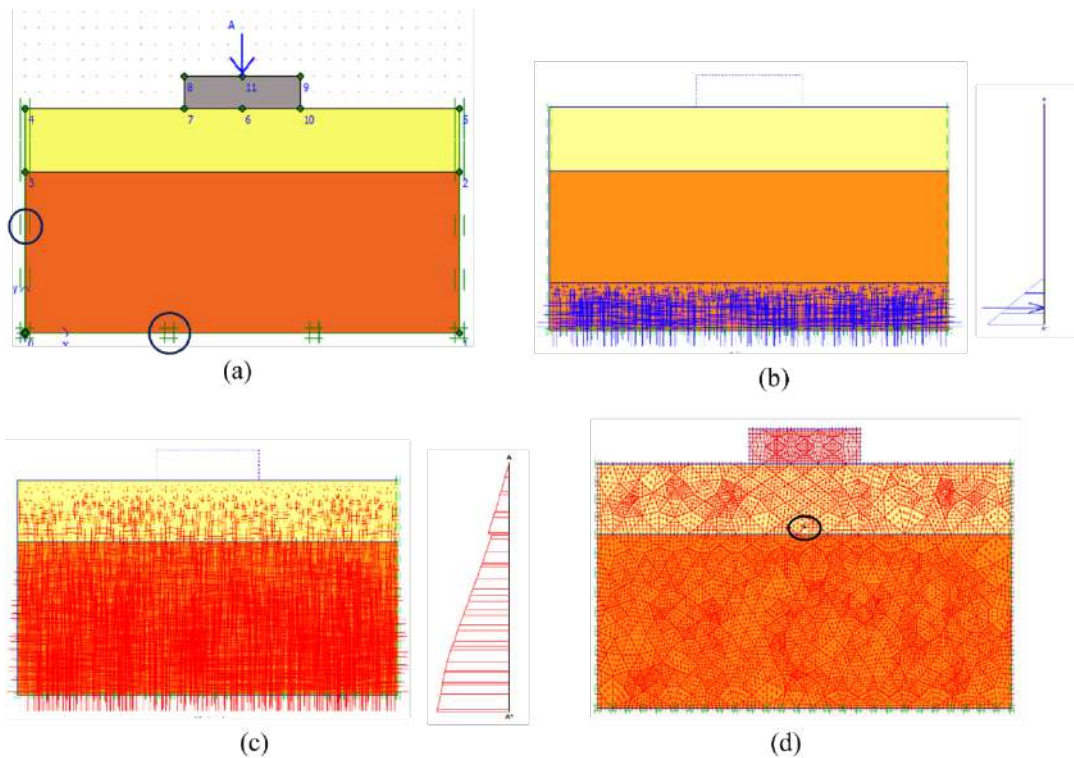


Figure 14. Development of the 2D numerical model

comparison of the effect of strength variation of stabilized topsoil layer on the shallow foundation. As shown in figure 1 (a), the vertical boundaries were restricted from moving to horizontal direction, allowing the simulation of vertical settlements, whereas the bottom horizontal boundary was restricted in moving in both vertical and horizontal directions. The effect of water table was not considered in the current study, in which the phreatic line was defined well below the influence zone of the foundation as shown in figure 1 (b).

The analysis was carried out stepwise, where the 1) initial condition, 2) after construction of foundation and 3) after construction of superstructure (i.e., application of vertical loads) were simulated and the factor of safety values were assessed in each step. This kind of stage-wise analysis in fact enables the analysis of a practical construction sequence of a typical shallow foundation. The total stress distribution at the initial stage (i.e., before constructing the foundation) is illustrated in

figure 1 (c), and the point of interest located in the topmost soil layer is shown in figure 1 (d), which is used for the sensitivity analysis and direct comparison of model results.

### 3. Results and Discussion

#### A. Foundation settlement analysis

The foundation settlement analysis was done in all the three stages of the construction sequence of shallow foundation as explained in section II (B).

Figure 2 illustrates the variation of the reduction in total settlement (%) of the point of interest selected under the foundation (see figure 1 (d)), against the quarry dust mix proportion (%). This reduction was measured relative to the total settlement of foundation in natural soil, in order to highlight the settlement reductions at different quarry dust mix proportions of stabilized soil. Figure 3 shows the colour maps of total displacement of foundation at 0%, 60% and 100% of quarry



dust mix proportions, which clearly shows how the displacement of underlying soil layer occurred at different mix proportions of quarry dust. The results are displayed only for the final stage (i.e., after the application of vertical loads), which is the most critical stage for a shallow foundation construction, compared to intermediate stages, as it gives the highest settlements due to exerted high loads from the super-structure.

In fact, the total settlement includes both vertical and horizontal displacement components, in which the vertical displacement is predominant due to vertical settlement of the foundation upon the applied vertical load. It is evident that the total settlement reduces gradually up to 60 – 80% of quarry dust mix proportion and then increases back at the case of total replacement of weak soil with quarry dust. Therefore, the results convey the idea that in the sense of soil stabilization, the total replacement of natural soil with quarry dust is not always the best option under given in-situ conditions. However, at all the cases, the total settlement of stabilized soil remains less than that of natural weaker soil.

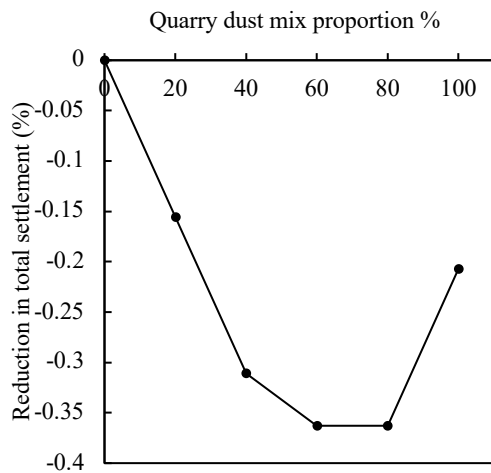


Figure 15. Reduction of the total settlement of shallow foundation with quarry dust mix proportions, relative to the settlement of natural soil.

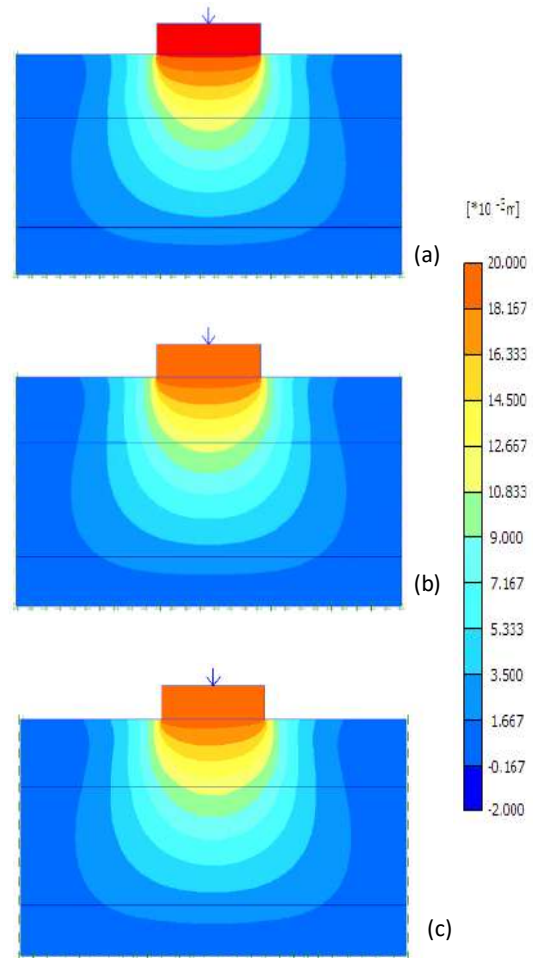


Figure 16. Colour maps of displacement after applying loads on the foundation (a) 0% quarry dust, (b) 60% quarry dust, (c) 100% quarry dust

### B. Factor of Safety (FOS) analysis

Application of loads on the foundation, if not the load exerted from the super-structure always increases with the finishing work at the latter stages of the construction project. Also, after completing the construction work, the super-structure loads increase substantially with the addition of both live and dead loads. Therefore, analysis of the factor of safety of the foundation after the application of service loads is critical. The infrastructure should in fact serve the purpose without failure during its serviceability period.

The factor of safety analysis was carried out for stages 2 and 3, as described in section II (B), and the values were directly compared, in

order to highlight the importance of considering a proper construction sequence (see figure 4).

As illustrated in figure 4, the factor of safety values were heavily affected after the application of loads on the foundation. In fact, the factor of safety values of the natural weak soil at the 1<sup>st</sup> phase and 2<sup>nd</sup> phase are 5.932 and 1.523, respectively, where the reduction is almost 74%. This proves the impact of the applied load towards the safety factors which is one of the main components when it comes to the design process of the foundation. The deviation of 4.409 of the factor of safety value highlights the importance of soil improving and the importance of the level of the improvement.

If the variation of factor of safety with quarry dust % is considered in detail, similar to previous analyses, the factor of safety value increases with the increasing quarry dust mix proportion. The increment has “invert U-shape” behaviour, where the 60% - 80% mix proportion yields the highest possible factor of safety. The further increment of quarry dust causes reduction in factor of safety – conveying a slight reduction in the soil strength, compared to the 80% case. Hence, the analysis suggests that there exists an optimum percentage of quarry dust to be mixed with the natural soil, that yields the highest stability of a shallow foundation.

This is basically due to the variation in soil strength parameters used for the strength analysis, i.e., cohesion and friction angle. In fact, according to Mohr-Coulomb material model, the shear strength of soil is governed by the combination of both cohesion and frictional angle (see Eq. 1).

$$\tau_f = c' + \sigma' \tan\phi' \quad [1]$$

where,  $\tau_f$  is the shear strength of soil,  $c'$  is the effective cohesion of soil,  $\sigma'$  is the effective normal stress and  $\phi'$  is the effective friction angle of soil.

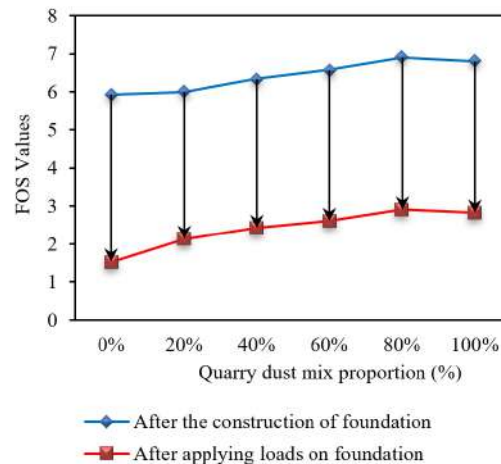


Figure 17. Variation of Factor of Safety of shallow foundation with quarry dust mix proportion, at different stages of construction.

The addition of sandy type quarry dust to the natural weak soil increases its friction angle due to high friction between sharp angular particles of quarry dust. This is the main reason for the initial rapid increment of foundation stability up to 60% of quarry dust mix proportion. In contrast, this simultaneously reduces the cohesion of the mixed soil, as the addition of large quantity of cohesion-less material (i.e., quarry dust) into clayey soil would hinder the cohesive nature of the mixed soil. This imbalance of two strength components will in turn affect the overall shear strength of the resultant mixture.

Hence, the combined variation in the strength parameters ultimately yields an optimum mix proportion, that can be used for the highest stability of the foundation. Hence, it is evident that fully replacement of soil with quarry dust is not the best option in all cases, but there exists an optimum mix proportion that results in the highest stability, with a lesser cost.

#### 4. Conclusion

The current study presents a numerical analysis of the effect of quarry dust on the geotechnical properties of selected weak soil and the resultant effect on the stability of a

shallow foundation. Following conclusions were made based on the findings of the study.

- With increasing quarry dust percentage in the mix, the cohesion of the mixed soil tends to decrease while the friction angle increases, which lead to observe a non-linear variation in the resultant shear strength and thus the behaviour of shallow foundation.
- In fact, the increase of quarry dust proportion in weak soil up to a certain percentage reduces the settlement while increasing the factor of safety of a shallow foundation. According to the current numerical results, the best improvement in stabilized soil in terms of displacement (i.e., settlement) is noticed at 60% - 80% and the highest factor of safety value was noted at 80% mix proportion. However, the factor of safety tends to slightly decrease when the natural soil is completely replaced by the quarry dust – i.e., at the 100% quarry dust mix proportion.
- This is basically due to the combined effect of cohesion and friction angle of stabilized soil, in which the imbalanced contribution of each component (i.e., from natural soil and quarry dust) has resulted in a slightly lower shear strength, yielding a lower factor of safety value.
- Hence, it is evident that fully replacement of soil with quarry dust is not always the best option but it has to be evaluated through a rigorous analysis.

Although, the optimum soil + quarry dust mix proportion is obtained as 60% - 80% in the current analysis, the proportion can be varied with many factors such as in-situ soil properties, quarry dust properties, ground condition, type of structure and the applied load. Hence, a detailed analysis should be carried out considering all the influential parameters, before deciding the optimum quarry dust percentage for a given construction.

Although, the conclusions are replicated in the experimental analysis found in literature, the most important aspect of shallow foundation design (i.e., factor of safety) has to be critically evaluated to assess the level of stability of the foundation. Hence, this study confirms that the stability level varies with the soil+quarry dust mix proportion and should be analysed in detail considering the given situation, incorporating experimental, numerical and analytical assessments.

## References

- Akter M. S., Jamal M., Ali M. F. and Ahmad N., 2018. 'Effect of Quarry Dust on Different Properties of Soil'. *i-Manager's Journal on Future Engineering and Technology*, 13(4), p.14.
- Burland J. B., 1990. "On the compressibility and shear strength of natural clays". *Géotechnique*, 40(3), pp.329-378.
- Caraşca, O., 2016. "Soil improvement by mixing: techniques and performances". *Energy Procedia*, 85, pp.85-92.
- Kumar A. and Biradar K., 2014. "Soft subgrade stabilization with quarry dust-an industrial waste". *International Journal of Research in Engineering and Technology*, 3(08), pp.409-412.
- Marr W. A., 1999. "Effective uses of Finite element analysis in Geotechnical Engineering". *Civil Engineering Practice-Boston*, 14(2), pp.89-98.
- Onyelowe Ke C., Okafor F. O. and Nwachukwu D., 2010. "Geophysical use of quarry dust (as admixture) as applied to soil stabilization and modification-a review". *ARP Journal of Earth Sciences*, 1(1), pp.6-8.
- Prakash K. S., Rao C. H., 2017, "Strength characteristics of quarry dust in replacement of sand". In *IOP Conference Series: Materials Science and Engineering* (Vol. 225, No. 1, p. 012074). IOP Publishing.

Ramadas T. L., Kumar N. D. and Aparna G., 2010, "Swelling and strength characteristics of expansive soil treated with stone dust and fly Ash". In Indian geotechnical conference-2010, GEOTrendz (pp. 16-18).

Soosan T. G., Jose B. T. and Abraham B. M., 2001. "Improvement of ground and highway sub-bases using quarry waste". Proceedings of international seminar on civil engineering,, 730-737.

Sridharan A., Soosan T. G., Jose B. T. and Abraham B. M., 2006, "Shear strength studies on soil-quarry dust mixtures". Geotechnical & Geological Engineering, 24(5), pp.1163-1179.

# Improving Turbidity Removal Efficiency in Slow Sand Filter during the Occurrence of High Turbidity Levels in Surface Water

N Anoja<sup>1</sup>, ME Sutharsan<sup>1</sup> and S Sarankan<sup>1#</sup>

<sup>1</sup>National Water Supply & Drainage Board, Sri Lanka

#edsutharsan@yahoo.com

**Abstract:** *The prominent drinking water treatment process practised to eliminate turbidity from surface water, especially during high turbidity occurrence in the surface water, is coagulation, sedimentation and rapid sand filtration for many years. However, the possibility of turbidity removal using a slow sand filter (SSF) was not extensively studied in the case of high turbidity occurrence in the surface water. This study aimed to evaluate the performance of SSF in terms of turbidity removal in surface water, when pre-adding poly-aluminium chloride (PACl) as a coagulant chemical along with the pre-treatment by roughing filter. One per cent of PACl is prepared and dosed at the rate of 20 mg/L with raw water into the water intake chamber before it reaches the SSF. The raw and treated water samples were collected every six-hour intervals. The raw water samples whose turbidity level more than 50 NTU were considered and analysed from 174 nos of trails. Turbidity level of raw water and filtered water was observed in the range of 50-313 NTU and 0.31-5.5 NTU respectively. The turbidity of treated water by SSF was observed to be well below the SLS 614;2013 acceptable limit of 2 NTU in 98.8% of the treated samples. It is observed the turbidity removal efficiency increases when the raw water turbidity level increases. The result shows turbidity of treated water from SSF was complying with the requirement in 98.5% of the trails, which enable the proper function of treatment plant during the high raw water turbidity by complying with SLS 614-2013 when adopting this methodology.*

**Keywords:** *Drinking water, Poly-aluminium chloride, Surface water treatment, Turbidity removal*

## 1. Introduction

There are many natural resources on the planet and water is one of them. Water is one of the basic needs not only for humans but also for plants, wildlife and other animals. In addition, the requirement of water as raw material is inevitable for all sorts of products in the industrial era. Hence, the contribution made by water to a country's economic development is huge in the present context. Though water is a basic human right, people over 785 million do not have access to basic drinking water facilities. Globally, it is estimated that over 2,000 million people consume drinking water from the faeces' contaminated water sources. Further, it is forecasted half of the world's population will be in water stress regions in another 5 years according to World Health Organization (World Health Organization, 2017).

There are many levels of water treatment available and practised at present. Household-level, community level and domestic level are the types of water treatment systems commonly available systems. The slow sand treatment method is adopted on all levels and this method can be applied even in the household level water treatment. A slow sand filter (SSF) was originally established by John Gibb, in Scotland (Ellis, 1987). The main advantages of SSF over the other filters are less energy requirement and cost-effective, which can be functioned well with minimal or no dependency on workman force and chemicals. SSF is one of the sustainable water treatment processes. In general, the physical, biological and chemical processes function together in

the removal of contaminants and other impurities from the raw water. Many developed countries such as Japan, Scotland and Netherlands are using SSF as a solution to treat water (Anggraini and Fuchs, 2019).

The extent to which suspended solids in water scattered or absorbed the light is termed turbidity. Nevertheless, the relationship between suspended solids and turbidity in terms of quantitative is not yet proven. The sunlight penetration is resisted by the high turbidity existence in water, which affects the process of photosynthesis. The clarity of water can be discussed in terms of the turbidity level. The transparency or clarity of the water is affected by the suspended solids and colour presence of water. There are many reasons for the suspended solid existence in water such as decayed vegetation, fungi, slit, and algae, which lead to delivering high turbidity in water. The quality of drinking water is judged by various parameters and turbidity is one of them (Agrawal, Sharma and Sharma, 2020). The famous treatment process practised to eliminate or reduce turbidity is coagulation, sedimentation and rapid sand filtration, by the water supply engineers. Many SSF pilot studies have been done by researchers using plastic and concrete materials for the frame and different graded gravel and sand as filter media in layers in the past. There are several factors mainly, water source features, temperature, hydraulic retention time, surface area, filtration rate, and filter media size influencing the design and the performance of the SSF. However, filter media grain size and depth control the efficiency of the water treatment (Anderson et al., 2009).

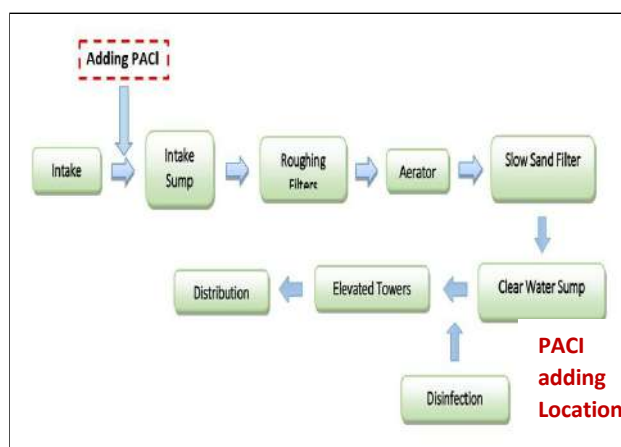


Figure 1. WTP layout and PACl mixing location

Different types of filter operations such as slow filter operation and fast filter operation were used with fine and coarse sand filter media by Ellis during his study in 1985. It was recorded that 60-65% removal of suspended solids and 70-75% removal of BOD5 in the study when using slow filter media (Ellis, 1987). Many findings suggest the SSF method can be used to treat different types of water and wastewater. In addition, drinking and wastewater treatment efficiencies of SSF have been about 99% for removal of turbidity, pathogens and suspended solids up to 99% is recorded as the efficiency of wastewater and drinking water SSF (Haarhoff and Cleasby, 1991). The prominent drinking water treatment process practised to eliminate turbidity from surface water, especially during high turbidity occurrence in the surface water, is coagulation, sedimentation and rapid sand filtration for many years. The efficiency and the function of SSF to treat drinking water, in the case of high turbidity occurrence in the surface water, when adding the pre-oxidation chemical have not been thoroughly studied, even though there was advanced development in the SSF techniques. Hence, the objective of the present study is to evaluate the performance of SSF in terms of turbidity removal from raw water when adding coagulant chemicals.

## 2. Materials and Methods

The water intake, PACl mixing point and treatment process are exhibited in Figure 1. Figure 2 shows that when the amount of rain exceeds the threshold limit, turbidity shows an upward trend and when the amount of rainfall decreases, turbidity decreases. Right after the 60 mm/hr heavy rain on 25th November 2020, turbidity level of 111 NTU was recorded. The following day turbidity increases to 280 NTU. After the heavy rainfall of 90 mm/hr on 6th December 2020 turbidity level of 350 NTU was recorded. No rainfall occurred between December 8 and 12, hence the turbidity levels decreased to 55 NTU. It was found by analysis the existing data, there is a clear correlation between rainfall and turbidity of the Dry Aru.

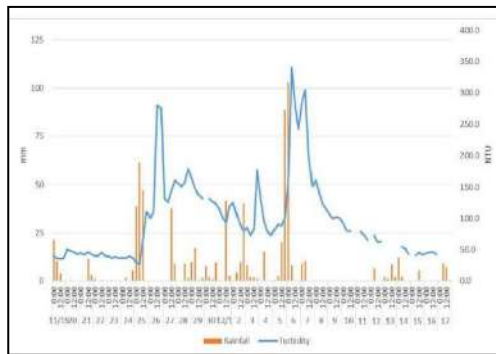


Figure 2. Rainfall vs Raw water turbidity level

The turbidity level of raw water generally satisfies this condition in the dry season. However, the record shows, that the turbidity of raw water increases to 100-350 NTU in the Kilinochchi water treatment plant during the rainy season, which resulted in stopping the plant's efficient operations. The treatment process of the Kilinochchi water treatment plant in Sri Lanka is pumping water from the intake to roughing filter to the aerator to SSF and finally to clear water ground sump. However, a new methodology was adapted and tested to the existing treatment process, by keeping the process as it is, encountering the threat of a higher level of turbidity in the raw water arises especially during the rainy season.

As per the WTP operation manual, raw water turbidity must be less than 30 NTU before entering into the slow sand filter to prevent clogging of the filter media of SSF (NWSDB, 1989). Therefore the methodology used was adding Poly Aluminium Chloride (PACl) as the coagulant chemical to activate the coagulation process from which the suspended solid particle can efficiently form clogs within a short period and be removed through the various filtration process.

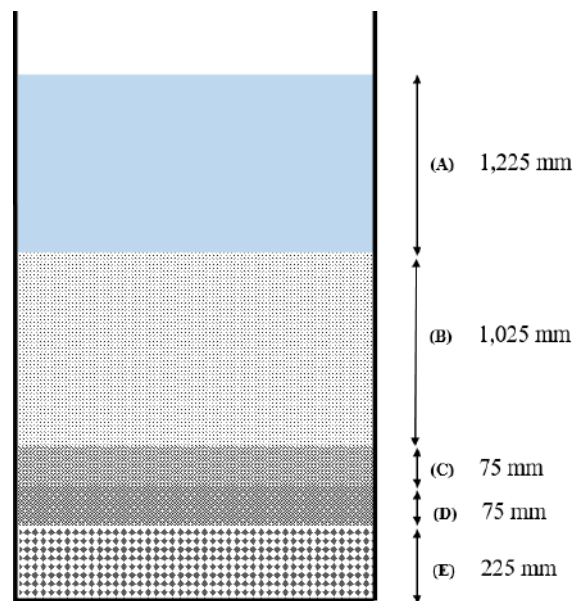


Figure 3. Cross-section of SSF

Where;

- (A) Water column over the filter media
- (B) Filter media sand layer
- (C) Filter gravel layer 1
- (D) Filter gravel layer 2
- (E) Filter gravel layer 3

Figure 4: Fine aggregates and gravels as filter media



A jar test conducted to choose the suitable chemical coagulant among alum and poly-aluminium chloride and to estimate minimum coagulant dose required to achieve certain water quality goals. Based on the findings from the jar test, one per cent (1%) of PACl was prepared and dosed at the rate of 20mg/L. The prepared solution was mixed with raw water into the water intake chamber before it reaches the roughing filter as shown in Figure 1. In addition, the inlet structure of roughing filter was modified to improve the mixing of PACl with raw water. The experiment was carried out for the water inflow rate maximum of 2000 m<sup>3</sup>/day. The filter media in SSF placed were 1025 mm thick layer of fine sand with a uniform coefficient of 1.78 and effective size of 0.32 along with gravel with various particle sizes of 5-9 mm, 5-16 mm, and 9-62 mm with a layer thickness of 75, 75, and 225 mm respectively as shown in Figure 3 (not to scale). The water depth over the filter media was 1,225 mm approximately.

Figure 4 shows the coarse and fine aggregates which have been placed in SSF as the filter

media. The turbidity level of raw water and the treated water from SSF were measured every six-hour intervals for one year. The turbidity is measured and analysed for 174 nos of trails. Turbidity was measured by a 2100Q turbidity meter at the site laboratory located in the water treatment plant site.

### 3. Results and Discussion

As representative test results, Figure 5 shows turbidity in raw water and treated water from a slow sand filter (SSF) when adding PACl as the coagulant agent in the intake chamber, with elapsed time obtained when the raw water turbidity exceeds the limit of 50 NTU. The raw water, before sending to SSF, generally be less than 30 NTU to prevent clogging of slow sand filter media (NJS Consultants Co., 2019)

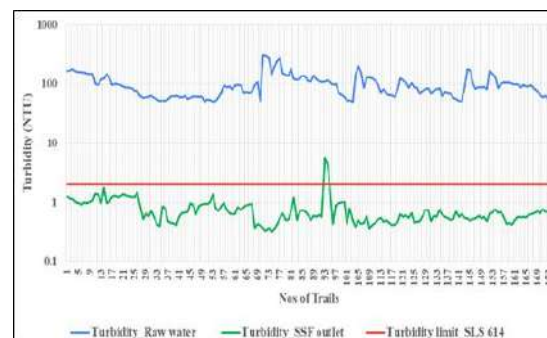


Figure 5. Comparison of turbidity in raw water and treated water

The result illustrates that the turbidity is removed significantly by the proposed methodology of with pre addition of PACl with raw water and with the pre-treatment and filtration by SSF. The turbidity of treated water by SSF was observed to be well below the SLS 614;2013 (SLSI, 2013) acceptable limit of 2 NTU in 98.8% of the treated samples when applying this method. Turbidity of raw water during the testing period by varying in the range of 50-313 NTU, whereas turbidity of the filtered water from SSF was observed between 0.31-5.5 NTU. The turbidity removal efficiency was calculated by using equation 1.



$$\text{Efficiency (\%)} = \frac{(\text{Influent Concentration} - \text{Effluent Concentration})}{\text{Influent Concentration}} \times 100 \quad (1)$$

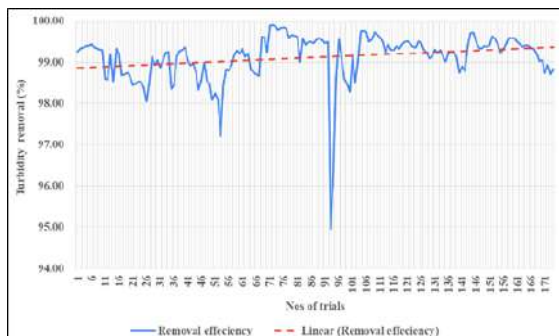


Figure 6. Turbidity removal efficiency vs trails

Figure 6 indicates that 171 out of 174 samples were observed to be above 98.5% efficiency in removing the turbidity. Further, there is a correlation observed between the time and the turbidity removal efficiency, where the efficiency increase with the days of operation. In a previous study, the same methodology was assessed through a prototype model of the same water treatment plant and turbidity removal efficiency found to be 82% and it was increasing with the increasing turbidity of the inlet water to the SSF. Consequently, the present study records the average turbidity removal efficiency of SSF as 98.5%.

In addition, it was recorded in a previous study that, a long operation of water treatment plant increased the turbidity removal efficiency (Jenkins, Tiwari and Darby, 2011). Further, it is also recorded that, drinking and wastewater treatment efficiencies of SSF have been about 99% for of removal of turbidity, pathogens and suspended solids up to 99% is recorded as the efficiency of wastewater and drinking water SSF (Haarhoff and Cleasby, 1991) and the findings are very much closer to the findings of the present study.

The turbidity removal efficiency by using this method was compared against the turbidity level of the raw water and plotted in figure 7. A positive correlation was observed between

removal efficiency and turbidity level of raw water. The turbidity removal efficiency increases when the raw water turbidity level increases.

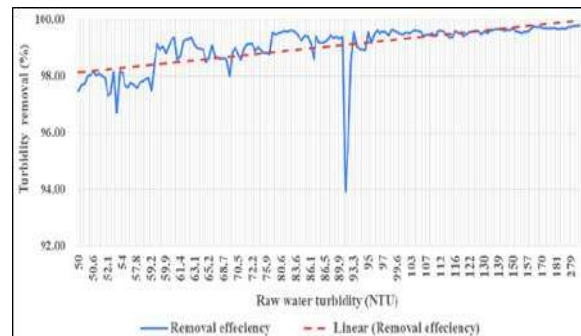


Figure 7. Turbidity removal efficiency vs raw water turbidity level

#### 4. Conclusion

The research objective was to evaluate the performance of slow sand filter (SSF) in terms of turbidity removal when pre-adding poly-aluminium chloride (PACl) as coagulating chemical for treating the surface water to supply potable water. The past year's records show the WTP stops its operation when raw water turbidity is high, especially during the rainy season. The result illustrates that the turbidity is removed significantly by adopting this methodology. It can be observed that the treated turbidity level is well below the threshold limit of 2 NTU, specified in SLS 614;2013 for drinking water, in most of the trails when using this method. The turbidity removal efficiency was observed to be increased with the days of operation. Further, the efficiency in turbidity removal by SSF increases when the raw water turbidity level increases. This method is very efficient and shall be applied as the solution for turbidity treatment for the higher turbidity issues in surface water in any potable water supply system.

#### References

Agrawal, A., Sharma, N. and Sharma, P. (2020) 'Designing an economical slow sand filter for

households to improve water quality parameters', *Materials Today: Proceedings*, 43, pp. 1582–1586. Available at: <https://doi.org/10.1016/j.matpr.2020.09.450>

Anderson, W.B. et al. (2009) 'Influence of design and operating conditions on the removal of MS2 bacteriophage by pilot-scale multistage slow sand filtration', *Journal of Water Supply: Research and Technology-Aqua*, 58(7), pp. 450–462.

Anggraini, A.K. and Fuchs, S. (2019) 'Influence of Gravel as Protection Layer on the Filter Run Time', *Teknik Sipil*, 15(1), pp. 56–60.

Ellis, K. V (1987) 'Slow sand filtration as a technique for the tertiary treatment of municipal sewages', *War. Res*, 21(4), pp. 403–410.

Haarhoff, J. and Cleasby, J. (1991) *Biological and physical mechanisms in slow sand filtration. Slow sand filtration*, American Society of Civil Engineers. New York.

Jenkins, M.W., Tiwari, S.K. and Darby, J. (2011) 'Bacterial, viral and turbidity removal by intermittent slow sand filtration for household use in developing countries: Experimental investigation and modeling', *Water Research*, 45(18), pp. 6227–6239. Available at: <https://doi.org/10.1016/j.watres.2011.09.022>.

NJS Consultants Co., L. (2019) *Operation and Maintenance Manual (Final Version, Rev.1)*. Kilinochchi.

NWSD (1989) *Design Manual D3, Water Quality and Treatment*. Colombo.

SLSI (2013) *Specification for Potable Water, SLS 614: 2013*. Colombo. Available at: <https://doi.org/10.1016/b978-0-444-59395-5.00011-x>.

World Health Organization (2017) *Guidelines for Drinking- Water Quality: First Addendum to the Fourth Edition*. Switzerland. Available at:

<https://www.who.int/publications/i/item/9789241549950>.

## Acknowledgment

The authors wish to acknowledge the assistance given by the Jaffna region of the National Water Supply and Drainage Board during this study.

## Author Biography



Ms. Anoja Niroshan graduated from the University of Sri Jayawardenapura with B.Sc (Hons.) in food science & technology with first class and poses a post-graduate degree M.Sc (Env) from OUSL. She is a member of the Institute of Chemistry, Sri Lanka. She is working as a Senior Chemist in the National Water Supply and Drainage Board, Sri Lanka at present.



Eng. M.E.Sutharsan is a Chartered Engineer, who graduated from the University of Peradeniya with a B.Sc (Hons.) in civil engineering with the second upper class and poses a post-graduate degree MBA from RUSL. He is a member of the Institute of Engineers, Sri Lanka (IESL). He is working as Chief Engineer in the National Water Supply and Drainage Board, Sri Lanka



Eng. S.Sarankan is a Chartered Engineer, who graduated from the University of Peradeniya with a B.Sc (Hons.) in civil engineering and poses a post-graduate degree in Executive Master in Management of Urban Water & Sanitation Service (France) and PGDip in Water Resource Engineering & Management. He is a member of the Institute of Engineers, Sri Lanka (IESL). He is working as Senior Engineer in the National Water Supply and Drainage Board, Sri Lanka.

# Study of Issues in Sludge Disposal and Management in Wastewater Treatment Plants

EMS Anuththara<sup>1</sup> and MB Samarakoon<sup>2#</sup>

<sup>1</sup>Department of Civil Engineering, General Sir John Kotelawala Defence University, Ratmalana, Sri Lanka

<sup>2</sup>Department of Civil Engineering, General Sir John Kotelawala Defence University, Ratmalana, Sri Lanka

#sanjaniekanayake@gmail.com

**Abstract:** *Improper methods of treatment, disposal and management of sludge generated by wastewater treatment plants has become a major environmental issue at present. This research focuses on identifying the environmental impact cause by the methods used when disposing and reusing the produced sludge as fertilizer, by the Biyagama CWWTP, Ratmalana/ Moratuwa WWTP, Ja-Ela/ Ekala WWTP and Raddolugama sewerage treatment plant. The sludge samples collected from the dumpsites were tested for heavy metals, nutrients, and organic compounds present in it. After analyzing the constituents present in the sludge, the issues in respective treatment plants and its procedures were identified. Moreover, the possibility of using the sludge as construction material, fertilizer and whether it satisfy the requirements to use as a fertilizer for crops cultivated for human consumption were discussed. In addition, a model limitation scale for the sludge standards was introduced through this study after observing various limitations maintained in other international standards. As per the results, only sludge from Raddolugama Plant was assured as safe for land application and sludge in Biyagama plant was found to be the most suitable for fertilization among the others although other minor hitches were found. Conclusively, ecofriendly and sustainable solutions were suggested to improve the sludge qualities and overcome the issues found and proposed how sludge could be utilized for greater uses than wasting a valuable asset.*

**Keywords:** *Sludge, Wastewater treatment plant, Sludge Disposal, Sludge management, Sludge fertilizer, Heavy metal contamination*

## 1. Introduction

Sri Lanka is a developing or an emerging country with a lower middle income status (World Bank Country and Lending Groups – World Bank Data Help Desk, no date). Massive amounts of wastewater are produced as industry progresses and population growth increases demand for food and water. According to the Central Environmental Authority (CEA), Sri Lanka's main industrial parks produce about 30 million cubic meters of wastewater annually (Jayalal and Niroshani, 2007). After being properly treated in a Wastewater Treatment Plant (WWTP), the treated effluent must be properly disposed of. Depending on the wastewater constituents and the standards that must be met for each disposal method, the method of treatment and the chemicals used during the treatment process may differ.

Screening, grit removal, primary settling (coagulation and flocculation), activated sludge treatment, filtration, and disinfection are the most common phases in wastewater treatment.

Sludge is an inevitable by-product of water treatment, and it can get produced at any above mentioned stage, albeit the clarification stage is the main source of sludge production (Turovskiy and Mathai, 2005)(Anjithan, B C L

Athapattu, N Ratnayake, 2015). Sludge, which is categorized as an industrial waste, comes in a variety of forms, including slurry, semi-solid, and solid, depending on the coagulants and other chemicals used to treat it. Even while sludge is a nutrient-dense waste product, it also includes pathogens and heavy metals that can harm the environment if disposed of without first being treated. Sludge treatment and disposal can also be highly costly. As a result, finding environmentally safe and cost-effective sludge removal and management strategies has become critical in recent years. Sludge management is the process of reducing the amount of sludge that must be disposed of.

The most common sludge treatment methods are conditioning, thickening, dewatering, stabilization and disinfection, and thermal drying. After the treatment process, it is disposed to the environment. There are several disposal alternatives, which are currently in use. They are; land spreading, incineration, landfilling, discharging to water courses and use as a soil conditioner or fertilizer for agricultural use.

On the other hand, these processes for treatment and disposal could be harmful to the public's health and the environment. Raw sludge frequently contains toxic compounds like heavy metals, pathogenic microorganisms, organic pollutants, as well as nutrients, grease, and fat. These substances have the potential to disrupt the ecosystem and living things when they are introduced into natural soil or water bodies. Some experts have emphasized the most common dangers connected with employing sludge as a fertilizer or soil conditioner. They are the risks of atmospheric pollution from gases such as ammonia and nitrous oxide, nutrient pollution from excess nitrogen and phosphorus, and soil contamination from chemical or biological contamination (Rorat et al., 2019)(Nkoa, 2014). These toxic contaminations could even increase pre-existing environmental problems (Rorat et al., 2019).

With the aim of analyzing the adverse effects of improper disposal of sludge and proposing suitable disposal and management methods with minimum environmental impact, the Central Wastewater Treatment Plant (CWWTP) at Biyagama Export Processing Zone (BEPZ), Ratmalana/ Moratuwa Wastewater treatment plant, Ja- Ela/ Ekala Wastewater treatment plant at Ekala Industrial Zone and Raddolugama Sewerage treatment plant were selected for this study. Observing the current methods of disposal of sludge in these selected treatment plants to identify the wrong approaches followed in them and their effects on the environment, identifying the constituents of the produced sludge, introducing a scaling for limitations of sludge parameters suitable for Sri Lanka and to identify effective methods to reuse, disposal and management in sludge were the main objectives when conducting this research. In order to achieve these, sludge and water samples were collected from selected locations and were tested for different physical and chemical parameters. Then the results were analyzed comparatively with standard limitation for land application of sludge and reusability of sludge as a fertilizer and the recommendations were given accordingly.

## **2. Methodology**

### *A. Site Visitation and Collection of Data*

Biyagama CWWTP, which is situated in the Biyagama Export Processing Zone, is currently maintained by the NWSDB. BEPZ is split into two sections: Block A and Block B. Block A companies send their treated effluents to the CWWTP's aeration lagoons, whereas Block B industries discharge their effluents to the Oxidation ditch. However, enterprises must meet particular water quality requirements in order to be permitted to transport their wastewater to the CWWTP. The biological treatment at CWWTP is based on the activated sludge process. The produced sludge is then

solar dried and then used for land filling, fertilizer or dumped to dump yards.

The biological treatment method used by the Moratuwa and Ja-Ela WWTPs both involves recycling activated sludge. The squeezed sludge from the belt filter is solar dried in greenhouses while the final effluent is discharged into the Dandugam River and sludge is utilized for composting or landfilling.

Raddolugama sewerage plant, which was commissioned to treat the toilet and kitchen wastewater that is discharged from the Housing schemes in that area, undergoes the same biological treatment as in Moratuwa and Ja- Ela WWTPs. The final sludge is solar dried to use as a fertilizer.

#### B. Collection of Sludge Samples

From the Biyagama CWWTP, samples were collected from the lagoon inlet, oxidation ditch inlet, ditch settling tanks, ditch clarifier drying bed, settling tank outlets and flocculation pond. From the Moratuwa, Ja- Ela and Raddolugama Treatment plants, sludge samples from the Belt filter press were taken. For the purpose of comparison of the sludge quality over the time, some past sludge reports were also collected from the Moratuwa and Biyagama WWTPs.

#### C. Laboratory testing and Analysing Data

The collected samples were then sent to laboratories to get tested for parameters which consisted color, moisture, odour, sand content, pH, Nitrogen content (N), Phosphorus content (P<sub>2</sub>O<sub>5</sub>), Potassium content (K<sub>2</sub>O), Magnesium content (MgO), Calcium content (CaO), Organic carbon, C/N ratio, Heavy metals (Hg, Mo, As, Cd, Cr, Cu, Pb, Ni, Zn, Se), Salmonella and Coliform (E-coli).

For the testing of the sludge, standard methods such as APHA, CPSD- AN 00581, SLS 516, SLS 645, SLS 1246, USEPA methods, AOAC 999.10 (2012), AAS method were followed according to the respective parameters. As per these guidelines, the calculations were done to find the concentrations of each parameter.

$$\text{mg Ca/L} = \frac{A \times B \times 400.8}{\text{mL sample}}$$

$$\text{Calcium hardness as mg CaCO}_3\text{/L} = \frac{A \times B \times 1000}{\text{mL sample}}$$

where:  
*A* = mL titrant for sample and  
*B* = mg CaCO<sub>3</sub> equivalent to 1.00 mL EDTA titrant at the calcium indicator end point.

Figure 1. Example calculation of Ca concentration as per APHA3500 - Ca B method Source : (APHA, 2012)

For the analysis of the results to check whether the sludge parameters lie within the tolerance limits and whether the sludge from any WWTP pose any threat to the environment and the living organisms, most common codes that are used worldwide and in Sri Lanka were used. They were, European Standards (European Commission, Council Directive 86/278/EEC of 12 June 1986), SLS standards (Specification for compost from Municipal Solid Waste and Agricultural Waste), and US EPA standards (40 CFR Part 503).

### 3. Results and Discussion

#### A. Comparison of the Sludge Parameters and Their Concentrations

Based on graph above, it is evident that among the heavy metals studied, Zn and Cu have higher concentrations in 2021, while Mn has the highest concentration in 2020. Because the CWWTP only uses a biological treatment method, this could have been caused by a company sending pre-treated water to the CWWTP. This could be due to not adhering to the BOI tolerance limits while sending effluent to the CWWTP.

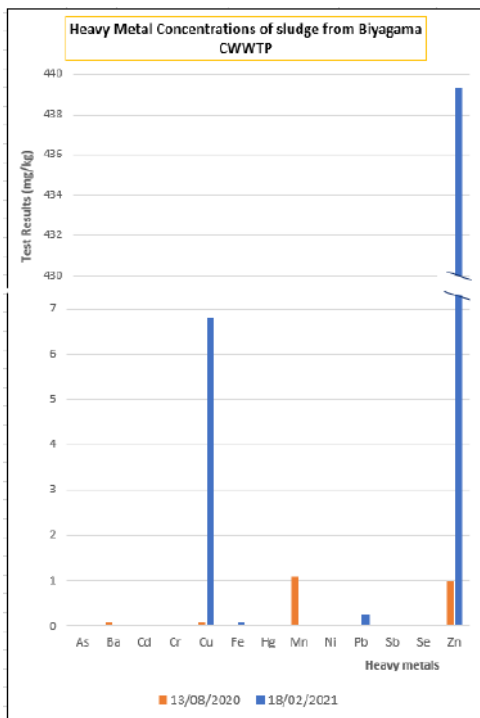


Figure 2. Heavy metal concentrations of sludge from Biyagama CWWTP

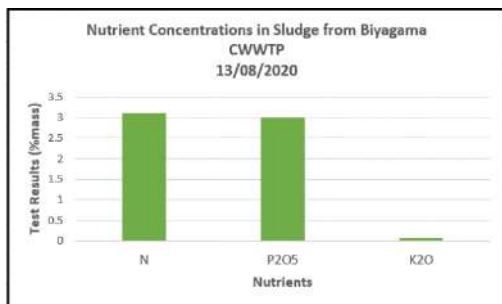


Figure 3. Nutrient Concentrations in sludge from Biyagama CWWTP dated 13/08/2020

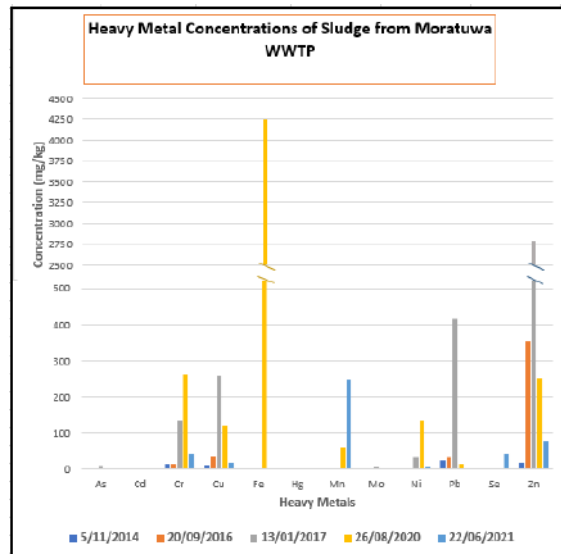


Figure 4. Heavy metal concentrations in sludge from Moratuwa WWTP

The most protruding element concentrations in this graph is displayed in the sludge sample dated at 26/08/2020. The iron contents have risen up to 4250 mg/kg. The sludge sample dated at 13/01/2017, also show some increase in the heavy metal concentrations compared to the other days. However, it is safe to say that the Moratuwa Plant has managed to decrease these parameters over the time, as of 22/06/2021 results show comparatively lower metal concentrations.

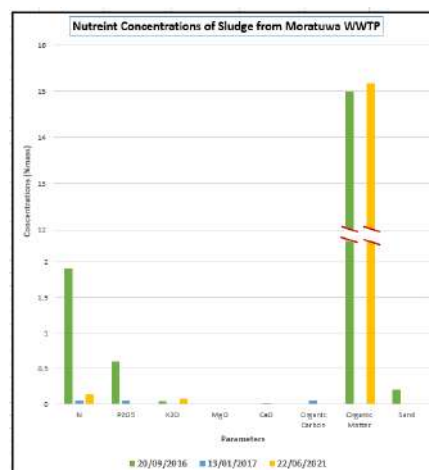


Figure 5. Nutrient concentrations of sludge from Moratuwa WWTP

Organic matter concentration in both 2016 and 2021 samples shows the peaks in those respective years.

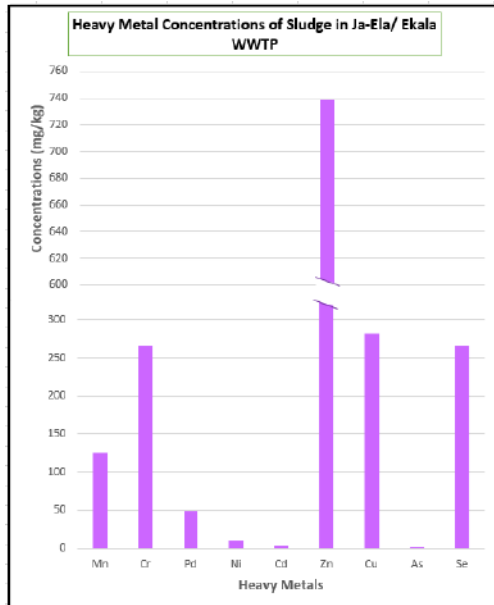


Figure 6. Heavy metal concentrations in sludge from Ja- Ela WWTP dated at 22/06/2021

The Zn level in the sludge sample has risen dramatically to 738.9 mg/kg, which could be attributable to the WWTP receiving extremely polluted industrial effluents or some factories exceeding the tolerance limits for industrial wastewater (effluents) discharged in to the common wastewater treatment plant, Biyagama.

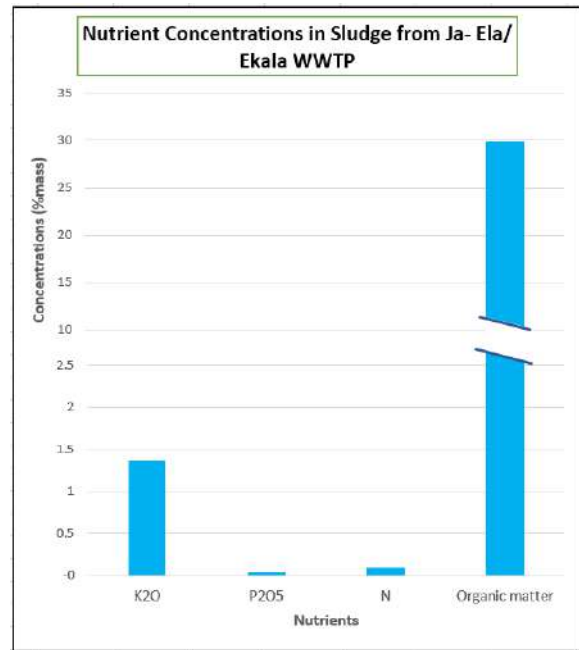


Figure 7. Nutrient concentrations of the sludge in Ja- Ela WWTP

The solar dried sludge sample from the Sewerage treatment facility suggests rather large quantities of Organic matter, as seen in the graph below. This is to be expected from a plant that handles domestic wastewater that has a high concentration of human excreta, food, and waste, among other things. It could also suggest that the treatment plant's efficiency in eliminating organic materials is low. Moratuwa WWTP sludge parameters show that the nutritional content of the sludge is lower than the SLS mandated limits. Although there is a noticeable improvement in the parameters as compared to previous Moratuwa WWTP reports. As a result,

Table 1. Comparison of sludge parameters with EU and EPA standards for suitability for land ap

Parameters	Test Results (mg/kg)									Standard Limitations (mg/kg)	
	Biyagama WWTP		Moratuwa WWTP					Ja- Ela/ Ekala WWTP	Raddolugama WWTP	EN Standards	EPA Standards (max)
	13/08/2020	18/02/2021	5/11/2014	20/09/2016	13/01/2017	26/08/2020	22/06/2021	22/06/2021	22/06/2021		
As	0.001	ND		3.6	7.1	<2.5	<2.0	<2.0	<2.0		41
Cd	ND	ND	ND	ND	2.9	0.8	<3.0	<3.0	<3.0	1 - 3	39
Cr	0.002	ND	13.4	14.2	133	262	44.1	265.1	63.6	1000	1200
Cu	0.1	6.81	11.9	37.7	259	120	17.2	282.0	11.5	50 - 140	1500
Hg	ND	ND	ND	1.8	ND					1 - 1.5	17
Mo					4.9						-
Ni		ND	3.2		35	134	<4.0	9.4	<4.0	30 - 75	420
Pb	ND	0.27	25.2	32.7	417	15	<2.0	48.8	<2.0	50 - 300	300
Se	ND				ND	2.5	44.1	265.1	63.63		100
Zn	1.0	439.33	17.0	353	2785	250	76.7	738.9	67.4	150 - 300	2800

Table 2. Comparison of sludge parameters with SLS and EU standards for suitability of the sludge generated from the WWTPs to use as a fertilizer for agricultural purposes

Parameters	Units	Test Results									Standard Limitations		
		Biyagama WWTP		Moratuwa WWTP					Ja- Ela/ Ekala WWTP	Raddolugama WWTP	SLS Standards	EN Standards	
		13/08/2020	18/02/2021	5/11/2014	20/09/2016	13/01/2017	26/08/2020	22/06/2021	22/06/2021	22/06/2021			
pH					6.7	5.8					6.5 - 8.5		
Organic Carbon	%mass				15	0.06		15.18	29.88	50.02	20	min	
Organic Matter	%mass				15	0.06		15.18	29.88	50.02			
N	%mass	3.1			1.9	0.06		0.15	0.09	0.31	1.0	min	
P <sub>2</sub> O <sub>5</sub>	%mass	3.0			0.6	0.058		0.01	0.04	0.02	0.5	min	
K <sub>2</sub> O	%mass	0.07			0.04	0.001		0.08	1.36	0.15	1.0	min	
MgO	%mass					0.012					0.5	min	
CaO	%mass					0.021					0.7	min	
As	mg/kg	0.001	ND		3.6	7.1	<2.5	<2.0	<2.0	<2.0			
Ba	mg/kg	0.1											
Cd	mg/kg	ND	ND	ND	ND	2.9	0.8	<3.0	<3.0	<3.0	10	max	20 - 40
Cr	mg/kg	0.002		13.4	14.2	133	262	44.1	265.1	63.6	1000	max	-
Cu	mg/kg	0.1	6.81	11.9	37.7	259	120	17.2	282	11.5	400	max	1000 - 1750
Fe	mg/kg	0.02	<0.1				4250						
Hg	mg/kg		ND	ND	1.8	ND					2	max	16 - 25
Mn	mg/kg	1.1					63	249.5	125.9	385.6			
Mo	mg/kg					4.9							
Ni	mg/kg		ND	3.2		35	134	<4.0	9.4	<4.0	100	max	300 - 400
Pb	mg/kg	ND	0.27	25.2	32.7	417	15	<2.0	48.8	<2.0	250	max	750 - 1200
Sb	mg/kg	0.01											
Se	mg/kg	ND				ND	2.5	44.1	265.1	63.63			
Zn	mg/kg	1.0	439.33	17	353	2785	250	76.7	738.9	67.4	1000	max	2500 - 4000
Faecal Coliform	per g				>110	ND					free		
Salmonella	per 25g		absent		absent	absent					free		
Color			Black			Black					Brown/ Grey to Dark black		
Moisture Content						0.061					<25%		
Odour			unpleasant			unpleasant					Shall not have any unpleasant Odour		
Sand Content	%mass				0.2	0.012					<10%		



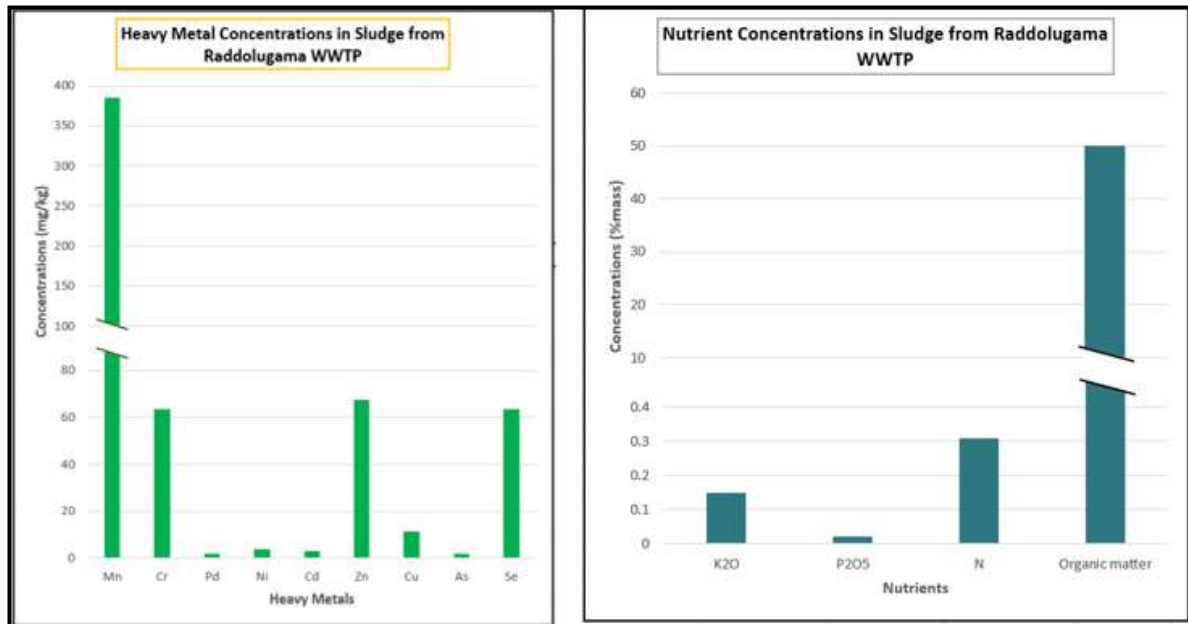


Figure 8. Heavy metal concentrations in sludge from Raddolugama Sewerage Treatment Plant dated 22/06/2021 and Nutrient concentrations of sludge from Raddolugama Sewerage Treatment Plant dated 22/06/2021

*B. Analysis of the Suitability of Sludge for Land Application*

From the results obtained, when compared with the European and US standards, it is apparent that only Raddolugama Sewerage treatment plant sludge can be assured as safe to use for land application.

*C. Analysis of Suitability of Sludge to use as a Fertilizer for Agricultural Purposes*

Based on the comparison of criteria, sludge from Biyagama CWWTP can be used as a fertilizer if an odour solution can be discovered. The most recent reports on the

indicate nutrient insufficiency.

Analysis of the issues which may have caused the variations in sludge parameters and how it can be improved through the existing plant

The biological treatment is used as a secondary treatment in the Biyagama, Moratuwa, and Ja-Ela treatment plants, while the raw water is treated chemically at the manufacturers' in-house treatment plants. In most cases, raw water is first biologically treated to remove organic matter and nutrients, and then chemically treated to minimize heavy metals and other characteristics for better quality. This could also be the cause of the sludge's high heavy metal and nutritional content, as mentioned above. Another problem noted in this investigation is the lack of an adequate odour control system. To prevent air pollution, some countries use effective scent control technologies. Chemical scrubbers are used in Germany to deodorize waste air (Frechen, 1988). In Denmark, they use a more ecofriendly alternative for chemical scrubbing. That is bio scrubbing (Hansen and Rindel,

2001). There are many other methods such as Bio filtration, activated sludge diffusion, bio trickling filtration, activated carbon adsorption, regenerative incineration, and a hybrid technology (bio trickling filtration coupled with carbon adsorption) (Estrada et al., 2011).

When industries deliver their pre-treatment effluents to WWTPs, however, the standards are not evaluated on a daily basis. Furthermore, even if changes in parameters are detected at the treatment plant's inlet, the individual factory that has exceeded the stipulated limits cannot be identified promptly so that corrective action can be taken. As a result, this study recommends establishing a mechanism for requesting a daily report of the factory outlet wastewater quality characteristics to the WWTP. When raw water is sent from the inflow to the oxidation ditch at the Biyagama CWWTP, it does not pass through a grit chamber. This could lead to a high sand content in the sludge. The maturation pond in the plant is not effective as the pond is covered in dense vegetation allowing very low light penetration. This may lead to eutrophication and eventually pollution of water.

*D. Proposing a Suitable Model Tolerance Limit Scale for Sri Lanka*

Table 3. Modelled limitation scale for sludge in land application

Parameter	Unit	Limit Value (max)
pH		6 - 8.5
Cd	mg/kg DM	5
Cr	mg/kg DM	100
Cu	mg/kg DM	400
Hg	mg/kg DM	2
Ni	mg/kg DM	30 - 50
Pb	mg/kg DM	150
Zn	mg/kg DM	1000
As	mg/kg DM	20-10
Mo	mg/kg DM	20
Faecal Coliform	per g	free
Salmonella	per 25 g	free

#### 4. Conclusion and Recommendation

This study focuses on finding environmentally and economically responsible ways to use or dispose of sludge produced as a byproduct of wastewater treatment. In order to examine the potential of sludge for use in agriculture as a fertilizer and the impact of land application, samples of sludge from four important treatment plants in Sri Lanka were evaluated for their qualities. Physical characteristics like color, moisture content, sand content, and chemical parameters like heavy metals and nutrients were examined in the sludge samples taken from the treatment plants, and these results were compared to EU, EPA, and SLS requirements.

The Biyagama facility's sludge, despite having an unpleasant smell, can be used as fertilizer, according to the findings. The other plants did not meet the necessary requirements. When it came to land application appropriateness, only the Raddolugama and Moratuwa treatment plants complied with EU and EPA regulations.

Sludge is a byproduct that is high in nutrients such as N, K, and P that are required for plant growth. As a fertilizer, sludge can be used directly as either a fertilizer or soil conditioner after treatment to obtain the necessary standards, or it can be mixed with compost to improve the nutrient quality. Moreover, at present, there is a promotion for production in Organic fertilizer in Sri Lanka with the limitations regulated for importing fertilizer by the current government. Hence this is an important opportunity to promote usage of sludge for fertilizer either by directly using as a fertilizer or soil conditioner after treating the sludge to obtain the necessary standards, or it can be mixed for compost and improve the nutrient quality, because sludge is a by product which is high in nutrients such as N, K, P which are needed for plant growth. Hence the sludge produced at Biyagama Plant can be used for fertilizer while adapting the odour control system used in the Moratuwa plant to solve its odour issue.

Sludge can also be used to create building supplies like cement and bricks. Since the sludge from Raddolugama and Moratuwa plants were tested positive for land applications, necessary treatments could be done to enhance its materialistic properties and use in raw material production or for landfilling. Recent research has revealed numerous promising advancements in sludge-based building materials.

Sludge is additionally employed in the creation of fuel. It is a good source for the manufacture of biofuel and can help with the current fuel problem and the high costs associated with utilizing it to generate energy.

Sludge must therefore be carefully handled and reused rather than being disposed of in landfills or dump yards. It represents a waste of a priceless resource. The correct treatment of sludge can reduce its negative impacts. However, laws for sludge treatment and disposal need to be addressed for disposing of sludge in any unfavourable ways that pose a harm to the organisms and environment.

### Acknowledgment

First, my most heartfelt sincere gratitude is express to my supervisor Dr. TMWRMB Samarakoon for his constant support, encouragement, exemplary guidance throughout the period of the final year project. I would also like to extend my deepest gratitude to Eng. (Mrs.) Champika J. Ranasinghe, Mrs. Kalyani Boteju, Mr. K.K.S Upulsiri Perera, Mrs. N.M. Samaranayake, Mrs. Harsha De Thennakoon, Mrs. Sumudu Habarakaduwa and Eng. (Mr.) N.U.K.Ranatunga. Finally yet importantly, I would like to thank Department of Civil Engineering of General Sir John Kotelawala Defence University, Sri Lanka for providing all the laboratory facilities to conduct my research. I would like to appreciate the support provided by my fellow colleagues and everyone else who stood by me.

### References

- Anjithan, B C L Athapattu, N Ratnayake, L. U. (2015) 'Sri Lanka Association for the Advancement of Science Proceedings of the 71 st Annual Sessions – 2015 Part I', d, p. 2015.
- APHA (2012) 'Standard Methods for the Examination of Water and Wastewater', p. 1496.
- Estrada, J. M. et al. (2011) 'A comparative analysis of odour treatment technologies in wastewater treatment plants',
- Environmental Science and Technology, 45(3), pp. 1100–1106. doi: 10.1021/es103478j.
- Frechen, F. B. (1988) 'Odour emissions and odour control at wastewater treatment plants in West Germany', Water Science and Technology, 20(4–5), pp. 261–266. doi: 10.2166/wst.1988.0175.
- Hansen, N. G. and Rindel, K. (2001) 'Bioscrubbing: An effective and economic solution to odour control at sewage-treatment plants', Water and Environment Journal, 15(2), pp. 141–146. doi: 10.1111/j.1747-6593.2001.tb00321.x.
- Jayalal, T. B. A. and Niroshani, S. L. N. (2007) 'Wastewater Production, Treatment, and Use in Sri Lanka', pp. 1–7.
- Nkoa, R. (2014) 'Agricultural benefits and environmental risks of soil fertilization with anaerobic digestates: A review', Agronomy for Sustainable Development, 34(2), pp. 473–492. doi: 10.1007/s13593-013-0196-z.
- Rorat, A. et al. (2019) 'Sanitary and environmental aspects of sewage sludge management', Industrial and Municipal Sludge: Emerging Concerns and Scope for Resource Recovery, (1), pp. 155–180. doi: 10.1016/B978-0-12-815907-1.00008-8.
- Turovskiy, I. S. and Mathai, P. K. (2005) Wastewater Sludge Processing, Wastewater Sludge Processing. doi: 10.1002/047179161X.
- World Bank Country and Lending Groups – World Bank Data Help Desk (no date).

Available at:  
<https://datahelpdesk.worldbank.org/knowledgebase/articles/906519-world-bank-country-and-lending-groups> (Accessed: 26 June 2021).

### **Author Biography**



EMS Anuththara has completed a BSc (Hons) in Civil Engineering from General Sir John Kotelawala Defence University, Sri Lanka. Her research interests include environmental engineering, Wastewater Treatment, Waste Management, Sewerage Disposal Methods, Sludge Management and Sustainable waste management.

# Assessment of Groundwater Quality due to Leachate Generated from a Solid Waste Dumpsite

LK Udamadura<sup>1</sup> and MB Samarakoon<sup>1#</sup>

<sup>1</sup> Department of Civil Engineering, General Sir John Kotelawala Defence University, Ratmalana, Sri Lanka

#lkudamadura@gmail.com

**Abstract:** In Sri Lanka, one of the main sources of groundwater pollution is the leachate generated from solid waste dumpsites. Karadiyana landfill is located 2km from Ratmalana airport, which receives nearly 500 tons of Municipal Solid Waste (MSW) daily. There is a considerable number of wells in the surrounding area, which are being used for drinking and other domestic purposes. The main focus of this study was to identify whether there is any effect of leachate on groundwater in nearby areas of Karadiyana dumpsite. Thus, well waters in nearby areas of the Karadiyana Dumpsite were collected. Subsequently, parameters such as pH, Electrical Conductivity (EC), Total Dissolved Solids (TDS), Total Phosphates and Ammoniacal Nitrogen included in these groundwater samples were determined. After the obtained concentrations were compared with permissible standards for drinking water, it was identified that some of the groundwater samples contained several contaminants exceeding the permissible limits. Moreover, the effect of distance on the degree of leachate contamination was also determined. Accordingly, it was suggested to identify the causing grounds for the anomaly obtained in these outcomes. As the conclusion, it was determined that for the time being, there is no significant effect of leachate on groundwater within the area starting from 400m away from the Karadiyana Dumpsite.

**Keywords:** Groundwater pollution, dumpsite, solid waste disposal, leachate, contamination

## 1. Introduction

As a consequence of population growth and urban development in developing countries, the rate of waste generation is increasing significantly. Most commonly, Municipal Solid Waste consists of everyday items that people throw after use such as batteries, electrical appliances, paint, glass, plastics, papers and food waste. Since Sri Lanka is a developing country, majority of MSW consists of food wastes, yard wastes and plastics. MSW, which includes these various constituents has a considerable degree of negative impact on environment and human health.

Out of numerous waste disposal practices such as incineration, waste compaction and thermal treatment plants, Sri Lanka uses open ground waste dumping method. Since aforementioned methods require more land and more technology for their operation, open ground waste dumping method is the waste disposal technique widely used in Sri Lanka (Dharmarathne and Gunatilake, 2013). The collected wastes are usually dumped in uncontrolled dumping grounds near residential buildings (Eseyin and Osu, 2019). This technique is more likely to be remain in Sri Lanka for a long time, since it seems to be one of the cheapest methods of waste disposal. Despite the fact that dumpsites are being used for waste management purposes, a huge number of adverse effects, especially for the neighbouring population of the dumpsite can be identified.

The adverse effects of dumpsites can be indicated as a main source of pollution of groundwater, surface water and soil, due to leachate contamination (Mishra et al., 2019).

Generation of leachate results, when dumped solid wastes comes in contact with groundwater or rain water. In view of this, it could be said that leachate is any liquid that passes through the dumped waste, while extracting the soluble or suspended solids and any other component present in it. Then, the leachate contaminated groundwater flows away from the dumpsite and get mixed with groundwater resources in the surrounding area of the dumpsite making those water resources polluted too('No Title', 1972). Leachate may contain high amounts of toxic substances including organic, inorganic and heavy metallic components. Due to leachate entering into subsoil and lastly into groundwater resources, groundwater of neighbouring areas of the dumpsite may become unsuitable for human consumption. But, the extent of effect of leachate contamination of groundwater resources depends on several factors including the depth of the water table, groundwater flow direction and concentration of contaminants(O et al., 2011).

Conventionally, when dumping wastes beforehand the ground should be prepared with necessary liners to prevent infiltration of leachate to groundwater or it is more effective to have a leachate collecting system. Introduction of a proper leachate controlling method to maintain leaching at the lowest level possible, is the primary method to protect surrounding water resources from leachate contamination(Przydatek and Kanownik, 2019). Accordingly, leachate can be properly collected and treated before disposing in to ecosystems.

As groundwater can be observed as a primary source of water supply in developing nations, this leachate contamination could lead to very critical environmental and health issues in Sri Lanka. Many researchers have conducted studies to determine the effect of leachate on groundwater and have identified that both groundwater and surface waters get polluted by leachate. Meanwhile it seems obvious that the damage cause to groundwater resources in

developing countries is considerably at a higher degree as a result of uncontrolled or semi-controlled open dumps. In addition to that, disposal of hazardous wastes along with MSW can be identified as another reason which increases the threat to groundwater resources in such countries.

This study was based on Karadiyana Dumpsite. It is a semi- controlled dumpsite which has been identified as one of the largest dumpsites in the country. Karadiyana dumping ground is situated in Thumbovila village in Western province, Sri Lanka. Nearly 575 tons of MSW is dumped to the dumping ground daily(Koliyabandara et al., 2017). The dumpsite has existed for over 30 years. The wastes from Panadura, Dehiwala, Kesbawa, Boralasgamuwa, Kotte and Mount Lavinia are dumped there. In addition, there is a compost plant which has been constructed as a solution for this huge amount of waste dumped in the dumping site.

## 2. Metodology and Data

### A. Selection of Locations to Collect Samples

In order to proceed the study, the area within 1km distance from Karadiyana dumpsite was divided into five regions having 200m intervals. From all the wells located within 1km radius of Karadiyana dumpsite, several wells were randomly selected to collect the groundwater samples. These samples were collected in such a way that it covers the whole perimeter included in 1km radius.



Figure 1. Considered regions around the dumpsite

Source:<<https://www.mapdevelopers.com/draw-circle-tool.php>>

### B. Sample Collection

Three samples from each selected well were collected, with the purpose of obtaining a mean value for the analysed parameters.

Transportation and Storage of Groundwater Samples Samples were collected into brown coloured bottles, in order to prevent the contaminants from breaking down. All the collected samples were stored in a cooler box until they were delivered to the laboratory. The reason for that was to prevent bacteria from multiplying inside the collected samples.

### C. Execution of Laboratory Tests

All the collected samples were evaluated for physical and chemical characteristics including pH, TDS, EC, concentration of Total Phosphates and concentration of Ammoniacal Nitrogen.

## 3. Results and Discussion

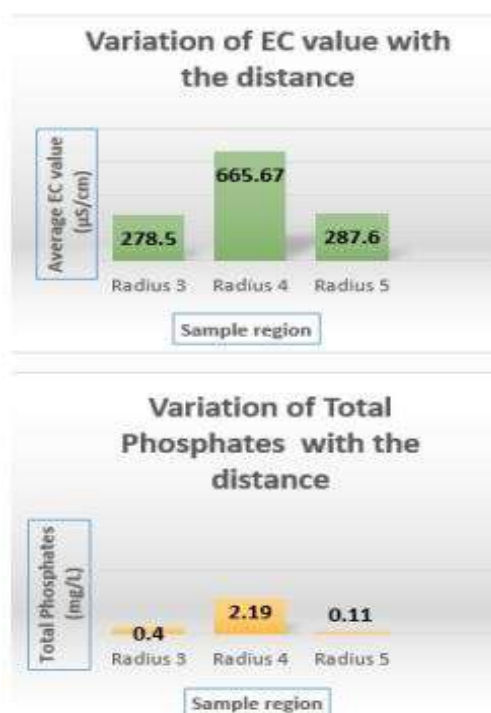
### A. Groundwater Characteristics

1) Variation of Groundwater Quality Parameters: The tested samples' pH values were between the range of 5.30 and 8.30. This indicates that tested water samples were varied from acidic to basic in nature. However, as per the specified requirement indicated in the first revision of SLS 614:2013-Specification of Potable Water, the majority of the pH values of the samples were within the allowable limits. TDS values for the samples that were examined ranged from 74.9 mg/L to 645.9 mg/L. Only one of the tested samples, from the fourth region, fell beyond the 500 mg/L TDS maximum permitted value given in the first revision of SLS 614:2013-Specification of Potable Water. Furthermore, it is evident from the results, that the samples taken from the fifth region have comparatively low TDS values.

All of the values obtained for electrical conductivity (EC) were less than 950  $\mu\text{S}/\text{cm}$ .

However, only one sample taken from the fifth region had an EC reading of 580  $\mu\text{S}/\text{cm}$ , which was above the limit permitted. With the exception of the aforementioned sample and the water samples taken from the fourth region, all the other samples had EC values below 400  $\mu\text{S}/\text{cm}$ , the upper limit specified by the World Health Organization (WHO). Additionally, the data clearly indicate that the samples collected from the fifth region have relatively low EC values.

However, results for the samples' Total Phosphates concentration were found to range from 0.07 mg/L to 5.6 mg/L. With the exception of one sample taken from region 4, none of the other samples were found to contain more total phosphates than its permissible amount, which is 2 mg/L in potable water.



Moreover, the concentration of ammoniacal nitrogen was found in the samples tested for the study to be between 0.1 mg/L and 4 mg/L. After analysis of the results, the concentration of ammoniacal nitrogen in half of the examined samples was found to be higher than the maximum allowable value, which is 0.5 mg/L according to the National Academy of Science.

Additionally, the samples taken from the fifth region exhibited the lowest ammoniacal nitrogen concentration values.

Table 1. Results for Groundwater Characteristics

Sample name	Parameter					
	pH	TDS (mg/L)	EC (µS/cm)	Total Phosphates (mg/L)	Ammoniacal Nitrogen (mg/L)	
Radius 3	Sample 1	5.30	168	223	0.6	0.2
	Sample 2	7.26	235.2	334	0.2	0.27
Radius 4	Sample 1	8.30	415	649	5.6	4
	Sample 2	7.00	285.3	424	0.09	3.5
	Sample 3	7.39	645.9	924	0.88	0.55
Radius 5	Sample 1	7.50	289	580	0.2	1.5
	Sample 2	5.63	74.9	111.3	0.07	0.1
	Sample 3	5.72	110.6	171.5	0.07	0.11

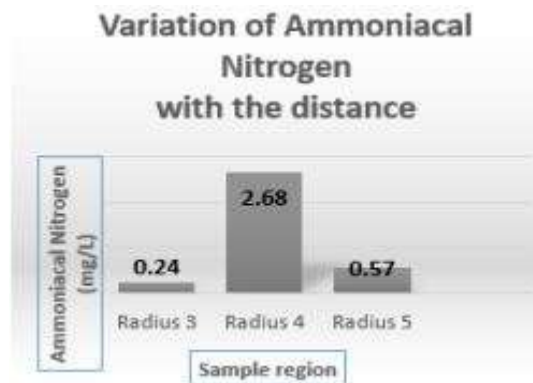


Figure 3. Variation of Parameters with the Distance

2) Effect of Distance:

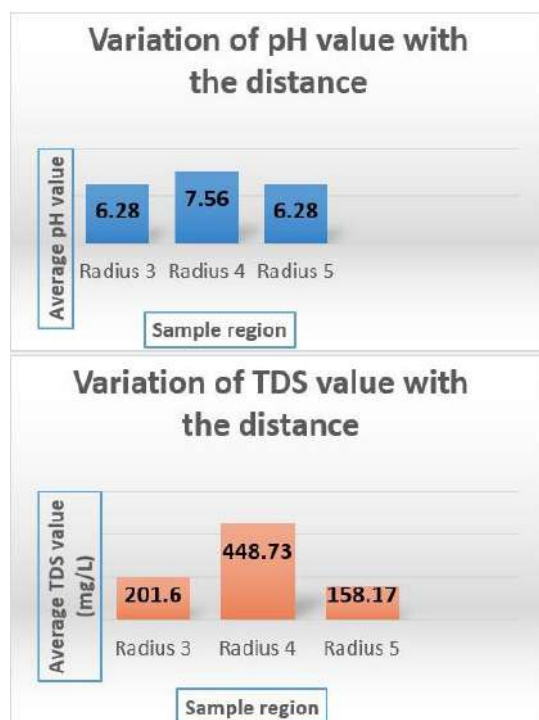


Figure 2. Variation of Parameters with the Distance

The results demonstrate that region 4 (radius 4 / R4) samples have greater average concentrations of all parameters than the other 2 regions. However both regions 3 and 5 have obtained the same average pH value. But, the average pH value determined from the samples from regions 3 and 5 indicates a value that is significantly below the acceptable pH level for drinking water. Waters in those places can be regarded of as being naturally more acidic because they have a low pH value.

When taking into account the TDS concentration results, it is clear that the samples taken from region 5, which is the location farthest from the dumpsite, generated the lowest value. This demonstrates the idea that leaching's impact tends to reduce with increasing distance from the dumpsite. However, based on the results, it can be determined that the average EC value of the samples that were collected from region 4 deviates significantly from those of the other two regions.

Furthermore, samples from region 5 have a lower average concentration of total phosphates than samples from region 3, which is much closer the dumpsite. The average concentration of Total Phosphates in samples from Region 4 is higher than that of the other two regions, and this value can be considered to be higher than the recommended



concentration for drinking water. When comparing groundwater samples collected from regions 3 and 5, the results for the average concentration of ammoniacal nitrogen exhibit relatively low values compared to those collected from region 4.

The results were expected to vary, with samples taken from regions 3 to 5 providing the concentration of water quality parameters in descending order. However, based on the results, there was a significant departure from the predicted results in the parameter concentrations of the samples collected from region 4. There are two possible explanations that could be used to justify the observed deviations:

- In region 4, there might be companies or production plants that discharge wastes that could degrade the quality of the groundwater in wells.
- Aquifers that are directly associated to the Karadiyana dumpsite may be found in the wells that were used for the study in region 4.

3) Groundwater Suitability: The SLS 614: 2013- Specification for Potable Water (First Revision)(For, 2013) specifies the following allowed maximum limits for each evaluated parameter.

Table 2. Specification for Potable Water

Characteristic	Maximum permissible requirement
pH	6.5 to 8.5
Electrical Conductivity (EC)	400 $\mu$ S/cm
Total Dissolved Solids (TDS)	500 mg/L
Total Phosphates	2.0 mg/L
Ammoniacal Nitrogen	-

Since there is no maximum permissible value for the concentration of Ammoniacal Nitrogen given in the SLS 614: 2013 – Specification for Potable Water (First Revision), the acceptable standard value given for that was identified as 0.5 mg/L according to the National Academy of Science(‘No Title’, 1972).

The average values of the tested parameters for each chosen location were taken into consideration in order to evaluate the appropriateness of the groundwater in the study area. However, the pH values for regions 3 and 5 exceed the acceptable limit for drinking water when the range in mean pH values of the samples is taken into account. Despite having a noticeably high value, the mean TDS value in region 4 is below the maximum limit for drinking water. Thus, it is possible to determine that the well waters in these 3 regions are acceptable for drinking purposes on the basis of the concentration of TDS values.

However, when comparing the mean EC values for these three regions, samples from region 4 have a high value that is higher than the standard EC limit for drinking water. This clarifies the fact that the well waters of region 4 are not directly suitable for consumption.

Based on the results for the concentration of Total Phosphates, samples from regions 3 and 5 mainly contained negligible levels. However, the total phosphate concentration of the wells in region 4 remained higher than the allowable limit, rendering the water in that area unsafe for residential use.

Based on the discussion above, it could be determined that the well water in region 4 is not at a level that is suitable for human consumption.

#### 4. Conclusion and Recommendation

Based on the results, it can be concluded that the leachate produced by the Karadiyana dumpsite appears to have a minimal effect on the quality of the groundwater in the vicinity, beginning 400 meters away from the dumpsite. However, it was also observed that some of the groundwater samples exhibited abnormal levels of Total Phosphates, Ammoniacal Nitrogen, and Electrical Conductivity. This could be an indication that the leachate produced in the landfill may have

collected over time in certain locations of the study area to some extent.

Furthermore, as the majority of the tested parameters were beyond the permitted limits specified by the SLS 614: 2013 Specification for Potable Water (First Revision), it has been concluded that the groundwater from wells in region 4 is not appropriate for immediate drinking.

However, over the time, threats to groundwater in these areas may increase due to leachate generated in Karadiyana dumpsite. Therefore, the need of enhancing waste management techniques can be identified as a very important measure in this regard. Conducting laboratory tests for water quality analysis in coming years may also help to identify the state of these groundwater. Additionally, further studies should be conducted in order to justify the reasons for the obtained anomaly in the results. It is also recommended to upgrade the Karadiyana dumpsite to a modernized dumpsite, with the purpose of restricting the generated leachate from mixing with groundwater resources.

## References

Dharmarathne, N. and Gunatilake, J. (2013) 'Leachate Characterization and Surface Groundwater', *International Journal of Scientific Research*, 3(11), pp. 1-7.

Eseyin, O. O. and Osu, I. C. (2019) 'Effect of Municipal Solid Waste (MSW) Leachate on Groundwater Quality in Port Harcourt, Nigeria', *Journal of Geography, Environment and Earth Science International*, (March), pp. 1-12. doi: 10.9734/jgeesi/2019/v19i330085.

For, S. (2013) 'Potable water'.

Koliyabandara, P. A. et al. (2017) 'Spatiotemporal Dynamics of Biogeochemical Species around Karadiyana Solid Waste Landfill, Sri Lanka', *AGUFM*, 2017, pp. B43B-2126. Available

at:

<https://ui.adsabs.harvard.edu/abs/2017AGU>

FM.B43B2126K/abstract (Accessed: 24 September 2020).

Mishra, S. et al. (2019) 'Impact of Municipal Solid Waste Landfill leachate on groundwater quality in Varanasi, India.', *Groundwater for Sustainable Development*, 9(May), p. 100230. doi: 10.1016/j.gsd.2019.100230.

'No Title' (1972).

O, A. A. et al. (2011) 'Assessment of groundwater

contamination by leachate near a municipal solid waste landfill', (January).

Przydatek, G. and Kanownik, W. (2019) 'Impact of small municipal solid waste landfill on groundwater quality', *Environmental Monitoring and Assessment*, 191(3), pp. 1-15. doi: 10.1007/s10661-019-7279-5.

## Acknowledgment

Final year individual research project is an immense opportunity for Civil Engineering Undergraduates to evolve important practical, academic knowledge and to integrate other essential skills in the selected Civil Engineering aspect. Hereby, I wish to express my gratitude to everyone who helped me to make this project successful.

First, I'd like to express my deepest thanks to Dr. TMWRMB Samarakoon for his advice, encouragement and support given throughout the project period. I would also like to express my acknowledgement towards the personnel of Environmental Laboratory of General Sir John Kotelawala Defence University and Anala Laboratory Services (Pvt) Ltd, Maharagama for their valuable contribution in providing me with laboratory facilities.

I would also like to appreciate the assistance given by T Gunasekara for making this project a success. Furthermore, I wish to extend my sincere gratitude to my beloved parents and my fellow colleagues from Intake 35 for encouraging me to complete this research. Finally, I would like to convey my heartfelt

appreciation to everyone who assisted me in various ways to complete this project.

### **Author Biography**



LK Udamadura has completed a BSc (Hons) in Civil Engineering from General Sir John Kotelawala Defence University, Sri Lanka. Her areas of interest in research are environmental engineering, particularly leachate contamination and analysis of ground water quality.